

Johanna Biederbick



**Population dynamics  
and trophic interactions  
of zooplankton in the  
Elbe estuary**

Dissertation

*For my loving parents,*

*Petra and Robert*

# **Population dynamics and trophic interactions of zooplankton in the Elbe estuary**

## **DISSERTATION**

zur Erlangung des Doktorgrades Dr. rer. nat. an der Fakultät  
für Mathematik, Informatik und Naturwissenschaften im  
Fachbereich Biologie der Universität Hamburg

vorgelegt von  
**Johanna Biederbick**

Hamburg  
2025

**Expected date of disputation:**

25<sup>th</sup> April 2025

**Examination committee:**

**Prof. Dr. Christian Möllmann** (first supervisor and examiner)

University of Hamburg

Faculty of Mathematics, Informatics and Natural Sciences

Department Biology

Institute of Marine Ecosystem and Fishery Science

**Dr. Rolf Koppelman** (second supervisor and examiner)

University of Hamburg

Faculty of Mathematics, Informatics and Natural Sciences

Department Biology

Institute of Marine Ecosystem and Fishery Science

**Prof. Dr. Jutta Schneider** (head of the examination commission)

University of Hamburg

Faculty of Mathematics, Informatics and Natural Sciences

Department Biology

Institute of Cell and Systems Biology of Animals

**Prof. Dr. Nicole Aberle-Malzahn** (recording clerk)

University of Hamburg

Faculty of Mathematics, Informatics and Natural Sciences

Department Biology

Institute of Marine Ecosystem and Fishery Science

**Dr. Andrej Fabrizius** (thesis committee chair and representative)

University of Hamburg

Faculty of Mathematics, Informatics and Natural Sciences

Department Biology

Institute of Cell and Systems Biology of Animals

## **Statement**

Although the work related to my thesis was predominantly planned and carried out by myself, it is important to note that research is a team effort. I received assistance from several colleagues, so that each chapter in this thesis is the work of more than one person. In accordance with the doctoral degree regulations, my contributions and those of my co-authors to the conception, realisation and composition of each chapter are given in a separate document attached at the end of the thesis. To acknowledge their contributions, I use the plural pronouns (we, us, our) throughout this thesis.

# Table of content

|                                                                                      |            |
|--------------------------------------------------------------------------------------|------------|
| <b>1. Summary</b> .....                                                              | <b>1</b>   |
| <b>2. Zusammenfassung</b> .....                                                      | <b>4</b>   |
| <b>1. Chapter 1: General introduction</b> .....                                      | <b>8</b>   |
| <b>2. Chapter 2: Spatio-temporal population dynamics of estuarine zooplankton</b> .. | <b>19</b>  |
| <b>3. Chapter 3: Population dynamics of <i>Eurytemora affinis</i></b> .....          | <b>51</b>  |
| <b>4. Chapter 4: Estuarine zooplankton trophic dynamics</b> .....                    | <b>80</b>  |
| <b>5. Chapter 5: Feeding ecology of <i>Osmerus eperlanus</i></b> .....               | <b>108</b> |
| <b>6. Chapter 6: Estuarine phytoplankton dynamics: Picophytoplankton</b> .....       | <b>133</b> |
| <b>7. Chapter 7: General discussion</b> .....                                        | <b>154</b> |
| <b>8. References</b> .....                                                           | <b>171</b> |
| <b>9. Acknowledgements</b> .....                                                     | <b>202</b> |
| <b>10. Eidesstattliche Versicherung / Declaration on oath</b> .....                  | <b>203</b> |
| <b>11. List of Publications</b> .....                                                | <b>204</b> |
| <b>12. Contribution of authors</b> .....                                             | <b>205</b> |

## Summary

Estuaries are highly productive transitional zones between freshwater and marine ecosystems, providing essential ecosystem services such as diverse habitats for humans and wildlife, coastal protection, nutrient cycling and carbon sequestration. Their dynamic physical and biochemical gradients challenge estuarine biota, resulting in the dominance of a few species with high plasticity to fluctuating environmental conditions through specialised feeding and reproductive strategies. Climate change and anthropogenic pressures may intensify these stressors on estuarine communities, potentially altering biodiversity and consequently ecosystem functioning. Zooplankton are an important component of the estuarine biota as primary and secondary consumers, playing a key role in food webs by maintaining trophic pathways. Despite their great importance for the ecosystem functioning, little is known about how variable environmental conditions affect the trophic interactions of zooplankton in estuaries (**Chapter 1**). This is particularly true for the highly modified Elbe estuary, one of the largest estuaries in northwestern Europe, where research on zooplankton population dynamics and trophic interactions is scarce despite recent morphological and biochemical changes in the ecosystem.

This dissertation integrates multiple studies and methodological approaches to assess the zooplankton community structures and their role in the food web of the Elbe estuary across spatial and temporal scales. This research aims to improve our understanding of natural and anthropogenic pressures on ecosystem functioning, offering a valuable basis for ecosystem-based management and conservation. To date, comprehensive studies of zooplankton population dynamics in the Elbe estuary are limited to the 1980s and 1990s, highlighting the need for new, detailed abundance data to enhance our knowledge of their spatio-temporal succession (**Chapter 2**). We conducted seasonal zooplankton sampling campaigns along the entire salinity gradient of the Elbe estuary and applied redundancy analyses to assess their relationships with the prevailing physico-biochemical conditions. The zooplankton community structure shifted along the salinity gradient from typical freshwater species to coastal taxa, while blooming conditions and turbidity affected

## SUMMARY

population structures based on their feeding characteristics. Overall, we observed a similar zooplankton community structure, but lower abundances compared to previous studies from the 1980s and 1990s. Morphological and hydrological changes, such as in flow velocity, sediment load and oxygen concentrations, may have contributed to the decline in species abundance.

The calanoid copepod *Eurytemora affinis* is the most dominant species throughout the estuary. Despite its dominance in the zooplankton community, little is known about the life history traits of *E. affinis* that are important for understanding its development and population maintenance under the estuarine gradients of the Elbe River. To address this, we conducted a detailed investigation of the *E. affinis* population dynamics by studying its growth, production and mortality rates through bi-weekly stationary sampling in the highly modified port region of the city of Hamburg (**Chapter 3**). Growth and production rates of *E. affinis* in this area were often higher than those reported in other estuarine studies, likely due to lower salinity stress and more favourable feeding conditions.

To improve our understanding of the spatio-temporal feeding conditions for zooplankton in the Elbe estuary and their impact on ecosystem trophodynamics, we identified available organic matter sources as potential food sources and examined feeding interactions among dominant species using a stable isotope approach (**Chapter 4**). We found a diverse mixture of particulate organic matter (POM) from riverine, terrestrial and coastal origins along the salinity gradient. The selected zooplankton taxa primarily derived their carbon source from high quality phytoplankton from the non-dredged freshwater area upstream of the port region, while the lower reaches were characterised by lower quantity and quality of algal food sources due to higher turbidity and intensive remineralisation processes. Selective feeding and food niche partitioning, along with shifts from herbivorous to detrital and heterotrophic food sources (e.g. microzooplankton) allowed species to cope with stressful feeding conditions, especially in winter and in the maximum turbidity zone (MTZ).

In addition, to investigate the impact of the estuarine zooplankton trophodynamics on higher trophic levels, we combined stable isotope and stomach content analyses on the most abundant fish species in the Elbe estuary, the European smelt *Osmerus eperlanus*

## SUMMARY

**(Chapter 5).** The study aimed to compare habitat exploitation between juvenile and adult smelt and to identify their feeding preferences to assess the trophodynamic role of estuarine zooplankton in a broader context. While adults may evade unfavourable food conditions by leaving certain areas, juvenile smelt were dependent on the prevailing food supply. We observed a dietary switch from zooplankton to increasing cannibalistic feeding preferences during ontogeny, with the limited food supply playing a key role in the selection of prey organisms. The presence of  $^{15}\text{N}$ -enriched juveniles in the MTZ suggested an extended food chain in this area, possibly due to unfavourable environmental conditions.

In the last study, we analysed the spatio-temporal distribution pattern of phytoplankton communities in the Elbe estuary as potential carbon sources for zooplankton, using a combination of flow cytometry and metabarcoding techniques **(Chapter 6)**. Major attention was given to the picophytoplankton, which contributed up to 70% to the total phytoplankton abundance and prevailed year-round in the Elbe estuary. Picophytoplankton may play an important role in sustaining primary production and thus food web structures under conditions of extreme temperatures, high turbidity and intense grazing pressure, which may be challenging for larger phytoplankton.

In summary, our studies have provided valuable new insights into the spatio-temporal dynamics of zooplankton populations and their trophic relationships across different trophic levels in the Elbe estuary **(Chapter 7)**. We were able to classify the Elbe estuary into four distinct zones, thereby providing a comprehensive overview of the food web dynamics based on our findings. We have synthesised these results in a schematic diagram that illustrates our main conclusions (Fig. 7.1).

## Zusammenfassung

Ästuare sind hochproduktive Übergangszonen zwischen Süßwasser- und Meeresökosystemen, die wichtige ökologische Dienstleistungen bieten, darunter vielseitige Lebensräume für Menschen und Wildtiere, Küstenschutz, Nährstoffaustausch und Kohlenstoffspeicherung. Ihre dynamischen physikalischen und biochemischen Gradienten stellen eine Herausforderung für die Biota der Ästuare dar, was oftmals zur Dominanz einiger weniger Arten führt, die sich durch spezialisierte Ernährungs- und Fortpflanzungsstrategien an schwankende Umweltbedingungen anpassen können. Der Klimawandel und anthropogene Einflüsse können diese Stressfaktoren für die Lebensgemeinschaften in den Ästuaren weiter verstärken, was die biologische Vielfalt und damit die Funktionsweise der Ökosysteme verändern kann. Zooplankton ist als Primär- und Sekundärkonsument ein wichtiger Bestandteil der ästuarinen Lebensgemeinschaft und spielt durch die Aufrechterhaltung der trophischen Pfade eine Schlüsselrolle in diesen Nahrungsnetzen. Trotz ihrer enormen Bedeutung für die Funktionsweise dieser Ökosysteme ist wenig darüber bekannt, wie schwankende Umweltbedingungen die trophischen Beziehungen des Zooplanktons in Ästuaren beeinflussen (**Kapitel 1**). Dies gilt insbesondere für das hochgradig modifizierte Elbeästuar, eines der größten Ästuare in Nordwesteuropa, in dem trotz der jüngsten morphologischen und biochemischen Veränderungen im Ökosystem nur wenig über die Populationsdynamik des Zooplanktons und deren trophischen Interaktionen bekannt ist.

In dieser Dissertation werden verschiedene Studien und methodische Ansätze integriert, um die Strukturen der Zooplanktongemeinschaften und ihre Rolle im Nahrungsnetz des Elbeästuars auf unterschiedlichen räumlichen und zeitlichen Skalen zu bewerten. Diese Untersuchungen sollen zu einem besseren Verständnis der natürlichen und anthropogenen Einflüsse auf die Funktionsweise des Ökosystems beitragen und ein wertvolles Instrument für ein ökosystembasiertes Management und den Naturschutz darstellen. Bislang sind umfassende Untersuchungen zur Populationsdynamik des Zooplanktons im Elbeästuar auf die 1980er und 1990er Jahre beschränkt, was den Bedarf an neuen, detaillierten

Bestandsdaten unterstreicht, um unser Wissen über ihre räumlich-zeitliche Entwicklung zu erweitern (**Kapitel 2**). Wir haben saisonale Beprobungen des Zooplanktons entlang des gesamten Salinitätsgradienten des Elbeästuars durchgeführt und Redundanzanalysen angewandt, um ihre Beziehungen zu den vorherrschenden physikalischen und biochemischen Bedingungen zu bewerten. Die Struktur der Zooplanktongemeinschaft verschob sich entlang des Salinitätsgradienten von typischen Süßwasserarten hin zu Küstenarten, während die durch die Trübung beeinflussten Blütebedingungen die Populationsstruktur in Abhängigkeit von ihren Ernährungsmerkmalen beeinflussten. Insgesamt beobachteten wir eine ähnliche Struktur der Zooplanktongemeinschaft, jedoch mit geringeren Abundanzen im Vergleich zu früheren Studien aus den 1980er und 1990er Jahren. Morphologische und hydrologische Veränderungen, wie beispielsweise in der Strömungsgeschwindigkeit, der Sedimentlast und den Sauerstoffkonzentrationen, könnten zu dem Rückgang der Zooplankton Bestände beigetragen haben.

Der calanoide Ruderfußkrebs *Eurytemora affinis* ist die häufigste Art innerhalb des Zooplanktons im gesamten Ästuar. Trotz seiner Dominanz in der Zooplanktongemeinschaft ist nur wenig über die lebensgeschichtlichen Merkmale von *E. affinis* bekannt, die für das Verständnis seiner Entwicklung und Populationserhaltung unter den Umweltbedingungen des Elbeästuars wichtig sind. Um dieses Thema aufzugreifen, führten wir eine detaillierte Untersuchung der Populationsdynamik von *E. affinis* durch, indem wir die Wachstums-, Produktions- und Mortalitätsraten mittels zweiwöchentlicher stationärer Beprobung im stark anthropogenen beeinflussten Hamburger Hafengebiet untersuchten (**Kapitel 3**). Die Wachstums- und Produktionsraten von *E. affinis* in diesem Gebiet waren häufig höher als in anderen Ästuarstudien, was wahrscheinlich auf geringeren Salzstress und günstigere Nahrungsbedingungen zurückzuführen ist.

Um die räumlich-zeitlichen Nahrungsbedingungen des Zooplanktons im Elbeästuar und deren Auswirkungen auf die Trophodynamik des Ökosystems besser zu verstehen, haben wir die verfügbaren Quellen organischen Materials als potenzielle Nahrungsquellen identifiziert und die Nahrungsinteraktionen zwischen den dominanten Zooplanktonarten mithilfe von stabilen Isotopen Untersuchungen analysiert (**Kapitel 4**). Entlang des

## ZUSAMMENFASSUNG

Salinitätsgradienten fanden wir eine vielfältige Zusammensetzung von partikulärem organischem Material fluvialen, terrestrischen und küstennahen Ursprungs. Die ausgewählten Zooplanktonarten bezogen ihre Kohlenstoffquelle überwiegend aus qualitativ hochwertigem Phytoplankton aus der flachen Süßwasserzone oberhalb des Hafengebietes, während der Unterlauf aufgrund höherer Trübung und intensiver Remineralisierungsprozesse durch eine geringere Quantität und Qualität der Algen gekennzeichnet war. Selektives Fressen, die Aufteilung von Nahrungsnischen sowie die Verlagerung von pflanzlichen zu detritischen und heterotrophen Nahrungsquellen (z. B. Mikrozooplankton) ermöglichten den Arten mit den schwierigen Nahrungsbedingungen, insbesondere im Winter und in der Zone maximaler Trübung, zurechtzukommen.

Um den Einfluss der Trophodynamik des Zooplanktons auf höhere trophische Ebenen im Ästuar zu untersuchen, kombinierten wir stabile Isotopen- und Mageninhaltsanalysen anhand des Europäischen Stint *Osmerus eperlanus*, welche die häufigste Fischart im Elbeästuar darstellt (**Kapitel 5**). Ziel der Studie war es, die Habitatnutzung von juvenilen und adulten Stinten zu vergleichen und ihre Nahrungspräferenzen zu ermitteln, um die trophische Rolle des Zooplanktons im Ästuar in einem größeren Kontext zu bewerten. Während adulte Stinte sich ungünstigen Nahrungsbedingungen entziehen können, indem sie diese Gebiete verlassen, sind juvenile Stinte von dem gegebenen Nahrungsangebot abhängig. Wir beobachteten einen Wechsel von Zooplankton als Hauptbeute hin zu kannibalistischem Fressverhalten im Laufe der Ontogenese, wobei das begrenzte Nahrungsangebot im Ästuar eine Schlüsselrolle bei der Auswahl der Beuteorganismen spielt. Das Auftreten von <sup>15</sup>N-angereicherten Jungfischen in der Zone maximaler Trübung deutet auf eine verlängerte Nahrungskette in dieser Zone hin, die möglicherweise auf ungünstige Umweltbedingungen zurückzuführen ist.

In der letzten Studie wurde das räumlich-zeitliche Verteilungsmuster der Phytoplanktongemeinschaften im Elbeästuar als potenzielle Kohlenstoffquellen für das Zooplankton mit einer Kombination aus Durchflusszytometrie und Metabarcoding untersucht (**Kapitel 6**). Der Schwerpunkt lag dabei auf dem Picophytoplankton, das bis zu 70% des gesamten Phytoplanktons ausmachte und ganzjährig im Elbeästuar vorkam. Das

## ZUSAMMENFASSUNG

Picophytoplankton spielt vermutlich eine wichtige Rolle bei der Aufrechterhaltung der Primärproduktion und damit der Strukturen des Nahrungsnetzes unter Bedingungen mit extremen Temperaturen, starker Trübung und hohem Fraßdruck, die für größeres Phytoplankton eine Herausforderung darstellen könnten.

Zusammenfassend lieferten unsere Untersuchungen wertvolle neue Einblicke in die räumlich-zeitliche Dynamik der Zooplanktonpopulationen und ihrer trophischen Beziehungen über verschiedene trophische Ebenen im Elbeästuar (**Kapitel 7**). Wir konnten das Elbeästuar in vier verschiedene Zonen unterteilen und damit einen umfassenden Überblick über die Dynamik des Nahrungsnetzes anhand unserer Ergebnisse geben. Wir haben diese Ergebnisse in einem schematischen Diagramm zusammengefasst, das unsere wichtigsten Schlussfolgerungen darstellt (Abb. 7.1).

## Chapter 1: General introduction

### Estuarine ecology under human pressure

Estuaries – derived from the Latin word *aestuarium*, meaning ‘tidal’ – are dynamic environments where freshwater from riverine systems converges and mixes with saltwater from the sea by tidal currents (Wolanski and Elliott, 2015). There have been several definitions of an estuary, but no uniform terminology exists. The most quoted and comprehensive definition of an estuary is given by Fairbridge (1980), who described estuaries as “*an inlet of the sea reaching into a river valley as far as the upper limit of tidal rise, usually being divisible into three sectors: (i) a marine or lower estuary, in free connection with the open sea; (ii) a middle estuary subjected to strong salt and fresh water mixing; and (iii) an upper or fluvial estuary, characterised by fresh water but subject to daily tidal action. The limits between these sectors are variable and subject to constant changes in the river discharge*”. The Venice System is currently the most widely used and accepted method for classifying estuaries based on salinity (Venice System, 1958). As salinity decreases from the sea to the river, the estuarine zones can be classified based on salinity into polyhaline (18 – 30), mesohaline (5 – 18), oligohaline (0.5 – 5) and freshwater (< 0.5) zones.

Estuaries serve as vital links between terrestrial, freshwater and saltwater ecosystems. They are characterised by unique physical forces and complex chemical and biological properties (see Fig. 1.1), such as rapid changes in currents, turbidity, salinity, nutrient concentrations, oxygen conditions and trophic pathways (Statham, 2012; Day *et al.*, 2013). Because of their dynamic nature, estuaries are highly productive areas that facilitate the transfer, recycling and storage of nutrients from both autochthonous and allochthonous sources across ecosystem boundaries (Wilson, 2002; Hyndes *et al.*, 2014). They provide essential ecosystem services, including not only carbon sequestration but also coastal and flood protection and diverse habitats that serve as refuge, feeding and nursery grounds for estuarine biota (Wilson, 2002; Koch *et al.*, 2009; Hyndes *et al.*, 2014; Wolanski and Elliott, 2015; Boynton *et al.*, 2018). However, only a few species can withstand the natural stressors of estuarine gradients, often resulting in the dominance of single key species and lower

species richness compared to adjacent freshwater and marine ecosystems (Whitfield *et al.*, 2012). Estuarine biota have evolved several behavioural and physiological adaptations, such as specialised feeding and reproductive strategies (e.g. Modéran *et al.*, 2012; Biederbick *et al.*, 2024; Martens *et al.*, 2024b), to exploit energy sources that would be highly stressful for most other organisms (Day *et al.*, 2013; Wolanski and Elliott, 2015).

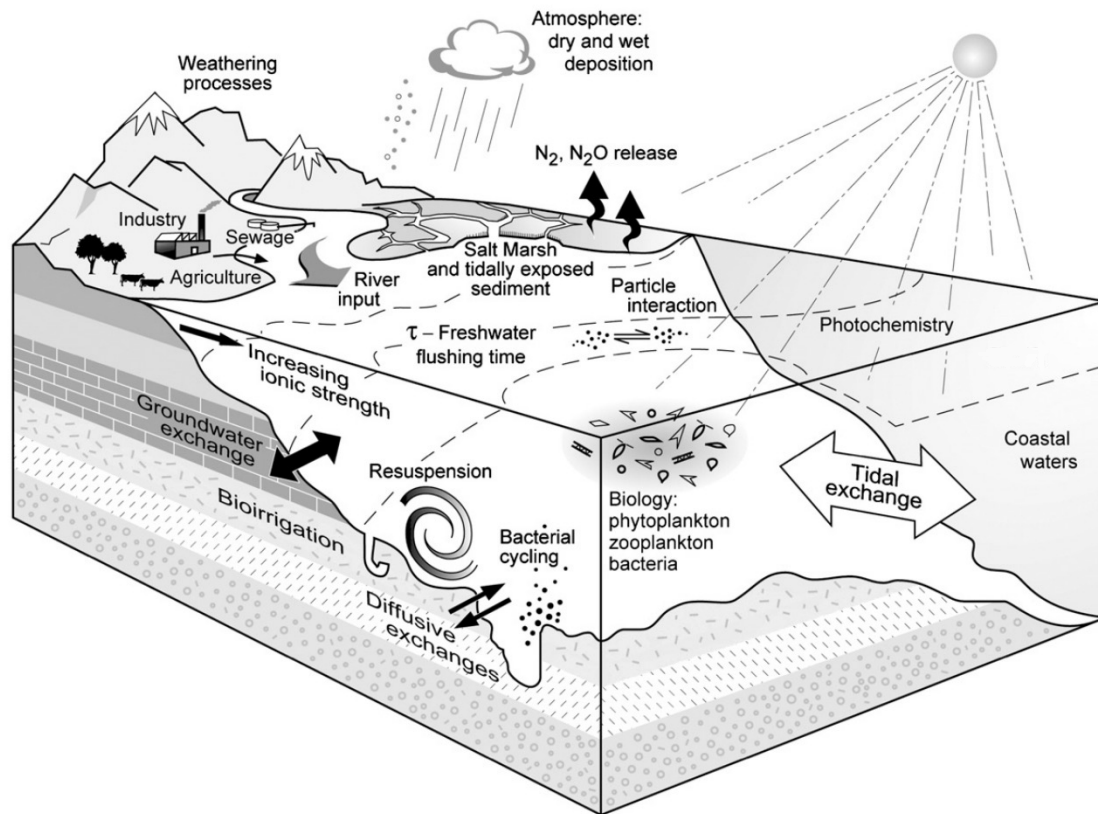


Fig. 1.1: Schematic overview of hydrodynamics and major biogeochemical processes in estuaries. Figure modified after Statham (2012).

Given that estuaries are valuable environments for ecological and economic purposes, human activities have modified these ecosystems worldwide to serve their own needs. Rapid population growth and development in coastal areas, along with increasing urbanisation and industrialisation are closely linked to human activities, such as tourism, land reclamation, waste disposal, agriculture, fishing and shipping (Kennish, 2002; Cloern *et al.*, 2016). These pressures are often accompanied by pollution, overexploitation and physical alteration of estuarine habitats through construction and dredging activities, all of which can significantly threaten these vital ecosystems (Blaber, 2000; Paerl, 2006; Kerner, 2007; Statham, 2012; Cloern *et al.*, 2016). In addition, climate change is likely to exacerbate

stress on estuarine communities. Climate-related changes are expected to increase the risk of eutrophication, harmful algae blooms, salinity stress and hypoxia in estuaries, which can potentially reduce biodiversity and consequently the ecosystem functioning (Statham, 2012; Cloern *et al.*, 2016; Robins *et al.*, 2016). Therefore, it is crucial to investigate the complex interplay between both natural and anthropogenic stressors on estuarine biota to provide decision makers with essential knowledge for ecosystem-based management and conservation efforts.

## Planktonic food webs in estuaries

The estuarine food web is essential for the transfer of energy within estuarine biota and across adjacent freshwater and marine ecosystems, thus contributing to the overall dynamic and functioning of these transitional zones. A key component of this food web is zooplankton, which serve as a vital trophic link between primary producers and higher trophic levels (Harris *et al.*, 2000). By feeding on algal and detrital sources, as well as smaller zooplanktonic species, zooplankton act as both primary and secondary consumers, while also serving as important prey for larger predators, such as fish (see Fig. 1.2). Their function in the food web contributes to the ecosystem stability and nutrient cycling.

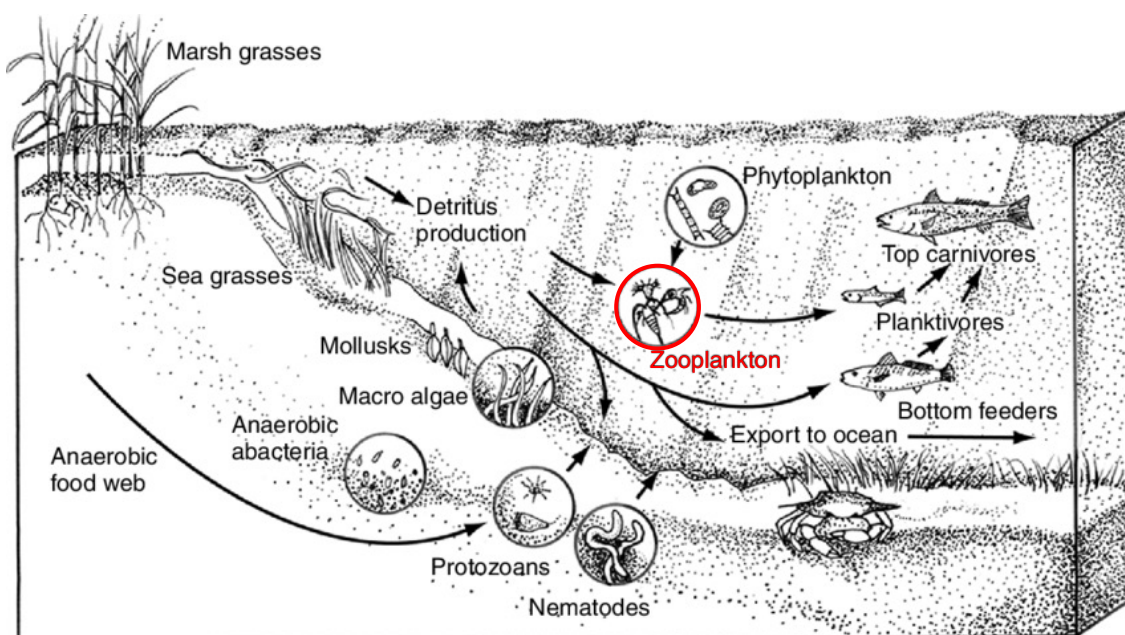


Fig. 1.2: Simplified estuarine food web diagram showing the main trophic links between estuarine biota. Black arrows illustrate the energy flow from sources to consumers. Zooplankton are highlighted in red. Figure modified after Day *et al.* (2013).

The term ‘plankton’ is derived from the Greek word *planao*, meaning ‘to wander’ (Harris *et al.*, 2000). It refers to all drifting organisms that lack the ability to withstand currents, as opposed to nekton, which includes actively swimming organisms. Planktonic organisms can be differentiated into phytoplankton and zooplankton species based on their morphology or nutrition mode (autotrophy vs. heterotrophy). While phytoplankton serve as primary producers capable of photosynthesis, zooplankton are primarily considered phagotrophic organisms that can be classified as herbivorous, detritivorous, omnivorous or carnivorous depending on their feeding preferences. Heterotrophic plankton also include mixotrophic organisms, meaning the combination of auto- and heterotrophy, which is often found in flagellates and ciliates (e.g. Muñoz-Marín *et al.*, 2020; Martens *et al.*, 2024b). Zooplankton can also be classified according to their life cycle (Harris *et al.*, 2000). Species that spend their entire life in the pelagic realm are referred to as holoplankton, unlike meroplankton, which spend only part of their life cycle in the water column. However, some holoplankton species, including cladocerans, copepods and rotifers, exhibit benthic resting stages by producing resting eggs that allow them to survive unfavourable environmental and feeding conditions, which has been often observed in estuarine systems (e.g. Johnson, 1980; Glippa *et al.*, 2011).

The term ‘zooplankton’ covers a wide range of organisms that may share similar feeding behaviours and life cycles, but they can also be distinguished by their size range (Harris *et al.*, 2000). Size classification was last comprehensively defined by Sieburth *et al.* (1978) (see

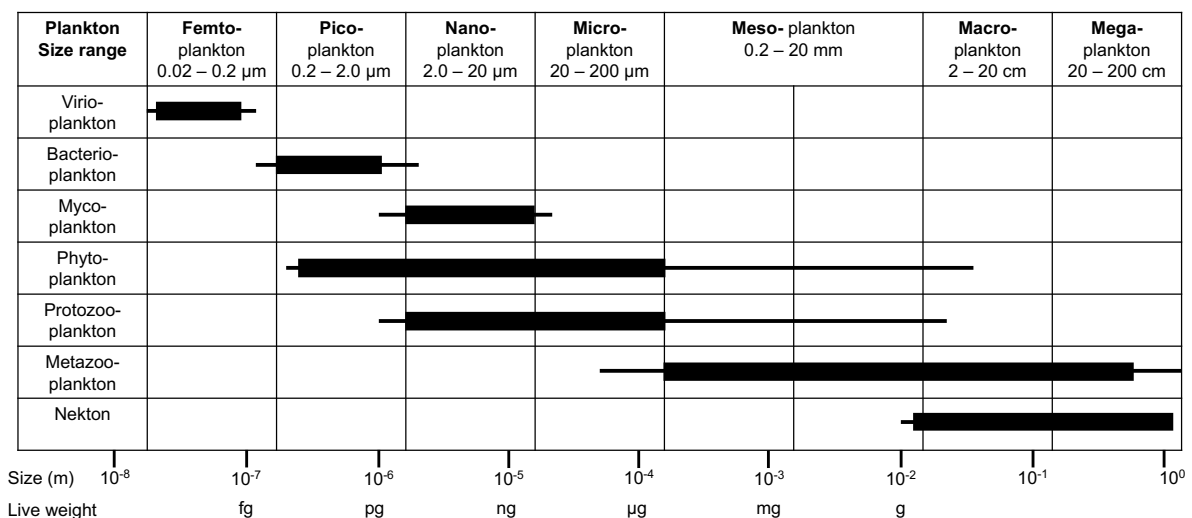


Fig. 1.3: Size spectrum of different taxonomic-trophic compartments of plankton including nekton. Redrawn and modified after Sieburth *et al.* (1978).

Fig. 1.3) and is an important aspect of quantitative plankton research. Zooplankton range from nanoplankton (2-20  $\mu\text{m}$ ) to megaplankton (20-200 cm) and are typically sampled with nets of different mesh sizes. In estuaries, where dynamic environmental conditions (e.g. turbidity, currents) can make effective quantitative sampling with nets difficult, alternative sampling devices such as bottles, pumps and traps are often used in addition to nets (Sluss *et al.*, 2011; Gutkowska *et al.*, 2012). The primary constituents of nanozooplankton are heterotrophic nanoflagellates, whereas most other protozoans, especially ciliates, rotifers and early life stages of crustaceans belong to the microzooplankton size class (20 – 200  $\mu\text{m}$ ) (Harris *et al.*, 2000). The mesozooplankton size class (0.2 – 20 mm) includes e.g. older stages of crustaceans, fish eggs, chaetognaths, ctenophores and appendicularians. Copepods are the most abundant crustaceans in the oceans and are also dominant in estuarine systems (Day *et al.*, 2013). They hatch from eggs and progress through six naupliar and six copepodite stages, with the final stage being the adult copepod (Mauchline *et al.*, 1998). Larger organisms, such as hydromedusae, mysids, amphipods, euphausiids are major components of the macrozooplankton (2 – 20 cm). There are only a few megazooplankton organisms, consisting mainly of jellyfish such as scyphozoa and siphonophores.

Body size typically determines food web relationships, as most consumers ingest prey items whole. In addition, the feeding type play a crucial role in trophic interactions. Filter feeders, including copepods, euphausiids, ciliates and rotifers, use various filtering techniques to exploit different food size spectra (Harris *et al.*, 2000). In particular, copepods and euphausiids are generally herbivorous and omnivorous, using their complex mouthparts and feeding apparatus to capture and selectively feed on large phytoplankton cells, organic detritus and nano- and microzooplankton, facilitated by a self-generated feeding current (Kiørboe, 2011). Ciliates and rotifers are often herbivorous, primarily grazing on pico- and nanoplankton, but they may also consume detrital sources and small protozoans (Gilbert, 2022). They use ciliary currents for feeding, which are less efficient in selective feeding compared to larger organisms (Kiørboe, 2011). In contrast, ambush feeders, including amphipods and fish larvae, are predators that can capture their prey either actively (i.e. by attacking) or passively (i.e. through prey movement), using appendages such as tentacles

and spines (Kiørboe, 2011). Cladocerans, mysids and ostracods are intermediates between ambush and filter feeders (Kiørboe, 2011). However, it is important to note that there are many exceptions within taxonomic groups. For instance, many copepods and euphausiids can also be carnivorous, for example *Cyclops* spp. and *Eudiaptomus* spp. (Brandl, 2005), or *Crangon crangon* (Pihl and Rosenberg, 1984). In addition, some species can even change their feeding mode, e.g. from herbivory to omnivory, when environmental and feeding conditions are detrimental, which has been observed for some estuarine zooplankton taxa (e.g. Modéran *et al.*, 2012).

In general, the functioning of food webs relies on the balance between nutrient supply, which drives primary production and thus food availability and quality for zooplankton (bottom-up control), and grazing pressure from higher trophic levels (top-down control) (Harris *et al.*, 2000). Estuarine environmental conditions can be challenging for zooplankton, which may have cascading effects on the food web dynamics. Despite their great importance in food webs, little is known about how variable environmental conditions affect the trophic ecology of zooplankton in estuaries. Assessing estuarine zooplankton community structures and their feeding relationships along spatial and temporal scales is of critical importance. To date, only a limited number of studies have focused on the trophic interactions of zooplankton in estuaries (e.g. Martineau *et al.*, 2004; Winkler *et al.*, 2007; Modéran *et al.*, 2012). Estuaries are unique ecosystems with distinct morphological characteristics and physico-biochemical dynamics (Day *et al.*, 2013). Consequently, comparisons of trophic relationships among different estuaries are inherently limited. The Elbe estuary, one of the largest estuaries in northwestern Europe, remains largely unexplored regarding zooplankton population dynamics and trophic interactions. It was therefore chosen as the area of study for this doctoral thesis.

## **The Elbe estuary**

The Elbe River has a total length of 1,094 km, starting in the Giant Mountains in the Czech Republic and ending in the North Sea at Cuxhaven (Boehlich and Strotmann, 2008). Its tidal section is about 142 km long, beginning at the weir at Geesthacht (Elbe-km 585), passing through the metropolis city of Hamburg (from Elbe-km 609 to 636) before entering the

German Bight (Elbe-km 727). The tidal estuary is described as a partially well-mixed water body that weakly stratifies in summer (Pein *et al.*, 2021) with a pronounced maximum turbidity zone (MTZ) located around Glückstadt (Elbe-km 674) (Papenmeier *et al.*, 2014). The hydrology is characterised by a semidiurnal, flood-dominated tide with a mean range between 3.5 m at Hamburg and 2 m at the weir (HPA, 2022). The water residence time ranges from two to four weeks, depending on the discharge rate, which averages about  $708 \text{ m}^3 \text{ s}^{-1}$  (measured at Neu-Darchau, Elbe-km 536; FGG Elbe, 2017). However, the hydrological conditions in the Elbe estuary have changed in recent decades due to climate change. In the last 30 years, the number of days with extremely low discharge rates ( $< 200 \text{ m}^3 \text{ s}^{-1}$ ) in summer has increased, which is associated with longer droughts in the Elbe catchment area (Weilbeer *et al.*, 2021).

The Elbe estuary provides an important socio-economic ecosystem service by linking the seaport of Hamburg, which is situated in the tidal freshwater zone, with international maritime traffic (Krysanova *et al.*, 2006). The first construction efforts in the Elbe estuary were carried out around the year 1000, when the first dikes were built for flood protection (Riedel-Lorjé and Gaumert, 1982). Since the early 19<sup>th</sup> century, when the harbour was greatly expanded, the morphology of the estuary has been altered multiple times through embankments, deepening and dredging events to improve access to the Hamburg port area (Riedel-Lorjé and Gaumert, 1982; Kerner, 2007; Li *et al.*, 2014). The navigation channel, originally in its pristine state with a depth of approximately 4 m (Kerner, 2007), has been deepened to about 20 m downstream of the port region since 2021 (HPA, 2022). These deepening events have caused a rapid drop in the bathymetry at the eastern edge of the city of Hamburg, resulting in longer water residence times and increased accumulation of suspended particles and siltation (Kerner, 2007; Li *et al.*, 2014; Geerts *et al.*, 2017).

In the 1980s, the Elbe was one Europe's most polluted rivers, suffering from poor waste water management and high levels of industrial organic compounds (Adams *et al.*, 1996; Krysanova *et al.*, 2006; Radach and Pätsch, 2007). Eutrophic conditions often led to hypoxia events, resulting in mass fish mortality (Thiel, 2011). Although the water quality began to improve after the implementation of the European Water Framework Directive following the

German reunification (Adams *et al.*, 1996), oxygen deficiency situations still persist in the Elbe estuary (Amann *et al.*, 2012; Schöl *et al.*, 2014; Kamjunke *et al.*, 2023). Recurring hypoxia events have been linked to changes in bathymetry that favour intense remineralisation processes (Adams *et al.*, 1996; Amann *et al.*, 2012; Geerts *et al.*, 2017; Sanders *et al.*, 2018). Most of the organic matter in the Elbe estuary consists of phytoplankton that originates from the shallow, non-dredged freshwater area upstream of the port region (Geerts *et al.*, 2017). When these algae reach the deep-water zone, they die off due to increased light limitation and sedimentation to deeper layers (Wolfstein and Kies, 1995; Kamjunke *et al.*, 2023; Steidle and Vennell, 2024), which in turn promote remineralisation processes (Sanders *et al.*, 2018; Dähnke *et al.*, 2022) and subsequently hypoxic conditions (Amann *et al.*, 2012; Geerts *et al.*, 2017).

Natural stressors, exacerbated by climatic and human-induced changes in the water regime of the Elbe estuary, have likely contributed to losses in biodiversity and biomass of both phytoplankton (e.g. Wolfstein and Kies, 1995; Geerts *et al.*, 2017) and fish (e.g. Theilen *et al.*, 2022; Theilen *et al.*, *subm.*; Illing *et al.*, 2024) over time. It can be assumed that these factors may also impact zooplankton population dynamics and their trophic interactions in the Elbe estuary.

## **Zooplankton in the Elbe estuary**

Research on the spatio-temporal population dynamics of zooplankton in the Elbe estuary has been carried out only occasionally. A major issue is the lack of permanent or long-term monitoring programmes with high spatial and temporal resolution. A possible reason for this may be that zooplankton are not classified as “biological quality elements” under the European Water Framework Directive, in contrast to fish fauna, benthic invertebrates, phytoplankton, macrophytes and phytobenthos, which are used to assess the ecological status and potential of rivers (BMUV/UBA, 2022). Previous investigations on zooplankton succession were initiated by governmental authorities and research institutions, resulting in a small number of reports, theses and peer-reviewed articles. Most of the existing literature on the population dynamics of zooplankton in the Elbe estuary is grey literature. In addition,

access to these earlier studies is often restricted, as most historical zooplankton data are not available in digital repositories or are not freely accessible through archives and libraries.

Zooplankton in the Elbe estuary was first studied in detail by Volk (1903) in the early 20<sup>th</sup> century, focusing on qualitative aspects. Thiemann (1934) was the first to provide a quantitative description of the Elbe zooplankton. This was followed by several other studies, including those by Schulz (1961), who examined phyto- and zooplankton from the riverine section of the Elbe to Cuxhaven, and by Nöthlich (1972), who primarily focused on the zooplankton population dynamics in the freshwater zone of the Elbe estuary. The most recent studies are limited to sampling campaigns conducted in the 1980s and 1990s (e.g. Fiedler, 1991; Peitsch, 1992; Bernát *et al.*, 1994; Holst, 1996; Holst *et al.*, 1998; Zimmermann-Timm *et al.*, 1998; Köpcke, 2002), prior to initiatives aimed at improving water quality. These studies do not consider recent environmental changes resulting from the last deepening campaigns in 1999 and 2021 (Kerner, 2007; HPA, 2022). Consequently, there is an urgent need for new data on the zooplankton community in the Elbe estuary, particularly in the light of recent morphological changes.

In contrast, feeding relationships of zooplankton in the Elbe estuary have been much less studied. Previous research has largely focused on the importance of zooplankton as food source for fish (e.g. Fiedler, 1991; Thiel *et al.*, 1996), rather than exploring trophic interactions within the planktonic food web. First attempts to study planktonic food web structures were made by Kerner (2004), who determined zooplankton grazing patterns by analysing carbon stable isotopes of planktonic organisms collected in the freshwater zone of the Elbe estuary. Therefore, a comprehensive seasonal and spatial investigation of the planktonic food web along the entire salinity gradient of the Elbe estuary is needed.

## **Objectives**

The overarching aim of this dissertation is to improve our understanding of estuarine zooplankton ecology, with major focus on population dynamics and trophodynamics, by integrating several studies and methodological approaches using the Elbe estuary as a model system. This research will provide a critical basis for future management and

conservation efforts by deepening our knowledge of the impacts of natural and anthropogenic pressures on the ecosystem functioning from a zooplankton perspective.

The first main objective of this thesis is to assess the spatial and temporal zooplankton species succession in the Elbe estuary in relation to the prevailing physico-biochemical conditions. To achieve this, we first conducted seasonal sampling campaigns to collect three different zooplankton size classes (i.e. micro-, meso- and macrozooplankton) using a combination of different sampling methods at six stations along the entire salinity gradient. This approach offers comprehensive insights into community structure, species abundance and biomass, which are addressed in **Chapter 2**. Further, we compared these new zooplankton datasets with relevant studies from the 1980s and 1990s.

In order to gain a deeper understanding of the population development and conservation of zooplankton in the Elbe estuary, in the following study (**Chapter 3**) we aimed to examine the growth, production and mortality of a selected key species, the calanoid copepod *Eurytemora affinis*. *E. affinis* is a highly ubiquitous estuarine calanoid copepod (Winkler *et al.*, 2011) that occurs throughout the entire Elbe estuary (Peitsch *et al.*, 2000) and serves as an important food source for local fish populations, particularly for the dominant species *Osmerus eperlanus* (Thiel *et al.*, 1996). To investigate its life history traits under the dynamic estuarine gradients, we carried out a bi-weekly stationary sampling campaign in the port region of the city of Hamburg to study the succession of its developmental stages from nauplii to adult copepodites. In addition, we compared our results spatially with a similar study conducted in the MTZ during the 1990s.

The second main objective of this thesis is to determine the spatio-temporal feeding conditions for zooplankton in the Elbe estuary and their impact on the trophodynamics of the ecosystem. We initially focused on the feeding interactions within the planktonic food web (**Chapter 4**). To achieve this, we applied a stable isotope analysis ( $\delta^{13}\text{C}$ ,  $\delta^{15}\text{N}$ ) to dominant meso- and macrozooplankton taxa, as well as to the ichthyoplankton of *O. eperlanus*, collected across different spatial and temporal scales. Additionally, we aimed to identify the dominant carbon sources that sustain the food supply for these planktonic consumers.

In **Chapter 5** we examined the influence of zooplankton trophodynamics on higher trophic levels to provide a comprehensive insight into the Elbe estuarine food web. We applied a combination of stomach content analysis and stable isotope techniques to study the feeding ecology of the key species smelt *O. eperlanus*, and consequently to assess the importance of zooplankton in their diet during ontogeny. The study also aimed to investigate spatial differences in feeding behaviour between juveniles and adults and to relate these variations to their habitat exploitation.

In the final study (**Chapter 6**) we focused on the first trophic level to distinguish and quantify the phytoplankton groups as potential food sources available to consumers. A metabarcoding approach was used in conjunction with flow cytometry to provide a comprehensive qualitative and quantitative characterisation of the phytoplankton communities, with particular emphasis on picophytoplankton. Although picophytoplankton have been documented in estuaries (Purcell-Meyerink *et al.*, 2017; Sathicq *et al.*, 2020), their ecological role in the Elbe remains unexplored, largely due to the limitations of traditional microscopy in detecting and classifying them.

## Chapter 2: Spatio-temporal population dynamics of estuarine zooplankton



Manuscript in preparation:

Biederbick, J., Möllmann, C., Russnak, V. and Koppelman, R. Spatial and temporal succession of zooplankton in an environment under anthropogenic pressure – the Elbe estuary in northern Germany.

**Title:** Spatial and temporal succession of zooplankton in an environment under anthropogenic pressure – the Elbe estuary in northern Germany

**Running title:** Spatio-temporal population dynamics of estuarine zooplankton

**Authors:** Johanna Biederbick<sup>1\*</sup>, Christian Möllmann<sup>1</sup>, Vanessa Russnak<sup>2</sup> and Rolf Koppelman<sup>1</sup>

<sup>1</sup>Institute of Marine Ecosystem and Fishery Science, University of Hamburg, Grosse Elbstrasse 133, 22767 Hamburg, Germany

<sup>2</sup>Helmholtz-Centre Hereon, Institute of Carbon Cycles, Max-Planck-Strasse 1, 21502 Geesthacht, Germany

\*Corresponding author

E-Mail: [johanna.biederbick@uni-hamburg.de](mailto:johanna.biederbick@uni-hamburg.de)

## Abstract

Estuarine zooplankton play a crucial role as primary and secondary consumers in estuarine pelagic food webs. They are exposed to strong fluctuations in physico-biochemical conditions and human stressors, such as dredging and intense agricultural land use, which affect the population dynamics on spatial and temporal scales. However, detailed community studies under certain estuarine conditions are rare and outdated for the highly turbid and dredged Elbe estuary (Germany). We provide a comprehensive overview of the micro- meso- and macrozooplankton population dynamics in the Elbe estuary by examining their spatio-temporal succession in relation to physical and biochemical gradients. For this, we applied a redundancy analysis on micro-, meso- and macrozooplankton assemblages and environmental data (chlorophyll *a* (Chl *a*), suspended particulate matter (SPM), dissolved nutrients, temperature, salinity, oxygen, pH) that were collected at six stations along the entire salinity gradient during seasonal sampling campaigns in 2021 and 2022. Salinity and Chl *a* were the primary factors affecting the spatial distribution of zooplankton, with highest Chl *a* concentrations restricted to the non-dredged section, where SPM levels were lowest. This autotrophic zone was favourable for a distinct freshwater assemblage consisting of cyclopoid and calanoid copepods (e.g. *Eurytemora affinis*), cladocerans (e.g. *Bosmina longirostris*), and rotifers (e.g. *Keratella* spp., *Brachionus* spp.), with abundances peaking at high Chl *a* concentrations, particularly in spring and summer. *E. affinis* emerged as the most abundant copepod throughout the entire estuary, exhibiting a marked tolerance to high SPM loads. Euryhaline species, such as *Acartia* spp., *Paracalanus parvus* and *Mesopodopsis slabberi* colonised the lower part of the estuary due to their affinity for higher salinities. We observed a similar community structure, but lower zooplankton abundance with respect to earlier studies which could be explained by the morphological and hydrological changes induced over the last decades. This study enhances our understanding of estuarine zooplankton population dynamics under various environmental conditions, which is essential for preserving these systems in the face of global change.

Keywords: Elbe estuary, zooplankton community, rotifers, copepods, mysids, spatio-temporal variability, environmental parameters

## Introduction

Zooplankton play a crucial role in food webs as link between primary producers and higher trophic levels (Barnett *et al.*, 2007) and can be used as biological indicators for ecosystem functioning (Modéran *et al.*, 2010; Selleslagh *et al.*, 2012). Estuaries are transition zones between freshwater and marine ecosystems and are consequently characterised by large fluctuations in physical and biochemical processes, such as salinity, discharge, tidal advection and substrate turnover (Day *et al.*, 2013). Transition zones are highly productive areas that have essential functions in the transfer and cycling of nutrients and provide an important habitat for crustaceans and fish (Wilson, 2002; Hyndes *et al.*, 2014). Anthropogenic pressures such as diking and dredging (Kerner, 2007), urbanisation and industrialisation (Paerl, 2006), as well as fisheries and aquaculture (Blaber, 2000) severely impact estuarine ecosystems on spatial and temporal scales. Estuarine zooplankton must therefore be able to adapt to large fluctuations in environmental conditions driven by natural processes and human activities. Assessing its community structure and distribution in response to physical and biochemical processes is important for understanding the functioning and managing of the ecosystem and to protect these habitats.

Effort has been made to enhance our understanding of environmental factors influencing zooplankton communities in the largest European estuaries, such as the Gironde (David *et al.*, 2005; Selleslagh *et al.*, 2012) and the Seine (Mouny and Dauvin, 2002) and the Scheldt estuary (Soetaert and Van Rijswijk, 1993; Tackx *et al.*, 2004; Mialet *et al.*, 2011). However, biochemical and physical processes can greatly differ between estuaries (Middelburg and Herman, 2007; Modéran *et al.*, 2010). For many other systems, such as the Elbe estuary, information on the variability in zooplankton community structure is still limited.

The Elbe estuary is one of Europe's largest estuaries, situated in north-west Germany, and flows into the North Sea. Like other systems, the Elbe estuary is heavily affected by human activities such as dredging and industrial use. The city of Hamburg, with the second largest harbour in Europe, is located about 100 km upstream in the tidal freshwater part of the Elbe. Due to dredging to enhance the accessibility downstream from the port area, the water depth increases rapidly causing high turbidity by longer residence time of water masses and

thus accumulation of suspended particles (Kerner, 2007; Papenmeier *et al.*, 2014). Riverine phytoplankton dies while passing the deeper and turbid water column in the port region because of light limitation (Wolfstein and Kies, 1995; Schöl *et al.*, 2014; Kamjunke *et al.*, 2023). This favours intense microbial degradation processes resulting in increasing oxygen deficiency situations in the port area (Geerts *et al.*, 2017; Sanders *et al.*, 2018). The Elbe estuary was also polluted with nutrients until the end of the 1980s due to the intensive use of fertilisers in agriculture, which led to eutrophication (Radach and Pätsch, 2007). Waste water management and the reduction of industrial organic compounds have improved the water quality of the Elbe estuary in the last decades (Adams *et al.*, 1996; Amann *et al.*, 2012). Several studies have shown that these changes may affect the zooplankton community. For example, Mialet *et al.* (2011) found a significant shift in the species distribution patterns and an increase in abundances in response to improved water quality in the Scheldt estuary. In addition, Marques *et al.* (2007) observed that zooplankton communities in the Mondego estuary suffered from regular dredging activities, which increased flow velocities and led to greater outflow of organisms, resulting in generally lower population densities.

The impact of past changes in the hydrological regime in the Elbe estuary on the structure of the zooplankton community remains uncertain. Detailed studies about environmental parameter influencing the zooplankton dynamics in the Elbe estuary are rare. The last published studies on estuarine Elbe zooplankton date back to sampling campaigns in the 1980s and 1990s, which provide information on population dynamics of rotifers (Holst *et al.*, 1998; Zimmermann-Timm *et al.*, 1998), copepods and mysids (Fiedler, 1991; Bernát *et al.*, 1994; Peitsch *et al.*, 2000; Köpcke, 2002). These studies were performed at the start of the efforts to improve water quality in the Elbe estuary and do not consider the recent environmental conditions impacted by the last deepening campaigns conducted in 1999 and 2021 (Kerner, 2007; HPA, 2022).

In this study, we aim to close this gap of knowledge for the Elbe estuary by characterising seasonal and spatial patterns in the zooplankton community structure, specifically focusing on abundances in relation to environmental conditions. We conducted seasonal sampling campaigns at six stations along the entire salinity gradient of the Elbe estuary in 2021 and

2022 to account for zooplankton spatio-temporal succession. Previous studies from the 80s and 90s (e.g. Fiedler, 1991; Peitsch, 1992; Holst, 1996; Köpcke, 2002) were re-analysed to compare patterns in zooplankton abundance and composition. We followed a multivariate approach on species biomass and distribution to (1) detect the most dominant taxa, (2) identify seasonal and spatial variations in the community structure of different zooplankton size classes, as well as (3) to uncover the prevailing environmental parameters that explain most of the species' succession, and (4) to compare our findings with studies from the last decades.

## Methods

### Study area

The Elbe River is one of the major rivers in Northwest Europe originating in the Great Mountains of the northern Czech Republic and enters the North Sea. Its tidal estuary extends approximately 142 km, beginning at the weir in Geesthacht (Elbe-km 585), passing through to the seaport of the metropolis city of Hamburg before reaching the German Bight at Cuxhaven (Elbe-km 727) (Fig. 2.1). Due to its substantial socio-economic importance, the estuary has undergone recurring hydrological modification, particularly dredging and straightening to maintain full access and enable expansion of the Hamburg Harbour (HPA, 2022). The hydrodynamics are characterised by a partially well-mixed water column (Pein *et al.*, 2021) with a long water residence time between two and four weeks depending on the river discharge (Amann *et al.*, 2012), exhibiting a marked maximum turbidity zone (MTZ) of about 30 km around Glückstadt at Elbe-km 674 (Papenmeier *et al.*, 2014). The Elbe estuary has a semidiurnal flood-dominated asymmetry with a mean tidal range between 3.5 m in the port area to 2 m at the weir (HPA, 2022), with a daily mean discharge rate of  $708 \text{ m}^3 \text{ s}^{-1}$  (FGG Elbe, 2017).

### Zooplankton sampling

Micro-, meso- and macrozooplankton samples were obtained during seasonal sampling campaigns at six stations in the Elbe estuary in 2021 and 2022 (Fig. 2.1). Seasonal sampling was conducted with the research vessel *Ludwig Prandtl* in May and July 2021, as well as in

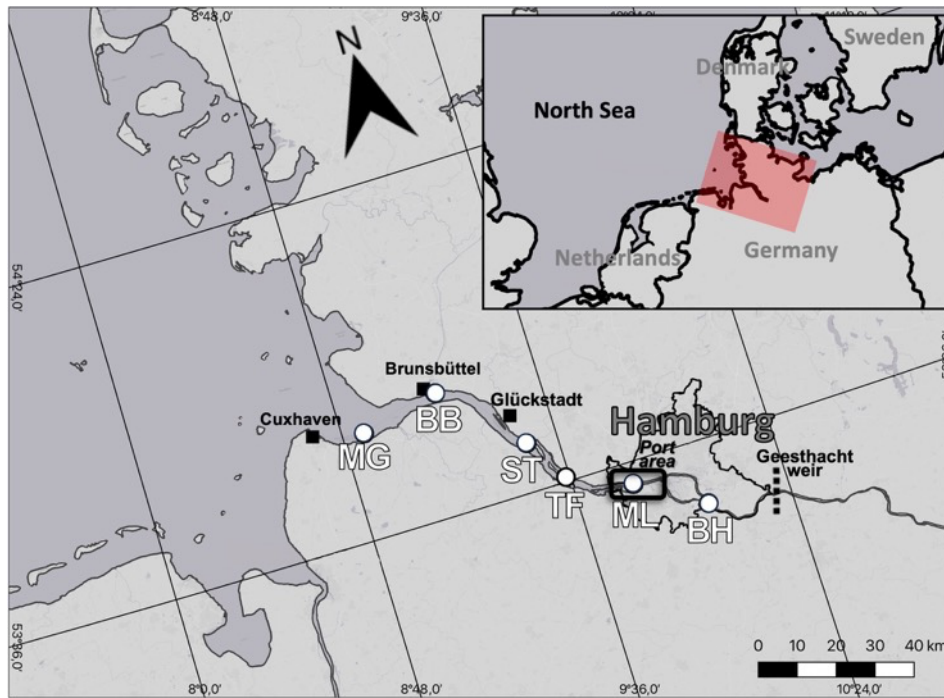


Fig. 2.1: Sampling locations in the Elbe estuary. Station names are abbreviated as followed: Bunthäuser Spitze (BH), Mühlenberger Loch (ML), Twielenfleth (TF), Schwarztonnensand (ST), Brunsbüttel (BB) and Medemgrund (MG) at Elbe-km 609, 633, 651, 665, 692 and 713, respectively. The weir at Geesthacht defines the upper tidal limit of the estuary. The background map has been provided by Esri, HERE, Garmin, © OpenStreetMap contributors, and the GIS User.

February, May, June and November 2022, respectively, and with the stow-net vessel HF567 *Ostetal* in August and November 2021, respectively (Table 2.1). Sampling was scheduled at the same time in the tidal cycle, ensuring consistent conditions between campaigns (see supplementary material for more details, Table S 2.1).

Table 2.1: Cruise schedule and data on mean temperature and river discharge rates (Q) for the respective sampling periods.

| Sampling periods | Dates                             | Season | Research vessel                   | Temperature (°C) |      | Q (m <sup>3</sup> s <sup>-1</sup> ) |
|------------------|-----------------------------------|--------|-----------------------------------|------------------|------|-------------------------------------|
|                  |                                   |        |                                   | Min.             | Max. |                                     |
| May 2021         | 07./08. May 2021                  | Spring | R/V Ludwig Prandtl                | 10.4             | 11.4 | 480                                 |
| Jul 2021         | 30. July 2021                     | Summer | R/V Ludwig Prandtl                | 21.7             | 22.7 | 666                                 |
| Aug 2021         | 25./26./27./28./29. August 2021   | Summer | Stow-net vessel<br><i>Ostetal</i> | 17.1             | 18.8 | 426                                 |
| Nov 2021         | 17./18./19./20./21. November 2021 | Autumn | Stow-net vessel<br><i>Ostetal</i> | 7.1              | 8.8  | 474                                 |
| Feb 2022         | 28. February 2022                 | Winter | R/V Ludwig Prandtl                | 4.4              | 5.8  | 1165                                |
|                  | 08./09./10./11. March 2022        |        | Stow-net vessel<br><i>Ostetal</i> |                  |      |                                     |
| May 2022         | 22. May 2022                      | Spring | R/V Ludwig Prandtl                | 16.2             | 19.6 | 345                                 |
| Jun 2022         | 20. June 2022                     | Summer | R/V Ludwig Prandtl                | 18.0             | 21.4 | 231                                 |
| Nov 2022         | 08. November 2022                 | Autumn | R/V Ludwig Prandtl                | 10.9             | 13.0 | 283                                 |

Micro- and mesozooplankton samples were obtained at each station with quantitative bucket hauls collecting 30 - 50 l of surface water at 0.5 m depth. Triplicate samples were taken and subsequently filtered through 55  $\mu\text{m}$  and 200  $\mu\text{m}$  gauze to separate the zooplankton into both size fractions. Macrozooplankton taxa were collected via a single horizontal tow at 0.5 m depth using a 1000  $\mu\text{m}$  ring trawl net (0.94 m aperture, 2.80 m net length) equipped with a mechanical flow meter (General Oceanics, Florida, USA; model number 2030R). Micro-, meso- and macrozooplankton was defined as organisms with a sieve size between 55 – 200  $\mu\text{m}$ , 200 – 2000  $\mu\text{m}$  and 2 – 20 cm, respectively. All zooplankton samples were fixed in sodium tetraborate buffered 37% formaldehyde solution at a final concentration of 4% after Omori & Fleminger (1976). Micro-, meso- and macrozooplankton samples were either entirely counted or subsampled using modified Hensen-Stempel pipettes (Perkins, 1957), Folsom (McEwen *et al.*, 1954) and Motoda (Motoda, 1959) splitters, respectively. At least 100 individuals of the most abundant taxa in each size fraction were counted and identified to the lowest taxonomic level possible using an inverted microscope (Leica Microsystems, Wetzlar, Germany; model number: DBMI3000B) and a dissecting microscope (Leica Microsystems, Wetzlar, Germany; model number: M125C) at 100X and 40X magnifications, respectively. Species- and stage-specific body lengths were determined from images of individual species using the image processing program “ImageJ” (version 4.13, Schneider *et al.*, 2012) and pooled across the sampling periods. Species dry weight (in  $\mu\text{g l}^{-1}$ ) were estimated applying length-weight regressions obtained from published literature (Dumont *et al.*, 1975; Mason, 1986; Mees *et al.*, 1994; Azeiteiro *et al.*, 1999; Wang and Zauke, 2002; Watkins *et al.*, 2011; see Table S 2.2 for more details). Species that were inconsistently recorded or observed only once were excluded from the analysis. Additionally, rare species, accounting for less than 1 % to the total abundance, were eliminated from the dataset to reduce noise in the multivariate analysis.

### **Environmental data**

Environmental parameters like temperature ( $^{\circ}\text{C}$ ), salinity, pH and oxygen saturation ( $\text{mg l}^{-1}$ ) were analysed in surface waters with an *in situ* Ferrybox system (see Petersen *et al.*, 2011

for further details) or obtained with a portable handheld sensor (Hanna Instruments, Vöhringen, Germany; model number HI98494) on-board of the RV *Ludwig Prandtl* and the stow-net vessel HF567 *Osteta*, respectively. Data on daily discharge rates were obtained from the nearest gauge station located upstream the weir in Neu Darchau (Elbe-km 536), which can be accessed via the Federal Waterways and Shipping Agency (WSV, 2023). Surface water samples were taken with multiple bucket hauls and filtered through pre-combusted, pre-weighted glass fibre filters (0.7 µm pore size, GF/F, Whatman, 450°C). The filtered water volume was adapted at each station according to the concentration of suspended organic matter to ensure proper coating of the filters. At each station, two filters were obtained for measuring suspended particulate matter (SPM) and chlorophyll *a* (Chl *a*) concentrations, while the filtrate was used for nutrient measurements. Filters and filtrate were transferred to centrifuge tubes and immediately stored at -20°C on board until further processing in the lab.

One half of the filters were freeze-dried at -80°C for 24 h and then weighed for SPM dry weight (in mg l<sup>-1</sup>). The other filters were used for Chl *a* extraction by adding 10 ml of 90% acetone, which were then stored cooled in darkness (5°C, 24 h) before centrifugation (3000 rpm, 4°C, 15 min). The absorbance of the extracts was determined using a PerkinElmer photometer (LAMBDA XLS, Waltham, USA; model number: L7110189) following the method of Jeffrey and Humphrey (1975). The filtrates were photometrically analysed for NO<sub>2</sub><sup>-</sup>, NO<sub>3</sub><sup>-</sup>, NH<sub>4</sub><sup>+</sup> and PO<sub>4</sub><sup>3-</sup> concentrations using an automated continuous flow analyser (Seal Analytical, Norderstedt, Germany; model number AA3) according to the method of Hydes et al. (2010).

## Data analysis

A permutational multivariate analysis of variance (PERMANOVA) was conducted to investigate the relationship between zooplankton community structures and the factor station, season, and year, including pairwise multilevel comparisons using the R package “pairwiseAdonis” (version 0.4, Martinez Arbizu, 2020). A transformation-based redundancy analysis (tb-RDA) was performed for each zooplankton size fraction to assess the impact of environmental data on the seasonal and spatial zooplankton succession using the R

package “vegan” (version 2.6-4, Oksanen et al., 2022). Individual taxa biomass was Hellinger transformed to reduce the influence of double zeros (Borcard *et al.*, 2011). Environmental data were z-standardised and then tested for collinearity by Pearson’s correlation. The parameter pH was subsequently eliminated from the analysis due to strong collinearity with oxygen saturation. To find the most parsimonious RDA model, a stepwise model selection based on AIC selection criterion was conducted. The explanatory variables were selected by backward and forward selection using the function *ordistep* of the “vegan” R package. The selected variables from the final RDA model are displayed in a correlation triplot for each zooplankton size fraction separately. For greater clarity in the correlation triplots, taxa with low affinities to environmental variables with species scores  $< 0.2$  were excluded in the selected model. A Monte-Carlo permutation test (with 999 iterations) was performed to test for significance of the global model, the RDA model axes, as well as the explanatory variables, which were retained in the RDA model after model selection. An adjusted  $R^2$  was calculated to estimate the amount of variability in the response data, which is explained by the explanatory variables. Due to technical issues, filtration could not be performed at all stations during the cruise in November 2021. Missing values were subsequently interpolated by multivariate imputations using the R package “mice” (version 3.16.0, van Buuren & Groothuis-Oudshoorn, 2011). All statistical analyses and visualisations were performed using R (version 4.3.2, R Core Team, 2023). The language of the finalised manuscript was corrected using the AI language model GPT-4 (OpenAI, 2023).

## Results

### Environmental conditions

Water temperatures ranged between 4.4°C in February 2022 to 22.7°C in July 2021 (Table 2.1). In May 2022, temperatures were up to 9°C higher than in May 2021. The highest discharge rates, reaching up to 1165 m<sup>3</sup> s<sup>-1</sup>, occurred during winter sampling, while the

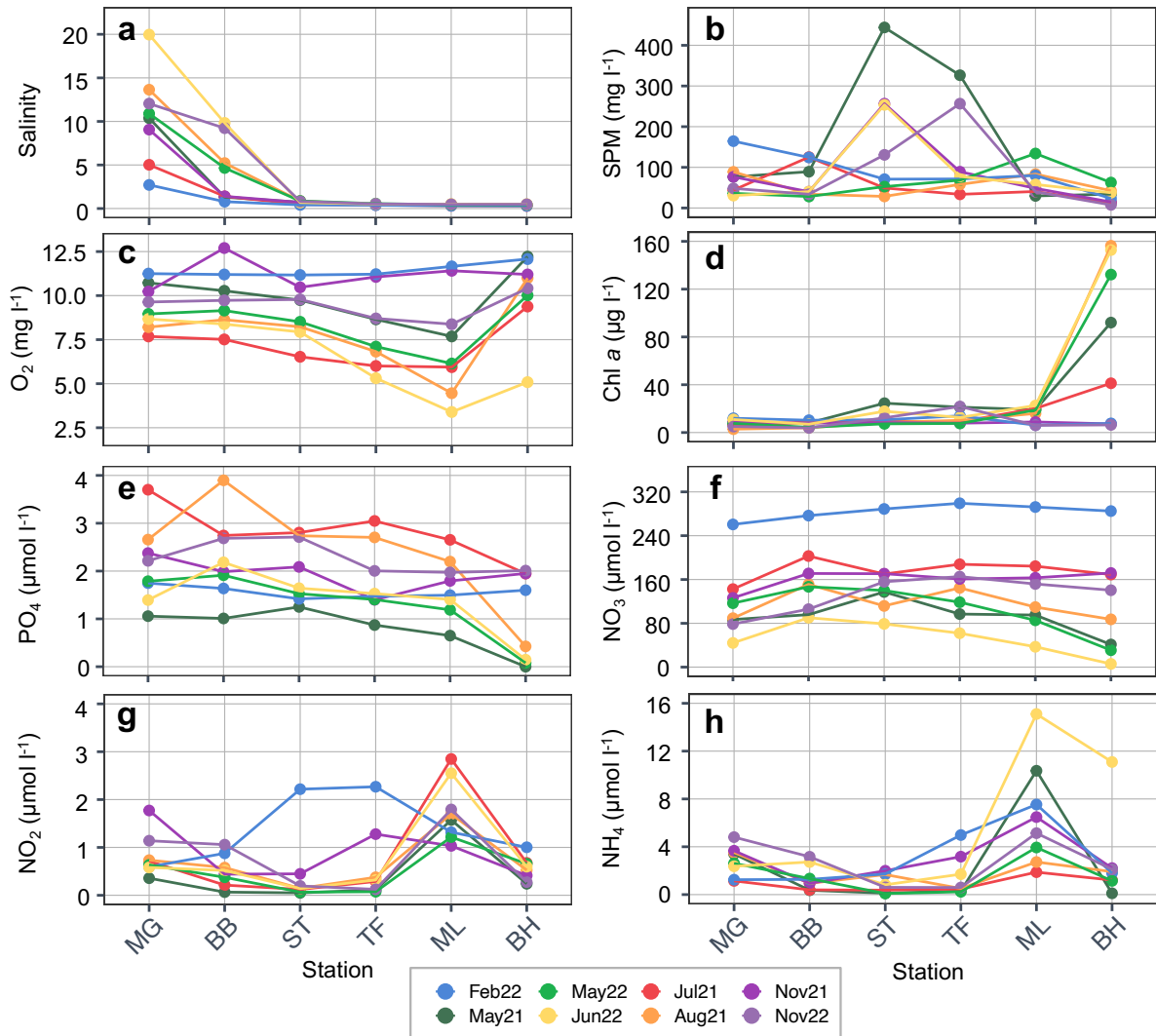


Fig. 2.2: Spatio-temporal variability in (a) salinity and concentrations of (b) suspended particulate matter (SPM) ( $\text{mg l}^{-1}$ ), (c) oxygen ( $\text{mg l}^{-1}$ ), (d) chlorophyll *a* (Chl *a*) ( $\mu\text{g l}^{-1}$ ), as well as dissolved (e) phosphate ( $\text{PO}_4$ ), (f) nitrate ( $\text{NO}_3$ ), (g) nitrite ( $\text{NO}_2$ ) and (h) ammonium ( $\text{NH}_4$ ) ( $\mu\text{mol l}^{-1}$ ) in the Elbe estuary in 2021 and 2022.

lowest rates ( $231 \text{ m}^3 \text{ s}^{-1}$  in June 2022) were recorded in summer. Salinity gradually increased downstream, with the strongest gradient observed in summer and the weakest in winter (Fig. 2.2). A freshwater zone (salinity  $<0.5$ ) extended upstream from station Twielenfleth (TF) throughout the year. A maximum SPM concentration of  $444 \text{ mg l}^{-1}$  was found at station Schwarztonnensand (ST), but peaks occurred also at the river mouth due to high discharge rates in February 2022. The lowest SPM levels were recorded at the uppermost station Bunthäuser Spitze (BH) throughout the year. Oxygen concentrations were negatively correlated with temperatures (Pearson,  $n = 48$ ,  $R = -0.78$ ,  $p < 0.001$ , see supplementary data, Table S 2.3) and decreased sharply towards the station in the port region, i.e. Mühlenberger Loch (ML), in spring and summer, with a minimum of  $3.4 \text{ mg l}^{-1}$  in

June 2022. High Chl *a* concentrations, reaching levels between 92 and 156  $\mu\text{g l}^{-1}$ , were observed exclusively at station BH in spring and summer, except for July 2021 with 41  $\mu\text{g l}^{-1}$ . Downstream of station ML, Chl *a* levels decreased sharply (below 23  $\mu\text{g l}^{-1}$ ). In autumn and winter, Chl *a* concentrations remained low at all stations. Nitrate ( $\text{NO}_3$ ) and phosphate ( $\text{PO}_4$ ) decreased with increasing Chl *a* concentrations (Pearson,  $n = 48$ ;  $\text{NO}_3$ :  $R = -0.42$ ,  $p = 0.003$ ;  $\text{PO}_4$ :  $R = -0.61$ ,  $p < 0.001$ ) towards station BH. Nitrite ( $\text{NO}_2$ ) and ammonium ( $\text{NH}_4$ ) concentrations were highest at station ML, especially during the summer.

Table 2.2: Results of the permutational multivariate analysis of variance (PERMANOVA) including values of significant multiple comparisons applied to the different zooplankton size fractions matrices. Hellinger distance was used to test for the effect of station, period and year on the zooplankton community composition.

| Size fraction    | Explanatory variable | df             | Pseudo-F | <i>p</i> -value     | Multiple comparison | <i>p</i> -value     |
|------------------|----------------------|----------------|----------|---------------------|---------------------|---------------------|
| Microzooplankton | Station              | 5              | 2.15     | <b>0.014*</b>       | BH-MG               | <b>0.012*</b>       |
|                  |                      |                |          |                     | BH-BB               | <b>&lt;0.001***</b> |
|                  |                      |                |          |                     | BH-ST               | <b>0.009**</b>      |
|                  |                      |                |          |                     | BH-TF               | <b>0.004**</b>      |
|                  |                      |                |          |                     | BH-MG               | <b>0.009**</b>      |
|                  | Period               | 6              | 2.44     | <b>0.002**</b>      | Jul21- Feb22        | <b>0.023*</b>       |
|                  |                      |                |          |                     | May22-Jul21         | <b>0.006**</b>      |
|                  |                      |                |          |                     | May22- Feb22        | <b>0.023*</b>       |
|                  |                      |                |          |                     | May22-Nov22         | <b>0.038*</b>       |
|                  | Year                 | 1              | 2.38     | 0.072               | 2021-2022           | n.s.                |
| Mesozooplankton  | Station              | 5              | 7.08     | <b>&lt;0.001***</b> | MG-BB               | <b>0.015*</b>       |
|                  |                      |                |          |                     | MG-ST               | <b>&lt;0.001***</b> |
|                  |                      |                |          |                     | MG-TF               | <b>&lt;0.001***</b> |
|                  |                      |                |          |                     | MG-ML               | <b>&lt;0.001***</b> |
|                  |                      |                |          |                     | BB-TL               | <b>0.048*</b>       |
|                  |                      |                |          |                     | BB-ML               | <b>0.043*</b>       |
|                  |                      |                |          |                     | BH-MG               | <b>&lt;0.001***</b> |
|                  |                      |                |          |                     | BH-BB               | <b>&lt;0.001***</b> |
|                  |                      |                |          |                     | BH-ST               | <b>&lt;0.001***</b> |
|                  |                      |                |          |                     | BH-TF               | <b>0.002**</b>      |
|                  | BH-ML                | <b>0.003**</b> |          |                     |                     |                     |
|                  | Period               | 7              | 1.02     | 0.434               |                     | n.s.                |
|                  | Year                 | 1              | 0.74     | 0.55                | 2021-2022           | n.s.                |
| Macrozooplankton | Station              | 4              | 6.31     | <b>&lt;0.001***</b> | MG-ST               | <b>0.003**</b>      |
|                  |                      |                |          |                     | MG-TF               | <b>&lt;0.001***</b> |
|                  |                      |                |          |                     | MG-ML               | <b>0.015*</b>       |
|                  |                      |                |          |                     | BB-ST               | <b>0.032*</b>       |
|                  |                      |                |          |                     | BB-TF               | <b>0.004**</b>      |
|                  |                      |                |          |                     | BB-ML               | <b>0.038*</b>       |
|                  | ML-TF                | <b>0.003**</b> |          |                     |                     |                     |
|                  | Period               | 5              | 0.89     | 0.54                |                     | n.s.                |
| Year             | 1                    | 0.84           | 0.40     | 2021-2022           | n.s.                |                     |

Abbreviations: df – degrees of freedom. Pseudo-f – Pseudo-F statistics. n.s. not significant.  
 Note: Significant differences are displayed in bold ( $p$ -value  $< 0.05$ : \*,  $< 0.01$ : \*\*,  $< 0.001$ : \*\*\*).

## Zooplankton community structure and abundance

A total of 25 major taxa were retained in the final dataset, consisting of seven microzooplankton, fourteen mesozooplankton and four macrozooplankton species (see

supplementary data, Fig. S 2.1). Overall, none of the three size classes exhibited interannual variability in their community structures (Table 2.2).

Microzooplankton biomass was higher in 2022 than in 2021, reaching high abundances in spring (May22) and summer (June), while species biomass remained low in autumn (November) and winter (February) (Fig. 2.3a). Microzooplankton abundance decreased sharply towards the river mouth. The microzooplankton species composition was dominated by the rotifers *Keratella* spp. and *Brachionus* spp., whose abundance gradually increased along the freshwater area upstream, peaking at station BH in May 2022 and June 2022, respectively. Both taxa comprised >80 % of the relative abundance in spring and summer, except for July 2021. Other rotifer species, such as *Notholca* spp. and *Synchaeta* spp., were found in higher relative proportions in autumn and winter and at stations in the

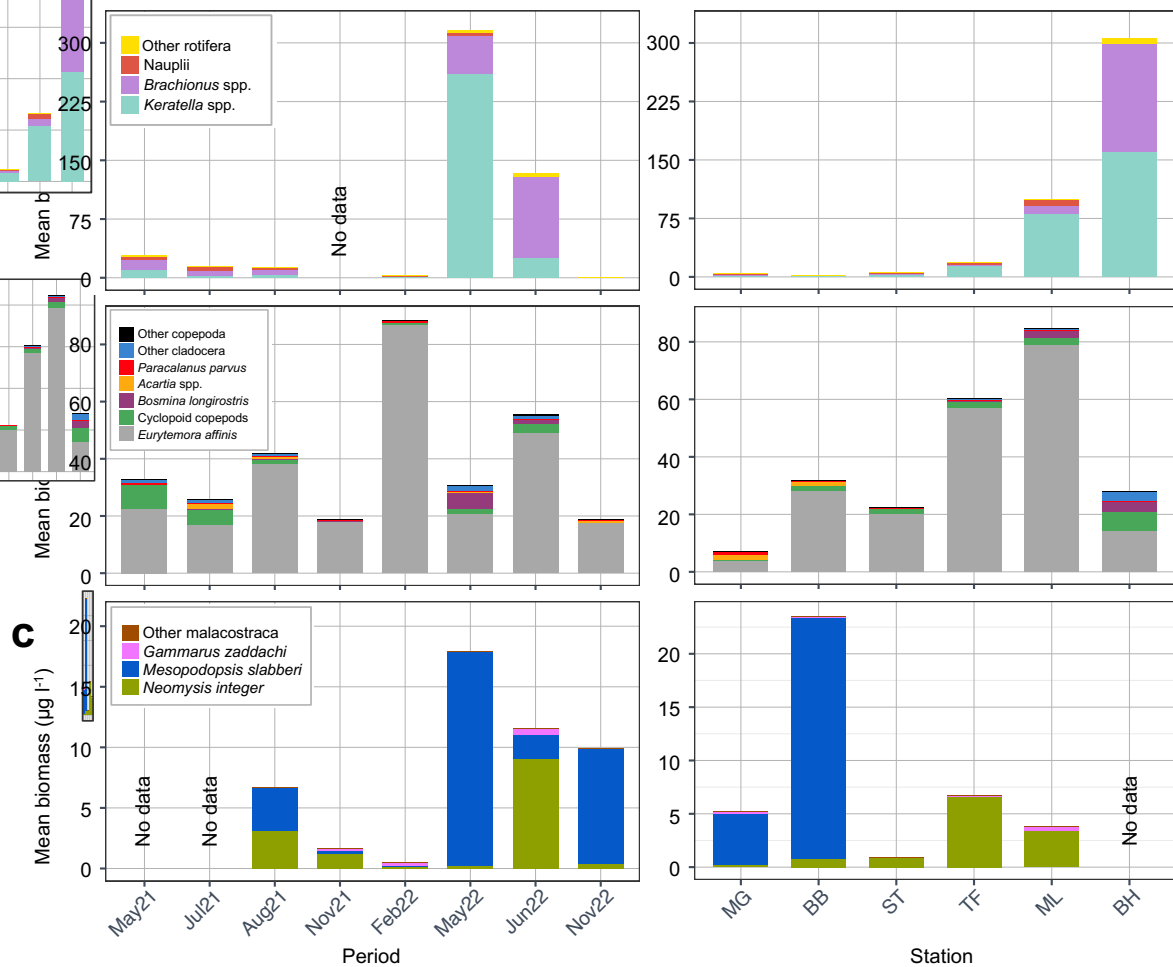


Fig. 2.3: Mean biomass data of dominant (a) micro-, (b) meso- and (c) macrozooplankton taxa from seasonal sampling along the entire salinity gradient (freshwater: BH, ML, ST; oligohaline: BB, mesohaline: MG) of the Elbe estuary in 2021 and 2022. Biomass data were meaned either over all stations per season (left plots) or over all periods per station (right plot).

brackish stretches, respectively (see supplementary data, Fig. S 2.1). Downstream of station BH, the community structure of the microzooplankton increasingly consisted of nauplii, which reached their highest abundance at station ML, especially in May and July 2021 (Fig. 2.3a).

Table 2.3: The results of selected RDA models for the three zooplankton size classes including the explained variance (adjusted  $R^2$  in %) by the explanatory variables. P-values and pseudo-F were obtained by Monte Carlo permutation tests (n=999 permutations).

| Ordination axis                                                                                                                                                                                                                                                                                                                                                  |                  |          |                 |                  |               |                 |                  |               |                 |
|------------------------------------------------------------------------------------------------------------------------------------------------------------------------------------------------------------------------------------------------------------------------------------------------------------------------------------------------------------------|------------------|----------|-----------------|------------------|---------------|-----------------|------------------|---------------|-----------------|
|                                                                                                                                                                                                                                                                                                                                                                  | Microzooplankton |          |                 | Mesozooplankton  |               |                 | Macrozooplankton |               |                 |
|                                                                                                                                                                                                                                                                                                                                                                  | $R^2_{adj.}$ (%) | Pseudo-F | $p$ -value      | $R^2_{adj.}$ (%) | Pseudo-F      | $p$ -value      | $R^2_{adj.}$ (%) | Pseudo-F      | $p$ -value      |
| Selected Model                                                                                                                                                                                                                                                                                                                                                   | 31.6             | 4.78     | <b>0.001***</b> | 34.9             | 5.20          | <b>0.001***</b> | 62.3             | 8.98          | <b>0.001***</b> |
| RDA Axis1                                                                                                                                                                                                                                                                                                                                                        | 14.6             | 11.02    | <b>0.003**</b>  | 22.4             | 20.02         | <b>0.001***</b> | 53.9             | 50.68         | <b>0.001***</b> |
| RDA Axis2                                                                                                                                                                                                                                                                                                                                                        | 11.2             | 8.48     | <b>0.003**</b>  | 8.9              | 7.92          | <b>0.006**</b>  | 5.4              | 5.08          | 0.176n.s.       |
| Explanatory variables                                                                                                                                                                                                                                                                                                                                            |                  |          |                 |                  |               |                 |                  |               |                 |
|                                                                                                                                                                                                                                                                                                                                                                  | Microzooplankton |          |                 | Mesozooplankton  |               |                 | Macrozooplankton |               |                 |
|                                                                                                                                                                                                                                                                                                                                                                  | Parameter        | Pseudo-F | $p$ -value      | Parameter        | Pseudo-F      | $p$ -value      | Parameter        | Pseudo-F      | $p$ -value      |
| Variables retained in the model                                                                                                                                                                                                                                                                                                                                  | Chl <i>a</i>     | 7.96     | <b>0.001***</b> | Sal              | 17.58         | <b>0.001***</b> | Sal              | 30.09         | <b>0.001***</b> |
|                                                                                                                                                                                                                                                                                                                                                                  | PO <sub>4</sub>  | 5.28     | <b>0.002**</b>  | NO <sub>2</sub>  | 1.49          | 0.206n.s.       | Chl <i>a</i>     | 7.80          | <b>0.001***</b> |
|                                                                                                                                                                                                                                                                                                                                                                  | Sal              | 3.58     | <b>0.011*</b>   | PO <sub>4</sub>  | 3.77          | <b>0.017*</b>   | NO <sub>2</sub>  | 2.54          | 0.077n.s.       |
|                                                                                                                                                                                                                                                                                                                                                                  | NO <sub>3</sub>  | 4.07     | <b>0.014*</b>   | Chl <i>a</i>     | 3.46          | <b>0.021*</b>   | Temp             | 5.97          | <b>0.008**</b>  |
|                                                                                                                                                                                                                                                                                                                                                                  | Temp             | 3.02     | <b>0.028*</b>   | SPM              | 2.54          | <b>0.047*</b>   | NO <sub>3</sub>  | 3.09          | <b>0.044*</b>   |
|                                                                                                                                                                                                                                                                                                                                                                  |                  |          | Q               | 2.33             | <b>0.049*</b> | Q               | 4.37             | <b>0.015*</b> |                 |
| Abbreviations: Chl <i>a</i> , chlorophyll <i>a</i> ; Temp, temperature; Sal, salinity; Q, river discharge; SPM, suspended particulate matter; NO <sub>3</sub> , nitrate; NO <sub>2</sub> , nitrite; PO <sub>4</sub> , phosphate; n.s. – not significant.<br>Note: Significant differences are displayed in bold ( $p$ -value < 0.05: *, <0.01: **, <0.001: ***). |                  |          |                 |                  |               |                 |                  |               |                 |

The highest mesozooplankton abundance was observed at station ML, followed by station TF in February, which resulted from high abundances of *Eurytemora affinis*. This taxon was the most dominant mesozooplankton species at all stations throughout the year, accounting for up to 98% of the total biomass (see supplementary data, Fig. S 2.1), with peaks mainly at station ML in February 2022 and during summer (i.e. August 2021 and June 2022) (Fig. 2.3b). Overall, the mesozooplankton biomass was lowest in November for both years and exhibited a decreasing trend towards the river mouth, with the lowest abundances found at station Medemgrund (MG). At the freshwater station BH, the mesozooplankton community consisted of cyclopoid copepods and cladocerans, such as *Bosmina longirostris*, with abundances peaking in spring and summer and gradually declining downstream (Fig. 2.3b). At station Brunsbüttel (BB) and MG, the mesozooplankton assemblage was dominated by *Acartia* spp. and *Paracalanus parvus*, and *E. affinis*, although the latter appeared in lower

densities compared to the freshwater stations (Fig. 2.3b). The highest abundances of *Acartia* spp. and *P. parvus* were recorded in July 2021 and February 2022, respectively.

The most abundant macrozooplankton taxa were *Mesopodopsis slabberi* and *Neomysis integer*, with peak abundances observed in May 2022 and June 2022, respectively (Fig. 2.3c). Both species exhibited spatially distinct assemblages (Table 2.2), with *M. slabberi* dominating at station BB and MG, while *N. integer* was mainly found upstream of station ST. In winter and at station ST, the macrozooplankton biomass was lowest, with *M. slabberi* being completely absent. *Gammarus zaddachi* was found along the entire salinity gradient, contributing up to approximately 10% of the relative biomass in the macrozooplankton assemblage (see supplementary data, Fig. S 2.1), with the highest abundances recorded in summer.

### Impact of environmental factors on the spatio-temporal zooplankton dynamics

The RDA model for microzooplankton retained the environmental parameters Chl *a*, PO<sub>4</sub>, salinity, NO<sub>3</sub> and temperature, listed in descending order of significance, explaining 31.6% of the total variation in species biomass (Table 2.3). The first axis (RDA 1) accounted for 14.6% of the total variability and described the seasonal variation in species abundance due to its strong correlation with temperature and Chl *a* (Fig. 2.4). The vectors of both environmental parameters pointed towards the freshwater station BH in spring and summer, where *Brachionus* spp. (Bra) clustered strongly. In contrast, nauplii (NAU) clustered in the opposite direction of axis 1 towards the stations ML, TF and ST. The second RDA axis, which explained 11.2% of the total variability in the microzooplankton abundance, was strongly associated with salinity, PO<sub>4</sub> and NO<sub>3</sub>. *Keratella* spp. (Ker) grouped in the contrary

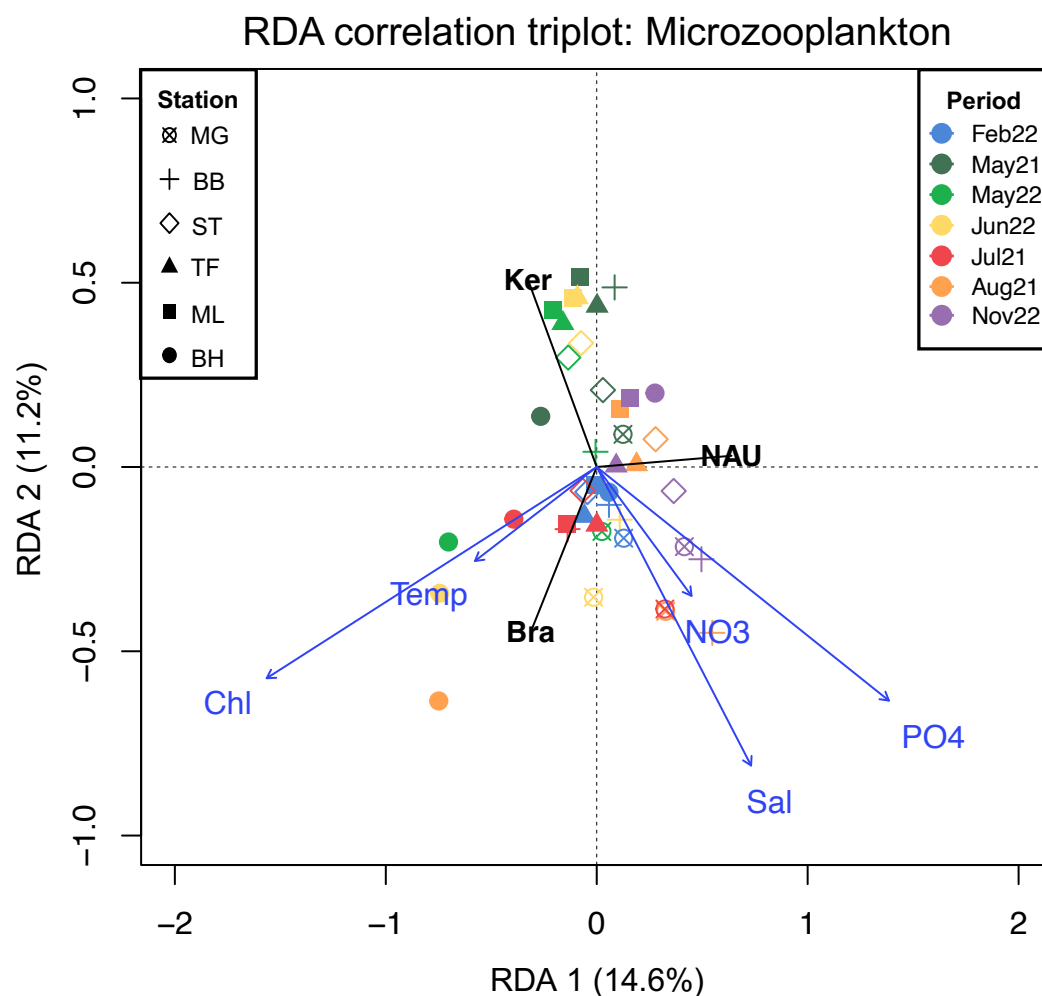


Fig. 2.4: Correlation triplot of RDA axis 1 and 2 explaining the total variability (in %) in the distribution pattern of microzooplankton species (black abbreviations) along environmental factors (blue abbreviations) per sampling period (colours) and station (symbols). Only taxa with species scores > 0.2 are shown. Abbreviations of the environmental parameters are explained in Table 2.3. Code of the species: Ker, *Keratella* spp.; Bra, *Brachionus* spp.; NAU, Nauplii.

direction of axis 2, which correlated with low salinity and nutrient concentrations at freshwater stations in spring (i.e. May 2021 and May 2022) and summer (i.e. June 2022).

Salinity,  $\text{NO}_2$ ,  $\text{PO}_4$ , Chl *a*, SPM and river discharge (Q) were included in the final RDA model of the mesozooplankton biomass, accounting for 34.9% of the total variation in the community structure (Table 2.3), with salinity explaining most of the ordination. RDA axis 1 explained 22.4% of the total variability in mesozooplankton biomass and exhibited a negative correlation with salinity and a positive correlation with river discharge (Fig. 2.5). *Acartia* spp. (Aca) and *Paracalanus parvus* (Par) clustered along axis 1 towards the stations MG and BB, where high salinity was prevalent, especially in summer. In contrast, *Eurytemora affinis* (Eur) aligned in the opposite direction between axis 1 and 2, correlating with high SPM and  $\text{NO}_2$  concentrations. These parameters were associated with the

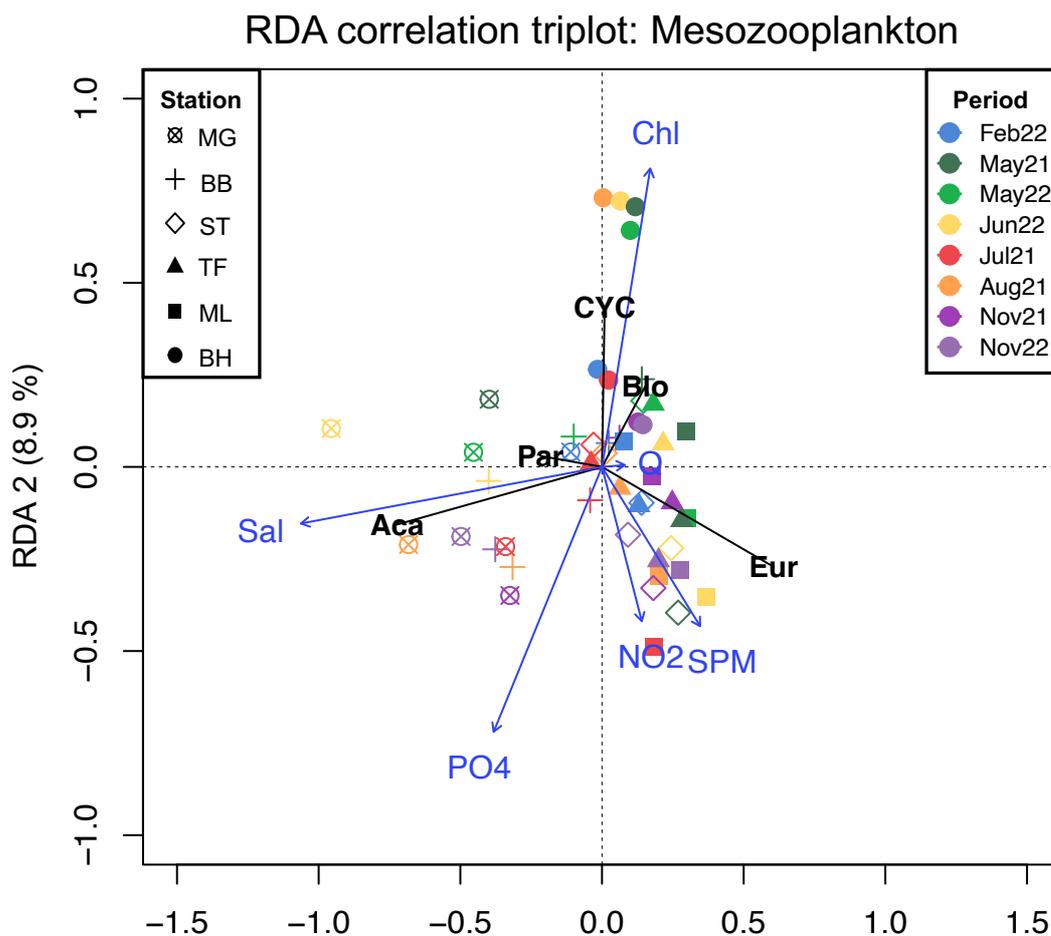


Fig. 2.5: Correlation triplot of RDA axis 1 and 2 showing the total variability (in %) in mesozooplankton community structure (black abbreviations) along spatial (stations as symbols) and temporal (colours) gradients of environmental factors (blue abbreviations). Only species with species scores > 0.2 are shown. Abbreviations of environmental parameters are explained in Table 2.3. Code of taxa: Aca, *Acartia* spp.; Par, *Paracalanus parvus*; CYC, cyclopoid copepods; Bio, *Bosmina longirostris*; Eur, *Eurytemora affinis*.

freshwater stations ST, TF and ML at the negative end of RDA axis 2, explaining 8.9% of the total variation. At the positive end of axis 2, cyclopoid copepods (CYC) and *Bosmina longirostris* (Blo) clustered towards station BH, which was characterised by low SPM, PO<sub>4</sub>, NO<sub>2</sub> concentrations and high Chl *a* levels, particularly in spring and summer.

The environmental parameters salinity, Chl *a*, NO<sub>2</sub>, temperature, NO<sub>3</sub> and river discharge explained 62.3% of the variation in the macrozooplankton community structure (Table 2.3). Only RDA axis 1 was significant, explaining the spatial variability of macrozooplankton biomass by salinity and Chl *a*, which grouped at the negative and positive ends of the axis, respectively (Fig. 2.6). *Mesopodopsis slabberi* (Mes) clustered at the negative end of axis 1 with high salinities at the stations MG and BB, while *Neomysis integer* (Neo) was strongly associated with high Chl *a* levels, corresponding to freshwater conditions upstream of the

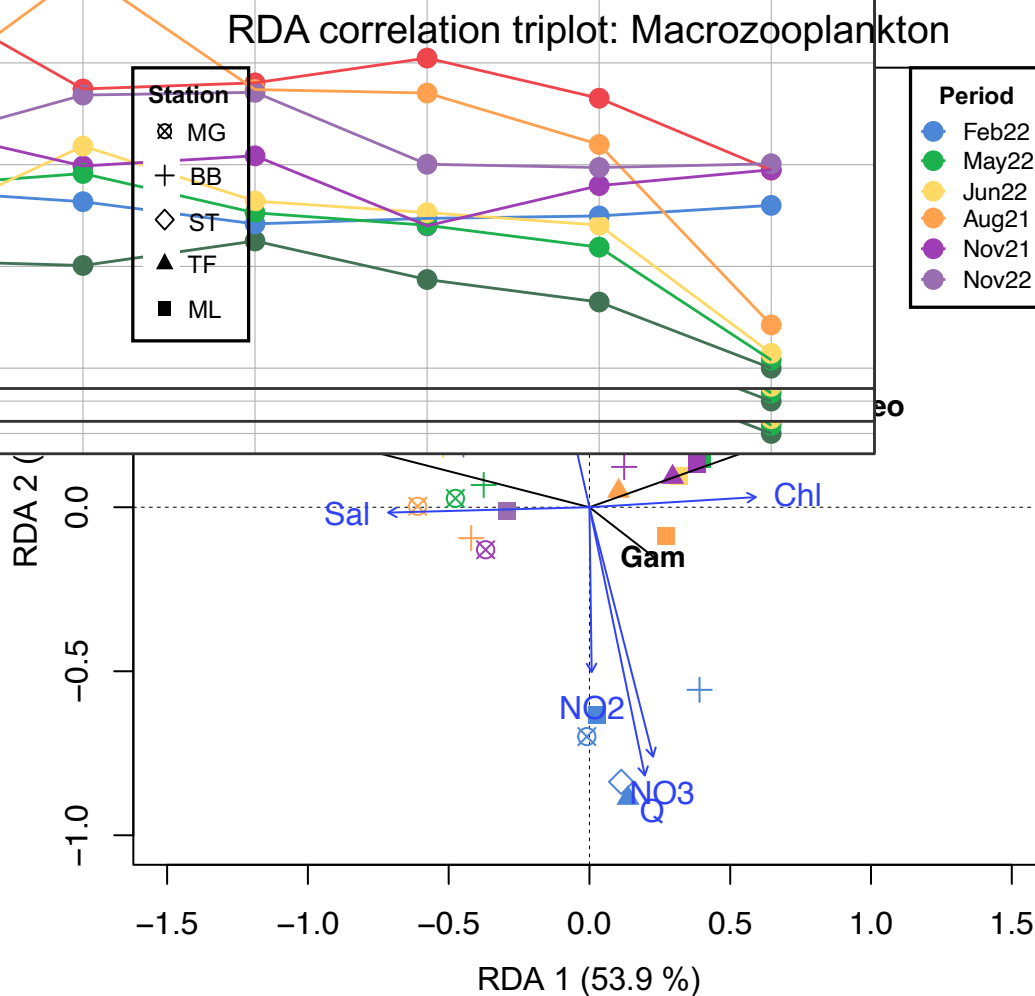


Fig. 2.6: RDA correlation triplot displaying total spatial (stations as symbols) and temporal (colours) variability (in %) in the macrozooplankton community structure of major taxa (black abbreviations) along environmental parameters (blue abbreviations). Only taxa with species scores > 0.2 are shown. Abbreviations of environmental parameters are explained in Table 2.3. Code of the species: Mes, *Mesopodopsis slabberi*; Gam, *Gammarus zaddachi*; Neo, *Neomysis integer*.

estuary. *Gammarus zaddachi* (Gam) clustered near the centre and showed only a weak affinity for high Chl *a* concentrations.

## Discussion

Research on zooplankton community dynamics in the Elbe estuary is limited and outdated due to the lack of permanent monitoring programs. Recurrent dredging and diking activities have resulted in hydrological changes in recent decades, including increased sediment accumulation and a rising risk of hypoxia (Kerner, 2007). These changes emphasise the need to examine the impact of the environmental conditions on the zooplankton assemblages in the Elbe estuary to improve our understanding of the ecosystem functioning. This study compares previous research on zooplankton population dynamics with our recent findings from 2021 and 2022, providing a new dataset on the spatio-temporal dynamics of micro-, meso- and macrozooplankton in the Elbe estuary.

## Zooplankton taxonomic composition

Species richness in the Elbe estuary was generally lower than in adjacent ecosystems, e.g. riverine sections of the Elbe (see Hromova *et al.*, 2024). This is common in estuarine systems as strong spatio-temporal variability in the environmental parameters, together with human stressors, limit the number of species that can tolerate such conditions (Day *et al.*, 2013). The number of dominant species in this study corresponds to those reported in other temperate estuaries in northern Europe (e.g. Azémar *et al.*, 2010; Modéran *et al.*, 2010). We found a high dominance of the rotifer species *Keratella* spp. and *Brachionus* spp. in the microzooplankton, which was also reported by Tackx *et al.* (2004) and Azémar *et al.* (2010) in the freshwater zone of the Scheldt estuary. It should be noted that large protozoans, particularly ciliates, belong to the microzooplankton size fraction (20 – 200 µm). In this study, however, the sampling design targeted organisms larger than 55 µm, which meant that protozoa were not consistently sampled, and are therefore not addressed further in this study. In addition, the microzooplankton taxa were only determined to the genus level, which is already sufficient to explain major ecological associations (see Azémar *et al.*, 2010 for further explanations), as species level identification is often difficult due to formaldehyde

fixation. *Eurytemora affinis* and *Acartia* spp. were the most dominant mesozooplankton taxa in our study, which is similar to the observations that have been reported in estuaries of the northern hemisphere, such as the Scheldt (Tackx *et al.*, 2004; Mialet *et al.*, 2011), the Gironde (David *et al.*, 2005), the Charente (Modéran *et al.*, 2010), the Seine (Mouny and Dauvin, 2002), the Chesapeake Bay (Kimmel and Roman, 2004; Hoffman *et al.*, 2008) and the St. Lawrence estuary (Winkler *et al.*, 2003). Mysid shrimps (mainly *Neomysis integer* and *Mesopodopsis slabberi*) and the amphipod *Gammarus zaddachi*, which are considered as typical suprabenthic estuarine species (Mees *et al.*, 1993), were also important pelagic constituents in the Elbe and other estuaries (e.g. Mouny *et al.*, 1998; Winkler *et al.*, 2003; Selleslagh *et al.*, 2012).

## **Spatial and temporal patterns of the zooplankton community and their relationship with the environmental parameters**

### **Microzooplankton**

In general, differences in the microzooplankton community structure were most strongly related to Chl *a* concentration, followed by NO<sub>3</sub>, PO<sub>4</sub>, temperature and salinity, indicating that changes in species composition were driven by both seasonal and spatial factors. The RDA analysis explained 31.6% of the total variation in the microzooplankton dynamics, suggesting that there might be additional parameters influencing species dynamics, which were not included in this study. For instance, biotic variables such as life history traits or predation were not further considered here. This was also true for the RDA results of the other zooplankton size fractions.

In the Elbe estuary, Chl *a* is not only a seasonal factor, but also has a spatial dimension, as high concentrations were restricted to the shallow upstream zone at station BH, which is consistent with the findings of Wolfstein and Kies (1995), Schöl *et al.* (2014), Geerts *et al.* (2017) and Kamjunke *et al.* (2023). The microzooplankton succession mirrored the spatio-temporal pattern of the Chl *a* concentrations, with the highest abundances at station BH in spring and summer, sharply declining towards the river mouth. At station BH, we identified a distinct species assemblage dominated by *Keratella* spp. and *Brachionus* spp., which were positively associated with high Chl *a* concentrations and temperature. Azémar *et al.* (2010)

also reported a positive correlation of the rotifer species *Brachionus quadridentatus* and *K. cochlearis* with Chl *a* concentration and high densities in the freshwater area of the Scheldt estuary. Species of the genera *Keratella* and *Brachionus* are known to prefer an algal diet, but also feed on fine detritus and protozoans as alternative food sources when food availability is limited (Hlawa and Heerkloss, 1994; Gilbert, 2022). Hence, they likely benefited from increased phytoplankton biomass during spring and summer, leading to their high densities at the uppermost station. Furthermore, our RDA results revealed a strong negative correlation between salinity and the two species, *Brachionus* spp. and *Keratella* spp. Both taxa typically dominate the freshwater sections of estuaries, as they can tolerate only a limited range of salinity (e.g. Park and Marshall, 2000; Azémar *et al.*, 2010; Hitchcock *et al.*, 2016).

In the deep-water zone (from station ML to MG), we identified a second microzooplankton assemblage characterised by increasing abundances of copepod nauplii and, occasionally, other rotifer species, such as *Synchaeta* spp. This rotifer is typically halophilic, occurring in brackish sections of estuaries (e.g. Park and Marshall, 2000; Azémar *et al.*, 2010), and was found in high densities at the river mouth in our study. Consequently, the rotifer abundance declined downstream from the port area, likely due to changes in salinity, as well as food availability and quality, as the system transitions to a turbid and more heterotrophic dominated state (Kamjunke *et al.*, 2023).

Since rotifers can be an important dietary component for cyclopoid and calanoid copepods in freshwater zones (Brandl, 2005), the decline in rotifer abundance from the port area downstream may also be related to increased feeding pressure from high abundances of crustaceans, such as *E. affinis*. Notably, the spatio-temporal distribution pattern of *E. affinis* alternated with peaks in rotifer abundance, which may indicate a potential predation relationship. Mialet *et al.* (2011) suggested a similar predation pattern of alternating population peaks between rotifers and *E. affinis* in the Scheldt estuary. However, predation relationships are not investigated further here, as this would require biochemical approaches, such as stable isotope and fatty acid biomarkers (Dalsgaard *et al.*, 2003; Layman *et al.*, 2012), which are beyond the scope of this study.

### Mesozooplankton

Salinity, followed by PO<sub>4</sub>, Chl *a*, SPM load and river discharge were the most important environmental parameters affecting the mesozooplankton distribution and succession. Unlike the pronounced temporal effects reported by e.g. Tackx *et al.* (2004), Selleslagh *et al.* (2012) or David *et al.* (2005), the PERMANOVA results indicated that changes in the mesozooplankton community structure were largely driven by spatial factors, as shown by the exclusion of temperature as an explanatory parameter in the RDA model. The lack of significant seasonal variability in the community structure may be due to the low temporal resolution of about 1.5 years. A longer sampling period may be required to capture notable temporal dynamics in the species structure.

We identified three distinct species assemblages in the Elbe estuary, with salinity being the most influential factor influencing their distribution. The mesozooplankton can therefore be classified into typical freshwater, freshwater-oligohaline and oligohaline-mesohaline assemblages (e.g. Mouny and Dauvin, 2002; Modéran *et al.*, 2010).

The freshwater assemblage was situated in the autotrophic zone at station BH and was characterised by cladocerans (e.g. *Bosmina longirostris*, *Daphnia longispina*, *Alona* spp.) and cyclopoid copepods, which are sensitive to high salinity and typically found in upper estuarine freshwater reaches (e.g. Soetaert and Van Rijswijk, 1993; Mouny and Dauvin, 2002; Mialet *et al.*, 2011). Cladocerans and cyclopoid copepods showed a positive correlation with rising Chl *a* concentrations in spring and summer, but a negative correlation with increasing PO<sub>4</sub>, NO<sub>2</sub> and SPM levels in the dredged zone. Freshwater cladocerans such as *B. longirostris* and *D. longispina* are filter feeders with a preference for a herbivorous diet (Bogdan and Gilbert, 1982). High concentrations of SPM, particularly inorganic particles, can disrupt food collection (Kirk, 1992) and hamper development of cladocerans (Kirk and Gilbert, 1990). Cyclopoid copepods rely on algal sources and rotifers in their diet (Brandl, 2005), so that the downstream decline in their abundance may also be linked to the decrease in rotifer biomass. In addition, cyclopoid copepods are less efficient at selective feeding compared to the dominant calanoid copepod *Eurytemora affinis* (Mialet *et al.*, 2011), which may contribute to their lower abundance in the deep-water section, where primary

production and rotifer densities were limited, probably due to increased SPM levels and salinity (Muylaert and Sabbe, 1999; Mouny and Dauvin 2002).

A freshwater-oligohaline species assemblage was found in the second zone from station ML to ST, dominated almost exclusively by *E. affinis*. High abundances of *E. affinis* at station ML coincided with peaks in nauplii abundance, which has been also reported by Köpcke (2002) in similar areas of the Elbe estuary. Their spatial distribution was attributed to the area's proximity to a freshwater tidal flat, which is an important retention and reproduction area for planktonic organisms and fish (Thiel *et al.*, 1995; Köpcke, 2002). *E. affinis* is a typical brackish species with a broad salinity tolerance (Devreker *et al.*, 2009), that can selectively feed on algal biomass, despite low primary production in turbid waters (Tackx *et al.*, 2003). While it predominantly consumes phytoplankton, *E. affinis* can also switch to a carnivorous diet by exploiting alternative food sources, such as protozoa or detritus, when primary production is limited (Modéran *et al.*, 2012; Biederbick *et al.*, 2024). This adaptive feeding strategy allows *E. affinis* to thrive in high SPM environments, thereby avoiding food limitation and competition. In fact, according to the RDA results, *E. affinis* correlated strongly with high SPM loads, likely due to its adaptation to turbid environments.

Other euryhaline calanoid copepods, such as species of the genus *Acartia*, rely heavily on a herbivorous diet and are unable to shift their food source (Gasparini and Castelt, 1997), allowing them to colonise only areas downstream of the MTZ, where food is more available (Modéran *et al.*, 2012). This could explain why *Acartia* spp. was found exclusively at the stations MG and BB, where turbidity was lower. The majority of taxa observed in the oligo-mesohaline section were typical coastal zooplankton of the North Sea (Fransz *et al.*, 1991), dominated by the euryhaline species *Acartia* spp. and *Paracalanus parvus*. *E. affinis* was also present, but at lower densities, probably being outcompeted by *Acartia* spp. and *P. parvus* due to rising salinity in the downstream section of the MTZ, which has been often observed in other estuaries (e.g. Soetaert and Van Rijswijk, 1993; David *et al.*, 2005; Modéran *et al.*, 2010).

### Macrozooplankton

Macrozooplankton assemblages were primarily driven by spatial gradients rather than temporal variations, with salinity and Chl *a* identified as the most important factors. The parameters NO<sub>2</sub>, NO<sub>3</sub>, temperature and river discharge were retained in the final RDA model (Fig. 2.6), however, the axis to which these parameters clustered was not significant in the explaining the species dynamics. The observed lack of significance might be attributed to limited sampling periods or stations (i.e. BH), which could not be sampled for technical reasons.

*N. integer* and *Gammarus zaddachi* were positively correlated with Chl *a* concentrations and negatively correlated with salinity, which may be related to their preference for oligohaline to freshwater conditions in estuarine environments (Mees *et al.*, 1993; David *et al.*, 2005; Selleslagh *et al.*, 2012). Both taxa are omnivores which can selectively feed on algal and detrital sources, while preferentially feeding on copepods to fulfil their nutritional requirements (David *et al.*, 2006; Modéran *et al.*, 2012). David *et al.* (2006) linked the distribution pattern of *N. integer* to its predatory behaviour towards *E. affinis*, which may explain its dominance in the upstream regions in our study. In contrast, *M. slabberi* was strongly correlated with high salinity, likely due to its marine origin (Mees *et al.*, 1993). This species enters the lower estuary mainly for reproduction (Mees *et al.*, 1993). In winter, when river discharge increased and salinity remained low throughout the estuary, *M. slabberi* was absent. Previous studies have shown that seasonal fluctuations in discharge can lead to significant changes in zooplankton assemblages, likely due to their response to changing hydrological conditions, including the position of the MTZ and the intensity of the salinity gradient (e.g. Holst *et al.*, 1998; Peitsch *et al.*, 2000). As a result, marine species, like *M. slabberi*, were absent from the lower reaches of the estuary when river discharge was high in winter, and were replaced by brackish species (e.g. *N. integer*) from the upper reaches.

### Changes in the species community and abundance of Elbe zooplankton

Zooplankton succession in the Elbe estuary was last extensively studied in the 1980s and 1990s (e.g. Fiedler, 1991; Peitsch, 1992; Bernát *et al.*, 1994; Holst, 1996; Holst *et al.*, 1998; Zimmermann-Timm *et al.*, 1998; Köpcke, 2002). Comparisons with previous studies are

often challenging due to methodological differences and variations in spatial and temporal resolution, which limit the ecological conclusions that can be drawn. Therefore, our results on spatio-temporal species succession are only comparable to similarly designed studies that focus on the most abundant taxa (see Fig. 2.7). In contrast to earlier studies, we applied a redundancy analysis for a more holistic examination of the relationships among zooplankton communities across multiple environmental variables. Our study also offers a higher spatial resolution by capturing zooplankton dynamics in the freshwater area upstream of the Hamburg Harbour, which has often been overlooked. Our findings indicate that this region is vital for freshwater taxa, especially rotifers, cladocerans and cyclopoids. Consequently, it is crucial to include this area in future research for a comprehensive understanding of zooplankton dynamics in the Elbe estuary.

The most dominant and abundant taxa in the zooplankton communities of the Elbe estuary have remained consistent, showing a distribution pattern largely comparable to previous studies (Fiedler, 1991; Peitsch, 1992; Holst, 1996; Köpcke, 2002). Holst *et al.* (1998) carried out the most recent investigations on estuarine rotifers and found a predominance of taxa of the genus *Keratella* (i.e. *K. cochlearis*, *K. quadrata*) and *Brachionus* (i.e. *B. calyciflorus*) in the freshwater section of the Elbe estuary, which they attributed to high food availability. Additionally, they noted a seaward decline in rotifer abundance associated with increasing turbidity and salinity stress, a trend that was also evident in our results (Fig. 2.7a). In addition, Fiedler (1991) and Köpcke (2002) found that *E. affinis* (Fig. 2.7b), together with *N. integer* (Fig. 2.7c), dominated the freshwater to oligo-mesohaline sections of the Elbe estuary, with high abundances in the port area (approx. at Elbe-km 630 to 640) and in front of the port region (ca. Elbe-km 650) in early spring and in summer, respectively, which is consistent with our findings. Both authors identified food limitation, high salinities and SPM

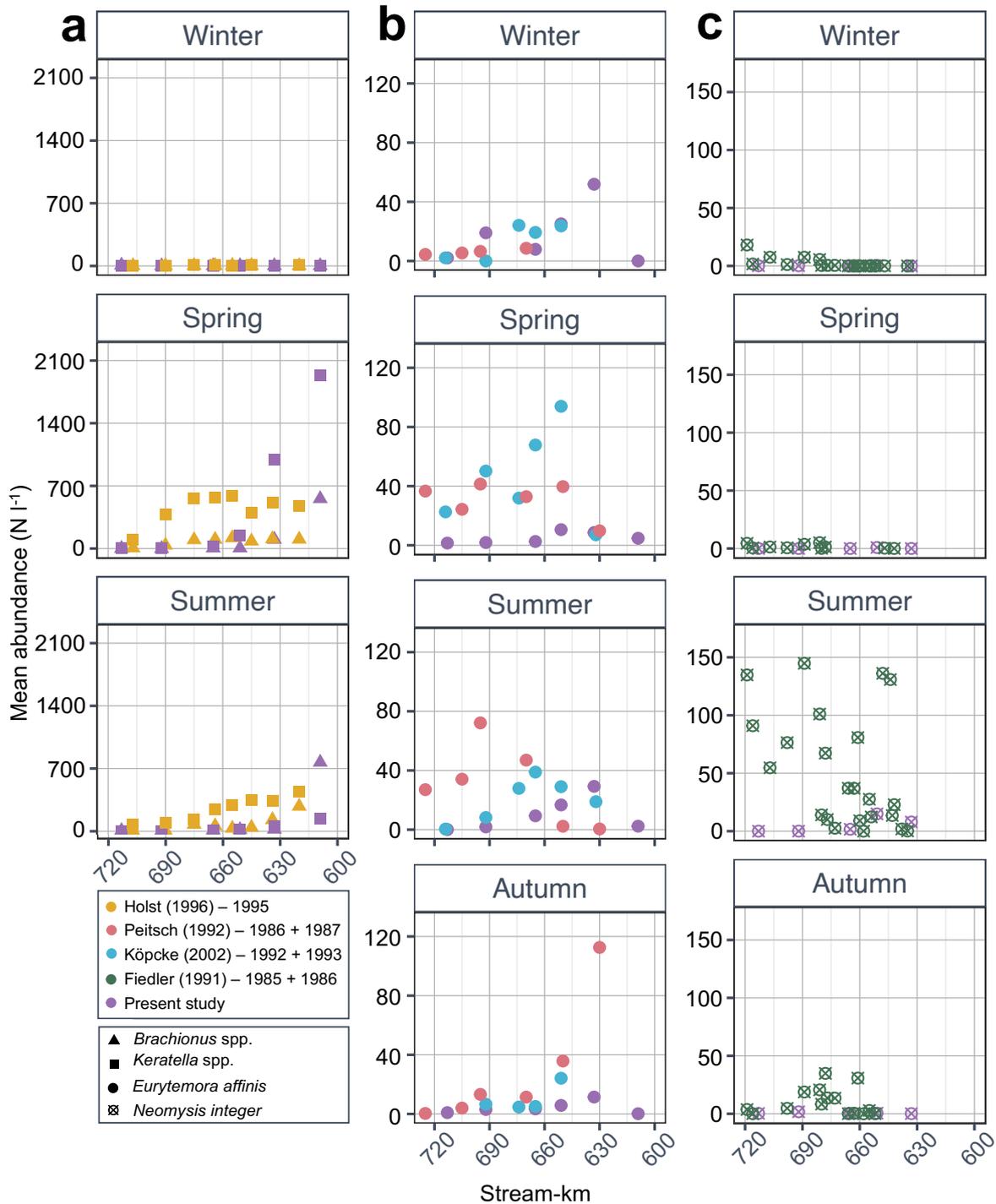


Fig. 2.7: Mean abundances of dominant taxa compared across studies in relation to our results: (a) *Keratella* spp. and *Brachionus* spp. from Holst (1996), (b) *Eurytemora affinis* from Peitsch (1992) and Köpcke (2002), and (c) *Neomysis integer* from Fiedler (1991).

concentrations, as well as hypoxia as key environmental factors affecting the population maintenance of *E. affinis* and *N. integer*.

While the overall zooplankton distribution patterns in our study closely resembled those found by Fiedler (1991), Peitsch (1992), Holst (1996) and Köpcke (2002), we noted a clear

decrease in the abundance of the dominant species (see Fig. 2.7). Over the past decades, the Elbe estuary has undergone strong changes in its hydrological regime due to multiple dredging campaigns (Kerner, 2007; HPA, 2022) and the implementation of enhanced waste water treatment (Adams *et al.*, 1996). Previous studies have shown that these changes can affect the development of zooplankton populations (e.g. Marques *et al.*, 2007; Mialet *et al.*, 2011). In the 1980s, the water quality in the Elbe estuary was poor due to intensive application of fertilisers in agriculture (Radach and Pätsch, 2007), resulting in recurring oxygen minimum zones with values below  $3.7 \text{ mg l}^{-1}$  (Amann *et al.*, 2012). Despite progress in pollution management, oxygen concentrations in the Elbe estuary have improved only slightly (Geerts *et al.*, 2017). Amann *et al.* (2012) argued that improved water quality may have promoted algal growth upstream, leading to increased oxygen consumption in the port area through enhanced remineralisation processes. In addition, recent deepening activities of the main channel have exacerbated the oxygen depletion by reducing flow velocities and thus the capacity for re-aeration in the Elbe estuary (Geerts *et al.*, 2017). In spring and summer, we observed a sharp decline in phytoplankton biomass and an increase in nutrients, particularly dissolved  $\text{NH}_4$  and  $\text{NO}_2$ , in the port region. Oxygen concentrations in this area also dropped below  $4 \text{ mg l}^{-1}$ , especially in summer, indicating potential degradation of phytoplankton and the release of dissolved  $\text{NH}_4$  and  $\text{NO}_2$  under oxygen consumption. Mialet *et al.* (2010) noted that mean oxygen levels below  $4 \text{ mg l}^{-1}$  may already be insufficient for *E. affinis* in the freshwater section of the Scheldt estuary.

Furthermore, dredging has led to a greater accumulation of SPM, particularly in the freshwater zone of the Elbe estuary (Kerner, 2007), which can negatively impact primary production (Wolfstein and Kies, 1995; Steidle and Vennell, 2024), thereby affecting the availability and quality of food for zooplankton (Biederbick *et al.*, 2024) and higher trophic levels, such as fish (Bernát *et al.*, 1994; Illing *et al.*, 2024). Similar effects were observed in smelt larvae (*Osmerus eperlanus*), the most abundant fish species in the Elbe estuary (Thiel *et al.*, 1995), for which high turbidity reduced prey consumption rates and survival (Illing *et al.*, 2024). High turbidity may be particularly harmful to organisms with limited ability to change their diet flexibly or feed selectively, such as cyclopoid copepods and filter feeders such as cladocerans, which showed a strong negative correlation with high SPM levels in

our study. Gasparini *et al.* (1999) showed that even for selective feeders like *E. affinis*, very high SPM levels can disrupt feeding and significantly reduce egg production rates. Additionally, elevated sediment input has amplified siltation in the shallow waters of the Elbe estuary (Li *et al.*, 2014). Consequently, the decline in zooplankton abundance may be linked to a loss of retention and reproduction areas, as suggested by Köpcke (2002). It is possible that hydrological and morphological changes in the Elbe estuary may have contributed to the observed decline in zooplankton abundance compared to data from the 1980s and 1990s.

## Conclusion

Our results indicate that variations in the zooplankton community structure were more strongly correlated with spatial factors than with seasonal ones, with Chl *a* and salinity being the most influential factors across all size classes. Blooming conditions were determined by low SPM concentration and high nutrient availability, which was restricted to freshwater stretches upstream the port area, where conditions were more favourable. In this autotrophic zone, we observed a predominance of freshwater taxa, including calanoid and cyclopoid copepods, cladocerans and rotifers, all positively correlated with high Chl *a* concentrations. *Eurytemora affinis* was the most abundant mesozooplankton species throughout the Elbe estuary and showed a broad tolerance to rising SPM concentrations, allowing it to thrive even in turbid regions. Coastal, euryhaline species like *Acartia* spp. and *Paracalanus parvus* became more abundant near the river mouth due to increased salinity. River discharge influenced the hydrological conditions in the Elbe estuary (e.g. MTZ position, salinity gradient), thereby affecting the colonisation of particularly euryhaline species in the lower reaches of the estuary. A decline in zooplankton abundance compared to earlier studies may be linked to strong morphological and hydrological changes in the Elbe estuary over the past decades. Further research is needed to evaluate the tolerance range of zooplankton species to these changes to predict long-term trends and develop effective water management strategies, requiring long-term data and mesocosm experiments. Furthermore, climate change is likely to alter the biochemical processes in estuaries faced by planktonic organisms (Robins *et al.*, 2016). Therefore, it is essential to

consider climatic drivers and human interventions when studying estuarine zooplankton dynamics.

## **Data availability**

The data to this article are available in the research data repository of the University of Hamburg, at <https://doi.org/10.25592/uhhfdm.15940>.

## **Acknowledgement**

The authors would like to thank the crew of the research vessel *Ludwig Prandtl* and the stow net vessel HF567 *Ostetal*, as well as Elena Hauten, Jesse Theilen and Raphael Koll for their assistance during the sampling. We would also thank Saskia Otto, Raquel Marques and Gregor Börner for helpful comments on the statistical analysis, Justus van Beusekom, Stefanie Schnell and Sven Stäcker for the technical support, as well as Martina Wichmann, Laura Öhm, Hanna Kaddoura and the technical interns for their assistance with sample processing in the lab.

## **Declaration of interest**

The authors have no conflicts of interest to declare.

## **Funding**

This project was funded by the German Research Foundation within the Research Training Group 2530: “Biota-mediated effects on Carbon Cycling in Estuaries” (project number 407270017; contribution to Universität Hamburg and Leibniz-Institut für Gewässerökologie und Binnenfischerei im Forschungsverbund Berlin e. V. (IGB)) and by the Bundesministerium für Bildung und Forschung (BMBF) within the project “Blue-Estuaries” (project number 03F0864C).

## Supplementary material

Table S 2.1: Overview of the sampling locations and tidal phases.

| Station (Abbreviation) | Coordinates   |                | Stream kilometre | Tidal phase |
|------------------------|---------------|----------------|------------------|-------------|
|                        | Latitude (°N) | Longitude (°E) |                  |             |
| Bunthäuser Spitze (BH) | 53.45         | 10.07          | 609              | Low tide    |
| Mühlenberger Loch (ML) | 53.55         | 9.82           | 633              | High tide   |
| Twielenfleth (TF)      | 53.61         | 9.57           | 651              | High tide   |
| Schwarztonnensand (ST) | 53.71         | 9.47           | 665              | High tide   |
| Brunsbüttel (BB)       | 53.89         | 9.19           | 692              | Low tide    |
| Medemgrund (MG)        | 53.84         | 8.89           | 713              | Low tide    |

Table S 2.2: Dry weight (DW) estimate of biomass (in  $\mu\text{g l}^{-1}$ ) in selected species based on length-weight regressions from respective references.

| Species (Stage)                    | Mean total size ( $\mu\text{m}$ ) | N   | Equation for biomass calculation                                                                       | Reference: |
|------------------------------------|-----------------------------------|-----|--------------------------------------------------------------------------------------------------------|------------|
| <i>Acartia</i> spp.                | 932                               | 133 | $\text{DW } (\mu\text{g l}^{-1}) = e^{(-14.051233 + 2.33 \cdot \text{Ln}(1000))} * (\text{ind./l})$    | Source 1   |
| <i>Alona</i> spp.                  | 509                               | 36  | $\text{DW } (\mu\text{g l}^{-1}) = 1.2 * (\text{ind./l})$                                              | Source 1   |
| <i>Asplanchna</i> sp.              |                                   |     | $\text{DW } (\mu\text{g l}^{-1}) = 0.51 * (\text{ind./l})$                                             | Source 1   |
| <i>Bosmina longirostris</i>        |                                   |     | $\text{DW } (\mu\text{g l}^{-1}) = 1.785 * (\text{ind./l})$                                            | Source 1   |
| <i>Brachionus</i> spp.             |                                   |     | $\text{DW } (\mu\text{g l}^{-1}) = 0.284 * (\text{ind./l})$                                            | Source 1   |
| <i>Chydorus sphaericus</i>         |                                   |     | $\text{DW } (\mu\text{g l}^{-1}) = 1.58 * (\text{ind./l})$                                             | Source 1   |
| <i>Corophium volutator</i>         | Head width: 1040                  | 37  | $\text{DW } (\mu\text{g l}^{-1}) = 2060 * (\text{ind./l})$                                             | Source 2   |
| Cyclopoid copepods                 | 938                               |     | $\text{DW } (\mu\text{g l}^{-1}) = e^{(-16.022785 + 2.59 \cdot \text{Ln}(938))} * (\text{ind./l})$     | Source 1   |
| <i>Daphnia cucullata</i>           | 822                               | 22  | $\text{DW } (\mu\text{g l}^{-1}) = e^{(1.609 + 2.84 \cdot \text{Ln}(840/1000))} * (\text{ind./l})$     | Source 1*  |
| <i>Daphnia galeata</i>             | 861                               | 27  | $\text{DW } (\mu\text{g l}^{-1}) = e^{(1.609 + 2.84 \cdot \text{Ln}(840/1000))} * (\text{ind./l})$     | Source 1*  |
| <i>Daphnia longispina</i>          | 869                               | 91  | $\text{DW } (\mu\text{g l}^{-1}) = e^{(1.609 + 2.84 \cdot \text{Ln}(840/1000))} * (\text{ind./l})$     | Source 1*  |
| <i>Eudiaptomus gracilis</i>        |                                   |     | $\text{DW } (\mu\text{g l}^{-1}) = e^{(-14.051233 + 2.33 \cdot \text{Ln}(1000))} * (\text{ind./l})$    | Source 1   |
| <i>Eurytemora affinis</i> (Male)   | 1554                              | 214 | $\text{DW } (\mu\text{g l}^{-1}) = e^{(1.05 + 2.46 \cdot \text{Ln}(1554/1000))} * (\text{ind./l})$     | Source 3   |
| <i>Eurytemora affinis</i> (Female) | 1655                              | 181 | $\text{DW } (\mu\text{g l}^{-1}) = e^{(1.05 + 2.46 \cdot \text{Ln}(1655/1000))} * (\text{ind./l})$     | Source 3   |
| <i>Eurytemora affinis</i> (C5)     | 1189                              | 109 | $\text{DW } (\mu\text{g l}^{-1}) = e^{(1.05 + 2.46 \cdot \text{Ln}(1189/1000))} * (\text{ind./l})$     | Source 3   |
| <i>Eurytemora affinis</i> (C4)     | 956                               | 147 | $\text{DW } (\mu\text{g l}^{-1}) = e^{(1.05 + 2.46 \cdot \text{Ln}(956/1000))} * (\text{ind./l})$      | Source 3   |
| <i>Eurytemora affinis</i> (C3)     | 762                               | 205 | $\text{DW } (\mu\text{g l}^{-1}) = e^{(1.05 + 2.46 \cdot \text{Ln}(762/1000))} * (\text{ind./l})$      | Source 3   |
| <i>Eurytemora affinis</i> (C2)     | 623                               | 188 | $\text{DW } (\mu\text{g l}^{-1}) = e^{(1.05 + 2.46 \cdot \text{Ln}(623/1000))} * (\text{ind./l})$      | Source 3   |
| <i>Eurytemora affinis</i> (C1)     | 473                               | 136 | $\text{DW } (\mu\text{g l}^{-1}) = e^{(1.05 + 2.46 \cdot \text{Ln}(473/1000))} * (\text{ind./l})$      | Source 3   |
| <i>Filinia</i> sp.                 |                                   |     | $\text{DW } (\mu\text{g l}^{-1}) = 0.45 * (\text{ind./l})$                                             | Source 1   |
| <i>Gammarus zaddachi</i>           | 9603                              | 160 | $\text{DW } (\mu\text{g l}^{-1}) = 1957 * (\text{ind./l})$                                             | Source 4   |
| Harpacticoida                      | 596                               |     | $\text{DW } (\mu\text{g l}^{-1}) = e^{(2.52652832 + 4.4 \cdot \text{Ln}(596/1000))} * (\text{ind./l})$ | Source 1   |
| <i>Keratella</i> spp.              |                                   |     | $\text{DW } (\mu\text{g l}^{-1}) = 0.26 * (\text{ind./l})$                                             | Source 1   |
| <i>Mesopodopsis slabberi</i>       | 6681                              | 251 | $\text{DW } (\mu\text{g l}^{-1}) = 757 * (\text{ind./l})$                                              | Source 5   |
| Nauplii                            | 162                               | 219 | $\text{DW } (\mu\text{g l}^{-1}) = e^{(1.435 + 2.48 \cdot \text{Ln}(162/1000))} * (\text{ind./l})$     | Source 3   |
| <i>Neomysis integer</i>            | 6264                              | 214 | $\text{DW } (\mu\text{g l}^{-1}) = 1201 * (\text{ind./l})$                                             | Source 6   |
| <i>Notholca</i> spp.               |                                   |     | $\text{DW } (\mu\text{g l}^{-1}) = 0.11 * (\text{ind./l})$                                             | Source 1   |
| <i>Paracalanus parvus</i>          |                                   |     | $\text{DW } (\mu\text{g l}^{-1}) = e^{(-14.051233 + 2.33 \cdot \text{Ln}(1000))} * (\text{ind./l})$    | Source 1   |
| <i>Pseudocalanus elongatus</i>     |                                   |     | $\text{DW } (\mu\text{g l}^{-1}) = e^{(-14.051233 + 2.33 \cdot \text{Ln}(1000))} * (\text{ind./l})$    | Source 1   |
| <i>Synchaeta</i> sp.               | 265                               | 25  | $\text{DW } (\mu\text{g l}^{-1}) = 0.265 * (\text{ind./l})$                                            | Source 1   |
| <i>Temora longicornis</i>          |                                   |     | $\text{DW } (\mu\text{g l}^{-1}) = e^{(-14.051233 + 2.33 \cdot \text{Ln}(1000))} * (\text{ind./l})$    | Source 1   |

Abbreviations: N – number of organisms used for size measurement; ind./l – individuals per litre. \* Pooled values of same genus from Source 1.

CHAPTER 2: SPATIO-TEMPORAL POPULATION DYNAMICS OF ESTUARINE ZOOPLANKTON

Source 1: Dumont, H. J., Van de Velde, I., and Dumont, S. 1975. The dry weight estimate of biomass in a selection of Cladocera, Copepoda and Rotifera from the plankton, periphyton and benthos of continental waters. *Oecologia*, 19: 75–97. <https://doi.org/10.1007/BF00377592>.

Source 2: Mason, C. F. 1986. Invertebrate populations and biomass over four years in a coastal, saline lagoon. *Hydrobiologia*, 133: 21–29. <https://doi.org/10.1007/BF00010798>.

Source 3: Watkins, J., Rudstam, L., and Holeck, K. 2011. Length-weight regressions for zooplankton biomass calculations - A review and a suggestion for standard equations. Cornell Biological Field Station Publications and Reports: 17.

Source 4: Wang, X., and Zauke, G. P. 2002. Relationship between growth parameters of the amphipod *Gammarus zaddachi* (Sexton 1912) and the permeable body surface area determined by the acid-base titration method. *Hydrobiologia*, 482: 179–189. <https://doi.org/10.1023/A:1021245715827>.

Source 5: Azeiteiro, U. M. M., Jesus, L., and Marques, J. C. 1999. Distribution, Population Dynamics, and Production of the Suprabenthic Mysid *Mesopodopsis Slabberi* in the Mondego Estuary, Portugal. *Journal of Crustacean Biology*, 19: 498–509. <https://doi.org/10.2307/1549259>.

Source 6: Mees, J., Abdulkarim, Z., and Hamerlynck, O. 1994. Life history, growth and production of *Neomysis integer* in the Westerschelde estuary (SW Netherlands). *Marine Ecology Progress Series*, 111: 43–57. <https://doi.org/10.3354/meps111043>.

Table S 2.3: Pearson correlation analysis of the environmental parameters.

|                 | Temp             | Q                | Sal         | SPM   | O <sub>2</sub>  | Chl <i>a</i>     | PO <sub>4</sub> | NO <sub>3</sub> | NO <sub>2</sub>  | NH <sub>4</sub> |
|-----------------|------------------|------------------|-------------|-------|-----------------|------------------|-----------------|-----------------|------------------|-----------------|
| Temp            |                  | <b>-0.49***</b>  | 0.07        | -0.20 | <b>-0.78***</b> | 0.25             | 0.23            | <b>-0.52***</b> | -0.16            | -0.04           |
| Q               | <b>&lt;0.001</b> |                  | -0.25       | 0.01  | <b>0.41**</b>   | -0.18            | 0.05            | <b>0.86***</b>  | <b>0.30*</b>     | -0.08           |
| Sal             | 0.62             | 0.09             |             | -0.18 | 0.05            | -0.22            | 0.20            | <b>-0.30*</b>   | -0.03            | 0.03            |
| SPM             | 0.18             | 0.98             | 0.22        |       | 0.03            | -0.06            | -0.13           | 0.04            | -0.25            | -0.23           |
| O <sub>2</sub>  | <b>&lt;0.001</b> | <b>0.004</b>     | 0.75        | 0.84  |                 | -0.01            | -0.21           | <b>0.44**</b>   | -0.13            | -0.28           |
| Chl <i>a</i>    | 0.08             | 0.22             | 0.13        | 0.66  | 0.93            |                  | <b>-0.61***</b> | <b>-0.42**</b>  | -0.07            | 0.15            |
| PO <sub>4</sub> | 0.12             | 0.73             | 0.18        | 0.37  | 0.16            | <b>&lt;0.001</b> |                 | <b>0.31*</b>    | 0.01             | -0.27           |
| NO <sub>3</sub> | <b>&lt;0.001</b> | <b>&lt;0.001</b> | <b>0.04</b> | 0.77  | <b>0.002</b>    | <b>0.003</b>     | <b>0.03</b>     |                 | 0.23             | -0.21           |
| NO <sub>2</sub> | 0.28             | <b>0.04</b>      | 0.87        | 0.08  | 0.39            | 0.62             | 0.99            | 0.11            |                  | <b>0.57***</b>  |
| NH <sub>4</sub> | 0.79             | 0.57             | 0.86        | 0.11  | 0.06            | 0.30             | 0.07            | 0.16            | <b>&lt;0.001</b> |                 |

The Pearson correlation coefficient is displayed above the diagonal, and the p-values are shown below the diagonal. Numbers in bold indicate significant correlation (p-value < 0.05: \*, <0.01: \*\*, <0.001: \*\*\*). Abbreviations: Chl *a*, chlorophyll *a*; Temp, temperature; Sal, salinity; Q, river discharge; SPM, suspended particulate matter; NO<sub>3</sub>, nitrate; NO<sub>2</sub>, nitrite; PO<sub>4</sub>, phosphate.

CHAPTER 2: SPATIO-TEMPORAL POPULATION DYNAMICS OF ESTUARINE ZOOPLANKTON

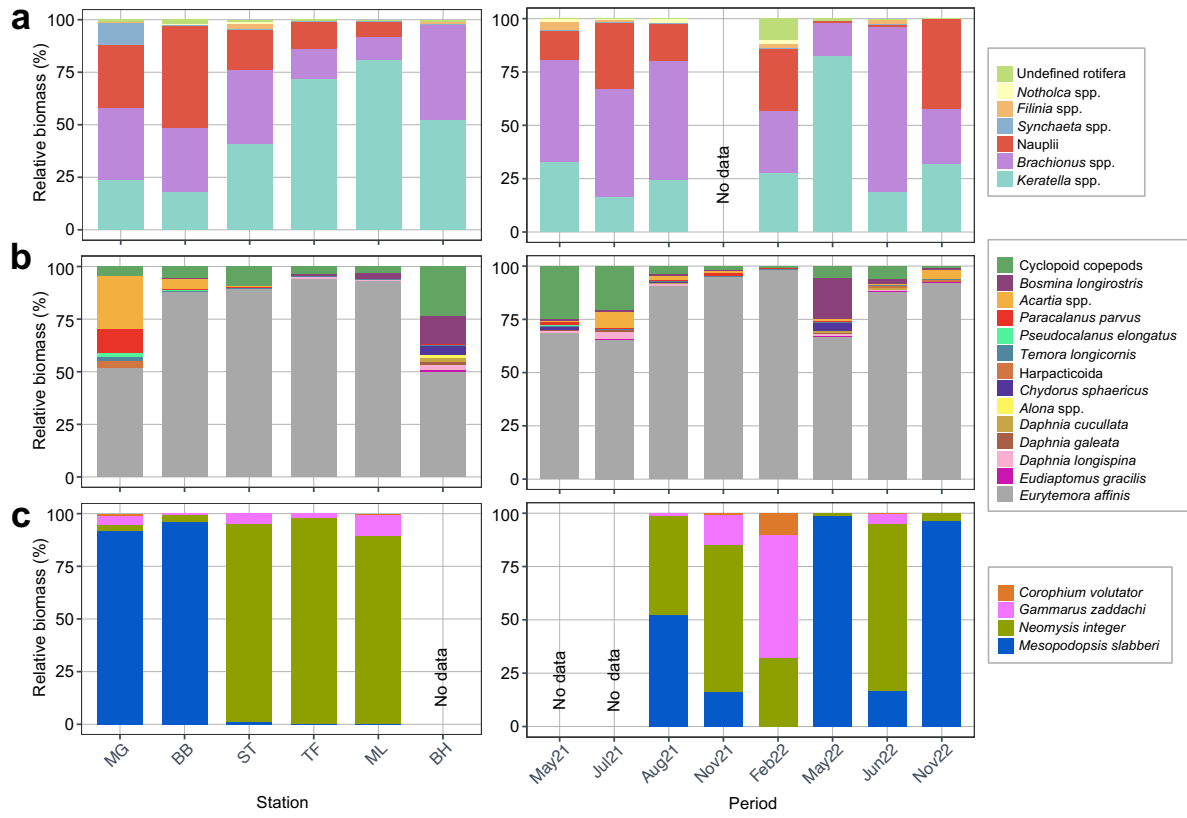
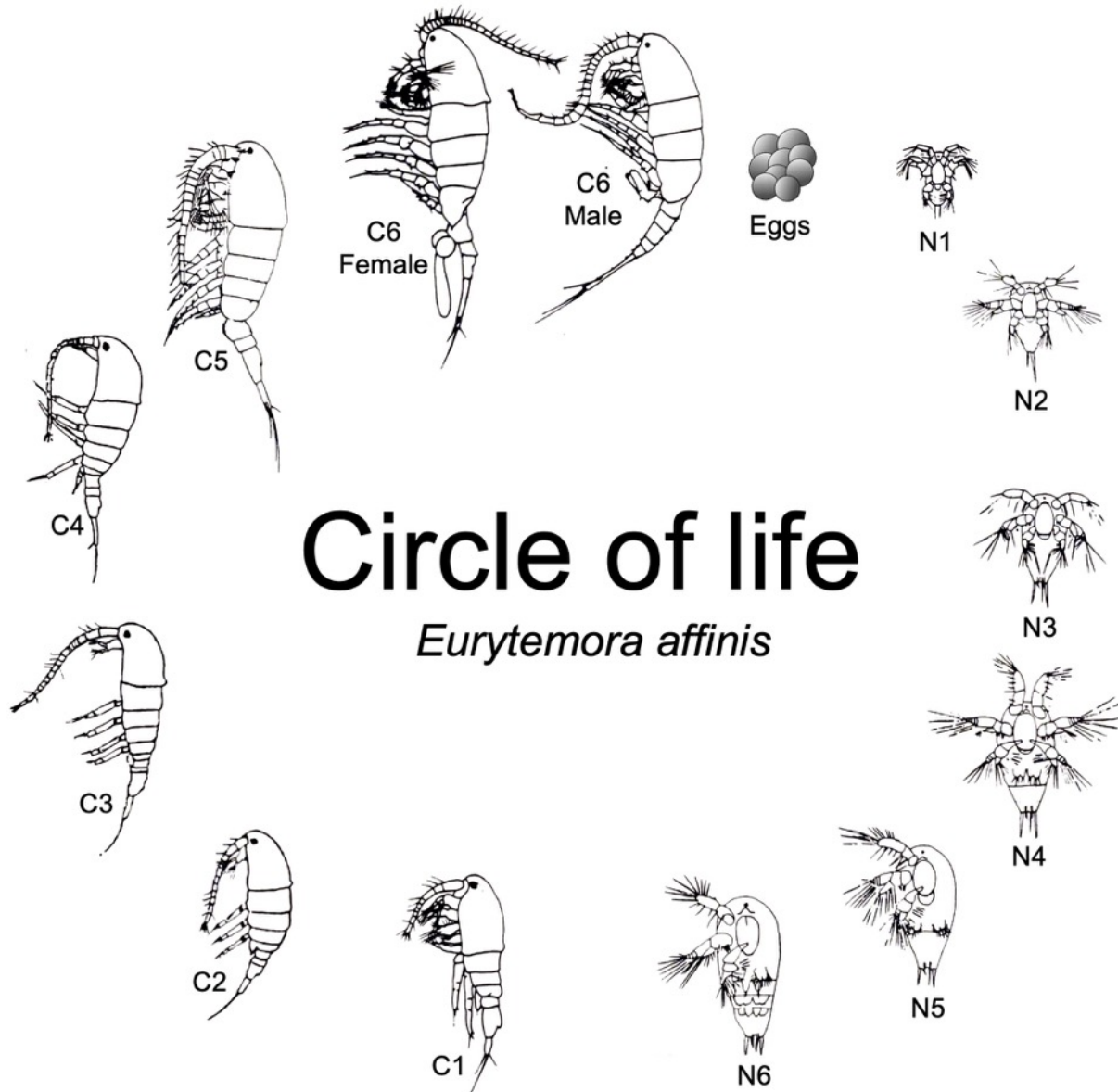


Fig. S 2.1: Spatial and seasonal variability in the relative biomass (%) of (a) micro-, (b) meso- and (c) macrozooplankton in the Elbe estuary in 2021 and 2022.

## Chapter 3: Population dynamics of *Eurytemora affinis*



Manuscript in preparation:

Biederbick, J., Renz, J., Russnak, V., Möllmann, C. and Koppelman, R. Population dynamics and production of *Eurytemora affinis* in the Elbe estuary.

Figure modified, from Peitsch (1992).

**Title:** Population dynamics and production of *Eurytemora affinis* in the Elbe estuary

**Running title:** Population dynamics of *Eurytemora affinis*

**Authors:** Johanna Biederbick<sup>1</sup>, Jasmin Renz<sup>1,2</sup>, Vanessa Russnak<sup>3</sup>, Christian Möllmann<sup>1</sup> and Rolf Koppelman<sup>1</sup>

<sup>1</sup>Institute of Marine Ecosystem and Fishery Science, University of Hamburg, Grosse Elbstrasse 133, 22767 Hamburg, Germany

<sup>2</sup>German Centre for Marine Biodiversity Research (DZMB), Senckenberg Research Institute, Martin-Luther-King Platz 3, 20146 Hamburg, Germany

<sup>3</sup>Helmholtz-Centre Hereon, Institute of Carbon Cycles, Max-Planck-Strasse 1, 21502 Geesthacht, Germany

\*Corresponding author

E-Mail: [johanna.biederbick@uni-hamburg.de](mailto:johanna.biederbick@uni-hamburg.de)

## Abstract

*Eurytemora affinis* is a highly abundant and ubiquitous euryhaline calanoid copepod found in estuarine systems of the northern hemisphere, where it plays a crucial role as a key species in the ecosystem functioning. Despite its dominance in the zooplankton community, the life history traits of *E. affinis* have rarely been studied, particularly in the Elbe estuary, one Europe's largest estuaries. Understanding these traits is crucial for elucidating its population dynamics and assessing its impact on the ecosystem production. We examined seasonal changes in *E. affinis* abundance, body size, growth and production rates, as well as mortality rates, through bi-weekly stationary sampling in the heavily dredged harbour area of the city of Hamburg in the Elbe estuary from April 2021 to July 2022. Peak abundances of up to approximately 600 ind. l<sup>-1</sup>, including nauplii and copepodite stages, occurred from April to early June and from August to early October in both years, with total biomass and secondary production reflecting these seasonal patterns. Our results suggest that temperature, followed by Chlorophyll *a* (Chl *a*) concentration were the most important environmental parameters impacting the population succession. Mortality rates were highest in the youngest (N1:6/C1) and oldest (C5/adult) stage groups, reaching up to 0.54 and 0.78 d<sup>-1</sup>, respectively. Growth and production rates of *E. affinis* were often clearly higher than in other estuarine systems, possibly due to low osmotic stress and more favourable feeding conditions resulting from lower suspended particulate matter and higher Chl *a* concentration in the area.

Keywords: Elbe estuary, *Eurytemora affinis*, life history traits, growth rates, mortality rates, spatio-temporal variability, environmental parameters

## Introduction

*Eurytemora affinis* (Poppe, 1880) is a euryhaline calanoid copepod found in estuarine habitats and adjacent coastal waters of the northern hemisphere. This species exhibits high plasticity in response to fluctuating salinities (Devreker *et al.*, 2004, 2007) and temperatures (Souissi *et al.*, 2016), which are affected by tidal mixing processes (Day *et al.*, 2013). The copepod inhabits areas, where food availability is highly variable and suspended matter is predominated by detrital sources (Modéran *et al.*, 2012; Biederbick *et al.*, 2024). *E. affinis* has a selective and omnivorous feeding behaviour, which allows it to efficiently consume various food sources even under high turbidity conditions (Tackx *et al.*, 2003; Cabrol *et al.*, 2015). It is a species complex that exhibits several distinct genetic traits with a similar morphology in different geographical regions (Winkler *et al.*, 2011). This taxa is the most dominant mesozooplankton species, found in freshwater to mesohaline zones throughout the year in numerous European estuaries, such as the Scheldt (Mialet *et al.*, 2011), the Seine (Mouny and Dauvin, 2002) and the Elbe (Bernát *et al.*, 1994; Biederbick *et al.*, *in prep.*), as well as in North American estuaries, including the St. Lawrence (Winkler *et al.*, 2003) and the Chesapeake Bay (Kimmel and Roman, 2004). Due to its high abundance, *E. affinis* plays a crucial role in estuarine carbon cycling, acting as a major consumer of primary producers and detrital sources, while also serving as important prey for mysids and fish (Thiel *et al.*, 1996; David *et al.*, 2016; Biederbick *et al.*, 2024). However, the population dynamics of *E. affinis* have not been thoroughly studied in all estuaries where it dominates the zooplankton community, although its life history traits may vary among populations and clades (see e.g. Lee *et al.*, 2013; Cabrol *et al.*, 2015). Specifically, research on the population dynamics of *E. affinis* in the Elbe estuary, one of the largest estuaries in northwestern Europe, is limited compared to studies conducted in other North American and European estuaries. It is crucial to gain information on the life history traits of this abundant copepod in the Elbe estuary to understand its population succession and, consequently, its impact on ecosystem services, like carbon sequestration.

Demographic parameters, such as growth, reproduction and mortality, give an indication of the seasonal and spatial development of the population. These parameters are closely

related, as individuals with shorter development times tend to reproduce earlier (Allan, 1976). Moreover, environmental parameters such as temperature are an important factor influencing the life history traits and thus the population dynamics of zooplankton by affecting e.g. individual metabolic rates, which subsequently lead to changes in survival, growth, reproduction and development time (e.g. McLaren, 1963; Allan, 1976; Devreker *et al.*, 2009; Souissi *et al.*, 2016). Salinity stress increases mortality and prolongs development times of *E. affinis*, mainly due to increased energy costs associated with osmoregulation (Devreker *et al.*, 2007, 2009). Limited food availability, difficulties in food selection, and low food quality can additionally negatively affect the population dynamics of *E. affinis*, resulting in reduced reproduction (e.g. Burdloff *et al.*, 2000), smaller body sizes (e.g. Souissi and Souissi, 2021) or lower secondary production (e.g. Burkill and Kendall, 1982). Consequently, environmental conditions that may influence the copepod's life history should be investigated when studying its population dynamics.

In the Elbe estuary, *E. affinis* is confronted with variable estuarine gradients that have been affected by multiple human-induced modifications as a result of recurring dredging and deepening events of the main channel to enable access to the port area of the metropolis Hamburg (Kerner, 2007). As a result, the hydrodynamics of the Elbe estuary are characterised by a high load of resuspended particles that reduce the available light (Wolfstein and Kies, 1995; Schroeder, 1997) and increase remineralisation processes (Amann *et al.*, 2012; Dähnke *et al.*, 2022), which, in turn, affect the available food quantity and quality for *E. affinis* (Biederbick *et al.*, 2024). Particularly in the port area, where the bathymetry experiences a sharp jump due to dredging activities (Hamburg Port Authority (HPA), 2022), the estuarine system shifts to a strongly modified habitat, where suspended matter accumulates as a result of reduced flow velocity (Kerner, 2007). The impact of these environmental conditions on the life history traits of *E. affinis* remains largely unexplored. So far, the demographic factors of *E. affinis* in the Elbe estuary were last studied by Peitsch (1992) in the late 1980s, focusing on production and mortality rates in the oligohaline zone of the estuary, approximately 80 km downstream of the port area. However, the hydrology of the Elbe estuary has changed considerably in recent decades due to further deepening events and ecosystem-based management (e.g. Amann *et al.*, 2012; Weilbeer *et al.*, 2021).

In the present study, seasonal changes in abundance, body size, growth and production rates, and mortality rates of *E. affinis* in the port region of the Elbe estuary will be investigated. A redundancy analysis will assess the stage-specific succession of *E. affinis* in relation to seasonal environmental changes. We hypothesise that the life cycles of *E. affinis* were affected by structural alterations in the Elbe estuary and harbour region. Our findings will be compared with results from other *E. affinis* populations in the northern hemisphere, in particular with investigations by Peitsch (1992) from April to September 1989.

## Methods

### Study site and sampling

The Elbe river belongs to the largest rivers in Europe, originating in the Czech Republic and discharging into the North Sea. The Elbe estuary is situated in Northwest Germany and spans approximately 142 km between the weir in Geesthacht (Elbe-km 585) and the German Bight at Cuxhaven (Elbe-km 727) (Fig. 3.1). It is characterised by a partially well-mixed water column (Pein *et al.*, 2021) and a long residence time of two to four weeks depending on river discharge (Amann *et al.*, 2012). The riverbed experiences a sudden drop in bathymetry of approximately 5 m to a depth of 20 m downstream from the overseas port

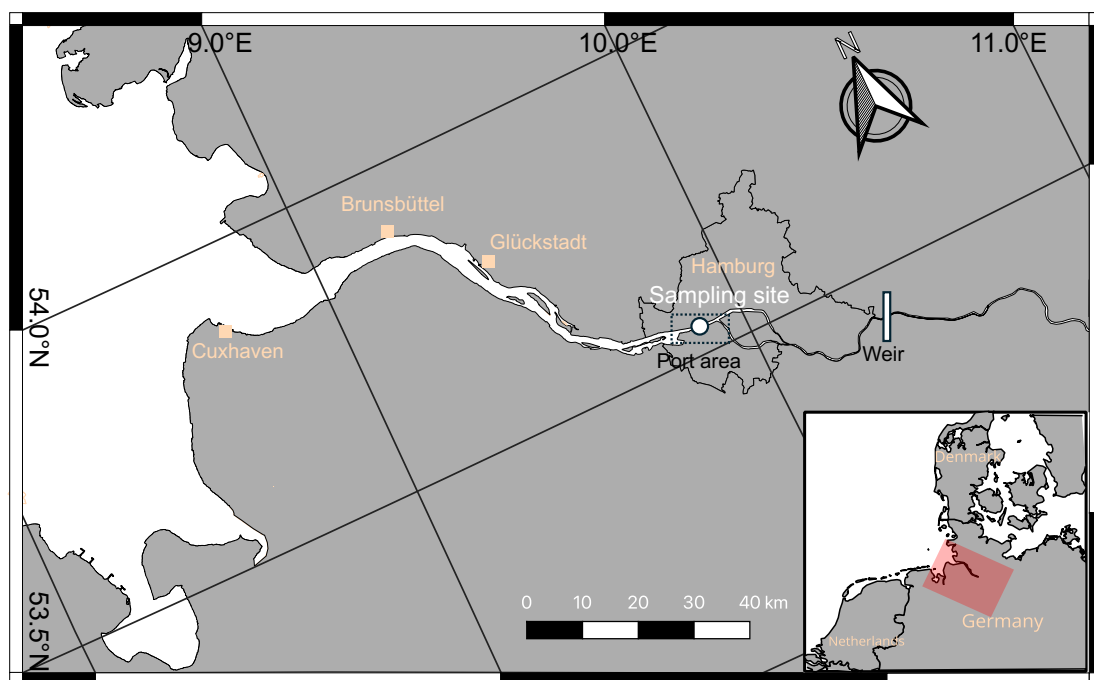


Fig. 3.1: Map of the Elbe estuary showing the sampling location at the pier Seemannshöft in the port area of Hamburg. The weir marks the upstream boundary where the river transitions into the estuarine zone.

of Hamburg (Hamburg Port Authority, HPA, 2022). We collected bi-weekly zooplankton samples and environmental data at a permanent sampling site from a pier (Seemannshöft, Elbe-km 629) located in the port area of Hamburg between 27<sup>th</sup> of April 2021 and 27<sup>th</sup> of July 2022 (Fig. 3.1). Sampling was conducted two hours prior to low tide during all samplings to ensure consistency between the sampling campaigns.

### **Environmental data**

Temperature (°C), oxygen saturation (%) and salinity were measured in surface water with a portable handheld sensor (Hanna Instruments, Vöhringen, Germany; model number HI98494). From May 13<sup>th</sup> to July 27<sup>th</sup>, 2022, the oxygen sensor was malfunctioning. For this period, oxygen concentrations were obtained from a permanent monitoring station of the Institute for Hygiene and Environment located at the pier Seemannshöft, which can be accessed online through the database of the Federal Waterways and Shipping Agency (WSV, 2023). Information on daily discharge was obtained from the nearest gauging station (Neu Darchau, Elbe-km 536) (WSV, 2023). We calculated mean discharge rates as an average over a one-week period to minimize short-term fluctuations. Water samples for the analysis of suspended particulate matter (SPM) and chlorophyll *a* (Chl *a*) concentrations were collected during each sampling campaign using multiple bucket hauls and subsequently filtered through pre-combusted and pre-weighted glass fibre filters (GF/F, Whatman, 0.7 µm pore size, 450°C). The volume of filtered water samples (approx. 100 to 500 ml) was adjusted for each season to ensure that the filters were adequately coated with suspended matter. Filters were transferred to tubes and immediately frozen at -20°C. For SPM dry weight measurements, filters were lyophilised at -80°C for 24 h and then weighed and standardised to mg l<sup>-1</sup>. Chl *a* was extracted in 90% acetone at 5°C for 24 h, followed by centrifugation (3000 rpm, 4°C, 15 min) and subsequently measured using a PerkinElmer photometer (LAMBDA XLS, Waltham, USA; model number: L7110189) following the method of Jeffrey and Humphrey (1975).

### **Zooplankton abundance**

Zooplankton samples were collected using quantitative bucket hauls of 30 to 50 l of surface water. The water volume was adjusted seasonally to collect sufficient biovolume. Triplicate

samples were taken during each sampling and filtered through 55  $\mu\text{m}$  and 200  $\mu\text{m}$  mesh to separate the samples into the microzooplankton (55 – 200  $\mu\text{m}$ ) size fraction for nauplius larvae, and the mesozooplankton (200 – 2000  $\mu\text{m}$ ) size fraction for copepodites including adults. Samples of nauplius larvae were collected only monthly. All zooplankton samples were preserved in 37% formaldehyde solution buffered with sodium tetraborate at a final concentration of 4% immediately after collection (Omori and Fleminger, 1976). Samples containing large numbers of nauplii or copepodites were subsampled using a modified Hensen-Stempel pipette (Perkins, 1957) or a Folsom splitter (McEwen *et al.*, 1954), respectively. At least 100 copepodites of *Eurytemora affinis*, as well as a minimum of 100 nauplius larvae were identified and counted, using a dissecting microscope (Leica Microsystems, Wetzlar, Germany; model number: M125C) and an inverted microscope (Leica Microsystems, Wetzlar, Germany; model number: DBMI3000B), respectively. Nauplii abundances were pooled across all stages, while adult individuals were differentiated into males and females. Sex ratios of adult individuals were calculated based on the proportion of males to females.

### Body size and dry weight

Prosome lengths of each copepodite and adult stage, as well as the total lengths of naupliar larvae, were measured monthly between August 5<sup>th</sup>, 2021, and June 28<sup>th</sup>, 2022. We assumed that the stage-specific sizes did not differ between the two years of sampling and assigned the monthly measured stage-specific size values to the respective sampling months. Total and prosome lengths of nauplii and copepodites, respectively, were taken from images of approximately 10 individuals per stage using the image processing program “ImageJ” (version 4.13, Schneider *et al.*, 2012). Individual dry weights (*DW*, in  $\mu\text{g}$ ) of nauplii, copepodites and adults of *E. affinis* were estimated from the respective size measurements using length-weight regressions of Christiansen (1988), for nauplius larvae:

$$DW = 6.3 L_t^{2.06} \quad (\text{Eq. 3.1})$$

copepodites and adults:

$$DW = 12.9 L_p^{2.92} \quad (\text{Eq. 3.2})$$

where  $DW$  is the individual dry weight of the respective stage in  $\mu\text{g}$ ,  $L_t$  the total length (in mm) and  $L_p$  the prosome length (in mm). We calculated mean individual dry weights for nauplii N1-N6 based on averaged total length measurements.

### Development time and growth rate

Development times ( $D$ , in days) were derived from a Bělehrádek equation (Bělehrádek, 1935) as a function of temperature ( $T$ , in  $^{\circ}\text{C}$ ) and the coefficients  $a$ ,  $\alpha$  and  $\beta$ :

$$D = a(T - \alpha)^{\beta} \quad (\text{Eq. 3.3})$$

Species-specific coefficients for *Eurytemora hirundooides*, which is a synonymous for *E. affinis* (Busch and Brenning, 1992), were applied as provided by Corkett and McLaren (1970), with  $a = 5527$ ,  $\alpha = 10.4$  and  $\beta = -2.05$ . The species-specific Bělehrádek equation was determined based on the development time from hatching of the first nauplius stage to the appearance of copepodite stage C1. For *E. affinis*, isochronal development is well-known (e.g. Roman, 1998; Peterson, 2001), with the first naupliar stage (N1) developing two to three times faster than subsequent stages (see e.g. Peitsch, 1992). A 2.5 times faster development time was calculated for N1, while assuming isochronal development for the other naupliar and copepodite stages. The duration of a generation of nauplii and copepodites of *E. affinis*, excluding eggs, is given by the sum of the stage-specific development times.

Stage-specific daily growth rates ( $g$ , in  $\text{day}^{-1}$ ) were calculated under the assumption of exponential growth, using the equation according to Breteler *et al.* (1982):

$$g = \frac{1}{D} \log_e \frac{DW_{i+1}}{DW_i} \quad (\text{Eq. 3.4})$$

where  $DW$  is the individual dry weight (in  $\mu\text{g}$ ) of successive development stages  $i$  and  $D$  the temperature-dependent development time (in days) estimated for each stage. Adult males were considered not to grow. Females were assumed to grow or produce eggs at a rate approximating the mean growth of the copepodite stages C1 to C5.

## Mortality rates

We calculated mortality ( $\beta$ , in  $\text{day}^{-1}$ ) of each stage using the vertical life table (VLT) approach of Aksnes and Ohman (1996), assuming that the daily recruitment to stage  $i$  and mortality rate, which is determined by the combination of stage  $i$  and  $i+1$ , is constant over the duration of the stage  $i$  and the consecutive stages. For nauplii and copepodite stages up to C4-C5, mortality was estimated by iteration, using the equation of Mullin and Brooks (1970):

$$\frac{\exp^{\beta D_{i-1}}}{1 - \exp^{-\beta D_{i+1}}} = \frac{N_i}{N_{i+1}} \quad (\text{Eq. 3.5})$$

where  $\beta$  is the mortality rate (in  $\text{day}^{-1}$ ) across two consecutive stages (stage  $i$  and  $i+1$ ),  $N$  is the abundance and  $D$  the development time of stage  $i$  and the successive stage  $i+1$ . Nauplii mortality rates were calculated based on averaged data on abundance and development times from N1 to N6.

Mortality rates of C5-adult stages were calculated based on the equation of Aksnes and Ohman (1996):

$$\beta = \frac{\ln\left(\frac{N_{C5}}{N_{Adult}} + 1\right)}{D_{C5}} \quad (\text{Eq. 3.6})$$

where  $\beta$  is the mortality rate (in  $\text{day}^{-1}$ ,  $\text{d}^{-1}$ ) and  $N$  is the abundance of copepodite stage C5 and an adult stages (female or males), and  $D$  the development time of copepodite stage C5. As the VLT approach is most efficient when averaging multiple values (e.g. over stations, periods) (Aksnes and Ohman, 1996), we calculated mean mortality rates by averaging rates during periods of high abundance, since low abundances (primarily in the winter period) often led to negative mortality estimates.

## Biomass and secondary production

Stage-specific biomass (in  $\mu\text{g l}^{-1}$ ) was estimated by multiplying the individual dry weights ( $DW$ ) by the abundance ( $N \text{ l}^{-1}$ ) of the respective stages. Secondary production was calculated by the stage-specific growth rates multiplied by their biomass. The total

secondary production of *E. affinis* was calculated by the sum of stage-specific (nauplii, copepodites, excluding eggs) secondary production.

### Statistical analysis

A transformation-based redundancy analysis (RDA) was conducted to examine the relationships between stage-specific abundances and environmental data, using the R package “vegan” (version 2.6-4, Oksanen *et al.*, 2022). Stage-specific abundances were Hellinger transformed to reduce double zeros (Borcard *et al.*, 2011). We excluded nauplii abundance data from the RDA because the monthly sampling schedule did not allow a concurrent analysis with the copepodite abundance data. Environmental data were z-standardised and checked for collinearity using Pearson’s correlation, which resulted in the exclusion of the parameter O<sub>2</sub> due to its high correlation with temperature. A Monte-Carlo permutation test (with 999 iterations) was conducted to assess the significance of the global model, the RDA model axes and the environmental parameters. An adjusted R<sup>2</sup> was calculated to estimate the proportion of variability in the abundance data that can be explained by the environmental variables. Visualisations and all statistical analyses were conducted using R Studio (version 4.3.2, R Core Team, 2023). Language correction of the finalised manuscript was done using the AI language model GPT-4 (ChatGPT; OpenAI, 2023).

## Results

### Environmental conditions

Water temperature at the pier Seemannshöft followed a cyclical annual pattern, with a minimum of 1.9°C measured at the end of December and maximum values of 22.3°C and 23.3°C in June 2022 and 2021, respectively (Fig. 3.2). The oxygen concentration exhibited a negative correlation with temperature (Pearson,  $r(31) = -0.81$ ,  $p < 0.001$ ), decreasing to below 30% saturation in June of both years. Oxygen saturation remained above 80% during the winter months. Chl *a* concentrations peaked at 59 µg l<sup>-1</sup> in April, which was followed by a second bloom in mid-July in both years (2021: 53 µg l<sup>-1</sup>, 2022: 33 µg l<sup>-1</sup>). In mid-June and

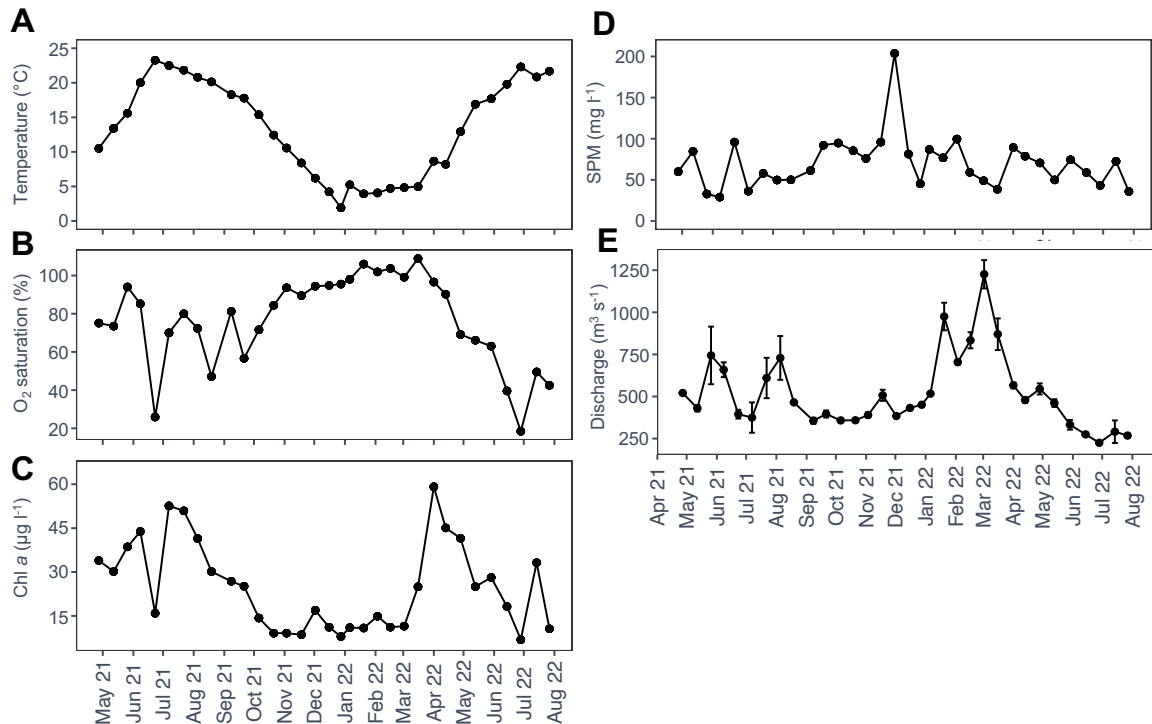


Fig. 3.2: Seasonal variability in the (A) temperature (°C) and concentration of (B) oxygen saturation (%), (C) chlorophyll a (Chl a, µg l<sup>-1</sup>) and (D) suspended particulate matter (SPM, mg l<sup>-1</sup>) at the pier Seemannshöft during the sampling campaigns. (E) Mean discharge rates (m<sup>3</sup> s<sup>-1</sup>) were calculated from weekly discharge rates, which were obtained from the last gauging station Neu Darchau (Elbe-km 536).

during the winter months, Chl *a* concentrations remained low at approximately 15 µg l<sup>-1</sup>. Water conditions were predominantly freshwater, characterised by stable and low salinities, with an average of  $0.47 \pm 0.12$ . SPM concentrations varied between approximately 50 and 100 mg l<sup>-1</sup> (mean:  $70 \pm 32$  mg l<sup>-1</sup>), with one peak of 204 mg l<sup>-1</sup> in December 2021. Mean discharge rates increased in late winter and early spring, reaching a maximum of  $1226 \pm 84$  m<sup>3</sup> s<sup>-1</sup> in March, followed by a decrease towards the summer months, with lowest values of  $225 \pm 4$  m<sup>3</sup> s<sup>-1</sup> in June.

### Abundance patterns

*Eurytemora affinis* was consistently present throughout the entire study period and exhibited a pronounced seasonal pattern, characterised by high variability during periods of peaking abundances (Fig. 3.3). *E. affinis* was most abundant during spring blooms, from April to early June, reaching maximum abundances of approximately 600 individuals per litre (ind. l<sup>-1</sup>), including nauplii and copepodites, in early June 2021 and late May 2022, respectively.

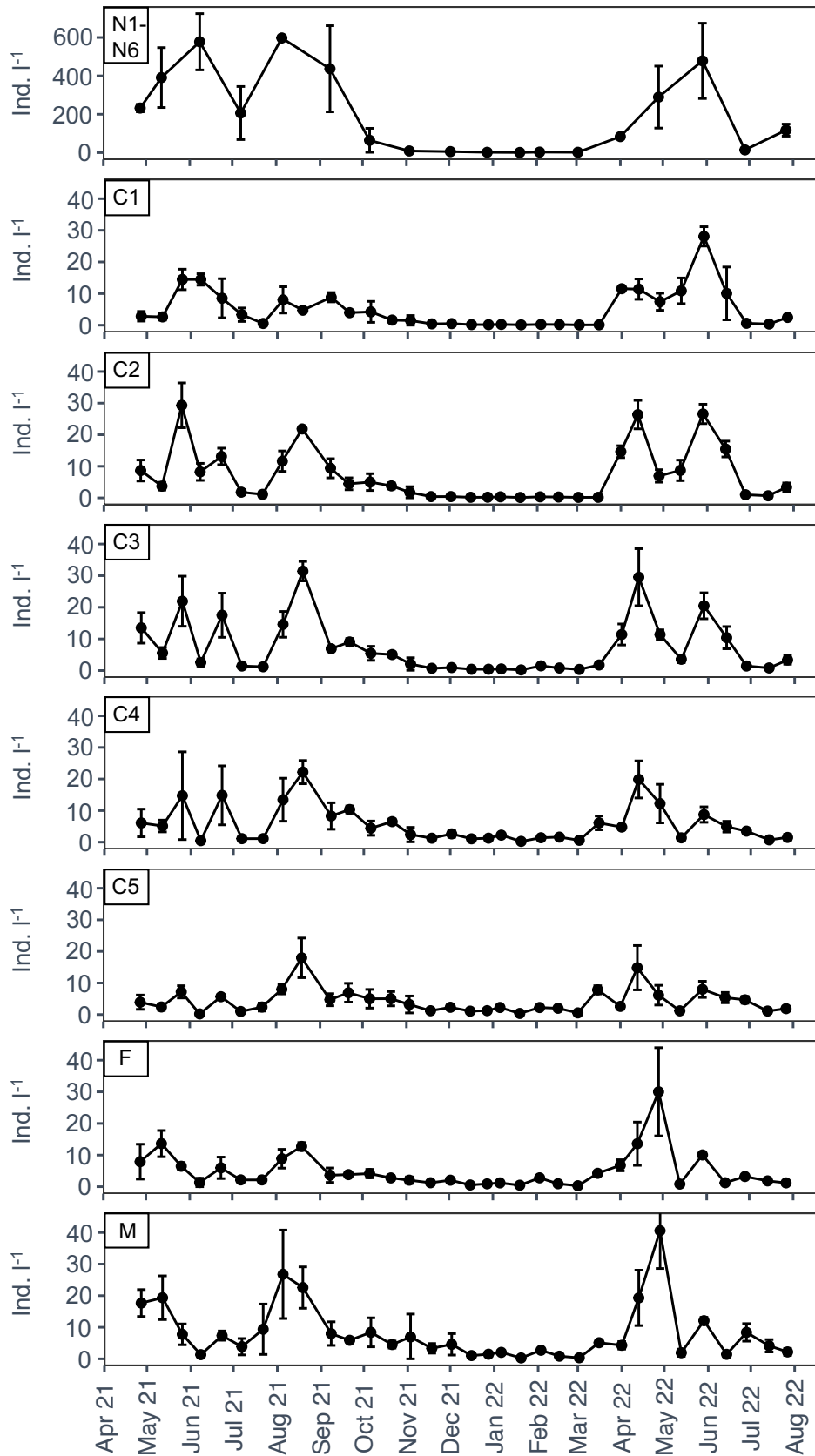


Fig. 3.3: Stage-specific abundance (individuals per litre, ind. l<sup>-1</sup>) of *Eurytemora affinis* during the different sampling periods at the pier Seemannshöft. Means are derived from triplicate samples. Nauplii stages (N1-N6) were pooled. For adult and younger copepodites, sexes are denoted as M (male), F (female) and C1 to C5 (copepodite stages). Please take note of the varying scales on the y-axes.

A second increase in the numbers of *E. affinis* occurred from the beginning of August to early October 2021, with the highest abundance reaching a total of 688 ind. l<sup>-1</sup> in early August 2021. Nauplii represented the largest proportion of the total abundance of *E. affinis*, ranging from approximately 200 to 580 ind. l<sup>-1</sup> during the spring and summer peaks. From the end of October to March, *E. affinis* abundance remained low across all stages, averaging less than 30 ind. l<sup>-1</sup> in total, with older copepodite (i.e. C4, C5) and adult stages dominating the population during winter. In general, the number of individuals of *E. affinis* showed a decreasing trend towards older stages, except for copepodite stage C1, which was frequently less abundant than stage C2. The number of adults was unevenly distributed by sex, with males almost always dominating the adult population (supplementary data, Fig. S 3.1). Throughout the entire sampling period, the ratio of males to females ranged between  $0.6 \pm 0.15$  and  $3.76 \pm 2.94$ , with an average of  $1.89 \pm 1.24$ .

Table 3.1: Results of the RDA model explaining the variance (adjusted R<sup>2</sup> in %) in the stage-specific abundance by the explanatory variables. Test statistics were obtained by Monte Carlo permutation tests (n=999 permutations). Significant differences are displayed in bold.

| Ordination axis                                                                                                                               |                                    |          |              |
|-----------------------------------------------------------------------------------------------------------------------------------------------|------------------------------------|----------|--------------|
|                                                                                                                                               | R <sup>2</sup> <sub>adj.</sub> (%) | Pseudo-F | p-value      |
| Selected Model                                                                                                                                | 17.4                               | 2.35     | <b>0.017</b> |
| RDA Axis1                                                                                                                                     | 15.1                               | 10.17    | <b>0.026</b> |
| RDA Axis2                                                                                                                                     | 0.1                                | 1.08     | 0.905        |
| Explanatory variables                                                                                                                         |                                    |          |              |
|                                                                                                                                               | Parameter                          | Pseudo-F | p-value      |
| Variables retained in the model                                                                                                               | Temp                               | 7.66     | <b>0.002</b> |
|                                                                                                                                               | Chl <i>a</i>                       | 2.55     | 0.066        |
|                                                                                                                                               | SPM                                | 0.66     | 0.504        |
|                                                                                                                                               | Q                                  | 0.54     | 0.612        |
|                                                                                                                                               | Sal                                | 0.34     | 0.769        |
| Abbreviations: Temp, temperature; Chl <i>a</i> , chlorophyll <i>a</i> ; SPM, suspended particulate matter; Q, river discharge; Sal, salinity. |                                    |          |              |

Seasonal variability in the abundance of *E. affinis* copepodites, including adults, was explained by up to 17.4% using the RDA model (Table 3.1). After model selection, the final parameters included in the RDA model were temperature, Chl *a*, SPM, river discharge (Q) and salinity. Only the first axis was significant, representing 15.1% of the total variability and reflecting temporal changes in the abundance of copepodites through its strong correlation with temperature. The Chl *a* concentration showed only a slight tendency to influence this temporal variability, while the other environmental factors appeared to play a minor role.

Both parameters, Chl *a* and temperature, clustered at the negative end of axis 1 in the correlation triplot towards the sampling months of May to August, where the youngest copepodite stages (i.e. C1-C3) were also grouped (Fig. 3.4). Older stages, including adults, clustered in the opposite direction towards the positive end of axis 1.

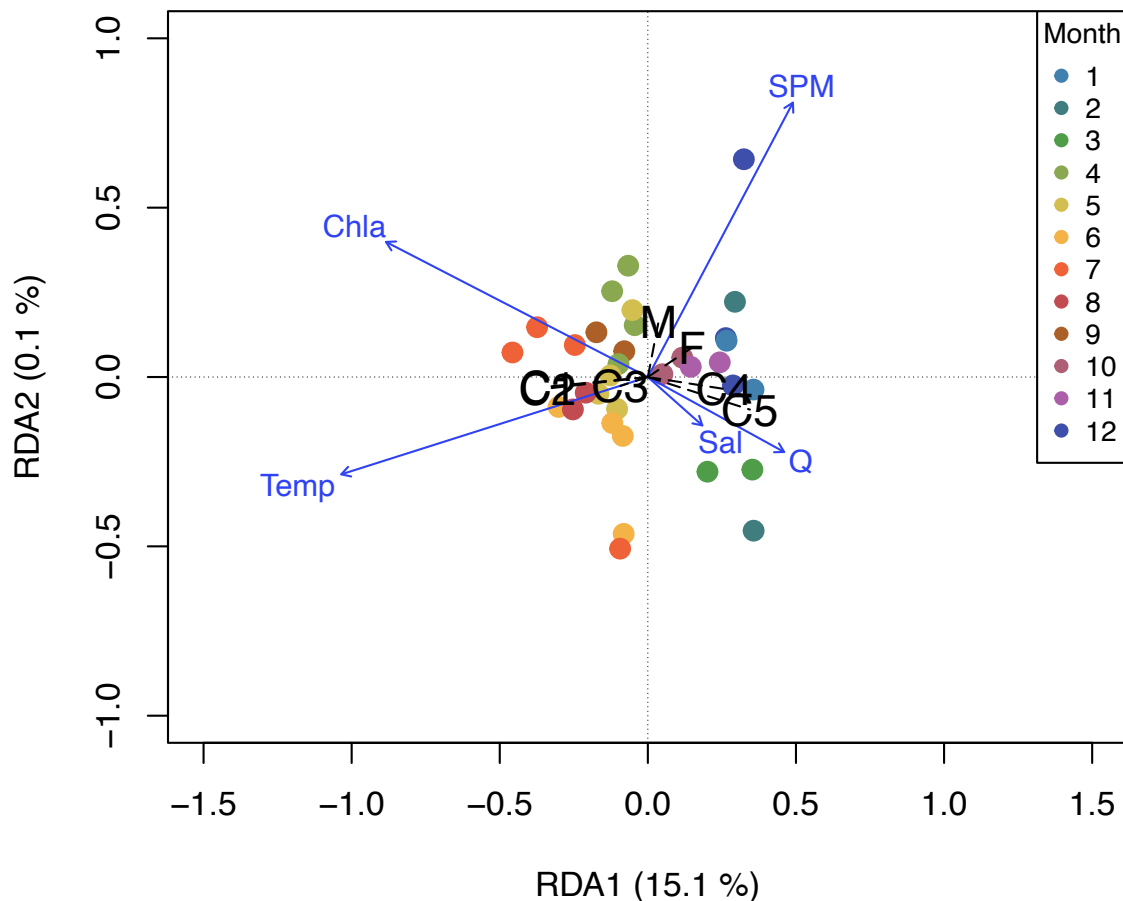


Fig. 3.4: Correlation triplot of RDA axis 1 and 2 explaining the temporal variability (in %) of the stage-specific abundance pattern. The RDA model only includes abundance data on copepodites, i.e. C1 to C5, female (F) and male (M) adults. See Table 3.1 for the explanation of the denotation of the environmental variables.

### Sizes, development and growth

Stage-specific total and prosome lengths exhibited a seasonal pattern, peaking in spring (i.e. April), with the lowest values for most stages occurring during winter and at the end of June (Fig. 3.5). Since stage-specific dry weights of *E. affinis* were calculated based on length-weight regressions (see Eq. 3.1 and Eq. 3.2), the individual dry weights followed the seasonal changes in body size with highest values in spring and the lowest in June and during winter

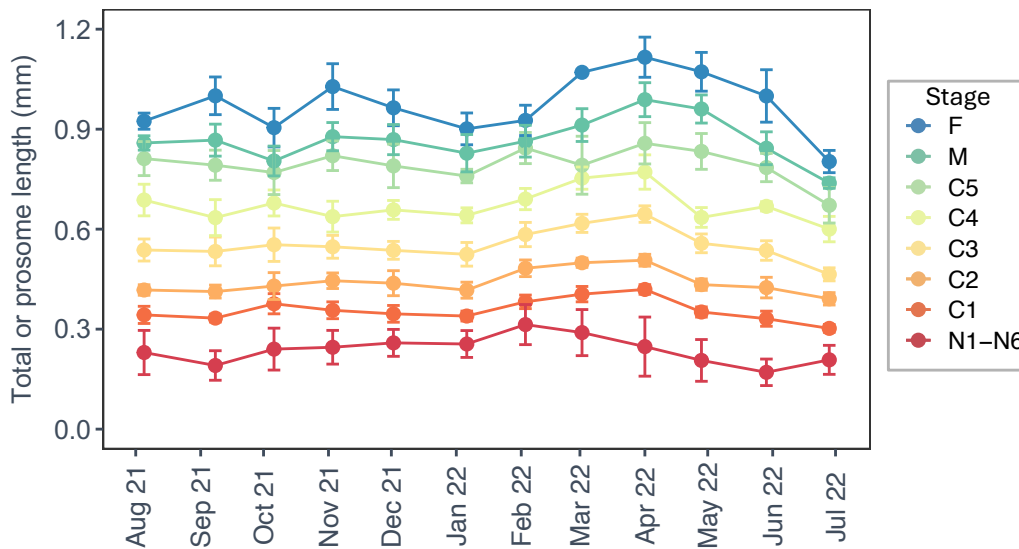


Fig. 3.5: Total length (mm) of nauplii (N1-N6, dark red) and prosome length (mm) of copepodites (C1 to C5), including females (F) and males (M) of *Eurytemora affinis*. Mean values are derived from size measurements of at least 10 individuals per stage and sampling date.

(see supplementary data, Table S 3.1). Total and prosome lengths increased progressively with each successive stage. Females of *E. affinis* had an average prosome length of  $0.97 \pm 0.09$  mm, which is approximately 0.1 mm larger than that of adult males ( $0.86 \pm 0.07$  mm) over the period studied.

Stage-specific development times were negatively correlated with temperature due to the application of a Bělehrádek equation (see Eq. 3.3) and are given in the supplementary material (see Table S 3.2). Under the assumption of isochronal development, stage durations did therefore not differ between stages within each sampling period, except for stage N1, which was assumed to have development times that were 2.5 times shorter than those of the other stages. Development rates varied from 0.72 days (d) per stage at 23°C in June 2021 to 5.63 d per stage at 1.9°C in December 2021. The total generation time, from naupliar to adults, ranged from 8.17 d (in June 2021) to 64.23 d (in December 2021), depending on the temperature.

Stage-specific growth rates were lowest in winter for all stages (see supplementary material, Fig. S 3.2), corresponding to reduced individual dry weights and extended stage durations during the winter months, according to Eq. 3.4. In contrast, growth rates peaked in late June or early July in both sampling years, although individual dry weights were highest in spring

(see Table S 3.1). Highest growth rates were observed for nauplii, with values ranging from 0.06 to 1.29  $d^{-1}$ . In general, daily growth rates decreased with each successive stage, with C5 copepodites exhibiting the lowest growth rates (0.02 to 0.39  $d^{-1}$ ), as growth rates of adult females were calculated from the means of C1 to C5 and males were assumed not to grow.

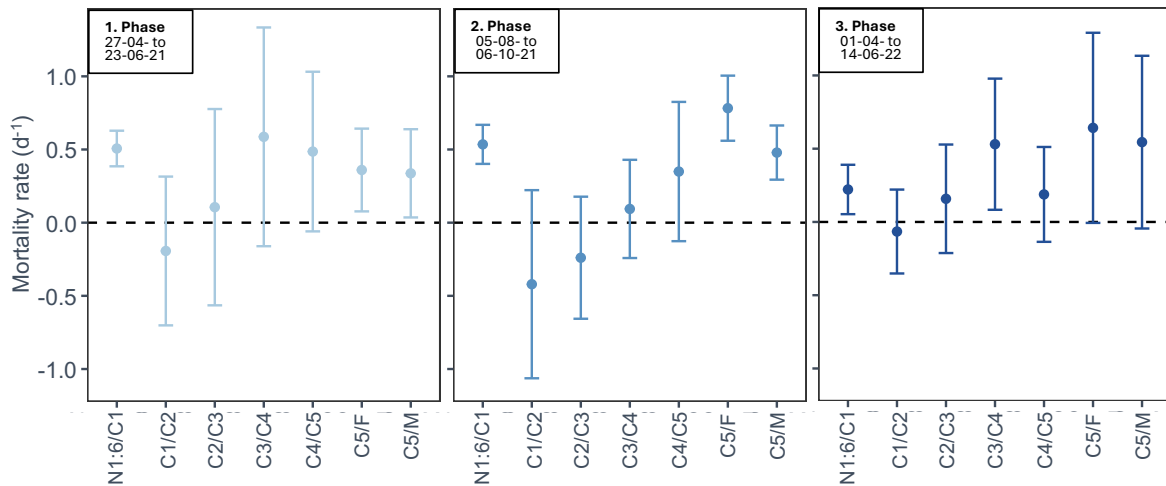


Fig. 3.6: Mean mortality rates (per day,  $d^{-1}$ ) across different stage groups of *Eurytemora affinis* during three distinct phases of high abundance. First phase (light blue): 27.04.21 to 23.06.21; Second phase (blue): 05.08.21 to 06.10.21; Third phase (dark blue): 01.04.22 to 14.06.22. Mean values were derived from triplicate samples and averaged over the respective sampling periods. Mean mortality rates of naupliar stages were calculated from averaged abundance data and development times from N1 to N6.

## Mortality

As estimates of mortality for *E. affinis* stage groups produced negative rates during periods of low and highly variable abundance, mean mortality rates were calculated only over periods of high abundance. Based on two spring assemblages peaking from April to June in both years, along with another assemblage that reached high abundances from August to October (see Fig. 3.3), three different mortality estimates per stage group were calculated (Fig. 3.6). Over the three periods, mean mortality rates were highly variable and showed an increasing trend with each subsequent copepodite stage, with maximum rates of  $0.34 \pm 0.30$  to  $0.54 \pm 0.59 d^{-1}$  for stage group C5/males and  $0.36 \pm 0.28$  to  $0.78 \pm 0.22 d^{-1}$  for C5/females, respectively, except for the stages C3 to C5 in phase 1. Stage group C1/C2 and partly C2/C3 exhibited negative mortality rates. Notably, mortalities for N1:6/C1 were higher than those of younger copepodite stages, with rates ranging from  $0.22 \pm 0.17$  to  $0.54 \pm 0.13 d^{-1}$ . No clear seasonal pattern was evident in the stage-specific mortality rates.

### Biomass and secondary production

The total biomass of *E. affinis* was high following periods of maximum abundance (Fig. 3.7). Nauplii reached a peak biomass of  $182 \mu\text{g l}^{-1}$  in early August 2021, while copepodites had a maximum of  $1067 \mu\text{g l}^{-1}$  in late April 2022, followed by a second, smaller peak ( $629 \mu\text{g l}^{-1}$ ) in August 2021. For both, nauplii and copepodites, biomass decreased to values below approximately  $50 \mu\text{g l}^{-1}$  and  $100 \mu\text{g l}^{-1}$ , respectively, between late June and mid-July, as well as during the winter months.

Peaks in secondary production followed the seasonal pattern of high abundance and biomass (Fig. 3.7). The total secondary production of *E. affinis* varied between 14 and  $135 \mu\text{g l}^{-1} \text{d}^{-1}$  for nauplii and 54 and  $231 \mu\text{g l}^{-1} \text{d}^{-1}$  for copepodites in the spring and summer

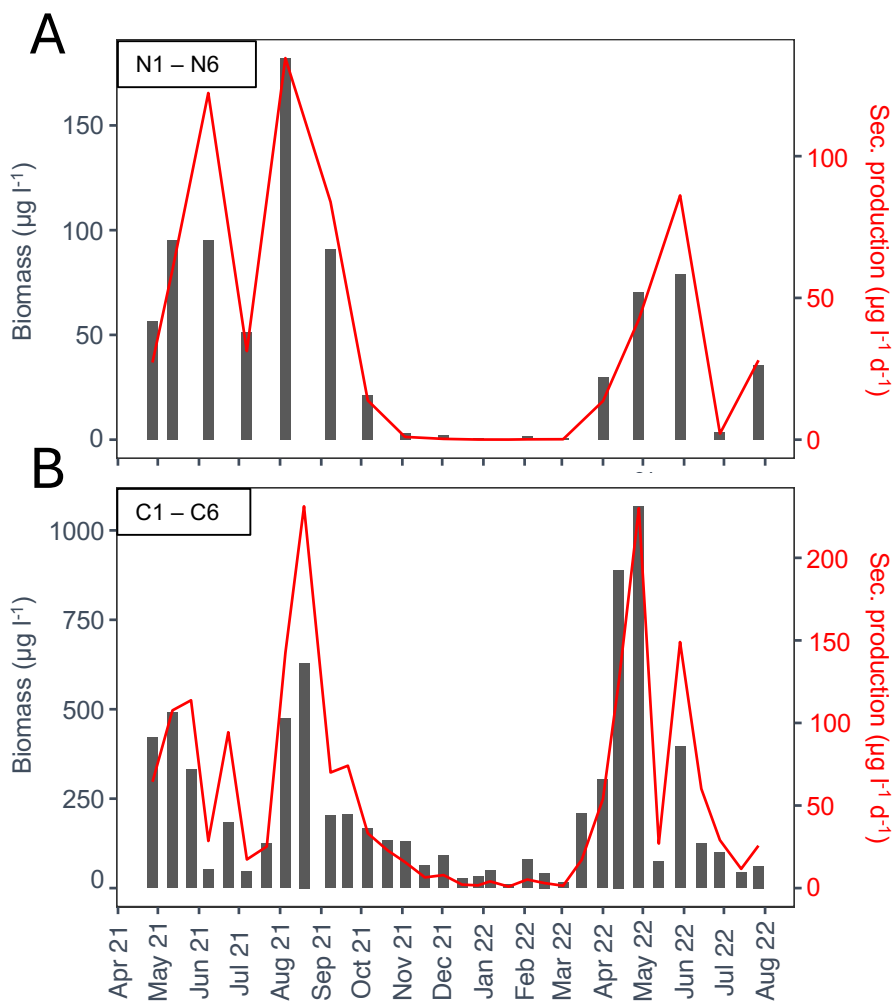


Fig. 3.7: Total biomass (black bars, in dry weight,  $\mu\text{g l}^{-1}$ ) and secondary production (red line, in  $\mu\text{g l}^{-1} \text{d}^{-1}$ ) of pooled (A) nauplii and (B) copepodite stages, including adults, of *Eurytemora affinis* during the sampling campaigns at the pier Seemannshöft.

growing seasons. In the end of June to mid-July, as well as in winter, the secondary production of pooled nauplii and copepodite stages decreased to rates below  $50 \mu\text{g l}^{-1} \text{d}^{-1}$ .

## Discussion

The population dynamics of the copepod *E. affinis* in the Elbe estuary remain largely understudied, particularly regarding key population dynamic parameters such as development time, growth rate, productivity and mortality. These parameters are important for understanding the seasonal stage-specific succession of *E. affinis*, especially considering the highly variable environmental conditions typical of estuarine systems. In this study, we assessed abundance patterns in relation to seasonal environmental changes, determined population dynamic parameters, and subsequently compared our findings with previous research, including the work by Peitsch (1992), as well as studies from other estuarine systems.

## Abundance patterns

Overall, the *E. affinis* population showed an increase in individual numbers during spring, from April to early June, followed by a second peak in abundance in late summer, from August to early October. The seasonal succession of *E. affinis* in the Elbe estuary was comparable to that reported in other estuaries, such as the Scheldt (Mialet *et al.*, 2011), the Seine (Mouny and Dauvin, 2002) or the Chesapeake Bay (Kimmel and Roman, 2004). However, peak abundances found in our study were often two to three times higher than in the respective studies, especially in late summer. In a long-term study on the distribution pattern of *E. affinis* in the Elbe estuary, conducted by Peitsch *et al.* (2000), peak abundances of typically 400 to 600 ind.  $\text{l}^{-1}$  were found in the harbour region during spring and summer. These findings align with our results, although the numbers fluctuated greatly and occasionally fell below 50 ind.  $\text{l}^{-1}$  in some years. In addition, in the oligohaline zone of the Elbe estuary, Peitsch (1992) displayed maximum abundances of 312 ind.  $\text{l}^{-1}$  in spring, while the summer assemblage from June to September remained below 40 ind.  $\text{l}^{-1}$ . Comparing the population dynamics of *E. affinis* among studies and estuaries can be highly challenging, not only because of individual hydrological conditions, but also due to methodological differences. Variations in sampling approaches, including differences in mesh sizes and

sampling schedules (e.g. tidal phase, frequency, depth), can lead to divergent maximum abundances between studies and should therefore be interpreted with caution.

Despite the above mentioned challenges, we mainly focused on comparing environmental factors and demographic parameters that may affect the seasonal succession of the *E. affinis* population across studies. Results from the RDA indicated that temperature was the most influential environmental factor affecting the seasonal stage-specific abundances of *E. affinis*. In particular, the abundance of young copepodite stages responded positively to increasing temperatures, which may be related to the high impact of temperature on reproduction rates. Several studies have shown that reproductive parameters of *E. affinis*, such as egg production rate, embryonic development time, and clutch size, are highly sensitive to temperature changes, often in combination with fluctuations in salinity that lead to salinity stress for the organisms (e.g. Hirche, 1992; Devreker *et al.*, 2009; Lloyd *et al.*, 2013). However, the RDA results showed that salinity was of minor importance for the stage-specific abundance pattern in our study. This outcome is probably a consequence of the stable, low salinity levels observed in the port area during the sampling period, which may have reduced any potential effects of salinity stress on the population dynamics. Peitsch (1992) studied egg production rates of *E. affinis* in the Elbe estuary and found maximum egg production rates in April, followed by a decline in June, with a subsequent rise at the end of July, which aligns with the seasonal pattern of abundance peaks observed in our study. The author attributed the increase in reproductive activity to the onset of the phytoplankton bloom, which was triggered by the rise in temperatures. High food availability and quality can enhance the fecundity of *E. affinis* (Gasparini *et al.*, 1999; Burdloff *et al.*, 2000) and thus influence the population growth (Allan, 1976; Mauchline *et al.*, 1998). However, our RDA results indicated that Chl *a* concentrations had only a slight influence on the stage-specific abundances of *E. affinis*, although Chl *a* concentrations peaked in April and mid-July at the time of increased abundances. The limited effect could result from the constrained explanatory power of the RDA, which explained only 17.4% of the total variability in the stage-specific succession. This suggests that additional factors, such as predation (see Thiel *et al.*, 1996), may play an important role in shaping the population dynamics that were not assessed in this study. Furthermore, our analysis lacked information

on reproductive parameters (e.g. clutch size, egg production rates), preventing us from drawing direct conclusions about population recruitment, which should be included into future research. In addition, we observed that maximum Chl *a* concentrations in the port region were six times higher than those in the brackish zone (see Peitsch, 1992), which is in agreement with recent studies on phytoplankton dynamics in the Elbe estuary (e.g. Kamjunke *et al.*, 2023; Martens *et al.*, 2024). In contrast to the port region, the oligohaline zone exhibited at least twice the SPM concentrations (over 200 mg l<sup>-1</sup>) according to Peitsch (1992), which may have caused stronger light limitation and consequently reduced phytoplankton growth. The study by Biederbick *et al.* (2024) suggests that *E. affinis* encounters suboptimal feeding conditions in the oligohaline zone, while organisms in the port region benefit from abundant high-quality phytoplankton due to the inflow from the upstream, non-dredged freshwater region. We therefore assume that the *E. affinis* population in the port region is likely less affected by food limiting conditions compared to that in the oligohaline zone (see Peitsch, 1992).

The winter sampling period was characterised by both low temperatures and limiting food conditions, which may have contributed to the decline of the *E. affinis* population. The winter population consisted almost exclusively of older copepodite stages (i.e. C4, C5) and adults, suggesting an overwintering strategy that may be associated with the formation of resting eggs, which is well-known for *E. affinis* (e.g. Ban and Minoda, 1994; Glippa *et al.*, 2011). A short-term decrease in abundance was also observed in mid-June in both years, coinciding with the end of the spring bloom, followed by a sharp drop in the oxygen saturation. This pronounced reduction in O<sub>2</sub> concentration after blooming conditions is widely documented and has often been linked to phytoplankton degradation processes, particularly in the port region of the Elbe estuary (Dähnke *et al.*, 2022; Kamjunke *et al.*, 2023). Mialet *et al.* (2010) and Appeltans (2003) found that in the Scheldt estuary the spatio-temporal distribution of *E. affinis* becomes limited at oxygen levels below 3 to 4 mg l<sup>-1</sup> in summer (approximately 35 to 47 % oxygen saturation). However, we could not detect a direct influence of O<sub>2</sub> on the stage-specific succession of *E. affinis*, despite oxygen saturation occasionally fell below these thresholds. This may be due to the limited temporal resolution of our study, which may not capture the effects of short-term oxygen fluctuations on the population dynamics.

### Population development, growth and production

Both field and laboratory studies demonstrated that *E. affinis* undergoes isochronal development that is closely linked to temperature changes (Peitsch, 1992; Mauchline *et al.*, 1998; Peterson, 2001), allowing us to calculate stage durations using a temperature-related regression (Corkett and McLaren, 1970). Isochronal development does not apply to the naupliar stage N1, which is a non-feeding stage that relies on lipid reserves for growth and must therefore develop faster to reach the first feeding stage (Peterson, 2001). We found stage-specific development times for *E. affinis* ranging from 0.72 d in summer to 5.63 d in winter. However, Peitsch (1992) assessed stage durations of *E. affinis* in the Elbe estuary using in situ measurements and found slightly longer development times than those derived from the Bělehrádek (1935) equation and explains these differences with food limitation in the oligohaline zone. Considering the better nutritional conditions in the port region, we assume that variations in development times were primarily influenced by temperature. Generally, individual body size is negatively correlated with temperature (Horne *et al.*, 2016; Evans *et al.*, 2020), which was most evident during the June sampling at maximum temperature. However, stage-specific body sizes, and hence individual dry weights, followed a seasonal trend aligned with the timing of the phytoplankton blooms, with the lowest body sizes in winter and during the collapse of the spring bloom, and the highest values in April. We assume that food conditions had a larger effect on individual length and thus individual dry weights of *E. affinis* than temperature, which is in line with the results of Peitsch (1992, 1995) for the Elbe, as well as for other estuarine systems (e.g. Burkill and Kendall, 1982). Multiple studies have shown that the egg production in copepods is often strongly associated with seasonal changes in the body size of adult females. Large females of *E. affinis* typically produce not only larger eggs, but also a greater clutch size than smaller individuals (Ban, 1994; Lloyd *et al.*, 2013; Souissi and Souissi, 2021). Consequently, the increased body sizes of *E. affinis* female adults in spring, likely resulting from rising temperatures and improved food conditions, may have promoted population recruitment, leading to greater abundances.

This relationship may also be reflected in the seasonal pattern of the growth rates, biomass and production rates, which were often clearly higher than those reported in other studies for *E. affinis* copepodites (e.g. Allan *et al.*, 1976; Burkill and Kendall, 1982; Peitsch, 1995). Stage-specific daily growth rates varied widely, ranging from 0.02 to 1.05 d<sup>-1</sup> for copepodites and peaking in summer, whereas Peitsch (1995) reported maximum growth rates of only up to 0.36 d<sup>-1</sup> in spring. Growth rates seemed less affected by seasonal variations in individual weights, which were highest in spring, and more influenced by shorter development times due to higher temperatures in summer. In addition, the total biomass of *E. affinis* peaked at 1067 µg l<sup>-1</sup> and 629 µg l<sup>-1</sup> during the spring and summer bloom, respectively, which was distinctly higher compared to that recorded in the oligohaline zone of the Elbe estuary (about 300 µg l<sup>-1</sup>) (Peitsch, 1995), the Chesapeake Bay (218 µg l<sup>-1</sup>) (Allan *et al.*, 1976) or the Bristol Channel (22 µg l<sup>-1</sup>) (Burkill and Kendall, 1982). Secondary production also followed the seasonal pattern of species abundance and total biomass, which was more than five times higher than production estimates for *E. affinis* copepodites reported by Peitsch (1995). Higher growth and production rates may be due to much higher Chl *a* concentrations, lower turbidity and smaller salinity fluctuations experienced by *E. affinis* populations in the port region of the Elbe estuary, compared to the other estuarine studies (e.g. Allan *et al.*, 1976; Burkill and Kendall, 1982; Peitsch, 1995). Increased energy costs associated with the need for food selection and osmoregulation might have limited the population growth of *E. affinis* in these respective studies.

## **Mortality**

Based on the sampling design of this study, we applied the vertical life table (VLT) approach of Aksnes and Ohman (1996) to calculate mortality rates. Unlike the horizontal approach, which requires tracking the same individuals of a cohort over time (e.g. Lagrangian sampling approach), the vertical method focuses on the overall population structure rather than individual cohort dynamics by assuming a stable, proportional stage structure with constant survival and recruitment rates at a single point in time (Ohman, 2012). The VLT approach mitigates the effect of spatial and temporal variability in the population dynamics, including advective processes, by determining average population mortality across multiple stations

and periods (Aksnes and Ohman, 1996). Consequently, we calculated mean mortality rates by averaging the rates during periods of peak abundances, resulting in two estimates for the spring assemblages and one for the summer assemblage. Winter mortality rates were often negative, particularly for young copepodite stage groups, likely due to their very low abundances. As a result, these estimates were excluded from the analysis.

Negative mortality rates were also observed for the stage group C1/C2 and, to a lesser extent, for C2/C3 during spring and summer growth seasons. Such negative estimates can occur when abundances fluctuate strongly between samples or when more individuals are present in the subsequent stage, which suggests a potential violation of the VLT assumptions (Aksnes and Ohman, 1996). We suspect that younger stages may have been underrepresented in our samples because they tend to drift downstream more easily than older stages, a phenomenon previously described by Peitsch and Kausch (1993) for *E. affinis* in the Elbe estuary. In general, the first copepodite stages tend to live near the surface and start to begin vertical migration at a later stage, such as C4 in *Calanus* for example (McLaren, 1963). Peitsch and Kausch (1993) assume that older stages of *E. affinis* migrate more efficiently to areas with lower water velocities, for e.g. to the bottom, resulting in a reduction in their displacement. This spatial segregation may also affect mortality estimates for nauplii, despite their high mortality rates. However, their greater abundance compared to C1 copepodites might have outweighed this effect.

Both the N1:6/C1 and C5/adult stage groups exhibited the highest mortality rates, reaching up to 0.54 and 0.78 d<sup>-1</sup>, respectively. A similar pattern was found for the Schlei fjord, where mortality rates of *E. affinis* C5/adult stage group ranged from 0.73 to 0.78 d<sup>-1</sup> (Christiansen, 1988). Peitsch (1992) reported mortality rates of up to 0.77 d<sup>-1</sup> for stage group C5/adult in the oligohaline zone of the Elbe estuary, while nauplii mortality was lower, peaking at 0.26 d<sup>-1</sup>. High mortality rates in the N6/C1 and C5/adult stage groups are common in copepods, as they are associated with high energy costs during the morphological transition to the first and last copepodite stage (e.g. Peterson, 2001; Marion *et al.*, 2016). Nauplii often face a large risk of predation mortality due to their limited swimming and escape abilities (Kiørboe and Sabatini, 1995), while adult copepods encounter high costs for reproduction efforts,

particularly in mate searching and egg production (Peterson, 2001; Kiørboe *et al.*, 2015). Several studies have shown that males often have higher mortality rates than females, due to shorter life spans and increased predation risk while searching for females to mate with (Mauchline *et al.*, 1998; Kiørboe, 2006; Kiørboe *et al.*, 2015). However, our results indicate slightly higher mortality rates for females than males, which might be also reflected in the male-skewed adult sex ratio. Unfortunately, we cannot determine whether these differences are of physiological origin, species behaviour or due to methodological limitations of this study. Mortality rates and sex ratios in *E. affinis* populations have been poorly studied, making comparisons very difficult and highlighting the need for future research.

## Outlook

We showed that improved food conditions during the spring and summer phytoplankton bloom in the port region likely enhanced the recruitment and growth of *E. affinis*, resulting in higher population abundances compared to the findings of Peitsch (1992) for the oligohaline zone of the Elbe estuary. Changes in temperature and food conditions have the most significant effect on the life history traits of *E. affinis*. Consequently, climate change related effects, such as warming and sea level rise, along with human-induced impacts on the water quality, e.g. increased turbidity due to further dredging events (Kerner, 2007; van Maren *et al.*, 2015), could affect the phenology, development times, growth, and survival of the *E. affinis* population in the Elbe estuary. The population dynamics of this most abundant copepod in the Elbe estuary (Peitsch, 1992; Bernát *et al.*, 1994) could impact the food web dynamics and consequently the ecosystem functioning, and should therefore be taken into account for ecosystem-based management.

## Data availability

Data are available in the research data repository of the University of Hamburg, at <http://doi.org/10.25592/uhhfdm.16618>.

## Acknowledgement

The authors would like to thank Laura Öhm, Julia Fuchs and Celine Imker for the support during the sampling process. We highly appreciate the technical support of Martina Wichmann in the lab.

## Declaration of interest

None to declare.

## Funding

This project was funded by the Deutsche Forschungsgemeinschaft (DFG, German Research Foundation) within the Research Training Group 2530: “Biota-mediated effects on Carbon Cycling in Estuaries” (project number 407270017; contribution to Universität Hamburg and Leibniz-Institut für Gewässerökologie und Binnenfischerei im Forschungsverbund Berlin e.V. (IGB)) and by the Bundesministerium für Bildung und Forschung (BMBF) within the project “Blue Estuaries” (project number 03F0864C).

## Supplementary material

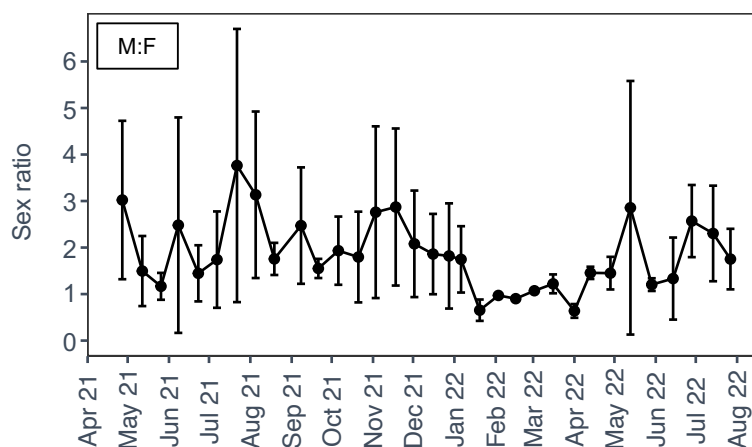


Fig. S 3.1: Sex ratio of males to females of *Eurytemora affinis* at the pier Seemannshöft for the respective sampling period.

CHAPTER 3: POPULATION DYNAMICS OF *EURYTEMORA AFFINIS*

Table S 3.1: Stage-specific individual dry weights ( $\mu\text{g}$ ) of *Eurytemora affinis* for the respective sampling period. The dry weights for nauplii (N1-N6, pooled) are based on average total length measurements.

| Stage<br>Date | Individual dry weight ( $\mu\text{g}$ ) |      |      |      |      |      |        |       |
|---------------|-----------------------------------------|------|------|------|------|------|--------|-------|
|               | N1-N6                                   | C1   | C2   | C3   | C4   | C5   | Female | Male  |
| 2021-04-27    | 0.24                                    | 0.61 | 1.12 | 2.34 | 3.43 | 7.57 | 15.81  | 11.47 |
| 2021-05-12    | 0.24                                    | 0.61 | 1.12 | 2.34 | 3.43 | 7.57 | 15.81  | 11.47 |
| 2021-05-26    | NA                                      | 0.51 | 1.06 | 2.09 | 3.98 | 6.36 | 12.89  | 7.83  |
| 2021-06-08    | NA                                      | 0.51 | 1.06 | 2.09 | 3.98 | 6.36 | 12.89  | 7.83  |
| 2021-06-23    | NA                                      | 0.39 | 0.83 | 1.37 | 2.91 | 4.03 | 6.79   | 5.32  |
| 2021-07-07    | 0.25                                    | 0.39 | 0.83 | 1.37 | 2.91 | 4.03 | 6.79   | 5.32  |
| 2021-07-22    | NA                                      | 0.57 | 1.01 | 2.10 | 4.32 | 7.01 | 10.24  | 8.27  |
| 2021-08-05    | 0.30                                    | 0.57 | 1.01 | 2.10 | 4.32 | 7.01 | 10.24  | 8.27  |
| 2021-08-19    | NA                                      | 0.57 | 1.01 | 2.10 | 4.32 | 7.01 | 10.24  | 8.27  |
| 2021-09-08    | 0.21                                    | 0.52 | 0.97 | 2.06 | 3.42 | 6.53 | 12.90  | 8.51  |
| 2021-09-21    | NA                                      | 0.52 | 0.97 | 2.06 | 3.42 | 6.53 | 12.90  | 8.51  |
| 2021-10-06    | 0.33                                    | 0.74 | 1.09 | 2.29 | 4.16 | 6.01 | 9.63   | 6.84  |
| 2021-10-21    | NA                                      | 0.74 | 1.09 | 2.29 | 4.16 | 6.01 | 9.63   | 6.84  |
| 2021-11-03    | 0.35                                    | 0.63 | 1.21 | 2.22 | 3.47 | 7.23 | 13.98  | 8.81  |
| 2021-11-18    | NA                                      | 0.63 | 1.21 | 2.22 | 3.47 | 7.23 | 13.98  | 8.81  |
| 2021-12-02    | 0.39                                    | 0.58 | 1.16 | 2.09 | 3.80 | 6.48 | 11.59  | 8.55  |
| 2021-12-16    | NA                                      | 0.58 | 1.16 | 2.09 | 3.80 | 6.48 | 11.59  | 8.55  |
| 2021-12-28    | 0.38                                    | 0.55 | 1.00 | 1.96 | 3.53 | 5.77 | 9.51   | 7.43  |
| 2022-01-06    | NA                                      | 0.55 | 1.00 | 1.96 | 3.53 | 5.77 | 9.51   | 7.43  |
| 2022-01-20    | 0.38                                    | 0.55 | 1.00 | 1.96 | 3.53 | 5.77 | 9.51   | 7.43  |
| 2022-02-03    | 0.58                                    | 0.78 | 1.54 | 2.68 | 4.37 | 7.84 | 10.32  | 8.42  |
| 2022-02-16    | NA                                      | 0.78 | 1.54 | 2.68 | 4.37 | 7.84 | 10.32  | 8.42  |
| 2022-03-02    | 0.49                                    | 0.92 | 1.70 | 3.16 | 5.64 | 6.52 | 15.74  | 9.87  |
| 2022-03-16    | NA                                      | 0.92 | 1.70 | 3.16 | 5.64 | 6.52 | 15.74  | 9.87  |
| 2022-04-01    | 0.36                                    | 1.02 | 1.77 | 3.59 | 6.05 | 8.24 | 17.77  | 12.47 |
| 2022-04-13    | NA                                      | 1.02 | 1.77 | 3.59 | 6.05 | 8.24 | 17.77  | 12.47 |
| 2022-04-28    | 0.24                                    | 0.61 | 1.12 | 2.34 | 3.43 | 7.57 | 15.81  | 11.47 |
| 2022-05-13    | NA                                      | 0.61 | 1.12 | 2.34 | 3.43 | 7.57 | 15.81  | 11.47 |
| 2022-05-29    | 0.16                                    | 0.51 | 1.06 | 2.09 | 3.98 | 6.36 | 12.89  | 7.83  |
| 2022-06-14    | NA                                      | 0.51 | 1.06 | 2.09 | 3.98 | 6.36 | 12.89  | 7.83  |
| 2022-06-28    | 0.25                                    | 0.39 | 0.83 | 1.37 | 2.91 | 4.03 | 6.79   | 5.32  |
| 2022-07-14    | NA                                      | 0.39 | 0.83 | 1.37 | 2.91 | 4.03 | 6.79   | 5.32  |
| 2022-07-27    | 0.30                                    | 0.57 | 1.01 | 2.10 | 4.32 | 7.01 | 10.24  | 8.27  |

Table S 3.2: Development time (in days, d) of *Eurytemora affinis* across naupliar stages (N1-N6, pooled) and copepodite stages (C1 to C6, including adults). Duration of a generation (excluding eggs) is given by the sum of stage-specific development times. Data on temperature (Temp, °C) are provided for comparison.

| Temp (°C) | Stage<br>Date | Stage-specific development times (d) |      |      |      |      |      |       |       |
|-----------|---------------|--------------------------------------|------|------|------|------|------|-------|-------|
|           |               | N1-N6                                | C1   | C2   | C3   | C4   | C5   | Adult | Total |
| 10.5      | 2021-04-27    | 10.28                                | 1.90 | 1.90 | 1.90 | 1.90 | 1.90 | 1.90  | 21.70 |
| 13.4      | 2021-05-12    | 7.88                                 | 1.46 | 1.46 | 1.46 | 1.46 | 1.46 | 1.46  | 16.63 |
| 15.6      | 2021-05-26    | NA                                   | 1.22 | 1.22 | 1.22 | 1.22 | 1.22 | 1.22  | 13.87 |
| 20.0      | 2021-06-08    | 4.77                                 | 0.88 | 0.88 | 0.88 | 0.88 | 0.88 | 0.88  | 10.07 |
| 23.3      | 2021-06-23    | NA                                   | 0.72 | 0.72 | 0.72 | 0.72 | 0.72 | 0.72  | 8.17  |
| 22.5      | 2021-07-07    | 4.06                                 | 0.75 | 0.75 | 0.75 | 0.75 | 0.75 | 0.75  | 8.56  |
| 21.8      | 2021-07-22    | NA                                   | 0.78 | 0.78 | 0.78 | 0.78 | 0.78 | 0.78  | 8.94  |
| 20.8      | 2021-08-05    | 4.52                                 | 0.84 | 0.84 | 0.84 | 0.84 | 0.84 | 0.84  | 9.54  |
| 20.1      | 2021-08-19    | NA                                   | 0.88 | 0.88 | 0.88 | 0.88 | 0.88 | 0.88  | 9.98  |
| 18.3      | 2021-09-08    | 5.37                                 | 0.99 | 0.99 | 0.99 | 0.99 | 0.99 | 0.99  | 11.33 |

CHAPTER 3: POPULATION DYNAMICS OF EURYTEMORA AFFINIS

|      |            |       |      |      |      |      |      |      |       |
|------|------------|-------|------|------|------|------|------|------|-------|
| 17.8 | 2021-09-21 | NA    | 1.03 | 1.03 | 1.03 | 1.03 | 1.03 | 1.03 | 11.76 |
| 15.4 | 2021-10-06 | 6.69  | 1.24 | 1.24 | 1.24 | 1.24 | 1.24 | 1.24 | 14.11 |
| 12.4 | 2021-10-21 | NA    | 1.59 | 1.59 | 1.59 | 1.59 | 1.59 | 1.59 | 18.11 |
| 10.6 | 2021-11-03 | 10.22 | 1.89 | 1.89 | 1.89 | 1.89 | 1.89 | 1.89 | 21.57 |
| 8.4  | 2021-11-18 | NA    | 2.37 | 2.37 | 2.37 | 2.37 | 2.37 | 2.37 | 26.96 |
| 6.2  | 2021-12-02 | 16.48 | 3.05 | 3.05 | 3.05 | 3.05 | 3.05 | 3.05 | 34.80 |
| 4.2  | 2021-12-16 | NA    | 3.96 | 3.96 | 3.96 | 3.96 | 3.96 | 3.96 | 45.15 |
| 1.9  | 2021-12-28 | 30.42 | 5.63 | 5.63 | 5.63 | 5.63 | 5.63 | 5.63 | 64.23 |
| 5.2  | 2022-01-06 | NA    | 3.45 | 3.45 | 3.45 | 3.45 | 3.45 | 3.45 | 39.32 |
| 3.9  | 2022-01-20 | 22.28 | 4.13 | 4.13 | 4.13 | 4.13 | 4.13 | 4.13 | 47.04 |
| 4.1  | 2022-02-03 | 21.87 | 4.05 | 4.05 | 4.05 | 4.05 | 4.05 | 4.05 | 46.18 |
| 4.7  | 2022-02-16 | NA    | 3.70 | 3.70 | 3.70 | 3.70 | 3.70 | 3.70 | 42.20 |
| 4.8  | 2022-03-02 | 19.64 | 3.64 | 3.64 | 3.64 | 3.64 | 3.64 | 3.64 | 41.46 |
| 5.0  | 2022-03-16 | NA    | 3.57 | 3.57 | 3.57 | 3.57 | 3.57 | 3.57 | 40.75 |
| 8.7  | 2022-04-01 | 12.42 | 2.30 | 2.30 | 2.30 | 2.30 | 2.30 | 2.30 | 26.21 |
| 8.2  | 2022-04-13 | NA    | 2.42 | 2.42 | 2.42 | 2.42 | 2.42 | 2.42 | 27.56 |
| 12.9 | 2022-04-28 | 8.21  | 1.52 | 1.52 | 1.52 | 1.52 | 1.52 | 1.52 | 17.33 |
| 16.9 | 2022-05-13 | NA    | 1.10 | 1.10 | 1.10 | 1.10 | 1.10 | 1.10 | 12.56 |
| 17.7 | 2022-05-29 | 5.60  | 1.04 | 1.04 | 1.04 | 1.04 | 1.04 | 1.04 | 11.83 |
| 19.8 | 2022-06-14 | NA    | 0.90 | 0.90 | 0.90 | 0.90 | 0.90 | 0.90 | 10.22 |
| 22.3 | 2022-06-28 | 4.11  | 0.76 | 0.76 | 0.76 | 0.76 | 0.76 | 0.76 | 8.67  |
| 20.8 | 2022-07-14 | NA    | 0.84 | 0.84 | 0.84 | 0.84 | 0.84 | 0.84 | 9.52  |
| 21.7 | 2022-07-27 | 4.27  | 0.79 | 0.79 | 0.79 | 0.79 | 0.79 | 0.79 | 9.02  |

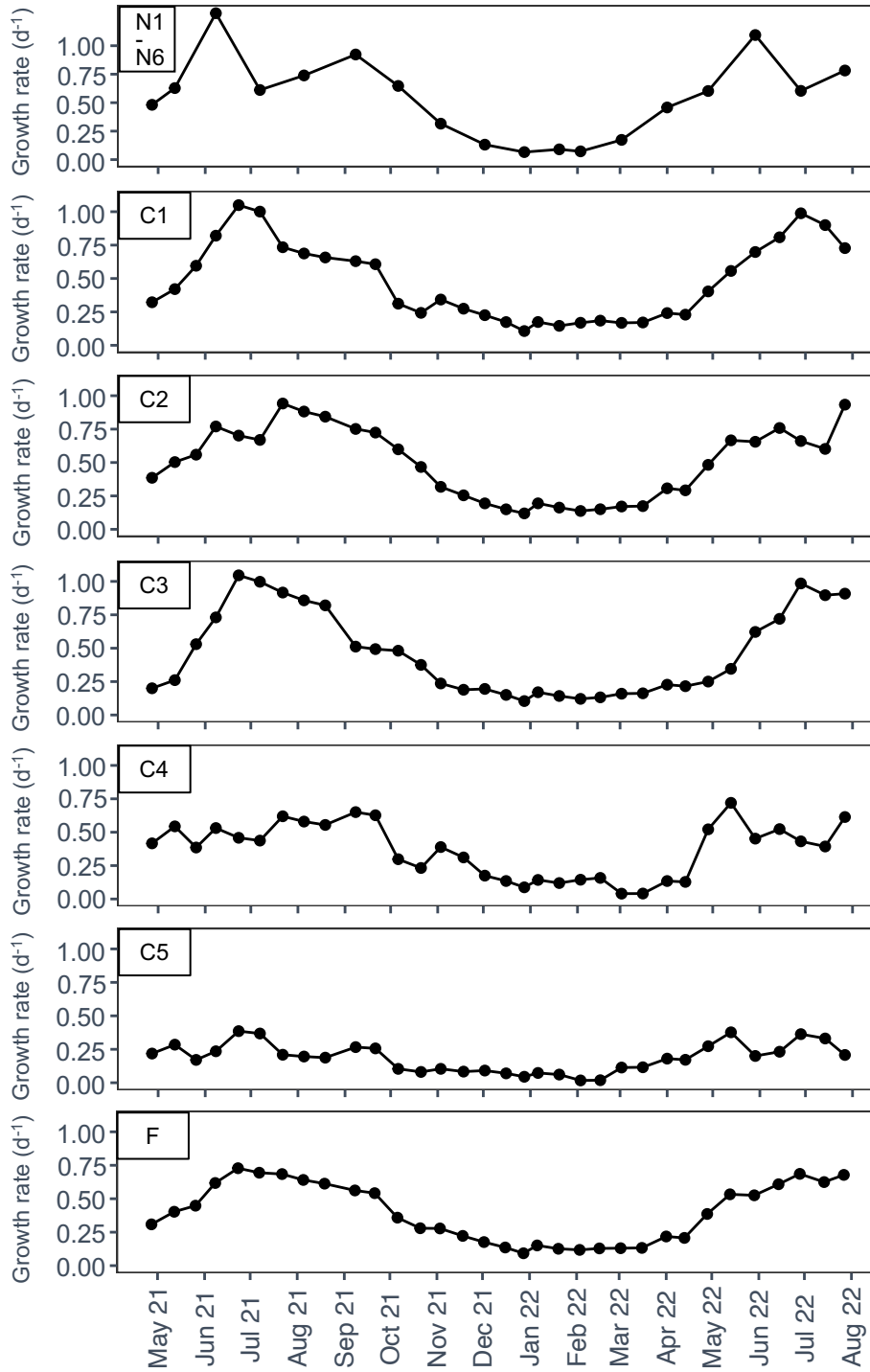
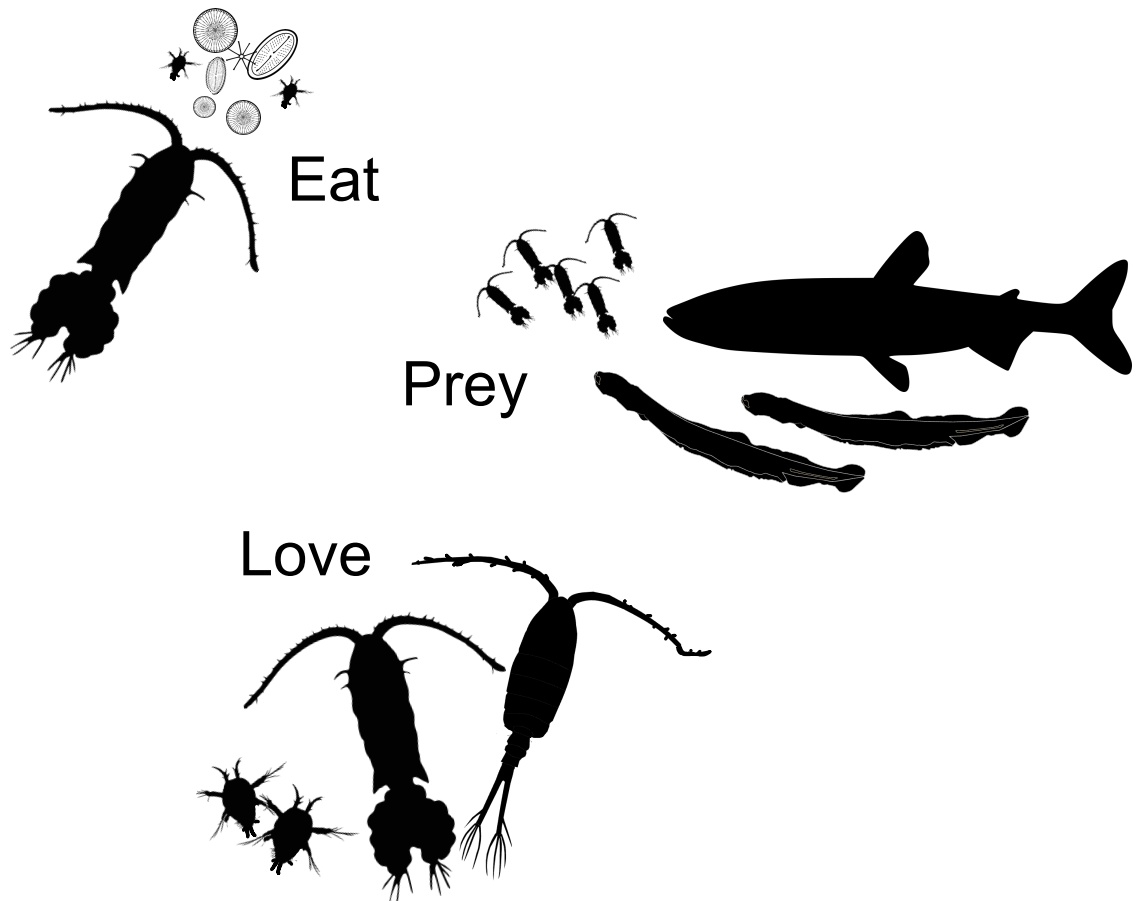


Fig. S 3.2: Stage-specific growth rates (per day,  $d^{-1}$ ) of nauplii (N1-N6, pooled) and copepodites, i.e. C1 to C5 and female (F) adults of *Eurytemora affinis*. Males were assumed not to grow. Growth rates of nauplii were averaged over all nauplii stages.

## Chapter 4: Estuarine zooplankton trophic dynamics



Manuscript published in ICES Journal of Marine Science (31/12/2024):

Biederbick, J., Möllmann, C., Hauten, E., Russnak, V., Lahajnar, N., Hansen, T., Dierking, J. and Koppelman, R. 2024. Spatial and temporal patterns of zooplankton trophic interactions and carbon sources in the eutrophic Elbe estuary (Germany), ICES Journal of Marine Science, 0(0). <https://doi.org/10.1093/icesjms/fsae189>

Pictograms used with permission from Elena Hauten.

**Title:** Spatial and temporal patterns of zooplankton trophic interactions and carbon sources in the eutrophic Elbe estuary (Germany)

**Running title:** Estuarine zooplankton trophic dynamics

**Authors:** Johanna Biederbick<sup>1\*</sup>, Christian Möllmann<sup>1</sup>, Elena Hauten<sup>1</sup>, Vanessa Russnak<sup>2</sup>, Niko Lahajnar<sup>3</sup>, Thomas Hansen<sup>4</sup>, Jan Dierking<sup>4</sup> and Rolf Koppelman<sup>1</sup>

<sup>1</sup>Institute of Marine Ecosystem and Fishery Science, University of Hamburg, Grosse Elbstrasse 133, 22767 Hamburg, Germany.

<sup>2</sup>Helmholtz-Centre Hereon, Institute of Carbon Cycles, Max-Planck-Strasse 1, 21502 Geesthacht, Germany

<sup>3</sup>Institute for Geology, University of Hamburg, Bundesstrasse 55, 20146 Hamburg, Germany

<sup>4</sup>GEOMAR Helmholtz Centre for Ocean Research Kiel, Wischhofstrasse 1-3, 24148 Kiel, Germany

\*Corresponding author

E-Mail: [johanna.biederbick@uni-hamburg.de](mailto:johanna.biederbick@uni-hamburg.de)

## Abstract

Zooplankton in estuaries encounter complex physical and biogeochemical processes that affect the quantity, quality and origin of their food sources. The knowledge about how zooplankton deal with highly variable organic matter sources is sparse. Here, we investigated the spatial and temporal patterns of zooplankton trophic dynamics and carbon sources in the intensively dredged, eutrophic Elbe estuary. For this purpose, we applied elemental and stable isotope analysis ( $\delta^{13}\text{C}$  and  $\delta^{15}\text{N}$ ) on particulate organic matter (POM) and dominant meso- and macrozooplankton species including ichthyoplankton from five stations along the entire salinity gradient of the estuary in 2022. The  $\delta^{13}\text{C}$  values of POM (-29.2 to -23.0 ‰) indicated a mixture of riverine, terrestrial and coastal carbon sources used by most taxa for their diet. *Eurytemora affinis* (-34.0 to -23.3 ‰) and *Mesopodopsis slabberi* (-22.2 to -20.0 ‰) exhibited a broader range in  $\delta^{13}\text{C}$  than POM, suggesting selective feeding on single POM components depending on the season. In winter and autumn, under high suspended matter loads and limited availability of high-quality autochthonous phytoplankton, zooplankton showed increased tendency for carnivory (higher  $\delta^{15}\text{N}$  values). Our study revealed a high trophic plasticity of estuarine Elbe zooplankton to buffer hydrological related alterations in their food source by dietary niche partitioning and a flexible switch in their feeding behaviour.

Keywords: Elbe estuary, estuarine zooplankton, trophodynamics, stable isotopes, allochthonous and autochthonous carbon sources, selective feeding

## Introduction

Planktonic organisms play an important role in the production and transfer of organic matter and energy in aquatic ecosystems (Barnett *et al.*, 2007; Koppelman *et al.*, 2009). Especially in estuaries, planktonic communities are affected by strong variability in environmental conditions, leading to complex food web structures. Estuaries are highly productive transition zones at the interface between freshwater and marine ecosystems and are characterised by physical (e.g. river discharge, tidal advection) and biogeochemical gradients (e.g. cycling of organic matter, nutrients and suspended solids) on various spatial and temporal scales (Hyndes *et al.*, 2014; Geerts *et al.*, 2017; Boynton *et al.*, 2018; Kamjunke *et al.*, 2023). These highly valuable habitats fulfil essential ecological functions such as transfer and sequestration of organic matter (Hyndes *et al.*, 2014), recycling and filtering of nutrients (Boynton *et al.*, 2018), refuge and nursery grounds for crustaceans and fish (Wilson, 2002), and coastal protection (Koch *et al.*, 2009). At the same time, estuaries are often severely impacted by anthropogenic stressors such as diking, dredging and eutrophication (Kerner, 2007; Cloern *et al.*, 2016).

Anthropogenic pressures and estuarine gradients impact the fate of organic matter transfer throughout different trophic levels, resulting in alterations of the food web structures and functions (Benfield, 2012). Estuaries are defined by strong tidal mixing and high concentrations of nutrients and suspended particulate matter, which affect the production of autochthonous organic matter (Turner *et al.*, 2022). Primary production is therefore often restricted to upstream freshwater areas, where light conditions are more favourable, and salinity stress and water turnover is reduced (Muylaert *et al.*, 2005). Fresh phytoplankton biomass, the most nourishing food source for zooplankton (Müller-Solger *et al.*, 2002), is therefore less accessible to primary consumers in turbid zones (Benfield, 2012). In addition, excessive loads of organic matter in estuaries facilitate microbial colonisation (Zimmermann-Timm *et al.*, 1998), resulting in intense remineralisation processes (Middelburg and Herman, 2007; Kamjunke *et al.*, 2023), which increase microbial pathways in the pelagic food web (Stoecker and Capuzzo, 1990; Lerner *et al.*, 2022). This leads to strong fluctuations in the quality of food sources, which can shift from fresh phytoplankton

to detrital, recalcitrant and less nutritious carbon sources (Müller-Solger *et al.*, 2002). Despite this high importance, the role and dynamics of detrital sources and autochthonous organic matter in the trophodynamic of estuarine zooplankton are still not well understood. Fundamental knowledge of trophic interactions within estuarine planktonic communities is needed to understand the impact of increasing human pressures on estuarine food webs and to provide a tool for ecosystem-based management and conservation.

Assessing the trophodynamics of estuarine zooplankton is difficult due to the potential diversity of different available organic sources, which include detrital, allochthonous material derived from terrestrial origin (e.g. C3 and C4 plants, soil organic matter), as well as primary producers from riverine and marine environments (e.g. phytoplankton, benthic algae), along with heterotrophic sources, such as flagellates, ciliates. Stable isotope analysis (SIA) is a powerful tool to disentangle the structure of planktonic food webs. Carbon isotope composition in consumers change little with the progression through a food web and thus reflect the time-integrated isotope composition of their diet (DeNiro and Epstein, 1978). In addition, trophic levels (TLs) for different organisms can be calculated based on their nitrogen isotope composition, which shifts in a predictable manner from one trophic level to the next (DeNiro and Epstein, 1981). In general, primary carbon sources differ markedly in their stable isotopic signal, making them distinguishable as dietary sources for planktonic consumers and has already been investigated in numerous estuarine studies (Thornton and McManus, 1994; Cloern *et al.*, 2002; Martineau *et al.*, 2004; Middelburg and Herman, 2007; Christianen *et al.*, 2017). Marine phytoplankton typically exhibit carbon and nitrogen isotopic values ranging between -22 and -17 ‰ and from 3 to 12 ‰, respectively, while freshwater algal material usually have  $\delta^{13}\text{C}$  values between -32 and -23 ‰ and around 5 ‰ for  $\delta^{15}\text{N}$  (Boutton, 1991; Maksymowska *et al.*, 2000; Finlay and Kendall, 2007). Benthic algae that contribute to the pelagic organic sources through resuspension exhibit  $^{13}\text{C}$ -enriched values between -22 and -11 ‰ and  $\delta^{15}\text{N}$  values from 3 to 9 ‰ (Maksymowska *et al.*, 2000; Christianen *et al.*, 2017). Terrestrial sources, including C3 and C4 plants, as well as soil organic matter, also have distinct isotopic characteristics; C3 plants and soil organic matter range between -27.0 and -26.0 ‰ for  $\delta^{13}\text{C}$  and from 3 to 18 ‰ for  $\delta^{15}\text{N}$ , whereas C4 plants are characterised by  $\delta^{13}\text{C}$  values between -17 to -9 ‰ and  $\delta^{15}\text{N}$  values from 3 to 7 ‰

(Maksymowska *et al.*, 2000; Cloern *et al.*, 2002; Finlay and Kendall, 2007). In addition, these terrestrial sources differ considerably in their carbon to nitrogen ratios as a result of degradation processes, with ratios ranging from 15 to 50 for terrestrial plants and from 8 to 25 for soil organic matter, in contrast to that of fresh algal sources (below 8) (Thornton and McManus, 1994; Finlay and Kendall, 2007). Moreover, stable isotopes also yield information about the width and overlap of the dietary niches of different organisms, and thus dietary niche differentiation (Newsome *et al.*, 2007). SIA provides time-integrated dietary information over longer time periods, contrary to conventional methods, such as gut content analysis and feeding experiments, which offer short-term insights into dietary preferences (Dalerum and Angerbjörn, 2005). The stable isotopic composition of organisms can therefore give a time- and space-integrated view of trophic interactions (Newsome *et al.*, 2007) and is thus ideal for highly dynamic habitats such as estuaries.

The Elbe estuary, a highly turbid environment characterised by strong estuarine gradients and anthropogenic stressors, has so far received limited attention in determining planktonic food web structures. It is one of Europe's largest tidal estuaries located in north-west Germany, and serves multiple ecological functions, including refuge for many zooplankton and fish species (Bernát *et al.*, 1994; Eick and Thiel, 2014). It is also of significant socio-economic importance, particularly due to its connection to the seaport of the city of Hamburg. Over the last decades, the Elbe estuary has experienced reoccurring morphological modifications due to channel diking and dredging events to facilitate access to Hamburg Harbour (Kerner, 2007; Papenmeier *et al.*, 2014). As a result, the navigation channel exhibits a rapid change in bathymetry, with water depths ranging from approximately 5 m at the eastern edge of the city of Hamburg up to 20 m downstream of the port area (Federal Waterways and Shipping Agency (WSV), 2023). This sudden increase in water depth results in longer water residence times in and downstream the port area, leading to enhanced accumulation of suspended particles and consequently to elevated turbidity (Kerner, 2007; Geerts *et al.*, 2017). Previous studies have indicated that this bathymetric jump in the port area contributes to a strong decline in phytoplankton biomass due to light limitation and sedimentation of algal cells to deeper layers (Wolfstein and Kies, 1995; Dähnke *et al.*, 2022; Kamjunke *et al.*, 2023; Steidle and Vennell, 2024),

which, in turn, increase remineralisation processes (Sanders *et al.*, 2018; Kamjunke *et al.*, 2023). Most of the particulate organic matter in the Elbe estuary therefore consists of allochthonous, decaying algae that originates from the shallow, non-dredged freshwater area upstream of the port (Geerts *et al.*, 2017). Downstream of the port area, the organic matter source contains allochthonous material from adjacent coastal regions, primarily marine-like substances (Tobias-Hünefeldt *et al.*, 2024), which are resuspended from deeper bottom water due to strong mixing forces (Spieckermann *et al.*, 2021). In addition, the Elbe estuary is characterised by a semidiurnal, flood-dominated tidal wave that leads to steady resuspension of organic substances from benthic sources into the water column (Spieckermann *et al.*, 2021).

Although the Elbe estuary is well-studied in terms of organic and particle matter dynamics, the role and fate of autochthonous and allochthonous organic matter in its planktonic food web, along with the spatio-temporal dynamics of utilising different organic matter sources by zooplankton, has never been fully investigated. So far, Kerner *et al.* (2004) have studied the carbon utilisation of micro- and mesozooplankton species only in the freshwater area of the Elbe estuary using carbon isotopes. The authors found marked shifts in the use of the consumers' carbon sources on a seasonal scale.

Here, we address this knowledge gap by investigating the trophodynamics of the planktonic food web along the entire salinity gradient of the Elbe estuary from seasonal samplings in 2022. We applied a carbon and nitrogen stable isotope analysis to five dominant zooplankton taxa in the Elbe estuary (see Fiedler, 1991; Bernát *et al.*, 1994; Eick and Thiel, 2014), including the calanoid copepod *Eurytemora affinis* (Pope, 1880), two mysids (*Mesopodopsis slabberi* (Van Beneden, 1861) and *Neomysis integer* (Leach, 1814)), the gammarid *Gammarus zaddachi* (Sexton, 1912), as well as fish larvae of *Osmerus eperlanus* (Linnaeus, 1758). As in many other temperate estuaries of the northern hemisphere (e.g. Martineau *et al.*, 2004; Hoffman *et al.*, 2008; David *et al.*, 2016), *E. affinis* is the most abundant calanoid copepod in the Elbe estuary, accounting for over 90% of the mesozooplankton abundance throughout the seasons (Bernát *et al.*, 1994) and thereby representing an important component of the planktonic food web (Kerner, 2004). In addition

to the ubiquitous suprabenthic gammarid *G. zaddachi*, the two sympatric mysids, *M. slabberi* and *N. integer*, contribute significantly to the total zooplankton biomass, dominating the brackish and freshwater sections of the Elbe estuary, respectively (Fiedler, 1991; Bernát *et al.*, 1994). The fish assemblage consists of more than 95% of the species *O. eperlanus*, which uses the estuarine part of the Elbe River as an important nursery and feeding ground (Eick and Thiel, 2014). We also collected bulk particulate organic matter (POM) at each station and analysed its stable isotopic composition to compare it with potential organic matter sources and to determine its availability to the selected zooplankton taxa across both spatial and temporal scales. The objectives of this study were to (1) determine the isotopic signatures of the local POM and selected zooplankton species across spatio-temporal dimensions, and to (2) compare their  $\delta^{13}\text{C}$  signatures with carbon baselines reported in the literature to assess the origin of their primary carbon source. In addition, the stable isotope approach enabled us to (3) gain insights in the consumers' trophic positions and dietary niches.

## Methods

### Study area

The Elbe River is one of the major rivers in Europe, discharging through the Czech Republic and Germany into the German Bight in the North Sea. Its turbid estuary has a length of 142 km reaching from the weir at Geesthacht (Elbe-km 585, Fig. 4.1) to the river mouth at Cuxhaven (Elbe-km 727). The main channel has been heavily dredged multiple times since the beginning of the last century from a depth of 4 m (Kerner, 2007) to approximately 20 m by 2021 (Hamburg Port Authority (HPA), 2022) to enable access to the Port of Hamburg, the third largest port in Europe for overseas traffic, located 39 km downstream of the weir. The tidal range varies from 2 m at the weir to 3.5 m in the port area (HPA, 2022). The water column is partially well-mixed (Pein *et al.*, 2021) and characterised by a long residence time of two to four weeks depending on river discharge (Amann *et al.*, 2012). It includes a

prominent maximum turbidity zone (MTZ) that extends 30 km and is located around Glückstadt (Elbe-km 674) (Papenmeier *et al.*, 2014).

Table 4.1: Overview of the sampling sites and tidal phases during sampling.

| Station (Abbreviation) | Coordinates              |                           | Elbe-km | Mean salinity $\pm$ SD | Tidal phase |
|------------------------|--------------------------|---------------------------|---------|------------------------|-------------|
|                        | Latitude ( $^{\circ}$ N) | Longitude ( $^{\circ}$ E) |         |                        |             |
| Bunthäuser Spitze (BH) | 53.45                    | 10.07                     | 609     | 0.4 $\pm$ 0.1          | Low tide    |
| Mühlenberger Loch (ML) | 53.55                    | 9.82                      | 633     | 0.4 $\pm$ 0.1          | High tide   |
| Schwarztonnensand (ST) | 53.71                    | 9.47                      | 665     | 0.7 $\pm$ 0.2          | High tide   |
| Brunsbüttel (BB)       | 53.89                    | 9.19                      | 692     | 6.1 $\pm$ 4.2          | Low tide    |
| Medemgrund (MG)        | 53.84                    | 8.89                      | 713     | 11.4 $\pm$ 7.1         | Low tide    |

Elbe-km: Stream kilometre

### Sample collection and processing

Sampling was performed during one-day cruises with the research vessel *Ludwig Prandtl* in the main channel at five stations along the entire salinity gradient in winter (February), spring (May), summer (June) and autumn (November) 2022 (Table 4.1). Sampling was scheduled to the same appointed time in the tidal cycle each time, ensuring consistent conditions between the campaigns. Stations were situated in the freshwater area upstream in the non-dredged channel (Bunthäuser Spitze (BH) at Elbe-km 609), within the port area (Mühlenberger Loch (ML) at Elbe-km 633), within the MTZ (Schwarztonnensand (ST) at

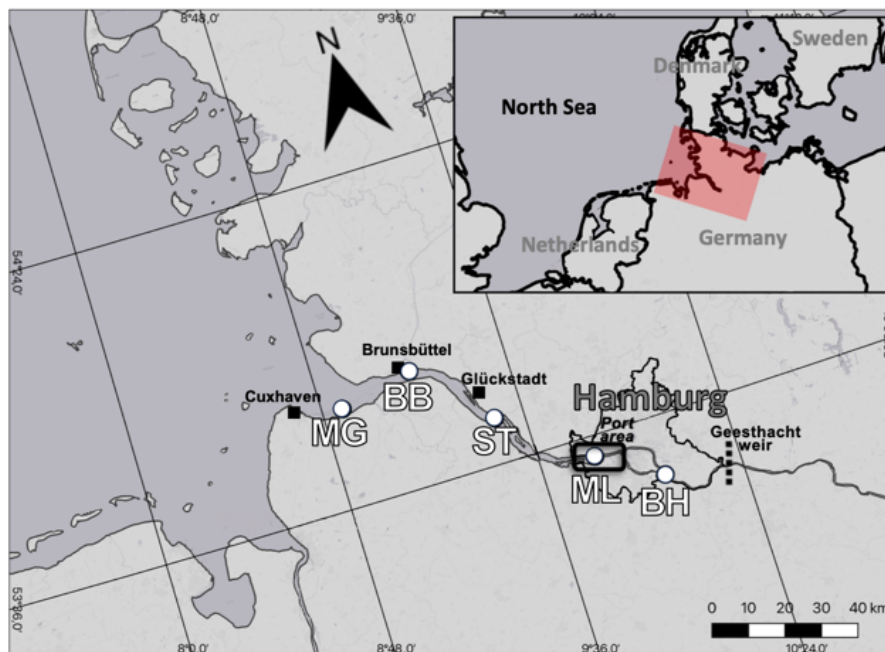


Fig. 4.1: Map of the Elbe estuary showing the five sampling locations. Station names abbreviated (see Table 4.1 for explanation). The weir at Geesthacht separates the estuary from the Elbe river. The background map has been provided by Esri, HERE, Garmin, © OpenStreetMap contributors, and the GIS User.

Elbe-km 665), in the oligohaline zone (Brunsbüttel (BB) at Elbe-km 692) and mesohaline zone in the river mouth (Medemgrund (MG) at Elbe-km 727) (Fig. 4.1). At each station, net samples were taken by single horizontal tows at 1 m water depth using plankton nets of 100  $\mu\text{m}$  (90 cm aperture, 3 m length) and 1000  $\mu\text{m}$  (0.94 m aperture, 2.8 m net length) mesh size. Mesozooplankton and macrozooplankton was defined as organisms with a size between 100 – 1000  $\mu\text{m}$  and 1 – 20 cm, respectively. Water samples were collected at 1 m water depth with multiple bucket hauls and filtered through pre-combusted and pre-weighted glass fibre filters (0.7  $\mu\text{m}$  pore size, GF/F, Whatman, 450°C). The filtered water volume was adjusted at each station based on the concentration of suspended organic material to adequately coat the filters with biomass. At each station, three filters were taken to measure either chlorophyll *a* (Chl *a*) concentrations, suspended particulate matter (SPM) and the stable isotopic (SI) compositions of POM samples (one replicate each). For the POM filters, water samples were sieved through 100  $\mu\text{m}$  mesh to remove large planktonic organisms. Filters and planktonic organisms from each haul were transferred to plastic trays and immediately stored at -80°C on board until further sorting and processing in the lab.

Temperature and salinity data were measured at each sampling site using an on-board *in situ* FerryBox system (see Petersen *et al.*, 2011 for further details). River discharge data were obtained from the closest gauge station located upstream of the tidal limit in Neu Darchau (Elbe-km 536). Daily discharge rates for the corresponding sampling date were used which can be accessed through the Federal Waterways and Shipping Agency (WSV, 2023). We compared temperature and discharge rates to historical monthly averages over short (2018-2022; past 5 years) and long-term periods (30 years) from the data portal of the WSV to check for the representativeness of the data (see supplementary material Table S4.1 for more details).

Zooplankton samples were defrosted on ice, sorted for dominant taxa by hand using ultra-fine tweezers under a stereomicroscope and rinsed twice in ultrapure water for removal of adherent particles. Dominant mesozooplankton (*Eurytemora affinis*), macrozooplankton (*Mesopodopsis slabberi*, *Neomysis integer*, *Gammarus zaddachi*) and ichthyoplankton (*Osmerus eperlanus*) taxa were analysed for stable isotopic composition. The individuals

were sorted into separate plastic vials, freeze-dried at  $-80^{\circ}\text{C}$  for 24 h and ground to fine powder before being transferred to tin capsules. Individuals of *E. affinis* was placed as whole animals directly into tin capsules after lyophilisation. For the analysis of elemental and stable isotopic composition, triplicates of at least three individuals each of macrozooplankton and fish larvae were used, if sufficient specimen were collected. Since the biomass of *E. affinis* was insufficient for triplicate measurements, single samples were analysed instead by pooling of approximately 100 adult individuals of *E. affinis*, which were equally mixed by sex.

Chl *a* was extracted by adding 10 ml of 90% acetone to the filters, which were then stored in darkness at  $5^{\circ}\text{C}$  for 24 h before centrifugation (3000 rpm,  $4^{\circ}\text{C}$ , 15 min). The absorbance of the extracts was measured at a wavelength between 630 and 750 nm using a PerkinElmer photometer (LAMBDA XLS, Waltham, USA; model number: L7110189), following the method described by Jeffrey and Humphrey (1975). Filters that were not used for Chl *a* measurements were freeze-dried at  $-80^{\circ}\text{C}$  for 24 h. SPM content was determined by weighting the dry filters. For the measurement of elemental and stable isotope ratios of POM, aliquots were cut out of the filter. Parts of the subsamples were placed into tin capsules for analysis of  $\delta^{15}\text{N}$  and C/N without prior treatment. The other aliquots were transferred to silver capsules and treated with HCL vapoured for 2 h under vacuum to remove carbonates for a separate  $\text{C}_{\text{org}}$  and  $\delta^{13}\text{C}$  analysis, as carbonates potentially causing a bias in the organic carbon measurements (Jacob *et al.*, 2005).

### **Analysis of elemental and stable isotope ratios**

Data on elemental and stable isotopic composition of planktonic organisms were compiled from three elemental analyser and isotope ratio mass spectrometer (IRMS) systems (see supplementary material (Table S4.2 for more details). SIA were performed using an elemental analyser (Euro EA CHNSO, HEKAtech, Wegberg, Germany; Thermo/Carlo Erba NC 2500, Milan, Italy; PDZ Europa ANCA-GSL, Sercon Ltd., Cheshire, United Kingdom) interfaced to an IRMS system (IsoPrime 100, Elementar, Langenselbold, Germany; DeltaPlus Advantage, Thermo Fisher Scientific, Bremen, Germany; PDZ Europa 20-20, Sercon Ltd., Cheshire, United Kingdom). Isotope ratios of carbon ( $\delta^{13}\text{C}$ ) and nitrogen ( $\delta^{15}\text{N}$ ) were expressed as parts per thousands (‰) differences from a standard reference material:

$$\delta X = \left[ \left( R_{\text{sample}} / R_{\text{standard}} \right) - 1 \right] \times 1000 \quad (\text{Eq. 4.1})$$

where  $X = {}^{13}\text{C}$  or  ${}^{15}\text{N}$  and the R the corresponding ratio  ${}^{13}\text{C}/{}^{12}\text{C}$  and  ${}^{15}\text{N}/{}^{14}\text{N}$ . Vienna Pee Dee Belemnite (VPDB) for carbon and atmospheric  $\text{N}_2$  for nitrogen were used as standard reference material. Helium was used as carrier gas.  $\text{CO}_2$  and  $\text{N}_2$  were used as working standards and were calibrated against international reference materials of the International Atomic Energy Agency (see supplementary material Table S4.2 for details).

### Statistical analysis

Seasonal and spatial variability in  $\delta^{13}\text{C}$ ,  $\delta^{15}\text{N}$  and C:N of POM, meso- and macrozooplankton including ichthyoplankton were identified using a non-parametric test, Kruskal-Wallis test, since isotope ratios were not normally distributed. Post-hoc multiple pairwise comparisons (Bonferroni corrected, Dunn's test; Dunn, 1961) were applied when differences were significant. C:N ratios were calculated based on their molar ratios. The ratio of chlorophyll *a* to SPM concentration (Chl *a*/SPM ratio) was used as an index for the phytoplankton availability that could potentially be consumed by the zooplankton (Irigoiien and Castel, 1995). Since it is difficult to separate phytoplankton from heterotrophic and detrital particulate matter including e.g. ciliates, flagellates, rotifers of similar size, POM was used as an indicator for a primary food source.  $\delta^{15}\text{N}$  ratios of the planktonic organisms were used to calculate trophic levels (TLs), assuming POM as an isotopic baseline for  $\text{TL} = 1$ . Prior trophodynamic studies on estuarine zooplankton indicate that our target species are not true herbivores, but rather omnivores with a pronounced tendency towards carnivorous feeding behaviour (e.g. Martineau *et al.*, 2004; David *et al.*, 2016). Given that trophic fractionation of nitrogen isotopes is typically higher for carnivores and other consumers with high-protein, animal-based diets, ranging from 3.3 to 3.4 ‰, compared to true herbivores, which exhibit a trophic enrichment factor (TEF) of 2 to 2.5 ‰ (Vander Zanden and Rasmussen, 2001; McCutchan *et al.*, 2003), we applied a TEF of 3.4 ‰ for our TL calculations. TLs were calculated based on the  $\delta^{15}\text{N}$  values of POM and the taxa from each station and season, according to the equation of Post (2002):

$$\text{TL} = 1 + (\delta^{15}\text{N}_{\text{zooplankton}} - \delta^{15}\text{N}_{\text{POM}}) / \text{TEF} \quad (\text{Eq. 4.2})$$

The relationships between elemental and isotope ratios of the consumers and environmental variables were assessed using Spearman rank correlation analysis (see results in the supplementary materials, Table S4.3). The multivariate ellipse-based model SIBER (software version 2.1.9, Jackson *et al.*, 2011) was applied to check for the species-specific isotopic niches. The trophic niches were calculated globally, as a minimum of at least five individual data points of  $\delta^{13}\text{C}$  and  $\delta^{15}\text{N}$  per taxon for each station and season are required to calculate either spatial or temporal niche space dynamics, which are not available in this study. Isotopic niche width ( $\%o^2$ ) was calculated by the standard ellipse function SEA (including 40% of the data) for each taxon, which was corrected for small sample size using a correction mode ( $\text{SEA}_c$ ). In addition, the overlap of isotopic niches was calculated by applying a Bayesian estimate of standard ellipses. The estimated Bayesian ellipses were tested for differences between taxa by comparing the proportion of their posterior distributions in terms of magnitude, which provides a direct measurement of the probabilities. All statistical tests and visualisations were performed using R software, software version 4.3.2 (R Core Team, 2024). An AI tool (ChatGPT, version GPT-4) was used to improve the writing style and readability of the final manuscript by identifying and correcting grammar and typographical errors.

## Results

### Environmental conditions

Temperatures at the examined stations ranged from 5.1 °C in winter to 21.4 °C in summer 2022 (Table 4.2), which falls within the range of averages recorded over the past 5 and 30 years (see supplementary material, Table S4.1). Salinity exhibited a gradual increase downstream, with the strongest gradient observed in summer and the weakest in winter. In spring and summer, strong phytoplankton blooms occurred exclusively at the uppermost freshwater station BH (132.2  $\mu\text{g l}^{-1}$  and 152.7  $\mu\text{g l}^{-1}$ , respectively), followed by a sharp decline in Chl *a* concentrations downstream from the harbour area. Chl *a* concentrations were positively correlated with temperatures (Spearman,  $n = 20$ ,  $r_s = 0.53$ ,  $p = 0.02$ , Table S4.3) and remained low at all stations during autumn and winter (maximal up to 12.3  $\mu\text{g l}^{-1}$ ). At station BH, generally low SPM concentrations were observed, which increased in the

downstream direction, reaching high values at station ST (up to 253.6 mg l<sup>-1</sup> in summer). In winter, SPM concentrations peaked at the river mouth (station MG), when river discharge was highest. The discharge rates followed the typical seasonal patterns reported for the Elbe estuary (see see supplementary material, Table S4.1), reaching their lowest values in summer.

Table 4.2: Environmental conditions during the sampling campaigns in the Elbe estuary. Data were obtained along the entire salinity gradient (freshwater: BH, ML, ST; oligohaline: BB, mesohaline: MG) in each season in 2022.

| Season | Station | Temperature (°C) | Salinity | Chl <i>a</i> (µg l <sup>-1</sup> ) | SPM (mg l <sup>-1</sup> ) | Discharge (m <sup>3</sup> s <sup>-1</sup> ) |
|--------|---------|------------------|----------|------------------------------------|---------------------------|---------------------------------------------|
| Winter | BH      | 5.1              | 0.3      | 7.6                                | 23.4                      | 1166                                        |
|        | ML      | 5.5              | 0.3      | 6.2                                | 80.1                      |                                             |
|        | ST      | 5.8              | 0.4      | 10.7                               | 70.8                      |                                             |
|        | BB      | 5.6              | 0.8      | 10.3                               | 124.3                     |                                             |
|        | MG      | 5.6              | 2.7      | 12.0                               | 164.3                     |                                             |
| Spring | BH      | 19.6             | 0.4      | 132.2                              | 62.6                      | 345                                         |
|        | ML      | 18.8             | 0.4      | 18.8                               | 134.0                     |                                             |
|        | ST      | 17.0             | 0.9      | 7.3                                | 52.6                      |                                             |
|        | BB      | 16.5             | 4.7      | 4.4                                | 28.2                      |                                             |
|        | MG      | 16.2             | 10.9     | 7.6                                | 36.1                      |                                             |
| Summer | BH      | 21.4             | 0.5      | 152.7                              | 37.5                      | 231                                         |
|        | ML      | 20.5             | 0.5      | 22.6                               | 57.9                      |                                             |
|        | ST      | 19.3             | 0.7      | 17.8                               | 253.6                     |                                             |
|        | BB      | 18.6             | 9.8      | 7.0                                | 40.3                      |                                             |
|        | MG      | 18.0             | 20.0     | 10.9                               | 30.6                      |                                             |
| Autumn | BH      | 10.9             | 0.5      | 6.4                                | 7.6                       | 283                                         |
|        | ML      | 12.8             | 0.5      | 6.0                                | 40.1                      |                                             |
|        | ST      | 12.7             | 0.8      | 12.3                               | 130.7                     |                                             |
|        | BB      | 12.5             | 9.2      | 3.9                                | 33.8                      |                                             |
|        | MG      | 12.4             | 12.0     | 5.0                                | 48.2                      |                                             |

Abbreviations: SPM – suspended particulate matter; Discharge – river discharge; Chl *a* – Chlorophyll *a* concentration.

### Spatial and temporal variation in quantity, quality and origin of particulate organic matter sources

The Chl *a*/SPM ratios were highest at the uppermost freshwater station (station BH) throughout the year with the largest ratio in summer (up to 4.1 \*10<sup>-3</sup>) (Fig. 4.2 A) caused by low SPM concentrations (Spearman, n = 20,  $r_s = -0.65$ ,  $p < 0.01$ , Table S4.3). Low Chl *a*/SPM ratios were consistently observed at station ST and BB during all seasons, where SPM levels were high. C:N ratios of POM decreased significantly with increasing Chl *a* concentrations (Spearman, n= 20, Chl *a*:  $r_s = -0.72$ ,  $p < 0.001$ , Table S4.3). Generally, C:N ratios of POM were significantly lower in summer compared to winter and autumn (KW test, Table S4.4)

and correlated negatively with rising temperatures (Spearman, temperature:  $n = 20$ ,  $r_s = -0.72$ ,  $p < 0.001$ , Table S4.3), with a slight increasing trend seawards (e.g. from 7.1 at the uppermost station BH to 10.4 at the oligohaline station BB in summer) (Fig. 4.2 B). At station ST, C:N ratios remained stable and high throughout the year. Similarly,  $\delta^{13}\text{C}$  values of POM exhibited an increasing trend downstream (Fig. 4.2 C), with seasonal means ranging between  $-26.9 \pm 2.2 \text{‰}$  at the uppermost freshwater station (station BH) and  $-24.2 \pm 0.9 \text{‰}$  at the river mouth (station MG) (supplementary material, Table S4.5). Salinity and river discharge were both positively and negatively correlated with  $\delta^{13}\text{C}$  values of POM, respectively (Spearman,  $n = 20$ ; salinity:  $r_s = 0.75$ ,  $p < 0.001$ ; river discharge:  $r_s = -0.60$ ,  $p < 0.01$ , Table S4.3). Moreover, in summer POM was significantly enriched in  $\delta^{13}\text{C}$  compared

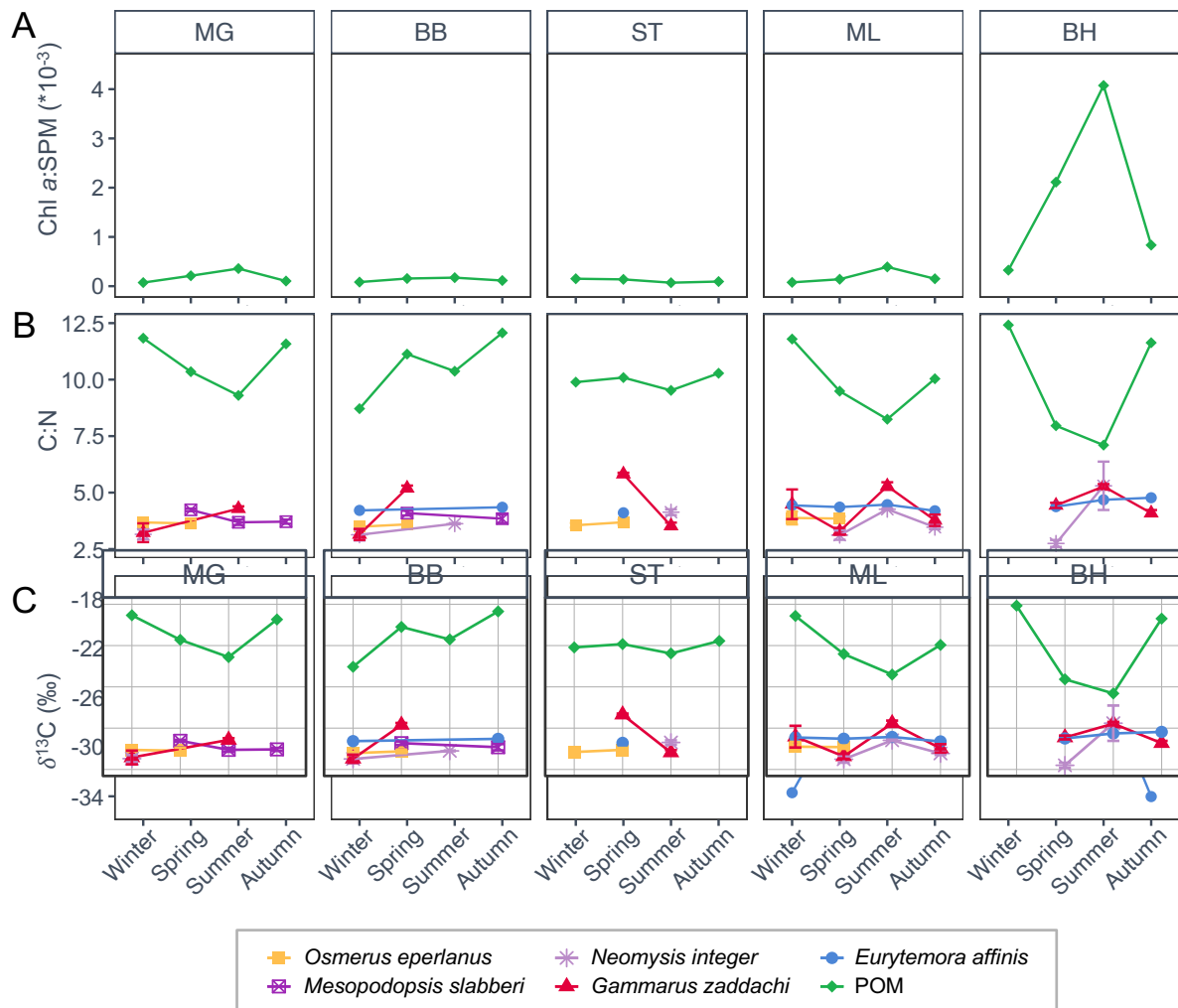


Fig. 4.2: Seasonal and spatial changes in primary production processes and the origin of the carbon source at five stations along the entire salinity gradient (freshwater: BH, ML, ST; oligohaline: BB; mesohaline: MG) of the Elbe estuary in 2022. Mean values ( $\pm$  SD) are given when triplicate samples were measured. (A) Variations in the ratio of chlorophyll *a* to suspended particulate matter concentration. (B) C:N ratio and (C)  $\delta^{13}\text{C}$  values of particulate organic matter (POM) and the zooplankton taxa.

to POM collected in winter (from  $-26.2 \pm 1.3$  to  $-24.1 \pm 0.8$  ‰, Table S4.5; KW test,  $p < 0.05$ , Table S4.4). There was no significant difference in the  $\delta^{15}\text{N}$  values of POM on the spatial and temporal scale (KW test, station:  $p = 0.9$ , season:  $p = 0.23$ , Table S4.4, Fig. 4.3 A).

### Trophic transfer of carbon sources and stable isotopic composition of consumers

$\delta^{13}\text{C}$  values of the zooplankton displayed more variations than the POM (Fig. 4.2 C). The planktonic consumers were generally enriched in  $\delta^{13}\text{C}$  in spring and summer compared to winter and autumn (KW test, Table S4.4), with this pattern being more pronounced in the freshwater section of the estuary. Most of the taxa collected at the freshwater station ML or BH had significantly more depleted and uniform  $\delta^{13}\text{C}$  values compared to individuals from the river mouth (station MG and BB) (KW test, Table S4.4), where  $^{13}\text{C}$ -signatures were more disparate. *M. slabberi*, which was only found at station BB and MG, was most enriched and showed the least variation in  $\delta^{13}\text{C}$ . *E. affinis*, however, showed neither significant spatial nor

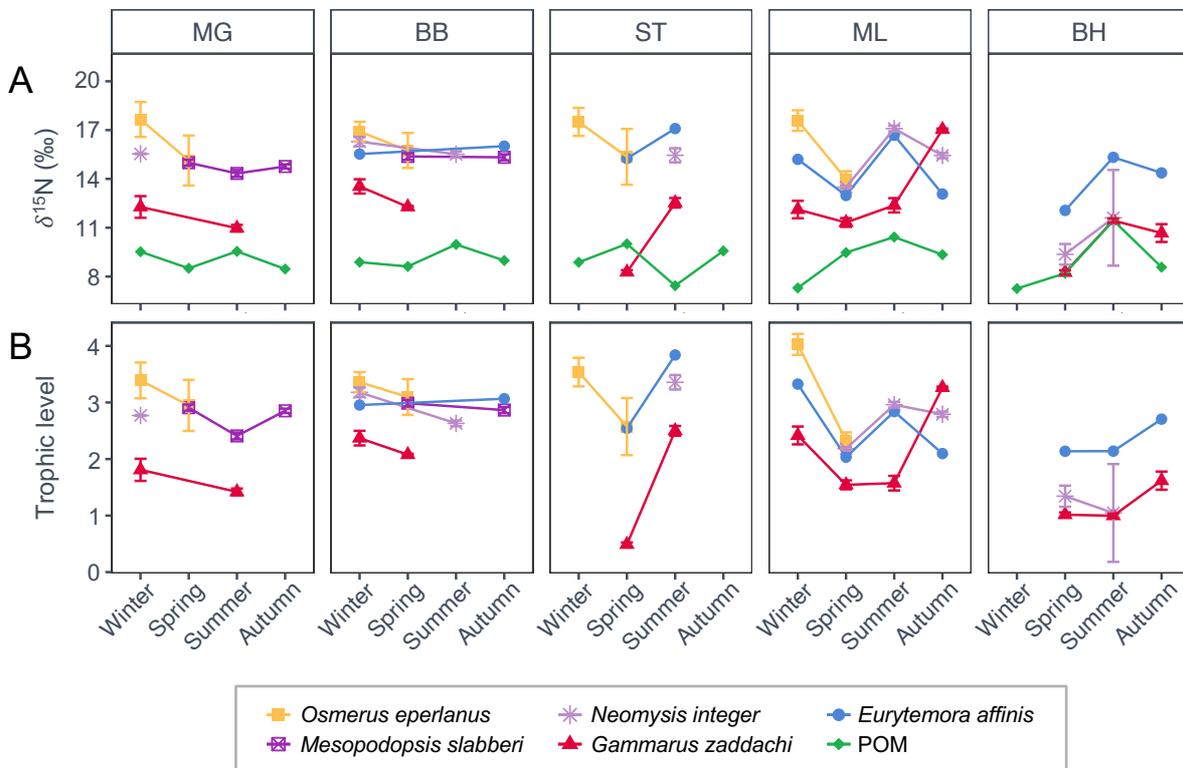


Fig. 4.3: Seasonal and spatial variability in (A)  $\delta^{15}\text{N}$  values and (B) trophic levels (TL) of the zooplankton taxa and particulate organic matter (POM) collected at five stations along the entire salinity gradient (freshwater: BH, ML, ST; oligohaline: BB, mesohaline: MG) of the Elbe estuary in 2022. POM is not depicted in the lower plot (B) since it was set as baseline (TL = 1) for all seasons and stations. Mean values ( $\pm$  SD) are given when triplicate samples were measured.

seasonal variability in its elemental and stable isotopic composition (KW test, Table S4.4), but had the lowest  $\delta^{13}\text{C}$  values (up to  $-34.0\text{‰}$  at station BH), especially in winter and autumn (Fig. 4.2 C). The other taxa, *M. slabberi*, *N. integer*, *G. zaddachi* and *O. eperlanus*, had TLs and  $\delta^{15}\text{N}$  values that were lower in spring or summer compared to winter and autumn (KW test, Table S4.4). Their  $\delta^{15}\text{N}$  values and TLs showed an increasing trend seawards from station BH to BB (Fig. 4.3, Table S4.5). In general, *G. zaddachi* exhibited significantly lower TLs and  $\delta^{15}\text{N}$  values compared to the other zooplankton species, which did not show major differences in their  $\delta^{15}\text{N}$  values or trophic positions (KW test, Table S4.4). However, in contrast to the other taxa, *O. eperlanus* at station ML displayed a trend of slightly higher TLs and  $\delta^{15}\text{N}$  values in winter, which became less distinct downstream (Fig. 4.3). In addition, the consumers' TLs correlated globally negatively with Chl *a*/SPM ratio (Spearman,  $n = 211$ ,  $r_s = -0.22$ ,  $p < 0.01$ ). The mean C:N ratios of the planktonic consumers, except for *E. affinis*, were significantly higher in summer and/or spring compared to winter and autumn (KW,

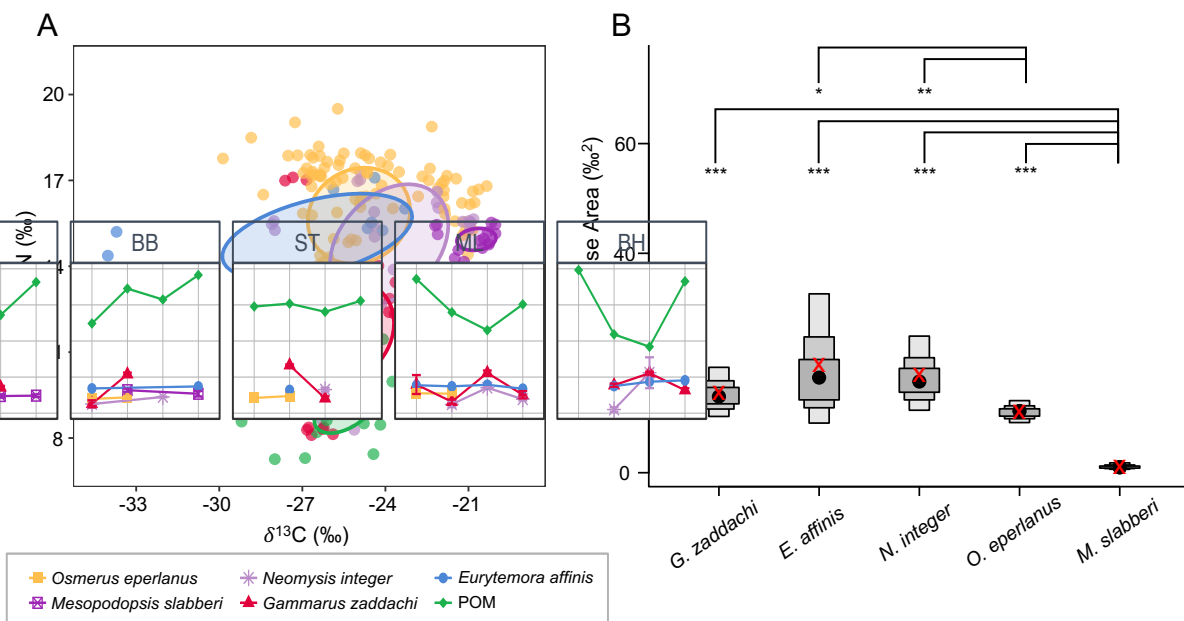


Fig. 4.4: Results of the overall niche space dynamics of the five dominant planktonic consumers and POM sampled in the Elbe estuary in 2022. (A) Stable isotope biplot of  $\delta^{13}\text{C}$  and  $\delta^{15}\text{N}$  of the taxa and POM including species-specific, small-size corrected standard ellipse areas ( $\text{SEA}_c$ ) (including 40% of the data per species). (B) Density box plots of estimated Bayesian standard ellipse area ( $\text{SEA}_b$ ) for the respective planktonic consumers, which indicate 50% (dark grey), 75% (grey) and 95% (light grey) credible intervals for mean estimations. Black dots depict the mean values of  $\text{SEA}_b$ , whereas the red cross represents the maximum likelihood estimate of  $\text{SEA}_c$ . The brackets above the density box indicate the probability that the posterior distribution of the  $\text{SEA}_b$  differs in magnitude between taxa (\*  $p < 0.05$ ; \*\*  $p < 0.01$ ; \*\*\*  $p < 0.001$ ).

Table S4.4). The taxa did not exhibit a clear spatial pattern in their C:N ratios (Table S4.4, Table S4.5).

### Stable isotopic niches of the zooplankton

Species-specific stable isotopic niches, based on averaged seasonal and spatial data using the standard ellipse for small sample size ( $SEA_c$ ), showed a high degree of overlap ranging from 17.7 % to 31.7 % between *E. affinis*, *N. integer* and *O. eperlanus* (Fig. 4.4 A, Table 4.3). *M. slabberi* exhibited a smaller and less variable isotopic niche, which did not overlap with those of the other taxa. *G. zaddachi* shared only one small overlap with the isotopic niche of *N. integer* (overlap 5.0 ‰<sup>2</sup>, 17.7 %, Table 4.3) and clustered at the bottom along the  $\delta^{15}N$  axis. Species-specific estimated niche widths ( $SEA_b$ ) ranged from the smallest niche of 1.2 ‰<sup>2</sup> for *M. slabberi* to the widest niche of 19.8 ‰<sup>2</sup> for *E. affinis* (Fig. 4.4 B). The width of  $SEA_b$  of *G. zaddachi*, *E. affinis* and *N. integer* were similar in their mean values.

Table 4.3: Results of the SIBER analysis including  $\delta^{13}C$  and  $\delta^{15}N$  values of the planktonic consumers collected in the Elbe estuary in 2022. Sample size (n), total area (TA), standard ellipse area without (SEA) and with correction of small sample size ( $SEA_c$ ) and the relative area of  $SEA_c$  overlap (in ‰<sup>2</sup> and %) between respective zooplankton species and the credible intervals of the estimated Bayesian standard ellipse area ( $SEA_b$ ).

| Species                      | n   | TA<br>(‰ <sup>2</sup> ) | SEA<br>(‰ <sup>2</sup> ) | $SEA_c$<br>(‰ <sup>2</sup> ) | Credible intervals |             |            | $SEA_c$ overlap                                                                                            |                                                                                                               |
|------------------------------|-----|-------------------------|--------------------------|------------------------------|--------------------|-------------|------------|------------------------------------------------------------------------------------------------------------|---------------------------------------------------------------------------------------------------------------|
|                              |     |                         |                          |                              | 50 %               | 95 %        | 99 %       | (‰ <sup>2</sup> )                                                                                          | (%)                                                                                                           |
| <i>Eurytemora affinis</i>    | 11  | 28.6                    | 17.8                     | 19.8                         | 14.0 – 21.4        | 8.5 – 32.5  | 6.0 – 40.7 | <i>G. zaddachi</i> : 0<br><i>N. integer</i> : 6.2<br><i>O. eperlanus</i> : 7.4<br><i>M. slabberi</i> : 0   | <i>G. zaddachi</i> : 0<br><i>N. integer</i> : 19.2<br><i>O. eperlanus</i> : 30.8<br><i>M. slabberi</i> : 0    |
| <i>Mesopodopsis slabberi</i> | 15  | 2.0                     | 1.1                      | 1.2                          | 0.9 – 1.2          | 0.6 – 1.8   | 0.5 – 2.2  | <i>G. zaddachi</i> : 0<br><i>E. affinis</i> : 0<br><i>N. integer</i> : 0<br><i>O. eperlanus</i> : 0        | <i>G. zaddachi</i> : 0<br><i>E. affinis</i> : 0<br><i>N. integer</i> : 0<br><i>O. eperlanus</i> : 0           |
| <i>Neomysis integer</i>      | 27  | 37.7                    | 17.2                     | 17.9                         | 14.7 – 19.2        | 11.1 – 24.9 | 9.6 – 28.8 | <i>G. zaddachi</i> : 5.0<br><i>E. affinis</i> : 6.2<br><i>O. eperlanus</i> : 7.1<br><i>M. slabberi</i> : 0 | <i>G. zaddachi</i> : 17.7<br><i>E. affinis</i> : 19.2<br><i>O. eperlanus</i> : 31.7<br><i>M. slabberi</i> : 0 |
| <i>Gammarus zaddachi</i>     | 39  | 43.4                    | 14.2                     | 14.6                         | 12.4 – 15.4        | 10.2 – 19.2 | 9.0 – 21.3 | <i>E. affinis</i> : 0<br><i>N. integer</i> : 5.0<br><i>O. eperlanus</i> : 0<br><i>M. slabberi</i> : 0      | <i>E. affinis</i> : 0<br><i>N. integer</i> : 17.7<br><i>O. eperlanus</i> : 0<br><i>M. slabberi</i> : 0        |
| <i>Osmerus eperlanus</i>     | 119 | 42.6                    | 11.0                     | 11.1                         | 10.3 – 11.6        | 9.1 – 13.1  | 8.6 – 14.0 | <i>G. zaddachi</i> : 0<br><i>E. affinis</i> : 7.4<br><i>N. integer</i> : 7.1<br><i>M. slabberi</i> : 0     | <i>G. zaddachi</i> : 0<br><i>E. affinis</i> : 30.8<br><i>N. integer</i> : 31.7<br><i>M. slabberi</i> : 0      |

## Discussion

Knowledge of zooplankton trophic interactions and carbon sources is incomplete for the intensively dredged, eutrophic Elbe estuary, which hampers understanding of food web structure and function. This study provides a better spatially and seasonally resolved view of the trophodynamics of the most abundant meso- and macrozooplankton taxa along the salinity gradient of the Elbe estuary based on carbon and nitrogen stable isotope analysis of dominant zooplankton taxa and of some potential food sources. Our focus is particularly on the spatio-temporal patterns of POM in terms of food availability (quantity and quality) and origin, as well as trophic segregation and shifts in carbon source utilisation among the dominant zooplankton taxa.

### The fate and sources of POM

Our results showed substantial seasonal and spatial variations in Chl *a* concentrations, Chl *a*/SPM ratios, C:N ratios and  $\delta^{13}\text{C}$  of POM. We found high Chl *a* concentrations exclusively at the uppermost freshwater station BH in spring and summer. When passing the Hamburg Harbour, a strong decline in phytoplankton biomass occurred with low Chl *a* concentrations at the downstream stations, which corresponds to the results of earlier studies in the Elbe estuary (e.g. Wolfstein and Kies, 1995; Kamjunke *et al.*, 2023). This rapid drop in phytoplankton biomass downstream of the port area has been attributed to light limitation, resulting from a high load of SPM that is accumulated and resuspended in the dredged section of the Elbe estuary due to the sudden change in the bathymetry and a respective decrease in flow velocity (Kerner, 2007; Geerts *et al.*, 2017). We found rising SPM concentrations along the dredged area of the estuary (from station ML to MG), with levels peaking at station ST. In February 2022, the MTZ shifted seawards as the SPM peak moved closer to the mouth of the estuary, likely due to the increase in river discharge rates in winter, as also suggested by Papenmeier *et al.* (2014). They reported for the area around Glückstadt, which is close to station ST in our study, a similar spatio-temporal pattern in the MTZ characteristics that align with our results, with high SPM concentrations (above  $150 \text{ mg l}^{-1}$ ) observed under low discharge conditions (below  $400 \text{ m}^3 \text{ s}^{-1}$ ). In contrast, the shallow tidal freshwater region upstream of the Hamburg Harbour is characterised by low turbidity

and reduced water turnover throughout the annual cycle (Wolfstein and Kies, 1995). This can favour intense phytoplankton blooms (Turner *et al.*, 2022) and might explain the high Chl *a* concentrations observed exclusively at station BH during warm periods. The Chl *a*/SPM ratio, as a proxy for phytoplankton availability (Irigoien and Castel, 1995), correlated negatively with the SPM concentrations, and thus may account for the high ratios exclusively detected at station BH. High loads of SPM may not only have impacted the available light but also led to a loss of phytoplankton due to enhanced sedimentation of plankton aggregates as a result of their stickiness. Phytoplankton produce sticky exudates during bloom conditions which increase their adhesion to other particles (Alldredge and Silver, 1988). Steidle and Vennell (2024) hypothesised that the previously reported decline in Chl *a* concentration in the Hamburg Harbour may be attributed to phytoplankton adhesion to negatively buoyant suspended particles, which subsequently sink to light-limited water layers. Consequently, high loads of SPM in the Elbe estuary can lead to distinct losses of primary producers as potential food source for planktonic consumers, particularly in the dredged sections downstream from the port area, and can be subjected to pronounced seasonal variations depending on river discharge rates.

C:N ratios give an indication of the quality of the organic matter sources, with values below 8 indicating fresh and high-quality POM and values above 8 representing detrital material, as algal detritus has increased C:N ratios due to diagenesis (Thornton and McManus, 1994; Sterner and Elser, 2003; Finlay and Kendall, 2007). Indeed, high Chl *a* concentrations in spring and summer coincided with a decline in C:N ratios below 8 for POM at station BH, indicating a higher contribution of high-quality POM in the upstream section of the estuary during these seasons. The negative correlation between C:N ratio and Chl *a* concentration in the present study aligns with the seasonal patterns observed in other river systems (e.g. Rhone River, Harmelin-Vivien *et al.*, 2010). When passing the port area, the C:N ratio of POM still showed a similar trend of decreasing values during spring and summer, but was distinctly enriched with values above 8, indicating a change in the organic matter composition to more detrital material and less fresh phytoplankton carbon sources. In the zone of maximum turbidity (station ST) we even observed poor POM quality year-round, as indicated by persistently high C:N ratios. These findings are in line with the spatio-temporal

pattern in organic matter processing and degradation that has been reported for resuspended (Spieckermann *et al.*, 2021) and particulate organic matter (Dähnke *et al.*, 2022; Kamjunke *et al.*, 2023) in the Elbe estuary. We hypothesise that the absence of high-quality food from the Hamburg Harbour seawards could be related to a shift from an autotrophic system at station BH towards a heterotrophic system along the dredged sections of the estuary. This shift is likely caused by light-limiting conditions and enhanced microbial processing, as associated with the high SPM load and reduced flow velocities (Kerner, 2007; Geerts *et al.*, 2017).

The local bulk POM in the Elbe estuary consisted of a mixture of multiple carbon sources, including riverine planktonic and terrigenous organic matter, as well as marine algal input, as indicated by intermediate  $\delta^{13}\text{C}$  values ranging from  $-26.9 \pm 2.2$  ‰ (station BH) to  $-24.2 \pm 0.9$  ‰ (at station MG), which is consistent with the stable isotopic composition of POM reported for other European (e.g. Scheldt, Gironde, Ems (Middelburg and Herman, 2007)) and North American estuaries like San Francisco (Cloern *et al.*, 2002) and St. Lawrence (Martineau *et al.*, 2004). The most seaward station (MG) was mesohaline and therefore does not represent a stable isotopic signal of true marine material, which is generally difficult to obtain in estuaries (Middelburg and Herman, 2007). Still, we observed a trend of  $^{13}\text{C}$ -enrichment downstream, suggesting an inflow of marine organic matter that was probably diluted upstream by tidal mixing processes. The  $^{13}\text{C}$ -signal of POM from the freshwater section is close to the carbon baseline for terrestrial C3-plants and also falls within the  $\delta^{13}\text{C}$  range for riverine phytoplankton (Boutton, 1991; Maksymowska *et al.*, 2000; Finlay and Kendall, 2007). While the low C:N ratios at station BH (e.g. values below 8 in spring and summer) and  $\delta^{13}\text{C}$  values ranging between  $-29.2$  to  $-24.1$  ‰ suggest the input of fresh algal material from the upstream freshwater section, the  $\delta^{15}\text{N}$  signal of POM at all stations (7.1 to 12.4 ‰) implies a pronounced contribution of terrestrial organic matter to the local POM (Maksymowska *et al.*, 2000; Finlay and Kendall, 2007). This is further supported by the significantly higher C:N ratios in winter and autumn, which are markedly greater than the typical ratio for fresh phytoplankton and more closely align with allochthonous material, such as terrestrial material and soil organic matter, that underwent diagenesis (Thornton and McManus, 1994; Finlay and Kendall, 2007). In addition, in winter, POM exhibited

significantly lower  $\delta^{13}\text{C}$  values compared to summer. The seasonal dynamics of the Elbe river discharge are typically characterised by elevated flow rates between January and March (see Table S4.1), which mostly result from high areal precipitation (Bartl *et al.*, 2009). We therefore assume that high river discharge rates during the winter sampling (i.e. in February) likely transported an increased amount of terrestrial material into the main channel of the estuary, resulting in a predominance of  $^{13}\text{C}$ -depleted terrigenous organic matter in the POM. In addition,  $\delta^{13}\text{C}$  values of POM are substantially influenced by species composition (Cloern *et al.*, 2002; Finlay and Kendall, 2007) and seasonal changes in the phytoplankton community structure are well known for the Elbe estuary (Martens *et al.*, 2024b, 2024c). In particular, for the year 2022, Martens *et al.* (2024b) observed a transition from the predominance of diatoms in summer to mixotrophic flagellates in winter in the Elbe estuary as a result of unfavourable light conditions. Since flagellates are more  $^{13}\text{C}$ -depleted than diatoms (Gearing *et al.*, 1984), a shift in the phytoplankton community towards a higher contribution of flagellates in the POM could have also led to depleted  $\delta^{13}\text{C}$  values observed during winter and autumn. In contrast, POM showed neither spatial nor temporal patterns in the  $\delta^{15}\text{N}$ , which is in line with findings from Middelburg and Herman (2007) across multiple European estuaries. As in our study, the authors explained the consistent  $\delta^{15}\text{N}$  values by a rapid nitrogen turnover driven by intense microbial activity paired with continuous lateral inputs from adjacent marshlands. Nevertheless, other components like respiration, photosynthetic rates as well as the dissolved inorganic carbon and nitrogen pool also influence the isotopic composition of aquatic primary producers (Finlay and Kendall, 2007), which were not assessed in this study.

### **Zooplankton diet and trophic segregation**

The  $\delta^{13}\text{C}$  values of the examined consumers in our study exhibited high variability, ranging from -34 to -20 ‰, which was consistent with stable isotope studies from estuaries of the northern hemisphere (Martineau *et al.*, 2004; Hoffman *et al.*, 2008; Modéran *et al.*, 2012; David *et al.*, 2016). Overall, the zooplankton species followed the general seasonal and spatial isotopic pattern of POM, which showed an enrichment of  $\delta^{13}\text{C}$  during seasons of high primary production and downstream towards the river mouth. All consumers had a wider

range of  $\delta^{13}\text{C}$  values compared to POM, indicating that the selected taxa did not directly consume POM as a whole, but were likely feeding on selective components that exhibited more seasonal and spatial differences in isotopic fractionation compared to bulk POM (Bouillon *et al.*, 2000). The discrepancy between the carbon isotopic composition of POM and the taxa appears to shift along the estuarine gradient, as organisms collected from upstream sites had more similar  $\delta^{13}\text{C}$  signatures than taxa sampled in the river mouth. Tidal mixing processes could have led to a larger variety of carbon sources (e.g. riverine and marine phytoplankton, resuspended benthic algae) at station BB and MG, allowing taxa to exploit a more diverse range of organic matter sources. However, assigning these components to certain primary carbon sources is difficult due to processes such as microbial diagenesis of organic matter or species-specific isotopic fractionation, which hamper the precise identification of the consumers' diet. Compound-specific stable isotope analysis or a combined biomarker approach using fatty acids would help in determining the origin of carbon sources in the consumers' diet when multiple sources are available and their isotopic signals may overlap (Cloern *et al.*, 2002; Finlay and Kendall, 2007).

The exploitation of distinct components of POM by the selected taxa is also reflected in the position and compactness of their isotopic niches. Most of the taxa showed an opportunistic feeding strategy, as reflected by their broad isotopic niche width. For *E. affinis*, *M. slabberi* and *N. integer*, the nitrogen isotopic signatures did not differ significantly among taxa, indicating that they largely shared food sources derived from the same trophic position, although mysids, particularly *N. integer*, are known to preferentially prey on *E. affinis* in estuarine systems (Modéran *et al.*, 2012; David *et al.*, 2016). Differences in the  $\delta^{15}\text{N}$  values between the consumers and POM were clearly higher, or in the case of *G. zaddachi*, lower than the typical trophic enrichment factor of 3.4 ‰ (Vander Zanden and Rasmussen, 2001). These results highlight that the consumers are highly selective feeders, likely relying on only a minor fraction of the local bulk POM, while fulfilling most of their carbon requirements from similar heterotrophic sources. Omnivorous feeding is widely documented in estuarine systems (e.g. Hughes *et al.*, 2000; Martineau *et al.*, 2004; David *et al.*, 2006; Hoffman *et al.*, 2008; Modéran *et al.*, 2012; Hitchcock *et al.*, 2016). Suspended organic matter, in particular detrital matter, is often populated by bacteria, protozoans and small metazoans, which can

be passively ingested by grazers feeding on these aggregates (Stoecker and Capuzzo, 1990) or actively preyed upon, as noted for e.g. *E. affinis* (Tackx *et al.*, 2003; Cabrol *et al.*, 2015). Feeding on heterotrophic sources is accompanied by a rise in the consumers'  $\delta^{15}\text{N}$  values, leading to an increase in food chain lengths (Lerner *et al.*, 2022). In addition, organic matter sources of terrigenous origin are often characterised by a  $\delta^{15}\text{N}$  signature that is enriched relative to autochthonous sources (Maksymowska *et al.*, 2000; Cloern *et al.*, 2002; Finlay and Kendall, 2007). Grazing on detrital, terrigenous sources could therefore also explain the high  $\delta^{15}\text{N}$  values of the zooplankton taxa. The inflow of allochthonous organic matter in the local POM has been documented as important carbon supply utilised by estuarine zooplankton when autochthonous sources are scarce, e.g. in winter under low-light conditions (e.g. Hoffman *et al.*, 2008; Hitchcock *et al.*, 2016). In fact, we observed a rise in the consumers'  $\delta^{15}\text{N}$  values and TLs seawards, as well as during winter and autumn, when the carbon dynamics in the Elbe estuary shifted to a predominantly heterotrophic system due to limiting primary production. Feeding on heterotrophic sources results in lower C:N ratios for the consumers (Elser *et al.*, 2000) as presented by the seasonal trends in the C:N ratios of consumers in this study. However, we cannot exclude the possibility that the seasonal changes in the C:N ratio may be derived from shifts in the lipid content, as lower lipid content in organisms is usually related to lower C:N ratios (Sterner and Elser, 2003).

Among the species, *E. affinis* exhibited the most depleted  $\delta^{13}\text{C}$  values, especially in winter and autumn. During periods of limited primary production or low food quality, *E. affinis* may have selectively consumed  $^{13}\text{C}$ -depleted constituents of the POM, either from autochthonous algae or terrestrial origin, and heterotrophic sources as indicated by the enriched  $\delta^{15}\text{N}$  signature, resulting in a broad isotopic niche width. The copepod probably preferentially consumed an increasing amount of autochthonous organic matter in the POM under phytoplankton blooming conditions in spring and summer, as indicated by their slightly enriched  $\delta^{13}\text{C}$  values. The ability of *E. affinis* to select its prey among suspended inorganic particles and to feed on detrital organic sources (Tackx *et al.*, 2003; Cabrol *et al.*, 2015) to cover its nutritional requirements are in line with the results of Kerner (2004) for the Elbe estuary and has also been reported for other estuaries (Martineau *et al.*, 2004; David *et al.*, 2006; Hoffman *et al.*, 2008; Modéran *et al.*, 2012; David *et al.*, 2016).

In contrast to this, *M. slabberi*, displayed  $\delta^{13}\text{C}$  values ranging from -22.2 to -20.0 ‰, generally up to 4 ‰ more  $^{13}\text{C}$ -enriched than those of the POM, exhibiting a narrow and unique dietary niche, which did not overlap with other taxa. The carbon isotopic signature of marine phytoplankton closely matched those of *M. slabberi*, suggesting that the mysid relied partly on marine algae to fulfil its carbon requirements. This might be further supported by their exclusive occurrence in the mouth of the estuary. In winter, this species was absent as it only migrates into the inner part of estuaries for reproduction and growth in spring (Hamerlynck and Mees, 1991). Nevertheless, we cannot definitively exclude microphytobenthos as potential food source, which falls within the range of  $\delta^{13}\text{C}$  range for *M. slabberi*, as it can constitute a considerable proportion of the total pelagic POM through resuspension from tidal flats (De Jonge and Van Beusekom, 1992). The tendency of *M. slabberi* to graze preferentially on a  $^{13}\text{C}$ -enriched, marine diet are in agreement with previous studies (e.g. Modéran *et al.*, 2012; David *et al.*, 2016). Food-niche partitioning allows *M. slabberi* to reduce food competition and to co-exist with the sympatric mysid *N. integer*, which fed on  $^{13}\text{C}$ -depleted components, similar to *E. affinis*. The exploitation of distinct carbon sources among sympatric mysids has also been noted by Winkler *et al.* (2007) for the taxa *Mysis stenolepis* and *Neomysis americana* in the St. Lawrence estuary.

*G. zaddachi* exhibited clearly lower  $\delta^{15}\text{N}$  values than the other consumers, indicating a preference for a primarily herbivorous diet, which is in line with previous studies (Korpinen *et al.*, 2006). Their  $\delta^{13}\text{C}$  values suggest a carbon source based on autochthonous riverine or detrital, terrestrial organic matter that have been noted for sister species (e.g. *Gammarus tigrinus*) in other estuaries (Hughes *et al.*, 2000; Hoffman *et al.*, 2008).

For *O. eperlanus*, our findings suggest an omnivorous to carnivorous feeding behaviour. In winter, the fish larvae exhibited slightly elevated  $\delta^{15}\text{N}$  values, approximately one trophic level higher than the other taxa. This pattern was most pronounced at station ML, which is located near a freshwater tidal flat that is recognised as an important area for the reproduction and retention of planktonic organisms (Fiedler, 1991; Peitsch *et al.*, 2000) and fish, such as *O. eperlanus* (Eick and Thiel, 2014). In this region, Thiel *et al.* (1996) analysed the stomach contents of early life stages of *O. eperlanus* and identified *E. affinis* and *N. integer* as the

main prey items, which were most abundant in the digestive tract of the fish larvae. In our study, the elevated  $\delta^{15}\text{N}$  values and TLs of *O. eperlanus* in late winter can likely be attributed to the high densities of copepods and mysids documented for this area near station ML (Fiedler, 1991; Peitsch *et al.*, 2000), which may have served as preferred food sources for the fish larvae. This feeding pattern might be also reflected in the large overlap in the  $\delta^{13}\text{C}$  values between *O. eperlanus* and both potential prey items, i.e. *E. affinis* and *N. integer*, which should not differ strongly if fish larvae preyed on them to any extent. In spring and at the stations downstream, we found that *O. eperlanus* exhibited lower TLs and  $\delta^{15}\text{N}$  values, close to those of the other zooplankton taxa (i.e. *E. affinis* and the mysids). This pattern may result from the limited availability of these potential prey items and could suggest that *O. eperlanus* preyed on similar food as *E. affinis* and *N. integer*. This dietary shift corresponds to the findings by Thiel *et al.* (1996), who observed that larvae of *O. eperlanus* transitioned to alternative prey items during the same period, which was linked to a decline in the *E. affinis* population resulting from high predation pressure. Additionally, the enriched  $\delta^{15}\text{N}$  values of *O. eperlanus* during the winter sampling could also be related to the fact that the fish larvae were only a few weeks old and likely fed from the yolk sac, indicating the isotopic signature of the adults, which the fish can retain for several weeks due to long tissue turnover rates (Vander Zanden *et al.*, 2015).

In summary, selective feeding might be an important strategy for the zooplankton in the Elbe estuary to optimise the use of available carbon sources to avoid competition and to survive stressful periods (i.e. winter and autumn) when food quality and availability (i.e. at the MTZ) is low. When primary carbon sources were limited, a switch to alternative food sources, like protozoans and small metazoans, was likely performed. Mixotrophic pathways have also been reported for phytoplankton taxa in the Elbe estuary, especially for taxa in the MTZ or during winter (Martens *et al.*, 2024b). The ability to feed opportunistically and use alternative sources of material is a crucial aspect of the trophic plasticity of planktonic consumers, helping to stabilise and maintain food web structures (e.g. David *et al.*, 2006; Hoffman *et al.*, 2008; Modéran *et al.*, 2012; Hitchcock *et al.*, 2016; Lerner *et al.*, 2022). This adaptability likely plays a central role for zooplankton in the Elbe estuary to cope with the environmental forces and to avoid competition.

## Conclusion

Our results highlighted that temporal and spatial variations in the quality and quantity of food for zooplankton in the Elbe estuary are influenced by primary production processes and the amount of suspended particulate matter in the water column resuspended by strong tidal mixing processes. Autochthonous algal material was mainly produced in the non-dredged freshwater area of the Elbe estuary upstream of Hamburg Harbour, which probably was subject to intense heterotrophic decomposition downstream of the port area. The stable isotopic signatures of POM indicate a mixture of coastal and riverine derived organic matter in the carbon source, which was predominated by the input of terrigenous matter from adjacent marshlands, especially during periods of high river discharge. High suspended matter loads and low availability of high-quality phytoplankton impacted the trophodynamics both temporally and spatially, reflected by a considerable increase in  $\delta^{15}\text{N}$  and, consequently, also an increase in trophic levels of the consumers. The investigated planktonic organisms were generally able to cope with strong variations in food quality and quantity due to opportunistic feeding behaviour. Selective feeding, portioning of dietary niches and switching from herbivorous to omnivorous nutrition allow species to co-exist and to optimise the use of allochthonous and autochthonous organic material. This trophic plasticity of the zooplankton may thus be an essential feature to withstand alterations in the hydrology of the Elbe estuary related to human disturbances (i.e. variations in turbidity and flow velocity) and natural estuarine gradients. This study helps to understand the impact of increasing human pressures on estuaries by providing a powerful tool for ecosystem-based management and conservation.

## Data availability

The data underlying this article are available in the research data repository of the Universität Hamburg, at <https://doi.org/10.25592/uhhfdm.14727>.

## Acknowledgements

The authors would like to thank the captain and crew of the research vessel *Ludwig Prandtl* for their help during the cruises (LP220228, LP220522, LP220613, LP221107), Nele

Martens, Stephanie Kondratowicz, Laura Öhm, Julia Fuchs and Celine Imker for support during the sampling process, Martina Wichmann and Marc Metzke for the technical support in the laboratory and Jan Conradt for helpful comments on the statistical analysis. We highly appreciate the comments of Dr. Rubao Ji and two anonymous reviewers for their valuable suggestions to improve this manuscript.

### **Declaration of interest**

The authors have no conflicts of interest to declare.

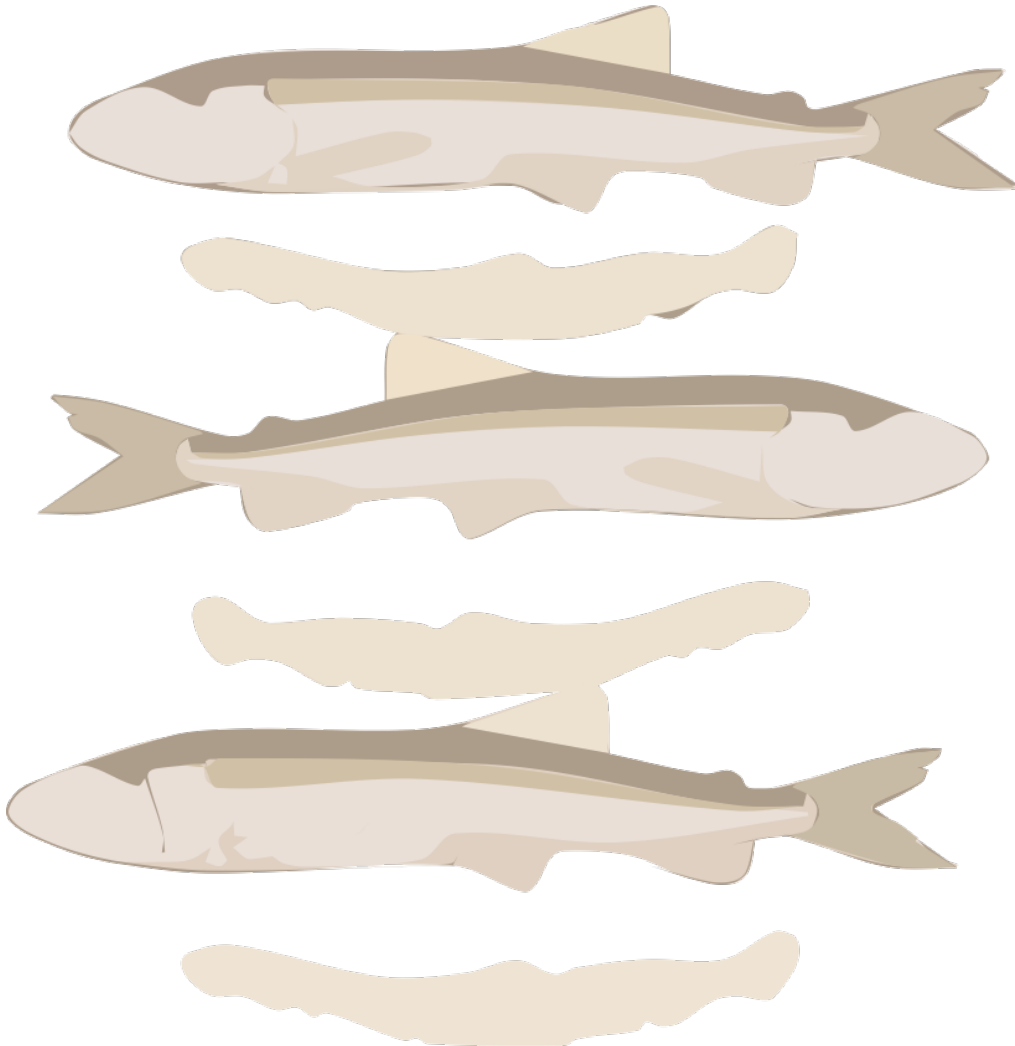
### **Funding**

This project was funded by the Deutsche Forschungsgemeinschaft (DFG, German Research Foundation) within the Research Training Group 2530: „Biota-mediated effects on Carbon Cycling in Estuaries” (project number 407270017; contribution to Universität Hamburg and Leibniz-Institut für Gewässerökologie und Binnenfischerei im Forschungsverbund Berlin e.V. (IGB)) and by the Bundesministerium für Bildung und Forschung (BMBF) within the project “Blue-Estuaries” (project number 03F0864C).

### **Supplementary material**

Supplementary data are available at *ICES Journal of Marine Science* online, at <https://doi.org/10.1093/icesjms/fsae189>.

## Chapter 5: Feeding ecology of *Osmerus eperlanus*



Manuscript in preparation:

Hauten, E., Biederbick, J., Funk, S., Koll, R., Theilen, J., Fabrizius, A., Thiel, R., Jensen, K., Grønkjær, P. and Möllmann, C. Characterising intraspecific habitat exploitation of anadromous key species *Osmerus eperlanus* along the salinity gradient of a large European estuary.

Figures modified and used with permission from Elena Hauten.

**Title:** Characterising intraspecific habitat exploitation of anadromous key species *Osmerus eperlanus* along the salinity gradient of a large European estuary

**Running title:** Feeding ecology of *Osmerus eperlanus*

Authors: Elena Hauten<sup>1\*</sup>, Johanna Biederbick<sup>1</sup>, Steffen Funk<sup>1</sup>, Raphael Koll<sup>2</sup>, Jesse Theilen<sup>3</sup>, Andrej Fabrizius<sup>2</sup>, Ralf Thiel<sup>4</sup>, Kai Jensen<sup>5</sup>, Peter Grønkjær<sup>6</sup>, Christian Möllmann<sup>1</sup>

<sup>1</sup>Institute of Marine Ecosystem and Fishery Science, University of Hamburg, Grosse Elbstrasse 133, 22767 Hamburg, Germany.

<sup>2</sup>Institute of Cell and Systems Biology of Animals (ICS), University of Hamburg, Martin-Luther-King-Platz 3, 20146, Hamburg, Germany

<sup>3</sup>Leibniz Institute for the Analysis of Biodiversity Change, Center for Taxonomy and Morphology, Martin-Luther-King-Platz 3, 20146, Hamburg, Germany

<sup>4</sup>Independent researcher, Lübeck, Germany

<sup>5</sup>Institute of Plant Science and Microbiology, Applied Plant Ecology, University of Hamburg, Ohnhorststrasse 18, 22609 Hamburg, Germany

<sup>6</sup>Institut for Biologi, Akvatisk biologi, University Aarhus, Ole Worms Allé 1 bygning 1134, 228, 8000 Aarhus C, Denmark

\*Corresponding author

E-Mail: [elena.hauten@uni-hamburg.de](mailto:elena.hauten@uni-hamburg.de)

## Abstract

Estuaries are both highly productive and challenging habitats for aquatic organisms due to their rapid changing environmental conditions, with salinity acting as an important driver for species composition and richness. In the Elbe estuary, one of the largest estuaries in Europe, the anadromous smelt *Osmerus eperlanus* dominates the fish community, making it a key species. During spring, juveniles and adults occupy the same habitat and thus share the same feeding grounds and resources. However, essential aspects of the feeding ecology and habitat use of these life stages remain unknown. Using integrated stomach content and stable isotope analyses of  $\delta^{13}\text{C}$  and  $\delta^{15}\text{N}$  of smelt muscle tissue, we found distinct habitat exploitation and movements patterns of juveniles and adults. We observed a high overlap of shared resources with mysids and gammarids being the most important prey species. However, an ontogenetic shift was found, with isotopic overlaps between the life stages decreasing upstream. Adults mainly fed on prey from the mesohaline and oligohaline sections, but less on upstream freshwater areas. Enriched  $\delta^{15}\text{N}$  values in the maximum turbidity zone indicated a locally extended food chain which primarily affected juveniles. Our results underline the importance of estuarine habitats serving as nursery and feeding areas for different life stages of migrating fishes. Our study contributes to a better understanding of habitat exploitation by the key species smelt along the estuarine salinity gradient. This knowledge further enhanced our expertise in smelt population dynamics, intraspecific interactions during ontogeny and the importance of estuarine services for migratory fishes.

Keywords: Estuary, food web, stable isotopes, key species, anadromous, nursery area

## Introduction

Estuaries are aquatic transition zones connecting marine and riverine habitats that are accessed by a variety of fish species as part of their life cycle to feed, seek refuge or spawn (Elliot and Hemingway, 2002; Thiel, 2011). Strong dynamic environmental processes cause high primary production rates (Schelske and Odum, 1962; Day *et al.*, 2013) and making them ideal for fish production (Haedrich, 1983; Elliot and Hemingway, 2002). However, the rapidly changing physico-chemical conditions, particularly the salinity gradient, present challenges for estuarine biota (Whitfield *et al.*, 2022). These environmental conditions lead to generalist feeding strategies of consumers (Mosman *et al.*, 2023), a lower species richness compared to adjacent freshwater and marine habitats (Whitfield and Harrison, 2020; Whitfield *et al.*, 2022) and the dominance of a few key species (Whitfield *et al.*, 2022).

The European smelt, *Osmerus eperlanus* (Linnaeus, 1758), represent such a key species in the Elbe estuary (Illing *et al.*, 2024), accounting for up to 96 % of the local fish community (Eick and Thiel, 2014). As an anadromous fish, smelt spend their adult life primarily in marine waters and migrate annually to freshwater areas of estuaries to spawn (Kottelat and Freyhof, 2007). The spawning migration takes place in late winter between February and March (Borchardt, 1988; Thiel and Thiel, 2015). Unlike other anadromous fishes, such as twaite shad (*Alosa fallax*) (Magath *et al.*, 2013), mature smelt remain in the estuary after spawning to exploit the habitat's benefits (e.g. high food supply, less predation) until summer (Borchardt, 1988).

Smelt play a critical role as a trophic link between lower and higher trophic levels (Illing *et al.*, 2024) and are also relevant for local fisheries (Eick and Thiel, 2014). Due to its anadromous life cycle, smelt use the estuary as a spawning ground, nursery and feeding area (Elliot and Hemingway, 2002), hence smelt exploit the estuary in various life stages throughout the year (Eick and Thiel, 2014; Eick, 2015). During spring, when the food supply peaks in the Elbe estuary (Borchardt, 1988; Eick and Thiel, 2014), juvenile and adult smelt exploit the same feeding areas. As the salinity gradient and other abiotic conditions (e.g. oxygen, turbidity) shape spatial estuarine community compositions (Henderson, 1989; Thiel

and Potter, 2001; Breine *et al.*, 2011), these local feeding areas differ in their quality and productivity throughout the river course (Selleslagh and Amara, 2008).

Ontogenetic niche shifts and habitat exploitation in the smelt genus *Osmerus* have been investigated in landlocked (e.g. Vinni *et al.*, 2004, 2005; Salujõe *et al.*, 2008; Hammar *et al.*, 2018; Rosinski *et al.*, 2020) and migrating populations (e.g. Franek, 1988; Taal *et al.*, 2014). However, these studies often overlooked the spatial characterisation of feeding areas and intraspecific features such as movement patterns or dietary preferences. Understanding how smelt exploit resources within the estuary is essential to determine whether intraspecific competition occurs and if distinct strategies for resource use and migrations have developed. This knowledge is critical for understanding population dynamics and promoting the conservation of this key species, especially considering the recent population decline (Illing *et al.*, 2024).

In this study, we applied a combination of stomach content and stable isotope analyses of white muscle tissue to investigate the feeding ecology of European smelt. Stomach content analyses provide direct observations of prey items and their quantities (Pasquaud *et al.*, 2008), offering taxonomic resolution (Lin *et al.*, 2007) and insights into predator-prey relationships, species-specific feeding strategies, and the main trophic pathways of a species (Leclerc *et al.*, 2014; Poiesz *et al.*, 2021). This method offers a snapshot of recently ingested prey (Klarian *et al.*, 2022), complementing stable isotope approaches.

Stable isotope analysis has emerged as a powerful tool to elucidate the functioning of ecological networks and food web structures (Pasquaud *et al.*, 2008). Nitrogen isotope ratios ( $\delta^{15}\text{N}$ ) exhibit stepwise per trophic level and thus indicate the trophic position of an organism in an ecosystem (DeNiro and Epstein, 1981). In contrast, carbon stable isotope ratios ( $\delta^{13}\text{C}$ ) are only little enriched per trophic level but offer insights into the production base of the food web (Peterson and Fry, 1987) and potential food source preferences of a species over a longer time frame (Kling *et al.*, 1992; Harvey and Kitchell, 2000).

In our study, we used both approaches, as the combination of these methods allows us to investigate whether the snapshots from the stomach contents are representative of the

general diet over longer periods of time or whether they only reflect short-term fluctuations in prey availability and the smelt's food preferences (e.g. Nielsen *et al.*, 2018). Goal was to (1) assess general feeding strategies and preferences of juvenile and adult smelt, to (2) examine these findings by analysing ontogenetic niche shifts, isotopic niche widths, and isotopic niche overlaps along the salinity gradient of the Elbe estuary. In addition, we employed a Bayesian mixing model (3) based on  $\delta^{13}\text{C}$  and  $\delta^{15}\text{N}$  data to reveal the habitat use and movement patterns of both life stages.

Our findings contribute to a deeper understanding of habitat exploitation by the estuarine key fish species smelt along the estuarine salinity gradient. This knowledge enhances our understanding of smelt population dynamics, intraspecific interactions during ontogeny, and the importance of estuarine services for migratory fish species.

## Material and methods

### Sampling

We collected smelt at five fishing stations covering the Elbe estuary from the river mouth to the city of Hamburg (Fig. 5.1). For comparability with previous studies (e.g. Magath and Thiel, 2013), we categorised the Elbe estuary into upper, middle, and lower sections, representing the salinity gradient in the area (Fig. 5.1a). Fishing was conducted with a commercial stow net vessel for 3-4 hours during high and low tide at each station from May 31<sup>st</sup> to June 4<sup>th</sup>, 2022. The stow net has an opening of 135 m<sup>2</sup> with a mesh size of 10 mm at the cod end. Additionally, a ring net with a mesh size of 1000  $\mu\text{m}$ , 94 cm diameter and a length of 2.8 m was used to collect potential prey organisms for stable isotope analysis. Standard measurements such as the total length of the fish (in cm) were recorded. Individuals were measured until normal distributions of the life stages were achieved to ensure a representative sample size (Fig. 5.1c). Smelt were grouped into juveniles (age group 1: 5.6 -13.4 cm) and adults (age group 2+: length > 13.5 cm) according to Lillelund (1961) (supplement material Table S 5.1). Further, we verified the life stages by examining the maturity stages of the fish at irregular intervals.

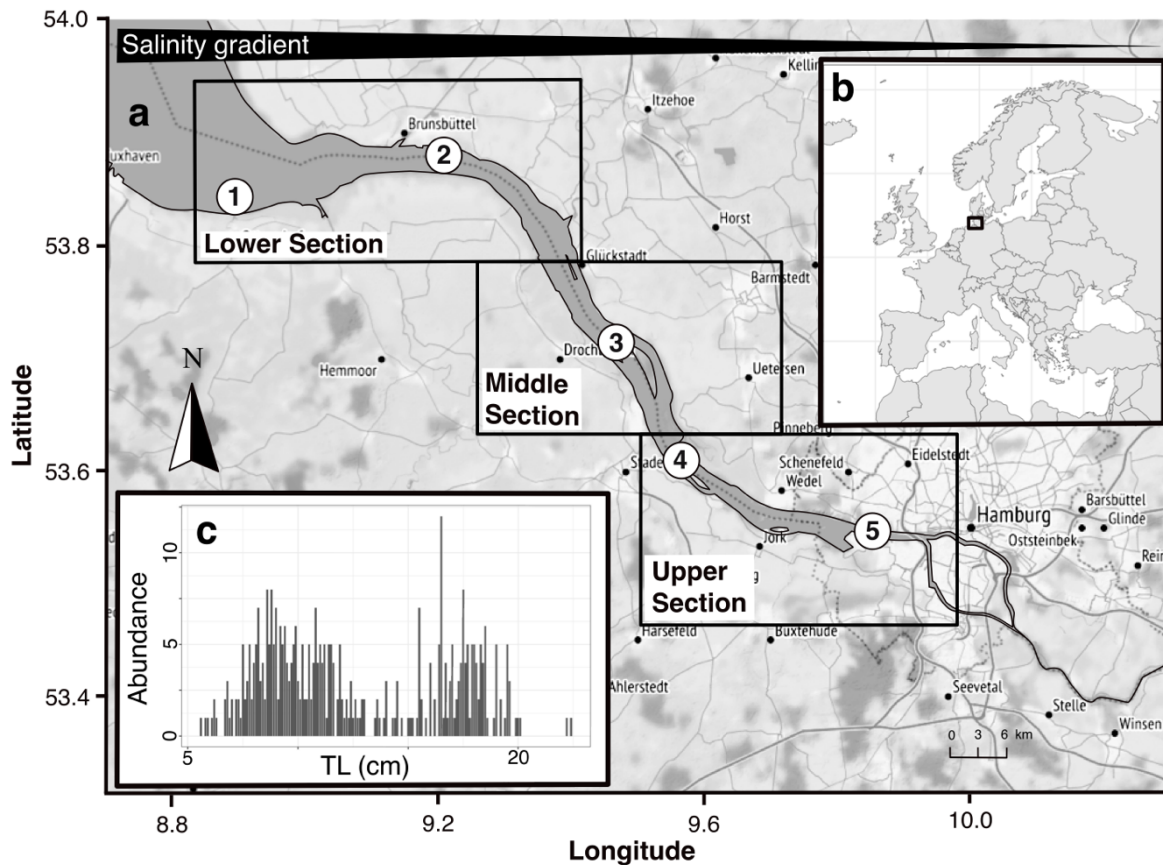


Fig. 5.1: (a) The Elbe estuary with sampling stations (1) Medemgrund, (2) Brunsbüttel, (3) Schwarztonnensand, (4) Twielenfleth and (5) Mühlenberger Loch along the salinity gradient. (b) The study area is located in Central Europe. (c) Barplot shows the abundance and TL = total length (cm) of sampled estuarine smelt *O. eperlanus* indicating the pattern of two occurring age groups.

### Stomach content analysis

For stomach content analysis ( $n = 265$ ) prey organisms were counted, measured, and determined to the lowest possible taxonomic level. Empty stomachs were excluded from the analysis. Highly digested fish that could not be identified properly were categorised as Pisces. Fragments of incomplete specimens were photographed and measured using the ImageJ software (Schneider *et al.*, 2012) to reconstruct biomasses using linear length-weight regression models according to Pihl and Rosenberg (1982), Mason (1986), Christiansen (1988), Marsh *et al.* (1989), Oesmann (1994), Peitsch (1995), Debus and Winkler (1996), Wang and Zauke (2002) and Lindén *et al.* (2003) (see supplement Table S 5.2). Numbers of fragmented organisms were estimated by counting heads or eyestalks and their biomasses were computed as mean values of intact individuals of the same species. Specimens that were found only very rarely, such as annelids, isopods or cladocerans were grouped into the category *other*.

Relative frequency of the biomass (%W) was calculated for all identified prey species per station and life-stage:

$$\%W = \left( \frac{\sum B_i}{\sum B_t} \right) \times 100 \quad (\text{Eq. 5.1})$$

where  $B_i$  is the stomach content weight of prey  $i$ , and  $B_t$  the total weight of the stomach content.

Prey-specific biomass (% $P_i$ ) is defined as the percentage of a prey taxon  $i$  averaged over all investigated fish stomachs in which prey  $i$  occurred and can be mathematically expressed as:

$$\%P_i = \left( \frac{\sum S_i}{\sum S_{t_i}} \right) \times 100 \quad (\text{Eq. 5.2})$$

where  $\sum S_i$  is the sum of weights of prey item  $i$  and  $\sum S_{t_i}$  the sum of all biomasses in stomachs where prey item  $i$  occurred (Amundsen *et al.*, 1996).

Frequency of occurrence (FO $_i$ ) was calculated by using the formula:

$$FO_i = \frac{n_i}{n} \quad (\text{Eq. 5.3})$$

where  $n_i$  is the number of stomachs that contain prey  $i$  and  $n$  is the total number of investigated stomachs (Amundsen *et al.*, 1996; Brown *et al.*, 2012).

We visualised prey-specific abundances ( $P_i$ ) and frequencies of occurrence (FO $_i$ ) using modified Costello plots to analyse feeding strategy, generalist-specialist dichotomy and niche width contribution based on stomach content data of juvenile and adult smelt (Amundsen *et al.*, 1996). Although the prey composition changes at the species level due to changing salinity conditions along the estuary, these species can be categorised into superordinate prey taxa. To generalise results of feeding patterns of smelt life stages using modified Costello plots, we therefore grouped the prey species into higher taxonomic levels, i.e. Copepoda, Mysidae, Amphipoda, Caridea, Pisces and *other* taxa.

### Stable isotope analysis

White muscle tissue was dissected from the dorsoventral bodyside of each smelt, rinsed with distilled water and subsequently stored at -80 °C on board. In the laboratory, all tissue samples were dried for 24 hours using a freeze dryer and homogenised using a tissue homogeniser and cell lyser. The powdered samples were weighed (0.8 – 1.2 mg) and filled into tin capsules. Stable isotope ratios of  $^{13}\text{C}$  and  $^{15}\text{N}$  in the samples were measured by the commercial laboratory of the UC Davis Stable Isotope Facility of the University of California using a continuous flow isotope ratio mass spectrometer (IRMS) PDZ Europa ANCA-GSL elemental analyzer interfaced to a PDZ Europa 20-20 isotope ratio mass spectrometer (Sercon Ltd., Cheshire, UK).

The final data is expressed relative to international standards VPDB (Vienna Pee Dee Belemnite) for carbon and atmospheric air for nitrogen using the delta notation:

$$\delta X = \left[ \left( R_{\text{sample}} / R_{\text{Standard}} \right) - 1 \right] \times 1000 \quad (\text{Eq. 5.4})$$

where  $X$  is the stable isotope value of C or N in permille (‰), and  $R$  the mass ratio of heavy and light stable isotope ratio ( $^{13}\text{C}/^{12}\text{C}$  and  $^{15}\text{N}/^{14}\text{N}$ ) for either the standard or the sample.

### Statistical analysis

Normality and variance homogeneity of  $\delta^{13}\text{C}$  and  $\delta^{15}\text{N}$  ratios were statistically tested using Shapiro-Wilk-tests and variance tests in R. Overall differences in isotopic values between juvenile and adult smelt were determined afterwards using the non-parametric Mann-Whitney U test ( $p < 0.05$ ). All statistical tests were performed using R (version 4.0.4, R Core Team, 2024).

The isotopic niche width among smelt life stages, overall and spatially separated via sections, were estimated using standard isotopic ellipses (‰<sup>2</sup>) using the SIBER package (Jackson *et al.*, 2011, version 2.1.6). Standard ellipse areas (SEA) were corrected for a small sampling size (SEA<sub>c</sub>). Further, we estimated isotopic niche overlap by the standard ellipse function containing ~ 40% of the isotopic data for each smelt group (juvenile vs. adult). A Bayesian standard ellipse was estimated (SEA<sub>b</sub>) to measure uncertainty by calculating

credible intervals around the individual data (Jackson *et al.*, 2011). Summary statistics of corrected SEA were used to determine confidence intervals (CI) of 95% and 40% for each group. To estimate the overall isotopic niche distribution of juvenile and adult smelt we calculated Layman metrics total area (TA), centroid (CD), nearest neighbourhood distance NND, and standard deviation of NND (SDNND) of each investigated group (Layman *et al.*, 2007).

Proportions of dietary isotope origins and spatial resource preferences of juvenile and adult smelt were determined using the SIMMR package (Parnell and Inger, 2016, version 0.4.5) which is based on a Bayesian mixing model (JAGS – Just Another Gibbs Sampler, Plummer, 2003). We used  $\delta^{13}\text{C}$  and  $\delta^{15}\text{N}$  data of smelt and their potential prey, concentrations of C (%) and N (%) of the selected prey organisms, including trophic enrichment factors (TEF) and smelt life stages to run the model. SIMMR applies Gaussian likelihood and fits the data to the model using Markov chain Monte Carlo (MCMC) (Parnell and Inger, 2016). TEF were set to 0.7‰ for  $\delta^{13}\text{C}$  and 3.0‰ for  $\delta^{15}\text{N}$  per trophic level (Sweeting *et al.*, 2007a, 2007b; Ankjærø *et al.*, 2012).

As SIMMR can only handle one model at a time, we analysed each section of the estuary separately for smelt age groups and finally compared the estimated proportions of all life stages and sections using the *compare\_sources* function. The more prey organisms are fed into the model, the more it leads to an overall depletion of the estimated proportions as the model is not able to distinguish between the sources. To avoid this effect, we chose the top three prey species per section that occurred most in terms of frequency and biomass based on stomach content and isotopic data. To generate isotopic information of zooplankton, we pooled mesozooplankton *Daphnia* spec. and calanoid copepod *Eurytemora affinis* from the upper section of the estuary, which are similar in their isotopic compositions and occurring simultaneously in this area (e.g. Riedel-Lorjé *et al.*, 1998). For Clupeidae we used isotopic values from the literature of young-of-the-year *Sprattus sprattus* from the southern North Sea by Das *et al.* (2003). Finally, we summarised the proportions calculated by the model per section to determine the spatial isotopic source origin.

## Results

### Stomach content analysis

We initially used stomach content analysis to identify the recent feeding history of smelt in the Elbe estuary (Fig. 5.2). Modified Costello plots demonstrate an overall mixed feeding strategy with varying degrees of generalization and specialization on different prey groups (Fig. 5.2a). We found the diet of juvenile smelt to be dominated by Mysidae (*Neomysis integer* and *Mesopodopsis slabberi*) and to a lesser degree on Amphipoda (Gammaridae and *Corophium volutator*). Rare taxa in juvenile smelt diets were Caridea (*Crangon crangon* and *Palaemon longirostris*), Copepoda and *other* group. Fish was rarely identified in stomachs of juvenile smelts but occurred occasionally in high abundances pointing towards a high-between-individual-variability. Compared to juvenile smelt, adults consumed fish more frequently, being the dominant food item together with Amphipoda. In addition, the diet of adult smelt was observed to contain less Mysidae than that of juveniles and only rarely Copepoda or prey assigned to the other prey group. Comparing the diets of smelt along the salinity gradient revealed the dominance of Mysidae (*N. integer* and *M. slabberi*) and Amphipoda (Gammaridae and *C. volutator*) in stomachs of juveniles to exist at all stations but the “Mühlenberger Loch” (station 5 in the upper section, Fig. 5.2b). At this least saline sampling station fish was dominating the diet of both juvenile and adult smelt. In contrast to the juvenile conspecifics, fish was also dominating the diet of adult smelt in the lower section of the Elbe estuary where highest salinities prevail. Here, the fish diet constituted mostly of Clupeidae, Gobiidae and smelt itself (i.e. cannibalism). Caridea (*C. crangon* and *P. longirostris*) was particularly found in smelt’s stomachs from the lower and middle sections in both life stages.

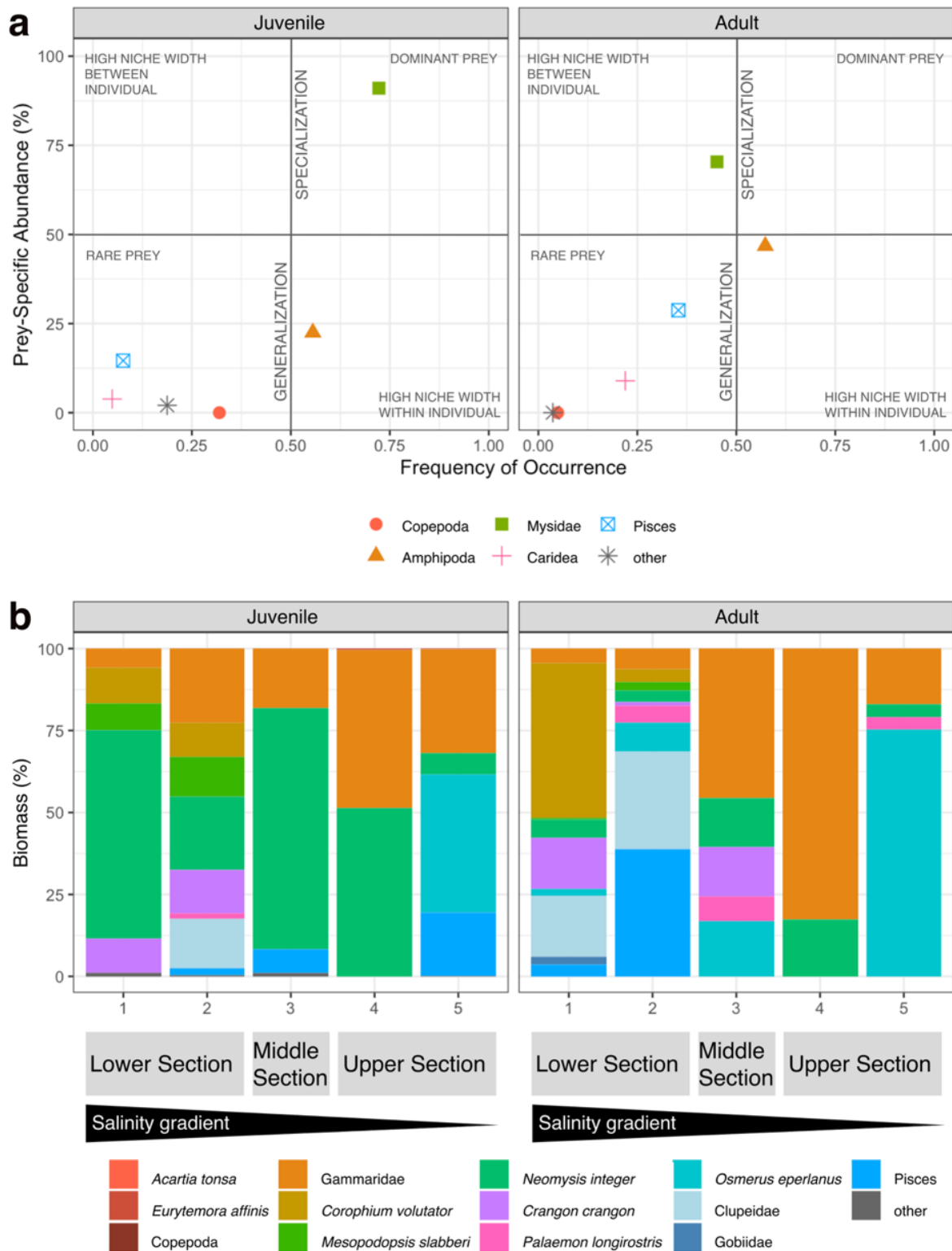


Fig. 5.2: Feeding preferences based on stomach contents of juvenile and adult smelt. **(a)** Modified Costello plots using prey taxa and averaged over sampling stations, and **(b)** percentage of biomass of prey species from smelt caught along the salinity gradient of the Elbe estuary.

## Stable isotope analysis

### Ontogenetic differences in isotopic niches

We first explored differences in stable isotope ratios between juvenile and adult smelt integrated over the entire sampling area in the Elbe estuary. We found juvenile smelts to have significantly (Mann-Whitney U test:  $W = 7112.5$ ,  $p < 0.01$ ) lower  $\delta^{13}\text{C}$  values compared to adults (Fig. 5.3a, Table 5.1). The  $\delta^{15}\text{N}$  values of juveniles were only slightly, but significantly lower (Mann-Whitney U test:  $W = 13418$ ,  $p < 0.01$ ) than of adults. Next, we analysed the overlap in isotopic niches using standard ellipse areas ( $\text{SEA}_c$ ) based on both isotope ratios together. We found a similar isotopic composition between both groups with an isotopic niche overlap of 16.4% (40% CI) of the  $\text{SEA}_c$  or 52.4% with 95% CI (Fig. 5.3b).

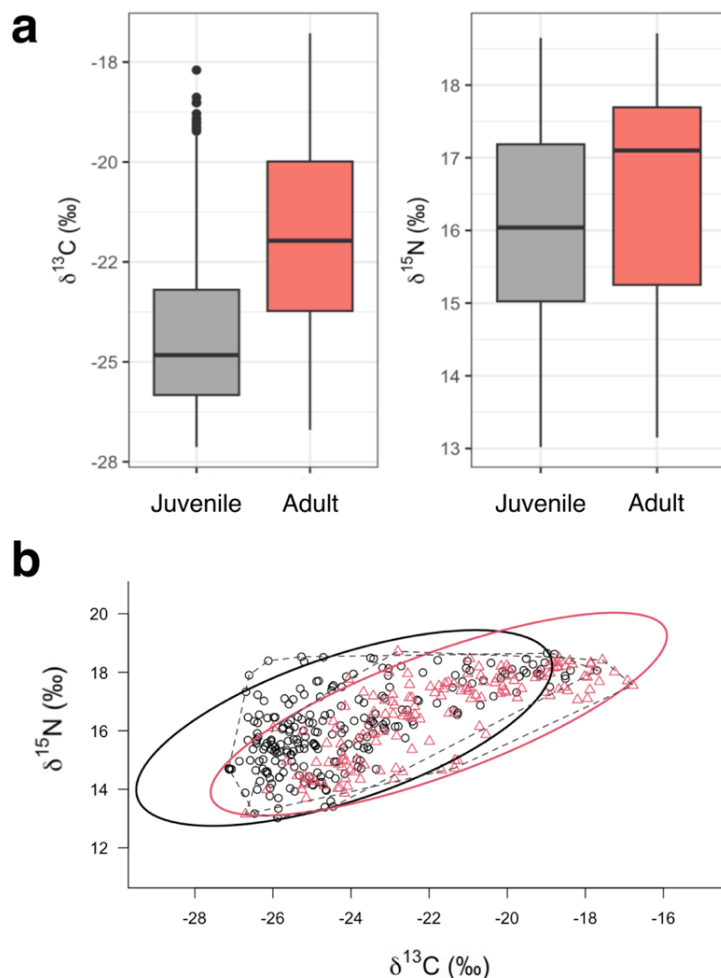


Fig. 5.3: Isotopic niches in juvenile and adult smelt aggregated over the Elbe estuary. **(a)** Boxplots with median as well as upper and lower quartiles of  $\delta^{13}\text{C}$  and  $\delta^{15}\text{N}$  of juveniles and adults. **(b)** Biplot of  $\delta^{13}\text{C}$  and  $\delta^{15}\text{N}$  ratios of juveniles (black circles) and adults (red triangles) with overall 95% CI ellipses (solid lines) and total area (TA) (dashed lines) of the isotopes.

Table 5.1: Characterization of isotopic niche width of smelt life-stages on a general (aggregated) and spatial scale (lower, middle and upper sections) using Layman metrics (TA = total area, CD = centroid, NND = nearest neighborhood distance, SDNND = standard deviation of NND) and SIBER calculations of standard ellipse areas (SEAc = standard ellipse area with correction) with n = sample size.

| Section    | Life-stage | n   | $\delta^{13}\text{C}$ (‰) | $\delta^{15}\text{N}$ (‰) | $\delta^{13}\text{C}$ range | $\delta^{15}\text{N}$ range | TA   | NND  | SDNND | SEAc (‰ <sup>2</sup> ) |
|------------|------------|-----|---------------------------|---------------------------|-----------------------------|-----------------------------|------|------|-------|------------------------|
| Aggregated | Juvenile   | 227 | -24.2 ± 2.2               | 16.1 ± 1.4                | 9.4                         | 5.6                         | 31.5 | 0.17 | 0.13  | 7.3                    |
|            | Adult      | 147 | -21.8 ± 2.4               | 16.6 ± 1.4                | 9.9                         | 5.6                         | 29.2 | 0.23 | 0.16  | 6.8                    |
| Lower      | Juvenile   | 95  | -22.8 ± 2.4               | 16.5 ± 1.3                | 8.9                         | 4.9                         | 21.6 | 0.26 | 0.19  | 5.3                    |
|            | Adult      | 100 | -20.9 ± 2.1               | 17.0 ± 1.2                | 8.2                         | 5.0                         | 22.8 | 0.25 | 0.19  | 5.7                    |
| Middle     | Juvenile   | 67  | -25.0 ± 1.4               | 16.2 ± 1.5                | 5.9                         | 5.4                         | 22.3 | 0.32 | 0.24  | 5.4                    |
|            | Adult      | 26  | -23.4 ± 2.5               | 15.6 ± 1.4                | 9.4                         | 4.1                         | 20.9 | 0.52 | 0.27  | 7.8                    |
| Upper      | Juvenile   | 65  | -25.4 ± 0.9               | 15.4 ± 1.1                | 3.6                         | 5.4                         | 13.6 | 0.25 | 0.21  | 3.2                    |
|            | Adult      | 21  | -23.7 ± 1.4               | 15.5 ± 1.2                | 5.4                         | 4.8                         | 12.1 | 0.61 | 0.54  | 4.0                    |

In addition, we analysed the spatial variation in isotopic niche overlap between juvenile and adult smelt along the salinity gradient of the Elbe estuary (Fig. 5.4). We found a pronounced decrease in isotopic niche overlap from mesohaline to freshwater conditions (Fig. 5.4a). In the lower, high saline section, juveniles showed a broader range of  $\delta^{13}\text{C}$  values. Furthermore, adults had higher  $\delta^{15}\text{N}$  values, except in the middle section. Standard ellipse areas (SEAc) from adult smelt caught at the middle and lower section of the Elbe estuary showed overall highest variation in isotopic ratios and revealed a broader isotopic niche width compared to its juvenile conspecifics (Fig. 5.4b). However, in the middle section the large SEAc and total area (TA) were mainly affected by three individuals containing low  $\delta^{13}\text{C}$  values, potentially derived from marine carbon pools (e.g. Peterson and Fry, 1987). These outliers influenced markedly the isotopic niche width of adults from the middle section but had less effect on the isotopic niche overlap between the life stages (isotopic niche overlap with outliers: 9.0% vs. without outliers: 10.6%).

Overall low values of mean nearest neighbor distances (NND) and standard deviation of NND (SDNND) revealed similar trophic ecologies of the life stages and an even distribution of trophic niches. However, these metrics differed slightly between the life stages. Juveniles showed smaller mean nearest neighbor distances (NND) and standard deviation of NND (SDNND) than adults, except for the lower section. Highest NND was estimated for adults from the upper and middle section.

In the middle and upper sections of the estuary both juvenile and adult smelts are well-separated in both  $\delta^{13}\text{C}$  and  $\delta^{15}\text{N}$  values. Further analyses of SEAc indicated that in the lower,

high saline section of the estuary, both life stages have a similar isotopic niche width (Fig. 5.4b, Table 5.1). Towards the middle and upper sections adults have increasingly large ellipse areas than juveniles, indicating a broader isotopic niche.

Overall, our analysis revealed distinct isotopic niches for juveniles and adults along the salinity gradient, showing greater dietary and/or habitat diversity, especially in the lower region.

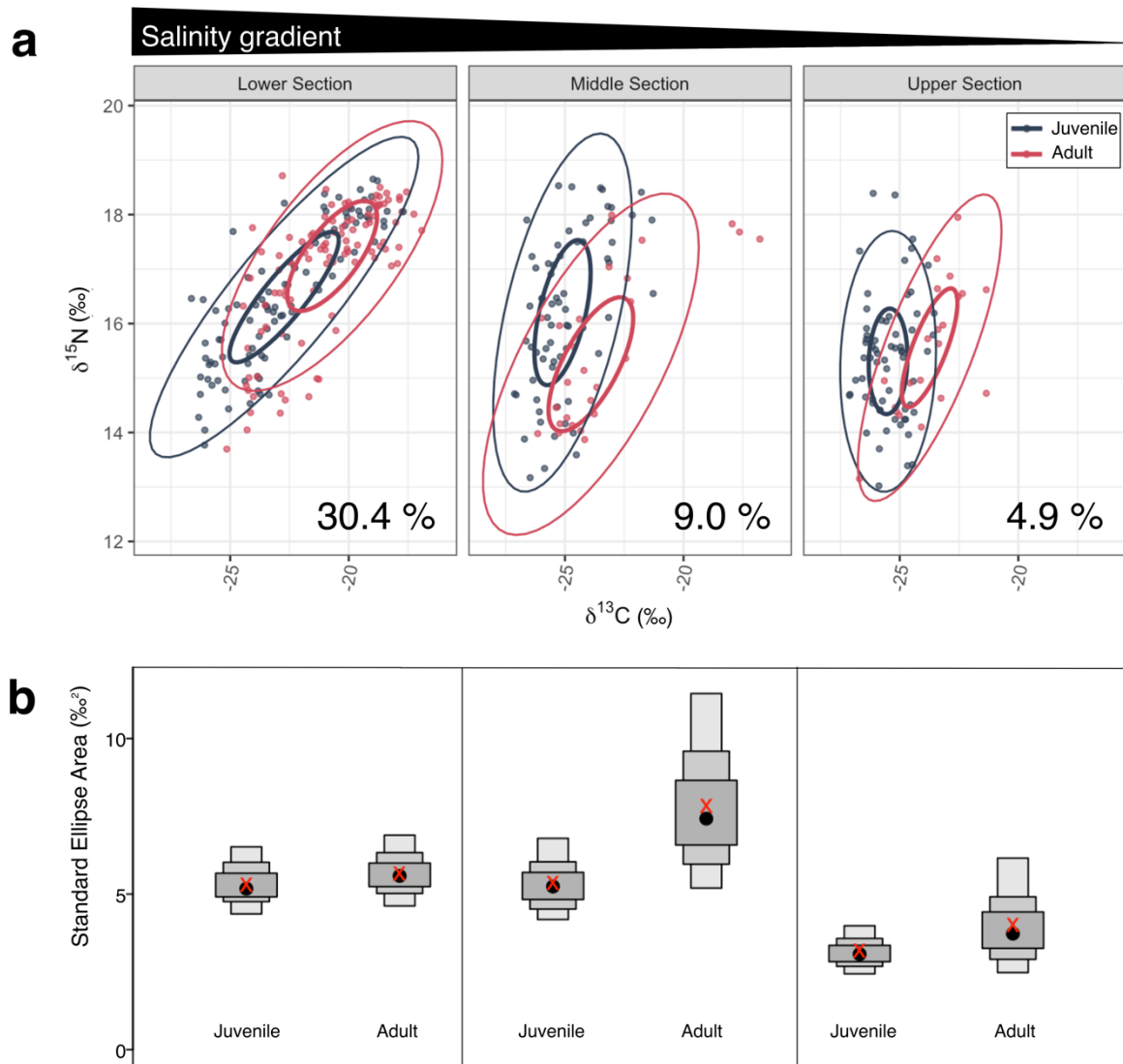


Fig. 5.4: Spatial variation in ontogenetic niches of juvenile and adult smelt along the salinity gradient. **(a)** Overlap of feeding niches across sections with standard ellipse area of 95% (outer ellipse) and 40% (inner ellipse) confidence intervals (CI). Overlaps were estimated using the 40% CI of both life-stages. Percentages indicate overlap between isotopic niches **(b)** Density plots of  $SEA_c$  ( $\text{‰}^2$ ) per section based on stable isotope ratios of  $\delta^{13}\text{C}$  and  $\delta^{15}\text{N}$ . Grey shaded areas show 95%, 75% and 50% confidence intervals with black dots represent the mode values and red crosses the corrected value.

### Spatial origin of food sources

We used Bayesian mixing models to explore the spatial origin of diet-derived carbon and nitrogen in juvenile and adult smelt. The main food items (identified through stomach content analysis and stable isotope analysis) in models for each section along the salinity gradient were used separately (see Material and methods section). Isoplots showed a generally good alignment of  $\delta^{13}\text{C}$  and  $\delta^{15}\text{N}$  of smelt and its food sources (Fig. 5.5a). We

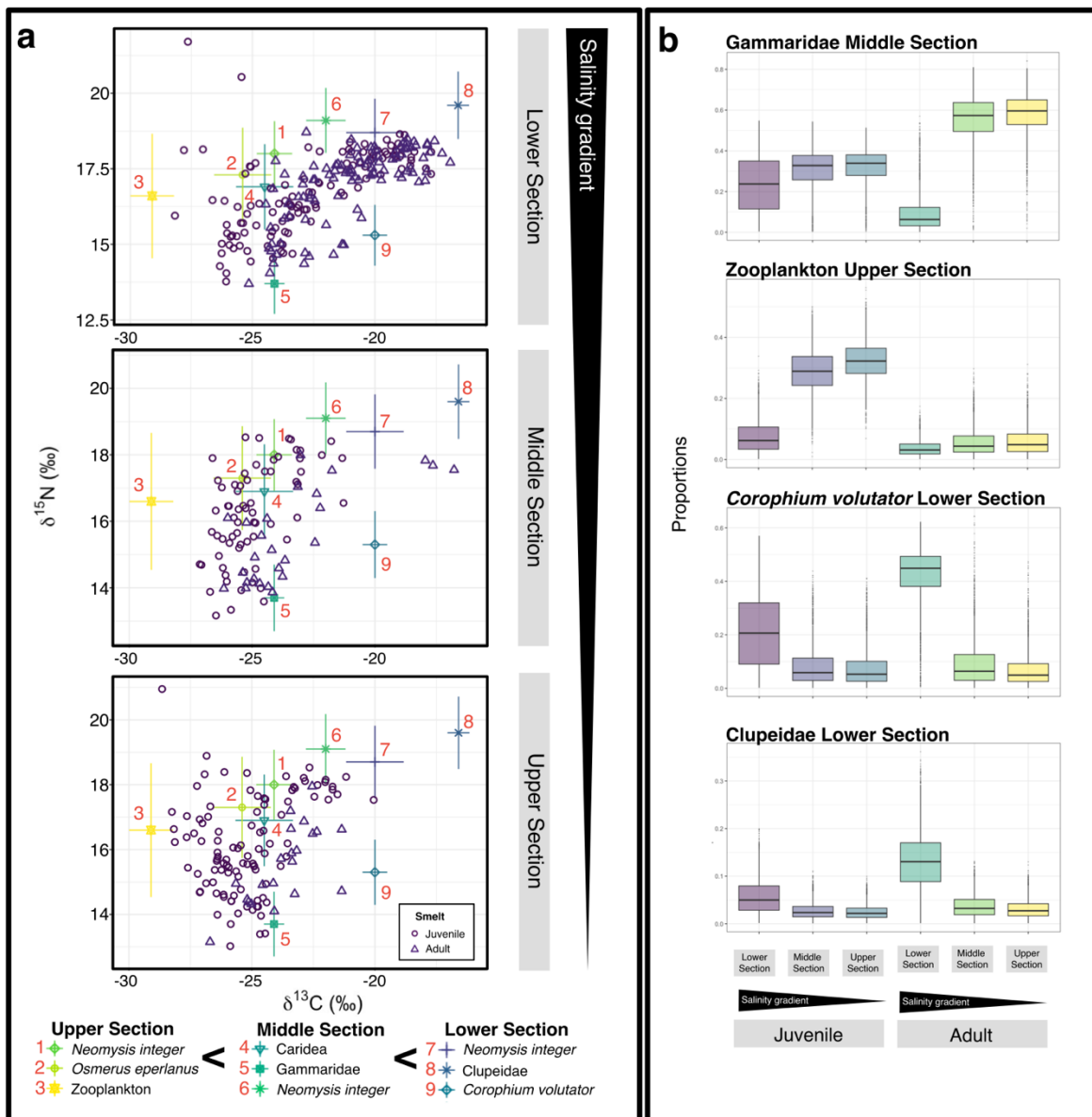


Fig. 5.5: Spatial feeding trends in smelt life stages using SIMMR output. (a) Isoplot of smelt (dots = juveniles, triangles = adults) from distinct sections with isotopic information of prey (containing TEF) from lower, middle and upper sections. Prey items (1-6) (red) differed in their isotopic values, ranging from low freshwater-derived sources in the upper section to high values derived from oligohaline/marine sources in the river mouth/lower section. (b) Proportions of most frequently assimilated prey type-based on  $\delta^{13}\text{C}$  and  $\delta^{15}\text{N}$ . Prey type of the respective section is shown above each panel.

furthermore observed higher  $\delta^{13}\text{C}$  in smelt individuals (both juvenile and adult) from the lower sections, compared to the middle and upper sections, indicating local marine habitat use. The difference between the lower section and the mostly freshwater sections is also demonstrated by the proportions of the main food components found in smelt (Fig. 5.5b). Juvenile and adult smelt from the lower section have both elevated proportions of Clupeidae and the amphipod *C. volutator* in their isotopic signatures. Adult smelt from the middle and upper sections on the other hand displayed higher values in Gammaridae compared to those from the lower section (while no difference in juveniles was found). Eventually, the mixing model for the upper section demonstrates the importance of zooplanktonic food that they feed upon in the middle and upper sections.

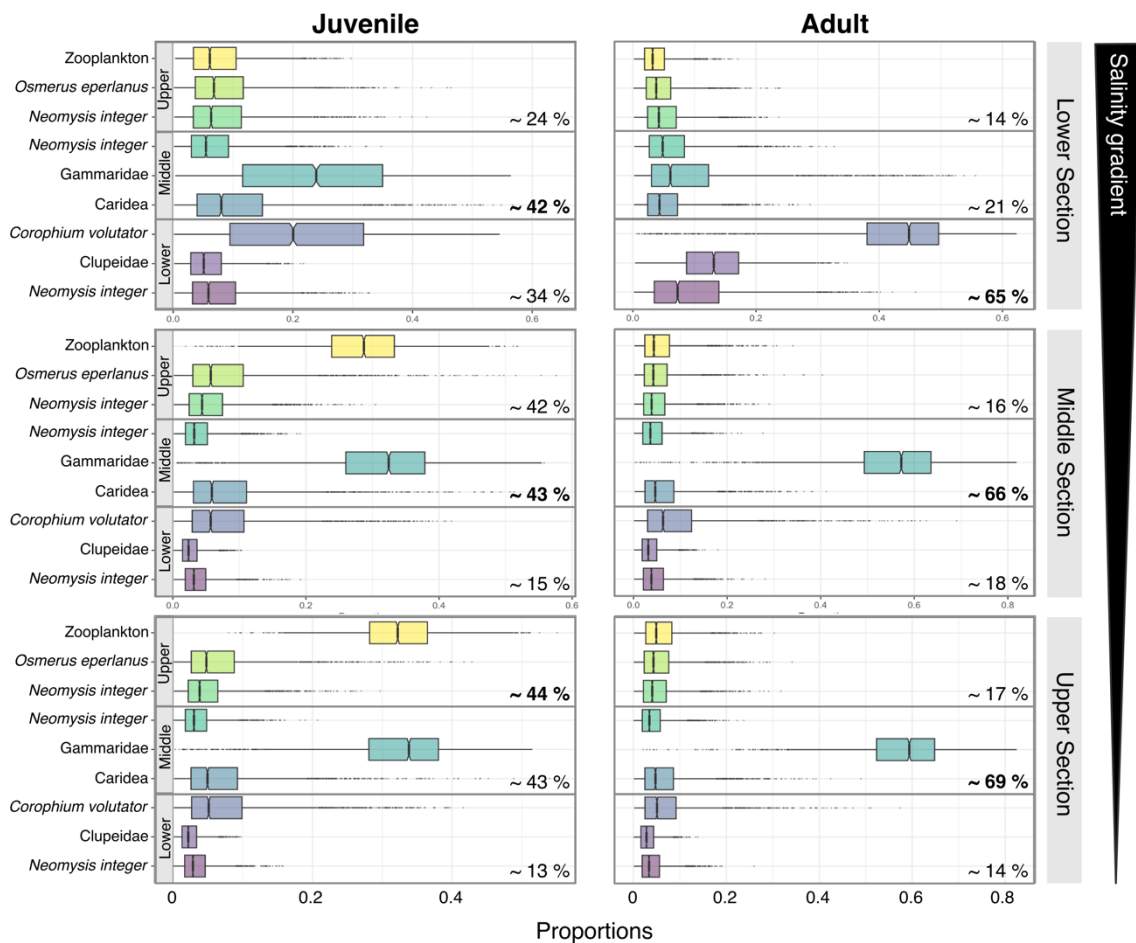


Fig. 5.6: Estimated proportions (%) revealed smelt movements in the Elbe estuary. Credibility interval plot of proportions of prey sources per section based on SIMMR for juvenile (left) and adult smelts (right) caught at lower, middle and upper sections along the salinity gradient. Proportions of prey groups were summed up per section to verify main feeding location of juvenile and adult smelt.

We explored mixing models for the three spatial sections including both life stages (Fig. 5.6). Proportions of food items are summed according to the section where smelt were sampled. The result confirms the spatial feeding patterns that were observed. Adult smelt from the middle and upper sections mostly feed in the middle section (highest aggregated percentages) and mainly rely on Gammaridae. In contrast, adult smelt from the lower section mainly fed locally with the highest proportion of the amphipod *C. volutator*. A similar pattern appeared for juvenile smelt where individuals caught at the middle and upper sections mainly consumed local food, i.e. Gammaridae in the middle section and zooplankton in the upper section. Juveniles from the lower section derived their food mainly from the middle section, the lower section, relying on Gammaridae and *C. volutator*, respectively.

We estimated the highest proportions derived from local and upstream areas for juveniles, especially from the lower and middle sections (Fig. 5.6). We observed the highest variation in stable isotope estimated proportions in adult smelt caught at the lower section. In addition, adults further fed frequently on food derived in the middle section but less on prey from the upper section.

## Discussion

Our study provides valuable insights into the feeding ecology and seasonal habitat exploitation of the European smelt (*Osmerus eperlanus*), a key species in the Elbe estuary. By utilising stable isotope-based Bayesian mixing models of  $\delta^{13}\text{C}$  and  $\delta^{15}\text{N}$ , along with stomach content analyses, we were able to assess both short-term and long-term dietary preferences, ontogenetic niche shifts and isotopic niche widths. This integrated approach allowed us to draw conclusions about spatial resource uses and migrations of smelt.

### Diet composition reflect salinity regime

Stomach data provide a snapshot of a fish's recent diet, whereas stable isotopes reflect the diet assimilated into the consumer's muscle tissue over a longer time period (Harvey and Kitchell, 2000), depending on individual growth and metabolic rates (Buchheister and Latour, 2010). Integrating these methods reduces uncertainties (Nielsen *et al.*, 2018) and

enhances the interpretation of food web datasets (Layman *et al.*, 2005; Davis *et al.*, 2012). In our study, this approach enabled us for a more comprehensive characterisation of smelt feeding ecology over a longer period of time.

Our analyses revealed that smelt from the river mouth exhibited a more diverse diet compared to those from the middle and upper sections of the Elbe estuary. Juvenile smelt in the lower section primarily consumed mysids (*M. slabberi* and *N. integer*), whereas adults mainly fed on marine organisms such as clupeid larvae and the amphipod *C. volutator*. The calculated proportions of clupeids and *C. volutator* similarly showed increased assimilation of isotopes from these prey organisms in smelt tissue, especially in those of adult specimens. The isotope proportions of juveniles in the middle and upper estuary revealed that zooplankton from freshwater and gammarids from the middle of the estuary made up major components of the diet. In contrast, zooplankton appears to play a subordinate role as a food source for adults. Interestingly, zooplankton was nearly absent from the stomach contents of both life stages, despite being a significant component of the isotopic derived diet of juveniles. This discrepancy likely reflects an ontogenetic shift in diet, where juveniles switch from small prey organisms to larger prey with increasing growth (e.g. Franek, 1988; Rochard and Elie, 1994; Vinni *et al.*, 2004; Taal *et al.*, 2014). However, the absence of copepods in the stomachs of juvenile smelt could also be a consequence of fast digestion or of the high feeding pressure on copepods, making a switch to another prey source likely. Rapid depletion in copepod densities due to increased predation by fish has repeatedly been observed in the Elbe estuary (Thiel, 2011).

Notably, at freshwater station Mühlenberger Loch (station 5), smelt larvae made up the largest proportion of the diet of juveniles and adults. Vinni *et al.* (2004) further demonstrated that smelt already show cannibalistic preferences at a total length of 7.8 cm, which promote higher growth rates in young fish.

To explore the ontogenetic shift from smaller to larger prey, we used standard ellipse areas (SEA<sub>c</sub>) to analyse stable isotope data from juveniles and adults (see Jackson *et al.*, 2011). We observed a significant shift in  $\delta^{13}\text{C}$  and  $\delta^{15}\text{N}$  values between the two life stages, though the isotopic niche shift was minor due to the high amount of shared prey organisms, such

as mysids and amphipods. The analysis of isotopic overlaps on a spatial scale along the salinity gradient indicated that the overall pattern was mainly influenced by isotope data from the river mouth, with ellipses shifting and overlap reducing towards freshwater conditions. This suggests that juveniles and adults may be feeding on prey from different  $\delta^{13}\text{C}$  pools in the more freshwater sections.

To account for potential outliers, we reanalysed the isotopic niche overlap in the middle section, excluding adults with marine-derived  $\delta^{13}\text{C}$  values ( $n = 3$ ). The resulting overlap of 10.6% was similar to the previous calculation of 9.0%, though the isotopic niche width decreased significantly from  $7.5\%{}^2$  to  $3.8\%{}^2$  without outliers. This narrowing of the isotopic niche suggests that migratory smelt contribute to isotopic variability and, consequently, to isotopic niche width.

### **Elongated food chain in middle estuary**

A unique feature of the middle section was the pronounced accumulation of  $\delta^{15}\text{N}$  in juvenile smelt, which did not occur in other sections. Typically, larger prey organisms of higher trophic levels are found in adult's stomachs, leading to higher  $\delta^{15}\text{N}$  values (DeNiro and Epstein, 1981; Fry, 1988). However, the elevated  $\delta^{15}\text{N}$  in juveniles here might be caused by anthropogenic influences such as wastewater (McClelland *et al.*, 1997; Donázar-Aramendía *et al.*, 2019), sewage treatment plants (Wayland and Hobson, 2001; Cole *et al.*, 2004; Morrissey *et al.*, 2013) or agricultural runoff (Heaton, 1986), all of which can increase nitrogen loads in the food web and further increasing  $\delta^{15}\text{N}$  values (Cabana and Rasmussen, 1996; McClelland *et al.*, 1997; Cole *et al.*, 2004). Sanders *et al.* (2018), however, identified nitrification hot spots in the Hamburg port area and the overall increased nitrate concentration that increased towards inland but did not measure high concentrations at the middle section of the Elbe estuary. Hence, the observed  $\delta^{15}\text{N}$  enrichment may have other causes here.

The middle section, located within the Maximum Turbidity Zone (MTZ) of the Elbe estuary, is characterised by high variation in salinities, turbid waters and nutrient fluxes from both upstream and downstream, driven by river runoff and the tidal inflow from the North Sea,

respectively (Kamjunke *et al.*, 2023). These conditions create a challenging environment that affects the entire aquatic food chain (Mosman *et al.*, 2023). Limited food supply and mixotrophic feeding strategies in this area (Martens *et al.*, 2024b) likely contribute to the extended food chain, where mesozooplankton such as the copepod *Eurytemora affinis* switch to a more carnivorous diet (e.g. increased consumption of rotifers) under low food availability (Modéran *et al.*, 2012). This extended food chain could lead to elevated  $\delta^{15}\text{N}$  values in juvenile smelt (Layman *et al.*, 2007; Biederbick *et al.*, 2024), indicating a reliance on local food supply and environmental conditions, while adults may avoid areas with low food availability or unfavourable environmental conditions (e.g. oxygen minimum zones) (Thiel *et al.*, 1995).

### **Spatial habitat exploitation and movements**

Our Bayesian models, applied separately to each fishing section for juveniles and adults, revealed major differences in dietary proportions between the river mouth and the more freshwater sections. Juveniles in the river mouth primarily assimilated prey from the middle and lower sections, while adults fed mainly within this region. In contrast, in the middle and upper sections, juveniles relied more on local and upstream food sources, while adults primarily consumed prey from the middle section. Due to the high proportions estimated from local and further upstream derived food sources in juvenile smelt, we conclude that their movements are potentially rather tidal dependent. Our findings reveal distinct habitat exploitation patterns and migration behaviours in juvenile and adult smelt. However, due to the variability of food organisms in the respective sections, we cannot be completely sure that we have accounted for all important food sources. Still, our models offer robust insights into the spatial feeding dynamics of smelt across the estuary.

### **Juvenile and adult prey competition**

In summary, our results enhance the understanding of the feeding ecology and seasonal habitat exploitation of smelt in the Elbe estuary. These insights could be applicable to trophic dynamics in other cool-temperate estuaries dominated by a key fish species.

During our sampling in May and June, both juveniles and adults were present throughout the study area, displaying distinct habitat exploitation strategies, as discussed above. Adults primarily fed in the river mouth and in the middle section of the Elbe estuary, while juveniles exploited local food sources. Nonetheless, we observed a large overlap of prey organisms, probably indicating intraspecific competition between the two life stages. As our findings illustrate the ability of adult smelts to leave areas with insufficient habitat conditions, the results promote a strategy of avoiding intraspecific competition when food supply is low. Additionally, estuaries are generally characterised by high biomass production and low species diversity (Platell *et al.*, 2006), which consequently forces exploitation of the same prey species by consumers. We therefore assume that the influence of competition within the species is rather low. Previous studies showed that the opportunistic feeding of smelt generally correlates with the food availability of a few prey species that occur in high biomass rates (e.g. Popov, 2006; Taal *et al.*, 2014) which further fluctuate on a temporal and spatial scale (Pothoven *et al.*, 2009; Taal *et al.*, 2014).

In spring, high productivity rates (e.g. plankton blooms, high zooplankton densities) are particularly notable in the Mühlenberger Loch (station 5) and the adjacent Hahnöfer Nebelbe, areas recognised as important nursery habitat for local fish species, especially smelt (Thiel *et al.*, 1995; Thiel, 2001). Thiel *et al.* (1995) observed here the highest smelt larvae densities especially in May. These areas are part of the Natura 2000 protected area network (Fricke *et al.*, 2021) and are characterised by large biomasses of *Eurytemora affinis* in spring (Köpcke, 2002). This copepod therefore serves as a key prey species for juvenile fish with increasing importance towards inland (Thiel, 2001). The high predation pressure on mesozooplankton in these areas often leads to a top-down induced decline in copepod biomass during spring (Köpcke, 2002; Thiel, 2011), prompting a shift to cannibalistic feeding behaviour in juvenile smelt. This dietary shift is supported by our analyses, which reveal a transition from zooplankton to cannibalism as a favoured feeding strategy in juvenile smelt during this period. Our findings underscore the importance of the Mühlenberger Loch as both a nursery and feeding ground for various smelt life stages (Thiel *et al.*, 1995; Thiel, 2001), highlighting its crucial role in the local estuarine food web.

## Conclusion

The findings of our study underline the importance of estuaries serving as essential nursery and feeding habitats for fish. Here we show that the feeding ecology of the key species smelt *Osmerus eperlanus* changes during its life cycle, as a result of changing diet during ontogeny and increasing movement ability in the adult stage. Juveniles showed a strong dependence on the local food supply, suggesting that they are more exposed to the prevailing environmental conditions than adults. Along the salinity gradient we observed increasing utilisation of distinct resources in juveniles and adults highlighting increasing ecological differentiation between the life stages as salinity increases.

Due to its high biomass rates, smelt inhabits a key function in the Elbe estuary, serving as an important nutrient source for other fish, birds, and marine mammals (Taal *et al.*, 2014; McCarthy *et al.*, 2019). In northern Europe, anadromous smelt populations show an overall depletion (McCarthy *et al.*, 2019), so does the Elbe smelt population in recent years (Illing *et al.*, 2024). Smelt population decline can have multiple reasons, such as low food availability and impairment or even loss of suitable spawning and nursery habitats (Sendek and Bogdanov, 2019). This study especially underlines the importance of intact nursery areas to ensure recruitment success of this key species. Based on our results, we conclude that particularly shallow areas are crucial for the development and growth of juvenile smelt and should be further considered as part of conservation strategies to protect the fish community in the Elbe estuary.

## Funding

This study was funded by the Deutsche Forschungsgemeinschaft (DFG, German Research Foundation) within the Research Training Group 2530: “Biota-mediated effects on Carbon cycling in Estuaries” (project number 407270017; contribution to Universität Hamburg and Leibniz-Institut für Gewässerökologie und Binnenfischerei im Forschungsverbund Berlin e.V.) This work was also supported by the project “Blue Estuaries” funded by the Federal Ministry for Education and Research under funding code 03F0864F.

## Acknowledgements

We would like to thank the fishing crew of the “Ostetal”, especially Claus Zeeck, Harald Zeeck and Dirk Stumpe for their technical support and fishing expertise. Moreover, we would like to acknowledge all students and technicians, especially Sven Stäcker, Joachim Lütke and Stefanie Schnell, who supported us during field and lab work.

## Supplementary material

Table S 5.1: Information on number of juvenile and adult smelt individuals caught at stations 1-5.

| Section | Station number | Station           | Juvenile (n) | Adult (n) |
|---------|----------------|-------------------|--------------|-----------|
| Lower   | 1              | Medemgrund        | 60           | 49        |
|         | 2              | Brunsbüttel       | 56           | 50        |
| Middle  | 3              | Schwarztonnensand | 68           | 25        |
| Upper   | 4              | Twielenfleth      | 43           | 4         |
|         | 5              | Mühlenberger Loch | 36           | 13        |

Table S 5.2: List of regressions to reconstruct prey biomasses based on measured fragments found in stomach contents of smelt (EXP= e<sup>^</sup> function)

|                               | Fragment               | Regression TL (mm)        | Regression weight (g)                 | Literatur               |
|-------------------------------|------------------------|---------------------------|---------------------------------------|-------------------------|
| <b>Pisces</b>                 |                        |                           |                                       |                         |
| <i>Osmerus eperlanus</i>      | Otolith diameter (OTO) | TL=-<br>16.634+39.248*OTO |                                       | Debus and Winkler 1996  |
| <i>Osmerus eperlanus</i>      | Lower jaw (LJ)         | TL=7.7098*LJ+4.7067       |                                       | Debus and Winkler 1996  |
| <i>Pomatoschistus microps</i> | TL                     |                           | W = EXP( 3.607 * ln(TL) + ln(0.0002)) | Pihl and Rosenberg 1982 |
| <b>Caridea</b>                |                        |                           |                                       |                         |
| <i>Crangon crangon</i>        | TL                     |                           | W = EXP(2.84 * ln(TL) + ln(0.3603))   | Pihl and Rosenberg 1982 |
| <b>Amphipoda</b>              |                        |                           |                                       |                         |
| <i>Corophium volutator</i>    | Head diameter (H)      |                           | W=EXP((0.36+0.35*H)/10)               | Mason 1986              |
| <i>Gammarus zaddachi</i>      | TL                     |                           | W=0.0029×TL <sup>2.88</sup> *0.001    | Wang and Zauke 2002     |
| <b>Mysidae</b>                |                        |                           |                                       |                         |
| <i>Mesopodopsis slabberi</i>  | TL                     |                           | W = 0.0000135*TL <sup>2.744</sup>     | Oesmann 1994            |
| <i>Neomysis integer</i>       | Eye                    | TL= -<br>4.479+29.988*Eye | W=0.0000022715*TL <sup>3.46</sup>     | Debus and Winkler 1996  |
| <i>Neomysis integer</i>       | Telson (TEL)           | TL=1.6125+TEL*6.25        |                                       | Debus and Winkler 1996  |
| <i>Neomysis integer</i>       | Standard               |                           | 0.0035                                | Debus and Winkler 1996  |

CHAPTER 5: FEEDING ECOLOGY OF OSMERUS EPERLANUS

|                           |               |                |                                                                  |                                 |
|---------------------------|---------------|----------------|------------------------------------------------------------------|---------------------------------|
| <i>Neomysis integer</i>   | TL            |                | $W=0.00000283*TL^{3.15}$                                         | Debus and Winkler 1996          |
| <i>Neomysis integer</i>   | Standard      | 1.82 ± 0.19 cm | 5.82±1.84 mg                                                     | Lindén et al. 2003              |
| <b>Copepoda</b>           |               |                |                                                                  |                                 |
| <i>Eurytemora affinis</i> | TL            |                | $W=12.9*TL^{2.92*0.000001}$                                      | Christiansen 1988, Peitsch 1995 |
| <b>Others</b>             |               |                |                                                                  |                                 |
| Annelida                  | Width, Length |                | $W = -49.509 + 0.280 (\text{Width})^2 + 9.205 (\text{Length})^2$ | Marsh et al. 1989               |

## Chapter 6: Estuarine phytoplankton dynamics: Picophytoplankton



Manuscript published in *Plant-Environment Interactions* (27/10/2024):

Martens, N., Biederbick, J., and Schaum, C.-E. 2024. Picophytoplankton prevail year-round in the Elbe estuary. *Plant-Environment Interactions*, 5(5), 1–11. <https://doi.org/10.1002/pei3.70014>.

Microscope images used with permission from Nele Martens.

**Title:** Picophytoplankton prevail year-round in the Elbe estuary

**Running title:** Estuarine phytoplankton dynamics: Picophytoplankton

Authors: Nele Martens<sup>1\*</sup>, Johanna Biederbick<sup>1</sup> and C.-Elisa Schaum<sup>1,2</sup>

<sup>1</sup>Institute of Marine Ecosystem and Fishery Science, University of Hamburg, Olbersweg 24, 22767 Hamburg, Germany.

<sup>2</sup>Center for Earth System Research and Sustainability, Bundesstrasse 53-55, 20146 Hamburg, Germany

\*Corresponding author

E-Mail: [nele.martens.mar@gmail.com](mailto:nele.martens.mar@gmail.com)

## Abstract

Picophytoplankton are important primary producers, but not always adequately recognised, e.g. due to methodological limitations. In this study, we combined flow cytometry and metabarcoding to investigate seasonal and spatial patterns of picophytoplankton abundance and community composition in the Elbe estuary. Due to the mixing of freshwater and seawater and the tidal currents this ecosystem is characterised by typical estuarine features such as salinity gradients and high turbidity. Picophytoplankton (mostly picoeukaryotes such as *Mychonastes* and *Minidiscus*) contributed on average 70 % (SD = 14 %) to the total phytoplankton counts. In summer picocyanobacteria (e.g. *Synechococcus*) played a more significant role. The contributions of picophytoplankton to the total phytoplankton were particularly high from summer to winter as well as in the mid estuary. However, at salinities of around 10 PSU in the mixing area of freshwater and seawater the proportion of picophytoplankton was comparably low (average 49 %, SD = 13 %). Our results indicate that picophytoplankton prevail in the Elbe estuary year-round with respect to cell counts. Picophytoplankton could occupy important niche positions to maintain primary production under extreme conditions where larger phytoplankton might struggle (e.g. at high or low temperature, high turbidity and in areas with high grazing pressure), and also benefit from high nutrient availability here. However, we did not find evidence that they played a particularly significant role at the salinity interface. Our study highlights the importance of including picophytoplankton when assessing estuarine phytoplankton as has been suggested for other ecosystems such as oceans.

Keywords: picocyanobacteria, picoeukaryotes, salinity, temperature, turbidity

## Introduction

Picophytoplankton (< 2-3  $\mu\text{m}$ ) are important primary producers in aquatic ecosystems from oligotrophic to eutrophic habitats (Moreira-Turcq *et al.*, 2001; Zhang *et al.*, 2015; Purcell-Meyerink *et al.*, 2017; Coello-Camba and Agustí, 2021; Takasu *et al.*, 2023). These tiny organisms fulfil crucial ecological functions, e.g. as food for nauplii larvae and filter feeders (Bernal and Anil, 2019; Richard *et al.*, 2022) and in carbon export (Puigcorb  *et al.*, 2015; Basu and Mackey, 2018). The small size of picophytoplankton allows them to occupy specific ecological niches, for example due to the high surface to volume ratio which might facilitate the uptake of required nutrients, and slow sinking velocity that can keep them in the euphotic zone (Raven, 1998; Massana, 2011). Short generation times and high standing genetic variation give picophytoplankton a comparatively high evolutionary potential (e.g. Schaum *et al.*, 2016; Barton *et al.*, 2020; Benner *et al.*, 2020). Picophytoplankton are more than likely to prevail in changing environments (see e.g. Benner *et al.*, 2020; Flombaum and Martiny, 2021; Tan *et al.*, 2022). Some picophytoplankton have been shown to appear under extreme conditions e.g. at high or varying salinity, turbidity and temperature (Belkinova *et al.*, 2021; Somogyi *et al.*, 2022).

Extreme living conditions are common across ecosystems, including estuaries. Estuaries are the interfaces between the freshwater and marine world and characterised by gradients and tidal-induced variation of environmental forcing (e.g. salinity, turbidity) and picophytoplankton can be an important group here (Moreira-Turcq *et al.*, 2001; Purcell-Meyerink *et al.*, 2017; Paerl *et al.*, 2020; Sathicq *et al.*, 2020). However, due to their small size picophytoplankton are still often not adequately recognised. This is largely due to difficulties in detecting and identifying these small-celled organisms with light microscopy (Bergkemper and Weisse, 2018). Moreover, it has been shown that picoeukaryotes cannot be thoroughly preserved with common fixation techniques, and abundances might decline with storage time (Nogueira *et al.*, 2023). Here, we applied flow cytometry and metabarcoding (the latter partially from Martens *et al.*, 2024b) to (1) investigate spatial and seasonal patterns in picophytoplankton abundance and composition in the Elbe estuary, (2) identify dominant taxa and (3) assess under which conditions (with respect to abiotic

factors) picophytoplankton and different players within (e.g. picocyanobacteria) might be particularly dominant.

## Materials and Methods

The Elbe estuary is located in the North of Germany, passing through the city of Hamburg, and enters the North Sea at Cuxhaven (Fig. 6.1a). As one of Europe's largest estuaries it is an important natural habitat and supplies the human population with essential ecosystem services (e.g. via port of Hamburg, recreation areas). The Elbe estuary has been experiencing intense anthropogenic pressure for centuries and further changes such as global warming or deepening of shipping channels might have additional impacts on the ecosystem functioning (see e.g. van Maren *et al.*, 2015). The tidal estuarine area is separated from the Elbe river by a weir at 586 km distance from the river source. A total of 50 surface water samples (ca. 0 - 2 m depth) were taken from seven stations along the Elbe estuary during different sampling campaigns (Fig. 6.1a, supplementary Table S6.1). Samples were taken aboard the research vessel *Ludwig Prandtl*, the fishing vessel *Ostetal*, and from two different piers (Dockland, Seemannshöft) in Hamburg. Further details about sampling in the different sampling campaigns - e.g. sampling method and sample volume - are given in the supplementary data (Table S6.1). Twenty-five samples were taken around the city of Hamburg (approx. 623 - 633 km) and used as a seasonal dataset (Fig. 6.3) and 29 samples from longitudinal sampling of six stations (609 - 713 km) covering three different seasons (spring and summer each 2021 and 2022 as well as winter 2022) were used as a spatial dataset (Fig. 6.2, supplementary Fig. S2).

Of each sample, 3 - 5 technical replicates à 20 µL were analysed using flow cytometry (BD accuri C6 plus) with a flow rate of 66 µl min<sup>-1</sup> and regular cleaning and mixing between the samples. Phytoplankton cells could be distinguished from other suspended matter by their cytometric properties (e.g. fluorescence, size) which were also used to identify different groups of phytoplankton (see e.g. Read *et al.*, 2014; Ning *et al.*, 2021; Thyssen *et al.*, 2022; and supplementary material Fig. S1). Picophytoplankton in the included samples from the Elbe estuary could be divided into two major groups: picoeukaryotes and picocyanobacteria. Picocyanobacteria differed from picoeukaryotes in their fluorescence properties. This group

had a higher phycocyanin- and lower chlorophyll-fluorescence (Fig. S1). Notably, some larger cells might be excluded from our analysis due to detection limits and low sample volume. However, we know from former data (see e.g. NLWKN, 2023; Martens *et al.*, 2024b) that taxa  $< 40 \mu\text{m}$  (e.g. *Stephanodiscus*, *Cyclotella*) are dominant in most seasons and areas of the Elbe estuary.

For the spatial dataset, 16S rRNA metabarcoding as well as 18S rRNA metabarcoding from another study (see further information in Martens *et al.*, 2024b) were included to add information about picophytoplankton taxa in the Elbe estuary (Fig. 6.2, Fig. S2). Samples for 16S rRNA sequencing were processed in the same way as shown for the 18S data (Martens *et al.*, 2024b), however, reads were assigned using the BLAST database (carried out by biome-id Dres Barco & Knebelsberger GbR). In both datasets, we selected taxa that are in

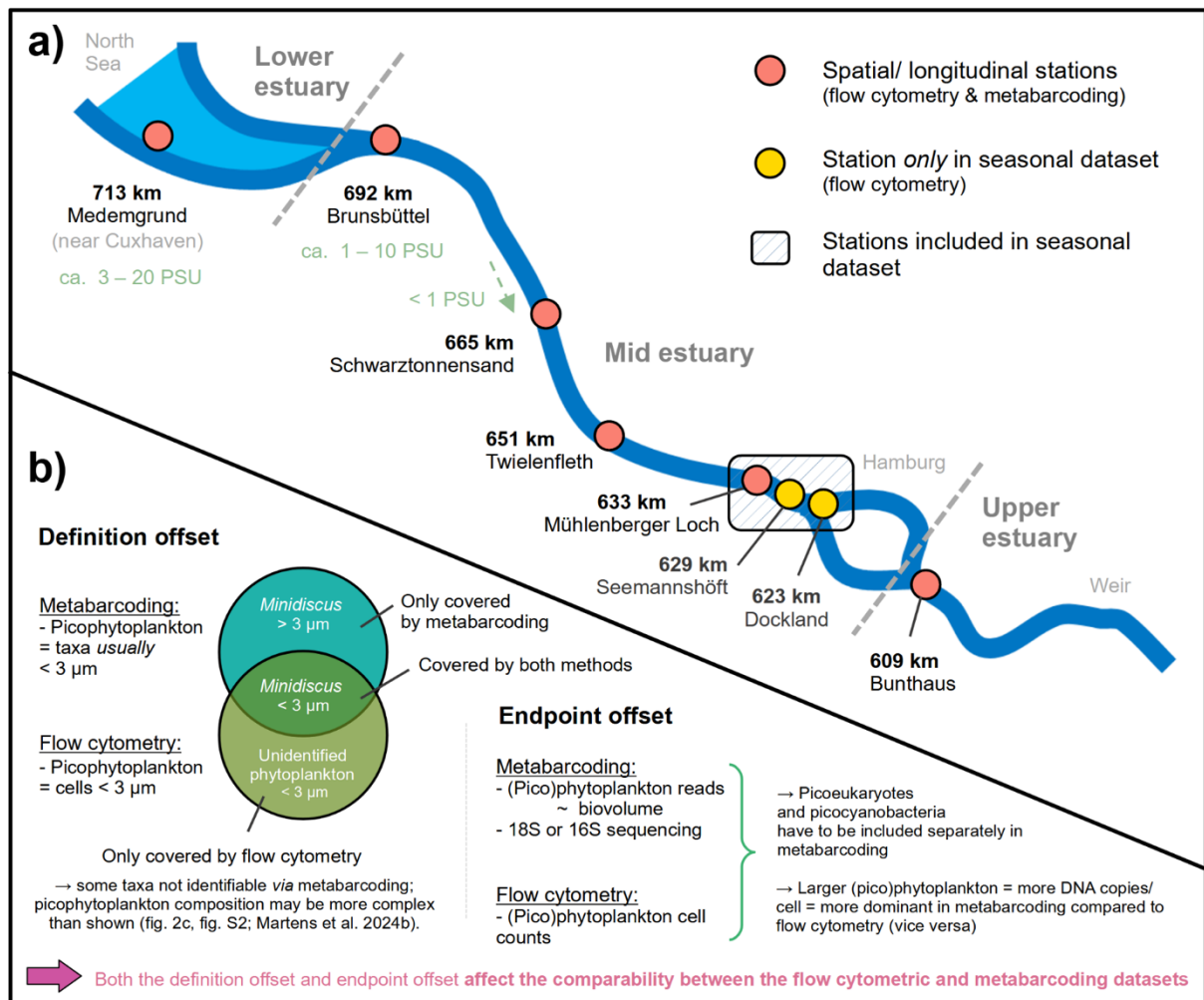


Fig. 6.1: Study area (Elbe estuary) and sampling stations of the seasonal and spatial dataset (a) and schematic overview of the offset between the measured endpoint and definition of picophytoplankton by the different methods (b). In (a) “km” metric indicates the approximate distance from the spring of the Elbe river in the Czech Republic (stream km). In (b), the text within the circles provides examples.

general considered picophytoplankton (e.g. *Synechococcus*, *Choricystis*, *Mychonastes*, *Minidiscus*). These are taxa that are usually  $< 3 \mu\text{m}$ , however, this might not always apply for every species, morphotype and cell within a population. We kept colony forming taxa that might appear solitary where single cells can be  $< 3 \mu\text{m}$  (e.g. *Microcystis*) - as well as unidentified cyanobacteria - in the dataset as they might add to the picocyanobacteria counts in the cytometry data. Note that the definition of picophytoplankton in the metabarcoding data are based on taxa identity and their usual size ranges, while in flow cytometry the definition is exclusively based on the actual cell size ( $< 3 \mu\text{m}$ ) (Fig. 6.1b). Furthermore, while in flow cytometry we detect abundance, metabarcoding results are rather correlated with biovolume. This is due to the size dependence of DNA copies per cell (Godhe *et al.*, 2008) and as a result, larger (picophytoplankton) taxa might appear more dominant in metabarcoding compared to flow cytometric data without being more abundant in terms of cell counts. Consequently, what is included in “picophytoplankton” and how dominant it is can to some extent differ between the methods (see Fig. 6.1b for further details). In addition, missing or insufficient data in metabarcoding (e.g. due to unidentifiable taxa, no sampling at 651 - 665 km in 2021 and low read numbers) make the comparison with flow cytometry rather difficult. For instance, we excluded data from samples with less than 100 picocyanobacteria, respectively picoeukaryotes reads in metabarcoding (Fig. S2). The number of picophytoplankton reads per sample varied from 147 to 6108 (average 1733) in the 18S dataset and 113 to 5692 (average 2155) in the 16S dataset.

Data were processed in R (version 4.1.3), including the packages tidyverse (version 1.3.2), ggplot2 (version 3.4.0), lubridate (version 1.9.2), scales (version 1.2.1) and MuMIn (version 1.47.5). We also used LibreOffice Draw (version 7.1.2.2) for overview figures and addition of text notes and chatPT (GPT-4) to streamline R code and to check the finalised manuscript for common grammatical and typographical errors. For spatial analyses, we obtained potentially interesting patterns from the figures showing cell counts and contributions of picophytoplankton groups along stations (Fig. 6.2a,b) and then carried out an ANOVA `av()` and Tukey test `TukeyHSD()` from the package `stats` (version 4.3.1) to assess whether the observed patterns were significant. To do so, we partially clustered different stations together, e.g. those in the mid estuary (see also Fig. 6.1, Fig. 6.2a,b, Table S6.2). In Fig. 6.2a,b

and Fig. 6.3 we used GAMs for curve fitting with `geom_smooth()` from `ggplot2` and the formula  $y \sim s(x, bs = "cr", k)$ . The  $k$  value describes the number of knots. Knots are the boundaries of the piecewise splines that define the GAM. They describe how often the fitted curve can change e.g. in terms of direction and steepness. The higher the  $k$  value, the more complex the GAM. The  $k$  values were determined based on the lowest AIC as obtained from `uGamm()` from the package `MuMIn` and `AIC()` from `stats` (see Table S6.3).

To set the phytoplankton distributions into context with the environmental conditions, additional abiotic parameters (water temperature, salinity, turbidity,  $PO_4$  and  $NO_3$ ; see also Fig. 6.4 and Table S6.4) were obtained during the sampling campaigns. Temperature, salinity and turbidity were measured with a FerryBox (Petersen *et al.*, 2011) during the sampling cruises. For samples taken from the pier in Hamburg (i.e. at Seemannshöft or Dockland, see Fig. 6.1a, Table S6.1), temperature and salinity were measured with a portable handheld sensor (Hanna Instruments, Vöhringen, Germany; model number HI98494). Nutrient analysis was carried out by Helmholtz-Zentrum hereon. Samples for  $NO_3$  and  $PO_4$  analysis were collected through the flow-through pump system of the FerryBox and filtered through combusted, pre-weighted GF/F filters (4 h, 450 °C), and stored in acid-washed (10 % HCl) PE bottles at  $-20$  °C. Three replicates each were analysed using an automated continuous flow system (AA3, Seal Analytical, Germany) and standard colorimetric techniques (Hansen and Koroleff, 2007), and the mean values were included in this study. A Spearman rank correlation with the function `rcorr()` from the package `Hmisc()` (version 5.1-0) was applied to draw conclusions about the relationship of picophytoplankton groups with abiotic parameters (Fig. 6.4b, Table S6.4). Additionally, turbidity data were obtained from the FGG database (Die Flussgemeinschaft Elbe (FGG Elbe), 2024) to compare these qualitatively with the seasonal dataset, where turbidity was not measured.

## Results

Across seasons and stations, flow cytometry detected between  $2.3 \times 10^3$  and  $123 \times 10^3$  picophytoplankton cells  $mL^{-1}$  in the samples from the Elbe estuary. On average 70 % (SD = 14 %) and up to 99 % of the detected phytoplankton cells per sample were  $< 3 \mu m$ .

Picoeukaryotes were by far the most dominant group with an average contribution of 77 % (SD = 11 %) to the picophytoplankton cell counts, while picocyanobacteria played a role in summer (up to 53 %).

Across seasons, picophytoplankton, picoeukaryotes and picocyanobacteria were overall significantly more abundant at the uppermost station (609 km) than in the area further downstream (633 - 713 km) (Fig. 6.2a, ANOVA/ Tukey:  $p = 6.0 \times 10^{-11}$ ,  $p = 2.1 \times 10^{-10}$  and  $p = 3.7 \times 10^{-6}$ , respectively; see also Table S6.2). Contributions of picoeukaryotes to the phytoplankton cell counts were significantly higher in the mid estuary (633 - 692 km) compared to the upper station (609 km) (Fig. 6.2b, ANOVA/ Tukey:  $p = 0.009$ ; Table S6.2), while they showed no significant differences between the mid and lower, as well as the upper and lower stations (Fig. 6.2b, Table S6.2). As the picophytoplankton fraction was largely represented by picoeukaryotes, those patterns hold for the contributions of picophytoplankton to the phytoplankton cell counts as a whole (Fig. 6.2b, ANOVA/ Tukey:  $p = 0.031$  for comparison of the mid (633 - 692 km) and upper area (609 km); Table S6.2). In contrast, contributions of picocyanobacteria to the picophytoplankton did not express a distinct pattern along space across season (Fig. 6.2b).

*Minidiscus* and *Mychonastes* were the most dominant picoeukaryote taxa across seasons based on 18S rRNA reads (Fig. 6.2c). Therein, *Mychonastes* was more dominant in the upper to mid reaches of the estuary (approx. 609 – 665 km), and *Minidiscus* in the mid to lower area (approx. 651 – 713 km). *Nannochloropsis* was prominent at 609 km in early May (spring 2021) and at 692 to 713 km in February (winter 2022) (Fig. S2a). Here *Choricystis* also played a role (contributions up to approx. 20 %). Other picoeukaryotes such as *Bathycoccus* and *Picochlorum* were minor contributors to the 18S picophytoplankton reads. Results from 16S sequencing (Fig. 6.2c) show that *Synechococcus* and *Microcystis* might be the most relevant contributors to picocyanobacteria in summer 2021, where picocyanobacteria were particularly dominant (up to approx. 43% of the phytoplankton cells; see also Fig. 6.2b). Here *Microcystis* was more dominant at the upper stations (609 - 633 km) and *Synechococcus* at the lower stations (692 - 713 km) (Fig. 6.2c). Notably there is some degree of uncertainty to what extent *Microcystis* would fall into the size range of

picophytoplankton, due to colony formation and cell size. It is likely that *Synechococcus* reached significantly higher proportions among the cells  $< 3 \mu\text{m}$  than suggested in Fig. 6.2c. Minor contributors to the picocyanobacteria reads were e.g. *Prochlorococcus* and *Cyanobium* (“other” in Fig. 6.2c).

In our seasonal dataset from downstream of the city centre of Hamburg (623 - 633 km), the abundances and contributions of the different picophytoplankton groups expressed distinct patterns along the sampling dates. The complexity is reflected in the high  $k$  values (15 - 20) of the fitted GAMs (Fig. 6.3, Table S6.3). Picophytoplankton expressed seasonal peaks in spring, summer and fall, largely due to the respective peaks of picoeukaryotes during these seasons and high picocyanobacteria abundances around July to August with elevated abundances extending into October (Fig. 6.3a). Picophytoplankton contributions to the total phytoplankton were highest in a single sample from the temperature peak in summer (Fig. 6.3b), largely due to picocyanobacteria, and across different samples in fall, which is due to low abundance of larger-celled taxa combined with the fall peak of picoeukaryotes and the remains of the fading summer bloom of picocyanobacteria (Fig. 6.3a,b). In contrast, picophytoplankton were less dominant within the phytoplankton communities in spring (Fig. 6.3b) due to taxa  $> 3 \mu\text{m}$  blooming in parallel. Seasonal effects could also be observed in the spatial dataset as longitudinal data were obtained from different seasons (winter, spring and summer). Here, highest absolute abundances of picophytoplankton were observed in summer 2022 (Fig. 6.2a). Contributions of picophytoplankton to the total phytoplankton counts were overall highest in summer 2021 and in winter 2022 mostly due to picocyanobacteria as well as picoeukaryotes and low abundance of larger-celled phytoplankton, respectively (Fig. 6.2b).

CHAPTER 6: ESTUARINE PHYTOPLANKTON DYNAMICS: PICOPHYTOPLANKTON

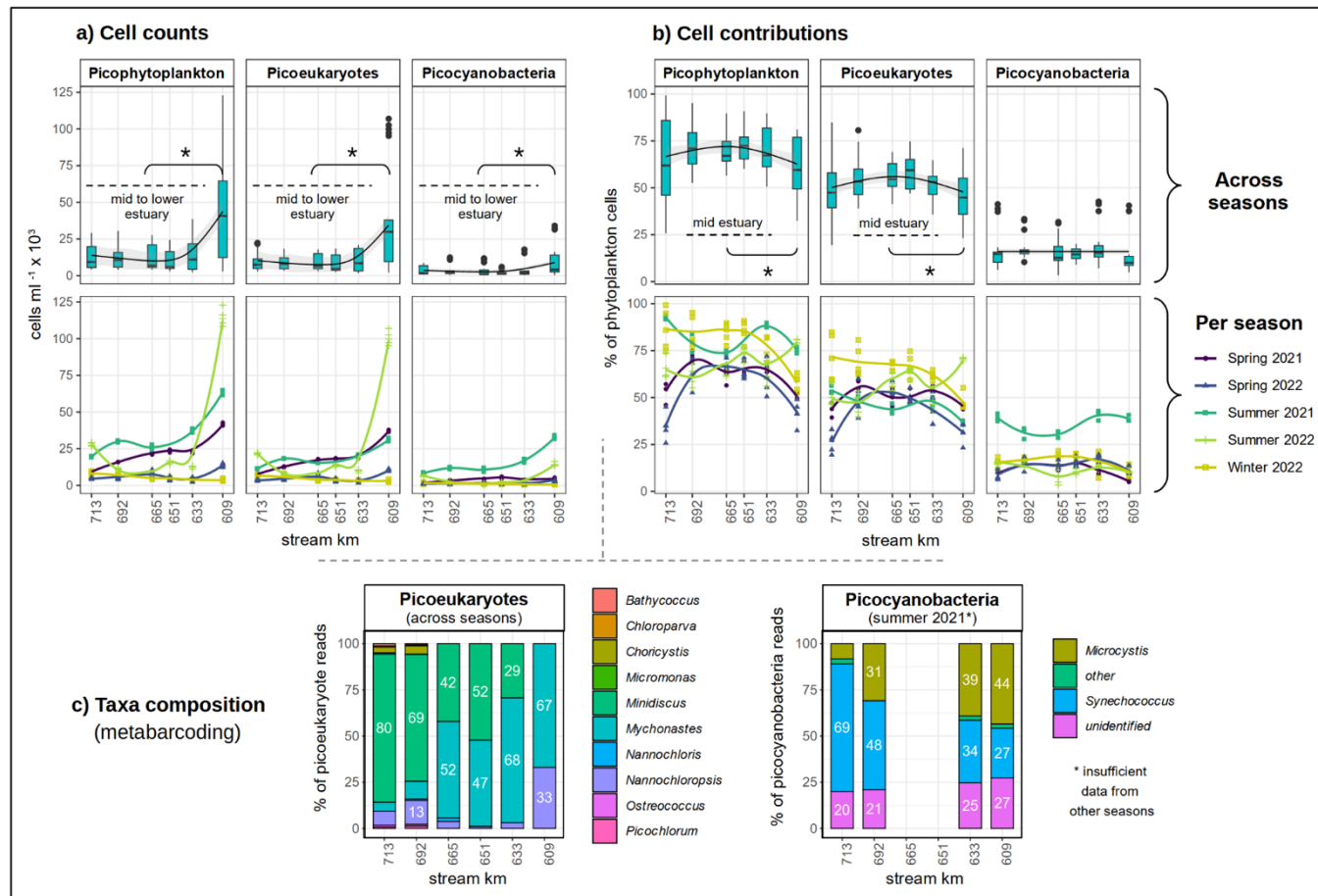


Fig. 6.2: Spatial distribution of different picophytoplankton groups along different stations (stream km). In (a) and (b), the top and bottom row show the same data, but in the top row these are shown across seasons (regression lines = method “gam” with chosen  $k$ ; see also Table S3) and in the bottom row they are shown per season (regression line = method “loess” for visual support). In the top row of (a) and (b) we additionally show where values were significantly different ( $p \leq 0.05$ ) between the upper estuary (609 km) and the mid estuary (633 - 692 km) respectively mid to lower estuary (633 - 713 km) according to an ANOVA and Tukey test (see also Table S2). Data in (c) is partially obtained from a former study Martens et al. (2024b). For clarity, labels are shown for values  $\geq 10\%$  only. Note that metabarcoding was not carried out at 651 - 665 km in 2021, hence the averaged composition of picoeukaryotes at these stations across seasons in (c) does only cover data from 2022. Beyond, it should be considered that metabarcoding includes phytoplankton that could not be identified to genus level and hence does not appear in (c) as they cannot be assigned to the size group of picophytoplankton. Metabarcoding data per season can be found in the supplementary data (Fig. S2). All data are shown in Table S5.

Abiotic conditions varied along seasons and stations (Fig. 6.4a). Temperature was highest in July (up to 23 °C in the spatial dataset at 665 km) and low in winter (down to 3 °C). Turbidity, salinity, NO<sub>3</sub> and PO<sub>4</sub> expressed spatial and seasonal patterns. Salinity was

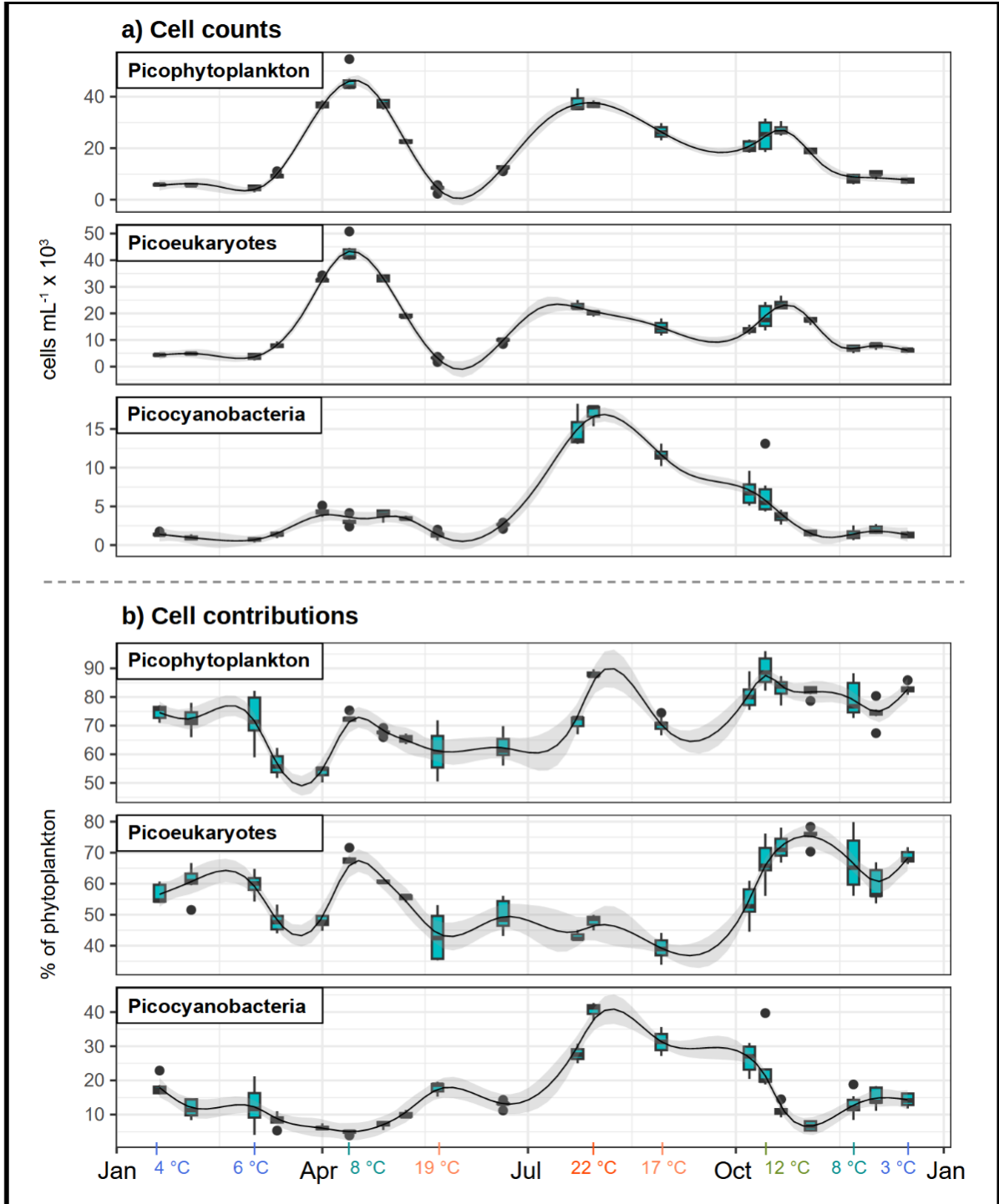


Fig. 6.3: Seasonal distribution of different picophytoplankton groups in the area around Hamburg (approx. 623 - 633 km). Horizontal scales show the sampling date independent of the year, i.e. day of the month. Data were merged when sampling was carried out < 5 days apart. Regression lines were added with `geom_smooth()` from `ggplot2` and the method “`gam`” with chosen `k` values (see also tab. S3). On the bottom we show the temperatures at certain time points (see further details in fig. 4a). All data are shown in tab. S5.

enhanced at the lowermost stations (692 - 713 km) and highest in summer 2022 and spring of both years. Compared to other seasons, turbidity was enhanced in winter 2022 and spring 2021, NO<sub>3</sub> in winter 2022 and summer 2021 and PO<sub>4</sub> in summer 2021. Note that we lack information about turbidity (as well as NO<sub>3</sub> and PO<sub>4</sub>) from fall, as this season was not included during the longitudinal sampling campaigns where turbidity was measured. However, we know from further database data that turbidity was also enhanced in fall 2021 (Fig. 6.3; Die Flussgemeinschaft Elbe (FGG Elbe), 2024). Turbidity, PO<sub>4</sub> and NO<sub>3</sub> concentrations were overall enhanced downstream of 609 km (Fig. 6.4a).

Picophytoplankton abundance was positively correlated with temperature (Fig. 6.4b,  $r = 0.59$  and  $0.53$  for the spatial and seasonal dataset,  $p < 0.001$  each). This was a result of high abundances of both groups in summer - for picoeukaryotes specifically in the spatial dataset

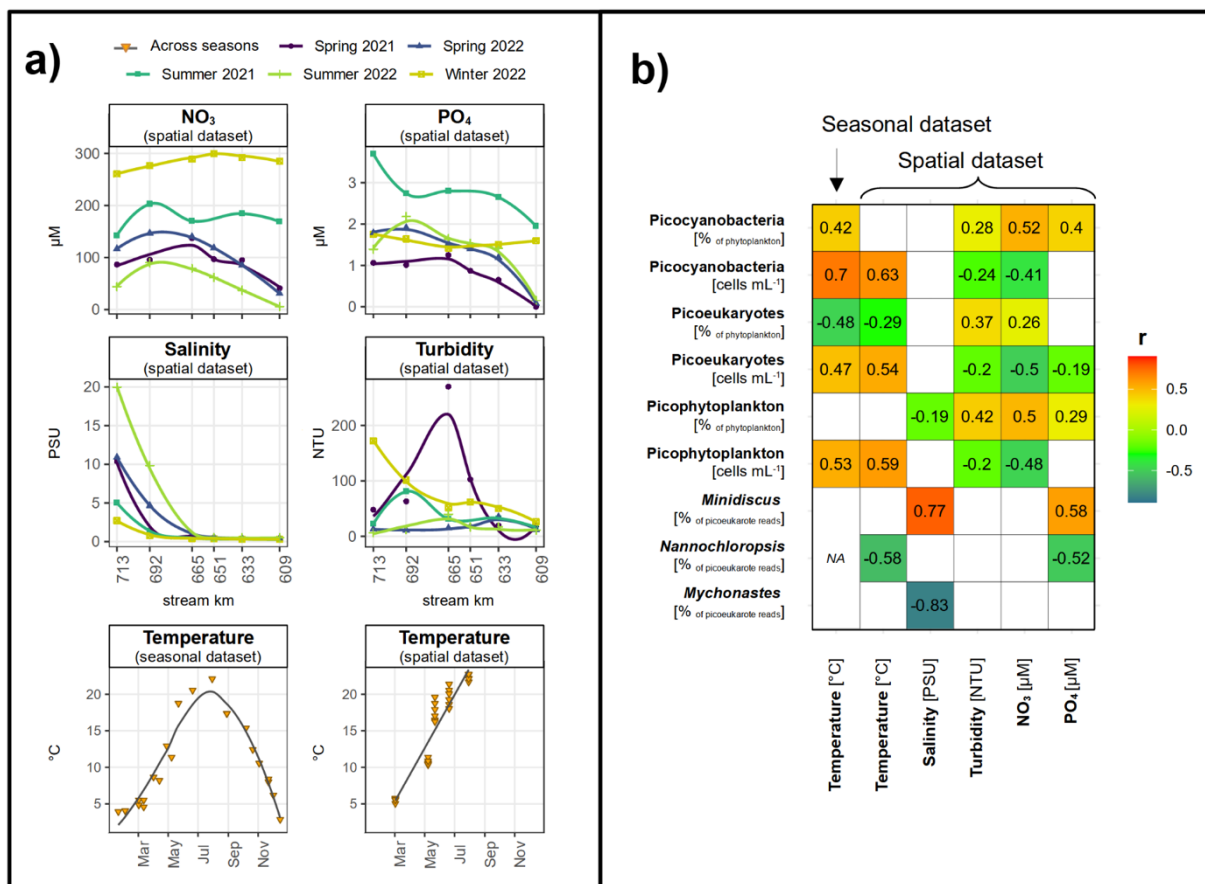


Fig. 6.4: Abiotic conditions (a) and correlation of different picophytoplankton groups with the abiotic conditions (b) in the spatial and seasonal dataset. Numbers and colour scheme in (b) show the correlation coefficient  $r$  calculated with spearman rank correlation for  $p \leq 0.05$  (see also tab. S4). 16S data were not included due to the low number of data points (see methods). Regression lines in a) were added with `geom_smooth()` from `ggplot2` and the method “`loess`” and “`lm`” as visual support. Note that one missing value of turbidity on July 29, 2021 (summer 2021) at 609 km was replaced by a value from July 26, 2021 at 609 km.

in summer 2022 (Fig. 6.2a), and for picocyanobacteria in general (Fig. 6.2a, Fig. 6.3a) - and low abundance of both groups in winter (Fig. 6.2a, Fig. 6.3a). Relative contributions of picoeukaryotes to the phytoplankton were negatively correlated with temperature (Fig. 6.4b,  $r = -0.29$  and  $-0.48$  for the spatial and seasonal dataset,  $p < 0.001$  each). Overall, this pattern arises from relatively high picoeukaryotes contributions to the phytoplankton in fall and winter where phytoplankton abundance was generally low, and enhanced picocyanobacteria contributions to the phytoplankton in summer (Fig. 6.2b, Fig. 6.3b). Picophytoplankton contributions to the phytoplankton cell counts were negatively correlated with salinity (Fig. 6.4b,  $r = -0.19$ ,  $p = 0.040$ ), largely due to low contributions at around 10 PSU at 713 km in spring 2021 and 2022 (Fig. 6.2b, Fig. 6.4a). Cell counts of picophytoplankton were negatively correlated with turbidity and  $\text{NO}_3$  (Fig. 6.4b, turbidity:  $r = -0.20$ ,  $p = 0.029$ ,  $\text{NO}_3$ :  $r = -0.48$ ,  $p < 0.001$ ) due to their high absolute abundance at 609 km - especially in summer - where turbidity and  $\text{NO}_3$  concentrations were rather low (Fig. 6.2a, Fig. 6.4a). In contrast, relative contributions of picophytoplankton to the phytoplankton were positively correlated with these parameters and additionally with  $\text{PO}_4$  (Fig. 6.4b, turbidity:  $r = 0.42$ ,  $p < 0.001$ ,  $\text{NO}_3$ :  $r = 0.50$ ,  $p < 0.001$ ,  $\text{PO}_4$ :  $r = 0.29$ ,  $p = 0.001$ ). This relationship with  $\text{PO}_4$ ,  $\text{NO}_3$  and turbidity is affected by the higher proportions of small cells in the mid to lower estuary, where these parameters achieved overall higher values compared to 609 km and by the seasonal importance of picocyanobacteria in summer 2021 (at high  $\text{PO}_4$ ) and picoeukaryotes in winter (at high turbidity and  $\text{NO}_3$ ) (Fig. 6.2b, Fig. 6.4a). Due to enhanced contributions to the picoeukaryotes reads from winter to spring compared to the other seasons (Fig. 6.2c), *Nannochloropsis* was negatively correlated with temperature (Fig. 6.4b,  $r = -0.58$ ,  $p = 0.010$ ). The negative relationship with  $\text{PO}_4$  (Fig. 6.4b,  $r = -0.52$ ,  $p = 0.022$ ) can be mainly explained by the high contributions of this taxon at 609 km in spring 2021, where  $\text{PO}_4$  was particularly low (Fig. 6.4a). *Mychonastes* was clearly associated with the freshwater reaches of the estuary (Fig. 6.2c, Fig. S2a), resulting in negative correlation with salinity (Fig. 6.4a,b;  $r = -0.83$ ,  $p < 0.001$ ). In contrast, *Minidiscus* was more dominant further downstream (Fig. 6.2c, Fig. S2a) and hence associated with higher salinity and higher  $\text{PO}_4$  values (Fig. 6.4a,b; salinity:  $r = 0.77$ ,  $p < 0.001$ ,  $\text{PO}_4$ :  $r = 0.58$ ,  $p = 0.010$ ).

## Discussion

### **Picophytoplankton dominate phytoplankton communities year-round**

We used flow cytometry to quantify picophytoplankton along the Elbe estuary and across seasons, and combined the results with composition data obtained from metabarcoding. Our results indicate that picophytoplankton - and therein picoeukaryotes - were the dominant groups of phytoplankton in the Elbe estuary with respect to abundance in the vast majority of the samples. Notably, different picoeukaryote taxa (precisely *Minidiscus* and *Mychonastes*) could each contribute up to 17 % to the eukaryotic phytoplankton reads, implying that this group was also relevant in terms of biovolume (see also Martens *et al.*, (2024b) and Fig. 6.1b). Considering their ubiquitous appearance throughout water bodies around the world (Purcell-Meyerink *et al.*, 2017; Sathicq *et al.*, 2020; Coello-Camba and Agustí, 2021; Takasu *et al.*, 2023), it is not surprising that picophytoplankton also play an important role in the Elbe estuary, even though empirical evidence has so far been scarce for this ecosystem. *Mychonastes* in particular has been found in various freshwater bodies (Shi *et al.*, 2018; Yang *et al.*, 2021, 2022; Zhao *et al.*, 2024) and *Minidiscus* is specifically known from marine and brackish habitats (Park *et al.*, 2017; Leblanc *et al.*, 2018; Fernandes and Correr-Da-Silva, 2020).

### **Picophytoplankton abundance follows distinct seasonal and spatial patterns**

The peak in picophytoplankton abundance in spring, summer and fall was likely associated with the elevated temperatures in these seasons (Fig. 6.2a, Fig. 6.3a, Fig. 6.4). Picocyanobacteria were in particular associated with extreme water temperatures (e.g. up to 22 °C) and this relationship has been observed in various studies before (e.g. Alegria Zufia *et al.*, 2021; Li *et al.*, 2024). However, other factors not measured in this study, such as sunlight availability and grazing as a factor to terminate blooms, may play an equally important role in shaping seasonal picophytoplankton patterns.

High picophytoplankton abundances at the uppermost station at 609 km (Fig. 6.2a) derive from the inputs of riverine phytoplankton and their growth in the relatively undisturbed area upstream of the city centre of Hamburg. A drop in phytoplankton abundance from 609 km

towards downstream of Hamburg is a well-known phenomenon from the area. This is partially explained by local grazing effects (Schöl *et al.*, 2009) but may also be affected by e.g. sinking in the current-calmed harbour basins (Wolfstein, 1996). Picophytoplankton abundance followed this pattern in our study and hence seem to be affected by these factors. An increase in picophytoplankton abundance in the vicinity of the North Sea (713 km) in summer 2022 may be explained by coastal inputs, especially as salinity was relatively high in this area and season (ca. 20 PSU).

### **Picophytoplankton are relatively important at extreme temperatures and low light availability**

The proportions of picophytoplankton within the phytoplankton communities (Fig. 6.2b, Fig. 6.3b) show the relative importance of this size group and can indicate where and when picophytoplankton grow better or get removed less quickly than larger phytoplankton. Picophytoplankton contributions to the phytoplankton communities indicate that picophytoplankton play a major role under extreme environmental conditions with respect to temperature and light availability. The proportions of picocyanobacteria within the phytoplankton communities were highest at high temperatures (e.g. 22 °C) following the patterns of their abundance (Fig. 6.2a,b). In contrast, though picoeukaryotes were positively correlated with temperature in terms of cell counts (Fig. 6.4b), and appeared most abundant at 609 km (Fig. 6.2a), their relative importance within the phytoplankton communities was highest at a combination of low temperature and low light availability (e.g. due to turbidity, low sunlight availability in winter). This derived from low contributions in summer in the seasonal dataset (Fig. 6.3b), as well as high contributions in winter 2022 (low temperature, high turbidity) and low contributions in summer 2021 (high temperature) in the spatial dataset and generally higher contributions in the mid estuary (633 - 692 km) where turbidity was overall higher (Fig. 6.2b, Fig. 6.4a). While further research is needed to disentangle the effects of temperature and turbidity, a positive relationship with turbidity has been observed before (e.g. in Somogyi *et al.*, 2017). Picophytoplankton might have specific strategies in light harvesting (Somogyi *et al.*, 2017, 2022; Liu *et al.*, 2020; Coe *et al.*, 2021; Soulier *et al.*, 2022). Additionally, we found that picoeukaryotes from the Elbe estuary were particularly skilled in utilising organic compounds (Martens *et al.*, 2024a). Making use of available

organic resources such as amino acids and carbohydrates can be an efficient strategy of phytoplankton to deal with - partially very variable - resource availability and provide a steady supply with nutrients (e.g. P, N), more complex substrates (e.g. amino acids) and energy (see e.g. Muñoz-Marín *et al.*, 2020; Reinl *et al.*, 2022). However, their higher contributions in the mid estuary might also be partially explained by them being removed less rapidly or distinctively by the lethal factors appearing in the area around Hamburg (e.g. grazing, sinking) (Wolfstein, 1996; Schöl *et al.*, 2009). For instance, small picophytoplankton cells can have a reduced sinking velocity compared to larger-celled phytoplankton. Moreover, while one of the key zooplankton taxa - *Eurytemora* (Schöl *et al.*, 2009) - may utilise picophytoplankton, for example, as part of aggregates (Wilson and Steinberg, 2010; Modéran *et al.*, 2012), they likely prefer to consume larger-celled phytoplankton, and hence, picophytoplankton might be eliminated less quickly by grazing. Lastly, the positive relationship of the contributions of different picophytoplankton groups with nutrients ( $\text{NO}_3$  and  $\text{PO}_4$ ) implies that those groups may benefit from high nutrient availability, for instance in seasons (e.g. winter) and areas (e.g. the mid to lower estuary, 633 - 713) with overall low phytoplankton concentrations.

### **Picophytoplankton are not specifically important at the salinity interface**

Picophytoplankton have been found to be important at extreme and highly variable salinities, e.g. in hypersaline lakes and in the Black Sea (Belkinova *et al.*, 2021; Somogyi *et al.*, 2022) and at intermediate salinities (e.g. 5 - 10 PSU) in estuaries (Wetz *et al.*, 2011), which are somewhat extreme for both freshwater and saltwater inhabitants. However, our data so far imply that picophytoplankton were overall more abundant and dominant at freshwater and rather high salinity (approx. 20 PSU) likely due to coastal inputs. Nevertheless, some picophytoplankton taxa, such as certain genotypes of *Minidiscus* (see also Martens *et al.*, 2024b) as well as *Ostreococcus*, *Bathycoccus*, and *Picochlorum*, which were particularly associated with intermediate salinities (approx. 1 - 10 PSU), have been associated with brackish habitats (e.g. in Hu *et al.*, 2016; Tragin and Vaultot, 2019) and high salinity tolerances (Foflonker *et al.*, 2016; Somogyi *et al.*, 2022) before. Those groups might fulfil significant ecological functions at the salinity interface of the estuary, e.g. as primary

producers and as food items for higher trophic levels, the latter regardless of whether they are in particularly good condition.

### **Taxa composition requires further investigations**

In our dataset, *Mychonastes* and *Minidiscus* were the dominant picoeukaryote taxa based on 18S sequencing, with *Nannochloropsis* playing a role in the colder seasons (Fig. 6.2c) and *Synechococcus* and *Microcystis* played a role as picocyanobacteria based on 16S sequencing. The results of the 16S sequencing were specifically limited as sufficient numbers of reads were often not obtained and we can mostly conclude that these taxa play a role but not further delve into quantitative analysis. However, also the eukaryotic picophytoplankton data are limited, as 18S sequencing (Martens *et al.*, 2024b) generated a lot of phytoplankton reads that could not be assigned to a specific genus. Those reads might partially belong to the group of picoeukaryotes and hence the composition of picoeukaryotes might be more complex than shown in our data (Fig. 6.2c, Fig. S2a). Moreover, in 2021, metabarcoding was not carried out at 651 - 665 km and hence we miss information about this area which was particularly interesting in the flow cytometric results (e.g. with respect to elevated picoeukaryote contributions, Fig. 6.2b). From our data, we can say that *Minidiscus* and *Mychonastes* are likely very important picoeukaryotes in the Elbe estuary. *Minidiscus* was more important from the mid to lower estuary and at elevated salinities (Fig. 6.2c, Fig. S2a, Fig. 6.4) which fits the general distribution of this taxon along brackish and marine habitats (Park *et al.*, 2017; Leblanc *et al.*, 2018; Fernandes and Corrêa-Da-Silva, 2020). In contrast, *Mychonastes* - appearing further upstream - is a genus well known from various freshwater ecosystems (Shi *et al.*, 2018; Yang *et al.*, 2022; Zhao *et al.*, 2024). Both taxa were more dominant in summer and spring (Fig. 6.2c, Fig. S2a), though a positive relationship with temperature was not significant in our data (Fig. 6.4b, see also Martens *et al.*, 2024b). Various studies imply that *Mychonastes* can be important throughout different seasons (Shi *et al.*, 2018; Yang *et al.*, 2022; Zhao *et al.*, 2024), so its higher contributions in summer and spring might be specific for the biome of our study area. Notably, some of the factors mentioned further above, that might be beneficial for picophytoplankton - especially in extreme environments - also apply for *Mychonastes*. For

instance, concerning light harvesting strategies, *Mychonastes* has been found to increase their chlorophyll *a* content and adjust their pigment composition to varying light availability, and *Mychonastes* appears tolerant of a broad range of light availabilities, which may help them survive under the fluctuating light conditions in the Elbe estuary (Malinsky-Rushansky *et al.*, 2002). Additionally, in our former study (Martens *et al.*, 2024a), we found that different strains of *Mychonastes* from the Elbe estuary had a high mixotrophic ability and a flexible strategy to acquire energy and nutrients may add in establishing dominance in our highly variable study area. Unfortunately, there are still few ecological data about *Minidiscus* to compare with. Yet, as a pico-diatom, *Minidiscus* plays a largely unique ecological role as it does not only benefit from its small size (e.g. with respect to a high surface to volume ratio) but also has a protective silica frustule that may prevent rapid removal by grazing and allow this taxon to appear more dominant in the lower and mid estuary.

### **Ecological significance and outlook**

Methodological limitations - such as an underrepresentation of samples with intermediate to higher salinities - might have affected some of our interpretations, however, consistent findings across a high number of samples included, e.g. with respect to the picophytoplankton dominance in terms of cell counts, make it inevitable to conclude that picophytoplankton play a key role in the Elbe estuary. Their high contributions under extreme conditions - e.g. high temperatures and low light availability - imply that they occupy ecological niches where larger phytoplankton might struggle to maintain primary production. Here they supply the higher trophic levels - such as micrograzers, filter feeders and nauplii larvae (see e.g. Bernal and Anil, 2019; Richard *et al.*, 2022) with energy and essential nutrients and hence maintain the food webs. Beyond, by maintaining primary production, picophytoplankton contribute to the upkeep of the biological pump (Basu and Mackey, 2018), that is, the transfer of carbon from (atmospheric) CO<sub>2</sub> towards aquatic biomass and finally carbon sequestration. However, due to their advantage at higher temperatures, (pico)cyanobacteria may become more dominant in the Elbe estuary under global warming (see also Flombaum and Martiny, 2021), which might affect food webs due to the relatively low nutritional value and possible toxicity of cyanobacteria (Ger *et al.*, 2016;

Sim *et al.*, 2023). Our results emphasise the importance to include the so far underrated group of picophytoplankton in (estuarine) research and provide insights into the comparability of techniques (e.g. flow cytometry, metabarcoding) for detecting (pico)phytoplankton communities.

## **Data Availability Statement**

Flow cytometric and metabarcoding data are provided in the supplementary material (Table S6.5). The metabarcoding raw data will be published on ENA. Flow cytometric raw data are available on request from the authors.

## **Acknowledgements**

We would like to thank the captain and crew of the research vessel Ludwig Prandtl and the fishing vessel Ostetal as well as Raphael Koll and Elena Hauten for their contributions to obtain samples, Vanessa Russnak, Leon Schmidt and Kirstin Dähnke (Helmholtz-Zentrum hereon) for providing environmental data, as well as Stefanie Schnell and Luisa Listmann for the technical support in the laboratory and Inga Hense and Hans-Peter Grossart for conceptual support. We acknowledge financial support from the Open Access Publication Fund of Universität Hamburg.

## **Conflict of Interest Statement**

We declare we have no competing interests.

## **Funding**

This project was funded by the Deutsche Forschungsgemeinschaft (DFG, German Research Foundation) within the Research Training Group 2530: „Biota-mediated effects on Carbon Cycling in Estuaries” (project number 407270017; contribution to Universität Hamburg and Leibniz-Institut für Gewässerökologie und Binnenfischerei im Forschungsverbund Berlin e.V. (IGB)).

## **Supplementary material**

Supplementary data are available at *Plant-Environment Interactions* online, at <https://doi.org/10.1002/pei3.70014>.

## Chapter 7: General discussion



*“Kein Buch und kein Gelehrter der Welt kann vermitteln, was die Natur ohne Worte lehrt. Es bedarf weder Stift noch Papier. Nur einen aufmerksamen Geist“*

– Unknown author.

## General discussion

Research on zooplankton in the Elbe estuary is limited, especially with regard to population dynamics and trophic relationships in relation to the prevailing environmental conditions in the estuary. This knowledge is essential for the management of such a highly modified habitat, which is affected by climatic and anthropogenic changes. Previous studies on zooplankton distribution patterns and their trophodynamics are either outdated, grey literature, restricted in scope and accessibility, or lack adequate spatial and temporal resolution.

The aim of this dissertation is to improve our understanding of estuarine zooplankton ecology, with a major focus on population dynamics and feeding relationships across spatial and temporal scales in the Elbe estuary. By integrating various methodological approaches, including quantitative and qualitative plankton sampling, microscopy and metabarcoding techniques, flow cytometry and stable isotope techniques, this doctoral thesis aims to provide insights into estuarine zooplankton research for future management and conservation efforts. This work contributes to the understanding of the spatio-temporal species succession of Elbe zooplankton and their trophic interactions within the planktonic food web, as well as their trophodynamic role for higher trophic levels. In this final chapter (**Chapter 7**), I will provide a comprehensive discussion that summarises and integrates the main findings from the five studies. I will also address broader issues that extend beyond the individual chapters and propose future research directions.

## Summary of the main findings

### Chapter 2: Spatio-temporal population dynamics of estuarine zooplankton

In this chapter, we found that the taxonomic composition of the micro-, meso- and macrozooplankton in the Elbe estuary is characterised by a few dominant species that overlap considerably with species assemblages found in other estuaries of the northern hemisphere, such as the Scheldt, the Gironde, the Seine, the Chesapeake Bay and the St. Lawrence estuary (see Mouny and Dauvin, 2002; Winkler *et al.*, 2003; Tackx *et al.*, 2004; David *et al.*, 2005; Hoffman *et al.*, 2008; Mialet *et al.*, 2011). In addition, we observed a similar

zooplankton community structure, but with clearly lower abundances of certain taxa compared to the most recent studies on Elbe zooplankton from the 1980s and 1990s. Recent changes in the morphology and hydrology of the estuary due to climatic and anthropogenic pressures, including increased flow velocity and sediment loads, and recurrent hypoxia events, likely contributing to the decline in species abundances. The zooplankton species composition in the Elbe estuary was mainly influenced by spatial variations in salinity, followed by chlorophyll *a* (Chl *a*) and suspended particulate matter (SPM) concentrations, and also by the intensity of the river discharge. Our data indicate that seasonal changes in temperature and nutrient availability affected both the timing and intensity of phytoplankton blooms, which in turn had a significant impact on the temporal succession of the species. In the shallow freshwater area (station Bunthäuser Spitze, BH), we found high abundances of herbivorous freshwater taxa in spring and summer, such as the rotifers *Brachionus* spp. and *Keratella* spp., along with cladocerans like *Bosmina longirostris*, *Alona* spp. and *Daphnia longispina*, which probably benefited from the high Chl *a* concentrations, low salinity stress and reduced turbidity. The euryhaline calanoid copepod *Eurytemora affinis* was the dominant mesozooplankton species throughout the estuary, with highest abundances observed in the deep-water section of the freshwater to oligohaline zone. *E. affinis* thrived particularly well in highly turbid environments when primary production was low, likely due to its well-known efficient selective feeding behaviour and dietary adaptability. At the river mouth, we identified halophilic zooplankton taxa of coastal origin, such as *Acartia* spp., *Paracalanus parvus* and *Mesopodopsis slabberi*, which likely colonised the lower reaches due to tidal inflow and reduced discharge rates. Our findings highlight the ecological significance of the Elbe estuary as a transitional zone, providing a vital habitat for freshwater, brackish and marine zooplankton taxa.

### **Chapter 3: Population dynamics of *Eurytemora affinis***

In this study, we focused on life history traits of the calanoid copepod *E. affinis* collected in the Hamburg Harbour and compared these data with a comparative study conducted in the 1990s in the turbid oligohaline zone of the Elbe estuary. The *E. affinis* population in the port region reached high abundances in spring (from April to early June) and in late summer

(between August and early October), primarily influenced by rising temperatures. We found the largest stage-specific body sizes in spring, coinciding with the timing of the phytoplankton bloom. We suggest that, in addition to temperature, improved food conditions may have favoured growth and possibly recruitment, leading to higher abundances not only in summer but also in spring. The copepod was present year-round in the harbour area reaching lower abundances in autumn and winter, as well as after the phytoplankton bloom collapse in early summer, while overwintering mainly in older developmental stages. Both the youngest and oldest stage groups were characterised by the highest mortality rates, probably due to increased energy costs associated with the morphological transition to the first and last copepodite stages, investment in reproduction, and increased predation pressure. In contrast to organisms in the oligohaline zone in the reference study, the organisms in the port region reached higher abundances and increased growth and production rates, which may result from more favourable food conditions and lower salinity stress. The study emphasises how much the prevailing environmental conditions can affect the population dynamics of *E. affinis* and how these effects can vary greatly within the same estuary.

#### **Chapter 4: Estuarine zooplankton trophic dynamics**

The primary focus of this chapter was to investigate the spatio-temporal trophic interactions of the most dominant meso- and macrozooplankton species and the available sources of particulate organic matter (POM) as potential food for these organisms, using a stable isotope approach. The local POM consisted of multiple carbon sources due to tidal mixing processes, ranging from riverine-dominated autochthonous phytoplankton at the shallow freshwater station BH to primary sources of marine origin at the river mouth. Inputs from detrital and terrestrial sources to the local POM were especially evident in autumn and winter during periods of high discharge when primary production was low. Large amounts of high-quality phytoplankton were restricted to station BH in spring and summer, which declined in quantity and quality downstream of the port region (station Mühlenberger Loch, ML) and remained low throughout the year in the MTZ, likely due to increased turbidity, reduced flow velocity and intensified microbial processing. The  $\delta^{13}\text{C}$  values of the selected

zooplankton species exhibited a wider range than the local POM, suggesting that the organisms selectively feed on specific components of the POM. In particular, *E. affinis* and *M. slabberi* had markedly lower and higher  $\delta^{13}\text{C}$  values compared to other taxa, indicating efficient grazing on riverine and marine algal sources, respectively. In addition, high  $\delta^{15}\text{N}$  values for organisms collected in the MTZ, as well as during winter and autumn, suggested a shift in their diet towards more carnivorous feeding behaviour, including the consumption of heterotrophic sources. The ability to flexibly switch diets and exploit different food niches enables these organisms to cope with stressful feeding conditions. This study demonstrates the high trophic plasticity of these taxa, highlighting their ability to maintain food web structures under highly dynamic environmental conditions in the Elbe estuary.

### **Chapter 5: Feeding ecology of *Osmerus eperlanus***

In this study, we aimed to identify the main prey items of juvenile and adult smelt (*Osmerus eperlanus*) and their patterns of habitat exploitation and migration, using stable isotope and stomach content analyses. Both juveniles and adults shared a high proportion of prey organisms, particularly mysids (i.e. *Neomysis integer*, *M. slabberi*) and amphipods (i.e. *Gammarus* sp., *Corophium voluntator*). However, we observed an ontogenetic shift from a diet consisting of zooplankton taxa to an increasing preference for piscivorous species with growing fish length, which is also reflected in the higher  $\delta^{15}\text{N}$  values of adults. Both stages showed a generally more diverse diet in the river mouth compared to upstream areas, which is reflected by a wider isotopic niche width. We also found that the dietary overlap between juvenile and adult smelt decreased upstream, suggesting that they use different carbon sources. While adults primarily fed on prey organisms originating from the middle and lower section of the Elbe estuary, juveniles relied heavily on the local food supply, showing a higher preference for smaller zooplankton taxa such as copepods (i.e. *E. affinis*), particularly in the freshwater areas. At station ML, both juveniles and adults switched from zooplankton to cannibalistic feeding, possibly as a result of a top-down induced decline in copepod biomass. In the MTZ, we found higher  $\delta^{15}\text{N}$  values in juveniles compared to adults. This was likely due to their preferred planktivorous feeding behaviour, as unfavourable environmental conditions in the MTZ may have led to an extension of the local planktonic food chain. We

suggest that juvenile smelt are more affected by the prevailing environmental conditions in the Elbe estuary, while adults avoid stressful food conditions by leaving these areas. Our findings highlight the critical role of estuarine habitats as nursery and feeding grounds for migratory fish and their ability to use distinct resources when food conditions are unfavourable.

### **Chapter 6: Estuarine phytoplankton dynamics: Picophytoplankton**

The last study focused on the spatial and temporal dynamics of picophytoplankton in the Elbe estuary and how the prevailing environmental conditions affect their population dynamics. Using a metabarcoding approach combined with flow cytometry, the picophytoplankton was both taxonomically classified and quantitatively assessed. Picophytoplankton was present year-round in the Elbe estuary, making up to 70% of the total phytoplankton communities, thereby inhabiting a key role in this ecosystem. They can be divided into two main groups: Picoeukaryotes and picocyanobacteria. The picoeukaryotes, which represented the largest proportion of the picophytoplankton (up to 77%), were dominated by the freshwater species *Mychonastes* in the middle (at station Schwarztonnensand, ST) and upper estuarine zone (station MG and BH), while *Minidiscus*, a typical marine-brackish species, was dominant from station ST to the river mouth. Notably, during the summer, picocyanobacteria dominated the picophytoplankton community, accounting for 43% of the total abundance, with *Synechococcus* found in the lower reaches and *Microcystis* present at the freshwater stations BH and ML. Picophytoplankton made their highest contributions to the phytoplankton pool under unfavourable environmental conditions, such as extreme temperatures in summer and winter, as well as low light availability and increasing turbidity (e.g. in the MTZ). We assume that they occupy ecological niches where large-cell phytoplankton may have difficulty sustaining primary production, potentially due to adaptations in light-harvesting strategies and nutrient and carbon acquisition. This chapter highlights the ecological importance of picophytoplankton in the Elbe estuary in maintaining food web structures and underscores their ability to thrive under harsh environmental conditions.

## Plankton dynamics along spatial and temporal scales

Our investigations provide valuable insights into the spatial and temporal population dynamics of zooplankton (**Chapter 2** and **3**) and phytoplankton, in particular picophytoplankton (**Chapter 6**), as well as various organic sources of particulate matter (**Chapter 4**) in the Elbe estuary. Although the studies differ methodologically in terms of sampling techniques, species identification and quantification, they all highlight a consistent pattern: plankton communities in the Elbe estuary undergo significant changes in species succession along the salinity gradient and exhibit lower biodiversity compared to adjacent marine and riverine ecosystems (cf. Frasz *et al.*, 1991; Marques *et al.*, 2023; Hromova *et al.*, 2024). This pattern is reflected in the dominance of a few distinct key species (e.g. *Keratella* spp., *E. affinis*, *M. slabberi*) found in different sections of the estuary. A similar pattern has been noted in the literature on fish populations in the Elbe estuary, where the smelt *O. eperlanus* accounts for approximately 96% of the total fish population (Eick and Thiel, 2014), similar to the abundances of the dominant copepod *E. affinis* (see **Chapter 2** and Köpcke, 2002). The dominance of single key estuarine planktonic species and limited taxonomic richness have also been reported in other temperate estuaries (e.g. Mouny *et al.*, 1998; Azémar *et al.*, 2010; David *et al.*, 2016). This aspect is often attributed to the challenging physio-biochemical conditions prevailing in these systems, particularly salinity fluctuations, which only a few species can withstand (Day *et al.*, 2013).

Remane (1934) first described this characteristic paradigm for estuaries by developing a conceptual model that relates the distribution of species diversity to the number of species with different salinity tolerances along the salinity continuum. The 'Remane' model indicates that the diversity of freshwater taxa declines sharply within a salinity range of 0.5 to 5, with the lowest species richness observed between salinities of 5 and 7. This conceptual model serves as a basis for much of our understanding of plankton distribution in estuaries, as outlined in most textbooks (e.g. Day *et al.*, 2013). However, there are some exceptions due to specialised osmoregulatory strategies of certain species (e.g. Telesh *et al.*, 2011), which makes the model a subject of ongoing debate (see Whitfield *et al.*, 2012). In our studies on plankton population dynamics in the Elbe estuary (**Chapter 2** and **6**), we found that salinity

is a primary, but not the only factor influencing spatial succession and species richness. According to the results of the redundancy analysis, other environmental factors such as river discharge, Chl *a* and SPM concentrations also played an important role in influencing the species distribution patterns. For example, typical freshwater rotifers like *Keratella* spp. and *Brachionus* spp. declined sharply along the salinity gradient. This decline, however, was probably also associated with increased turbidity and the resulting limited food availability for these filter-feeding species in the brackish zones, while more euryhaline species became abundant in the river mouth at salinities >10, where turbidity decreased again.

However, it should be noted that not all taxonomic groups were identified to the species level, which limits our conclusions on species richness. For instance, rotifers were only identified to genus level, which was sufficient for our multivariate analysis to assess their population dynamics in relation to environmental parameters, as methodologically discussed in the study by Azémar *et al.* (2010), but is not ideal for studying species richness. There were also limitations in the species identification of picophytoplankton (see **Chapter 6**). In the multivariate analyses, we focused on examining only the species succession of the most abundant taxa that could be identified at the lowest possible taxonomic level. We also faced the methodological limitation that estuarine studies on zooplankton population dynamics are often difficult to compare with each other. This is partly due to the fact that estuaries exhibit unique physico-biochemical characteristics that significantly influence the distribution patterns of biota, making comparisons between habitats difficult (Benfield, 2012). Furthermore, even within the same estuary, there can be significant differences in outcomes due to methodological biases. Factors such as the sampling approach, the choice of sampling gear, the depth at which the sample is taken and the timing of sampling within the tidal cycle can affect the assessment of plankton populations (Harris *et al.*, 2000). These aspects have been carefully considered in the interpretation of the study results.

### **Feeding strategies of pelagic species in estuarine ecosystems**

As estuaries are generally characterised by low species diversity but high biomass production, organisms often feed on the same prey because consumers frequently encounter the same species (Platell *et al.*, 2006; Elliott and Whitfield, 2011). In this

dissertation, we investigated this aspect for the planktonic food web of the Elbe estuary using stomach content and stable isotope analyses of zooplankton organisms (**Chapter 4**) and the fish species *O. eperlanus* (**Chapter 5**). We observed significant overlap in the food sources utilised by both taxonomic groups, suggesting a generalistic feeding strategy. Additionally, we have shown in **Chapter 4** that both the quantity and quality of potential food sources in the Elbe estuary can vary greatly in space and time. Previous studies have indicated that planktonic taxa and fish species are quite flexible in their dietary adaptations to changing food conditions and supply in estuaries (e.g. Hoffman *et al.*, 2008; Modéran *et al.*, 2012; Taal *et al.*, 2014). This pattern was also evident in our two studies (**Chapter 4** and **5**). For example, the copepod *E. affinis* likely relied on high-quality phytoplankton in the upper shallow freshwater areas during the spring and summer blooms, whereas in the MTZ it persisted under continuously harsh feeding conditions (i.e. low primary production, high turbidity) by probably grazing on alternative organic matter sources (e.g. microzooplankton, detritus). We suggest that this opportunistic and selective feeding strategy is crucial for coping with the dynamic environmental conditions in estuaries and helps to maintain food web structures.

In **Chapter 4** and **5**, we have provided valuable and deeper insights into the pelagic food web of the Elbe estuary. However, it is important to note that food webs are much more complex than our studies can capture, as they also include important trophic processes such as the microbial loop (Azam *et al.*, 1983), which were not investigated in the present thesis. Instead, our studies focused mainly on feeding relationships of meso- and macrozooplankton taxa and smelt. The complexity of food webs is particularly evident in the results of stable isotope analysis of the prevailing particulate organic matter sources (see **Chapter 4**). It is generally difficult to separate phytoplankton from heterotrophic and detrital particulate matter (Stoecker, 1984; Sato *et al.*, 2007). Therefore, we were not able to generate stable isotope baseline data for various taxonomic groups that are typical components of the POM (e.g. ciliates, flagellates, phytoplankton). As a result, we analysed the entire seston as a bulk sample to obtain stable isotope reference values for the local mixture of organic matter sources. However, this approach overlooks trophic structures within the microzooplankton and heterotrophic relationships at the microbial level (e.g.

mixotrophy). In addition, it is important to mention that most of the seasonal sampling campaigns in the present studies provide only a one-day snapshot of the prevailing trophic interactions and plankton population dynamics, and may not necessarily represent the respective seasons comprehensively. Dynamic biochemical and physical processes in the estuary, along with the patchiness of plankton populations (Mackas *et al.*, 1985), can lead to rapid changes in the trophodynamics (Benfield, 2012). Sampling with greater spatial and temporal resolution may help to reduce this effect. For future pelagic food web studies in the Elbe estuary, it is important to include heterotrophic pathways from the microbial loop and to consider the trophic role of microzooplankton taxa.

### **Trophic relationships along the salinity gradient of the Elbe estuary**

Based on our findings on the population dynamics of planktonic organisms (**Chapter 2, 3 and 6**) and their trophic relationships (**Chapter 4 and 5**), we can classify the Elbe estuary into characteristic zones. These zones differ significantly due to their unique environmental conditions that influence the local trophodynamics. In the following section, we will describe these areas with reference to our results from the five studies in order to provide a comprehensive overview of the food web dynamics in the Elbe estuary. The key findings are summarised in a schematic diagram (see Fig. 7.1).

#### **Autotrophic zone upstream of the port area**

In the shallow freshwater zone where station BH is located, we observed high abundances of typical riverine and estuarine zooplankton taxa, such as the rotifers *Keratella* spp. and *Brachionus* spp., cladocerans like *Daphnia longispina*, *Bosmina longirostris* and *Alona* spp., as well as freshwater cyclopoid copepods (**Chapter 2**) (see Fig. 7.1). *Eurytemora affinis* was also highly abundant at this station, but it dominated most in the harbour area and the MTZ, which were species-poor in contrast to the other sites. High primary production was found at station BH, especially in spring and summer, characterised by elevated Chl *a* concentrations (up to 153  $\mu\text{g l}^{-1}$ ) and high quality POM (**Chapter 4**). We hypothesised that favourable environmental conditions upstream of the port region, including low turbidity combined with high nutrient availability from agricultural runoff and reduced water turnover, supported the intense phytoplankton blooms. Similar patterns have been reported in other

studies of the Elbe estuary (e.g. Amann *et al.*, 2012; Geerts *et al.*, 2017; Kamjunke *et al.*, 2023) and other river systems (e.g. Turner *et al.*, 2022). The phytoplankton community at station BH is primarily of fluvial origin (**Chapter 4**) and consists of large-cell diatoms (Martens *et al.*, 2024b) and picophytoplankton, which constitutes up to 70% of the total biomass (**Chapter 6**). The latter was abundant throughout the year, often outnumbering large-cell phytoplankton during extreme temperatures (e.g. in July 2021 and winter). We suggest that picophytoplankton occupy important niche positions during harsh environmental conditions and may serve as an important food source for small sized grazers. *E. affinis* tended to feed selectively on <sup>13</sup>C-depleted, riverine algal sources (**Chapter 4**). Filter-feeding organisms, such as cladocerans and rotifers are likely to benefit from the high quantity and quality of phytoplankton in this autotrophic zone, as reflected by their high abundances (**Chapter 2**).

However, the importance of this area for higher trophic levels, such as fish populations in the Elbe estuary, remains poorly understood. Most studies on zooplankton population dynamics have only sporadically investigated this zone (e.g. Schulz, 1961). Our findings indicate that the shallow freshwater area upstream of the port region is an important habitat for planktonic organisms and provides unique features for the pelagic food web in the Elbe estuary. The favourable conditions for planktonic organisms in this zone contrast sharply with the heavily modified areas downstream, highlighting the importance of this area for future research.

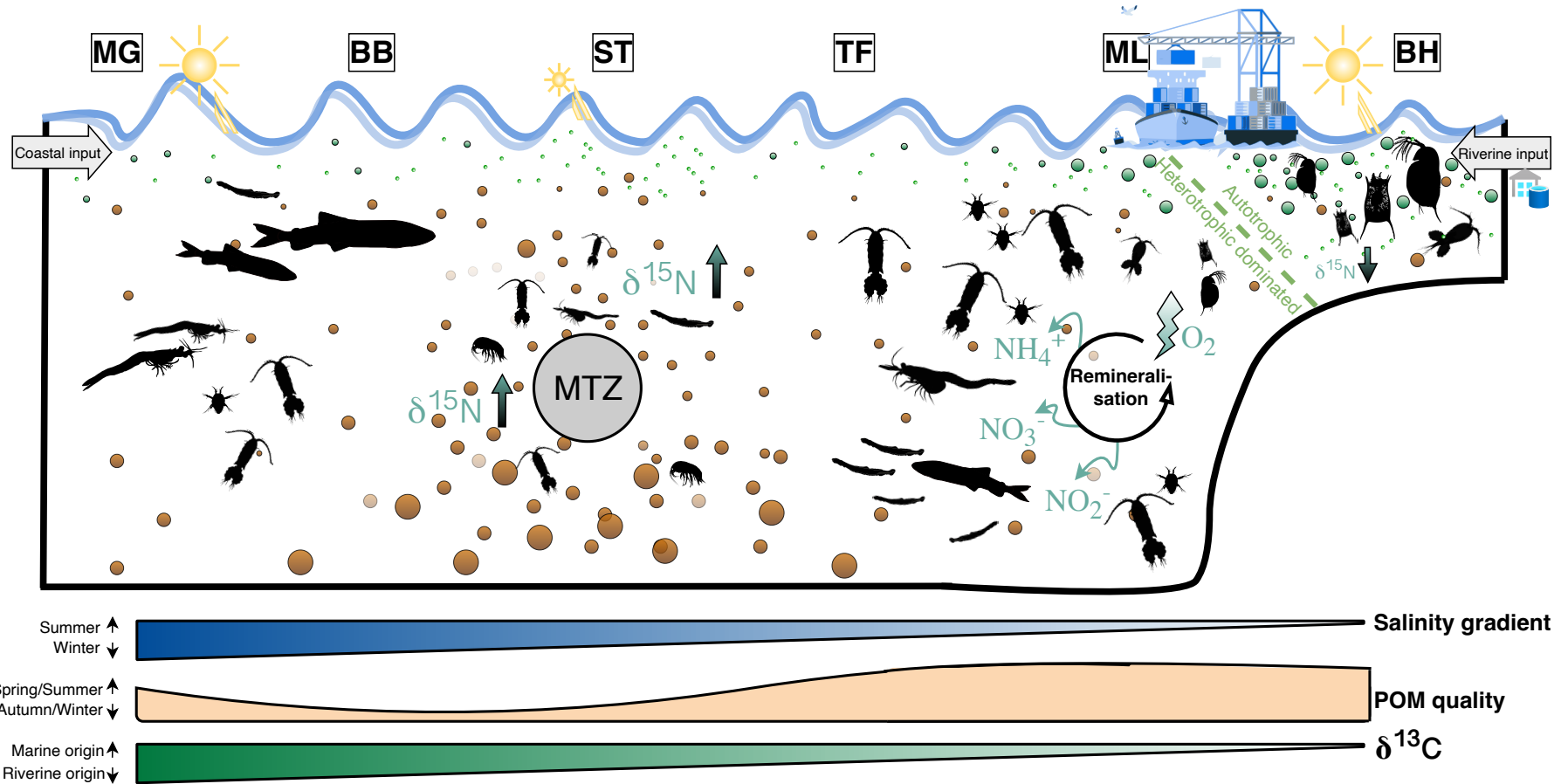


Fig. 7.1: Schematic overview of the key findings. The figure provides a simplified spatial representation of the key zooplankton species (shown as pictograms) and the prevailing environmental conditions, including salinity (indicated by the lower blue bar), turbidity (represented by brown dots), light availability (reflected by the size of the sun) and primary production (represented by green dots) at the sampling stations in the main channel of the Elbe estuary (from station MG to BH). The arrows and bars illustrate physical and biochemical processes such as remineralisation and release of nutrients, enrichment and depletion of carbon ( $\delta^{13}\text{C}$ ) and nitrogen ( $\delta^{15}\text{N}$ ) stable isotopes in selected zooplankton taxa and particulate organic matter (POM), and the inflow of riverine and coastal waters. Pictograms were used with permission from Elena Hauten.

## The port region

The Hamburg port area can be described by the findings from the stations Mühlenberger Loch (ML), Seemannshöft, Dockland and Twielenfleth (TL), the latter being situated in front of the harbour. The port region was characterised by an abrupt decline in primary producers and high-quality POM (**Chapter 2, 4 and 6**; see Fig. 7.1). This decline has been attributed to the rapid increase in water depth and reduced flow velocities, and the resulting accumulation and deposition of suspended particles (Kerner, 2007; Geerts *et al.*, 2017). As a consequence, the phytoplankton community in the port region experiences light limitation and increased sinking processes into deeper layers (Kamjunke *et al.*, 2023; Steidle and Vennell, 2024). Our findings showed that the local POM is primarily affected by the influx of riverine organic matter from the upper shallow freshwater zone (**Chapter 4**). This organic material undergoes intense remineralisation processes upon entering the harbour area at elevated temperatures, which is reflected in the rising nutrient concentrations followed by a massive drop in O<sub>2</sub> levels (**Chapter 2 and 3**). Sanders *et al.* (2018) identified this zone as a hotspot for nitrification processes in the Elbe estuary.

The zooplankton population in the harbour area was characterised by decreasing abundances of rotifers, cyclopoid copepods and cladocerans, which remained low even downstream of the port region. We assume that the decline of these taxonomic groups was related to the drop in Chl *a* concentrations and increased salinity stress. In contrast, the euryhaline copepod *E. affinis* was the most dominant species and occurred in high abundances. It is known for its highly selective feeding strategy (Gasparini and Castelt, 1997; Tackx *et al.*, 2003; Kiørboe, 2011), which may have allowed it to thrive in this area under increasing SPM concentrations. The decline in rotifers and possibly in primary producers may also be related to high predation pressure from *E. affinis*. However, due to the lack of baseline stable isotope data for rotifers and autochthonous phytoplankton, we were unable to find a direct link between these potential feeding interactions.

Growth conditions for *E. affinis* were likely more favourable in the port region, as indicated by the higher abundances and growth rates examined in **Chapter 3**, compared to those in the MTZ, as shown by Peitsch (1992). This may stem from lower salinities and better grazing

conditions for a herbivorous diet, with the latter also reflected in the lower  $\delta^{15}\text{N}$  values of *E. affinis* in the port region (see **Chapter 4**).

Furthermore, we observed higher abundances of *E. affinis* in the marginal zone at the pier (**Chapter 3**) compared to the main channel (**Chapter 2**). According to Köpcke (2002) and Steidle and Vennell (2024), side channels and marginal zones are crucial for maintaining the plankton populations in the Elbe estuary, providing refuges from strong advection processes. These areas are often characterised by shallow water and reduced turnover, which enhance the local primary production compared to the navigation channel (Kafemann, 1992; Köpcke, 2002), potentially explaining the higher abundances of *E. affinis* at the pier. In addition, both stations, ML and Seemanshöft, are located near the freshwater tidal flat Hahnöfer Nebelbe, which is recognised as a hotspot for reproduction and nursery grounds for zooplankton taxa, particularly *E. affinis* and *N. integer*, as well as fish species like *O. eperlanus* (Fiedler, 1991; Thiel *et al.*, 1995; Köpcke, 2002; Eick and Thiel, 2014). Thus, it is not surprising that we recorded the highest abundance of these taxa in the port region. These abundance patterns may also be linked to the feeding behaviour of *O. eperlanus*, particularly juvenile smelt. At station ML, juveniles showed a strong preference for mysids and copepods, as indicated by the stable isotope analyses discussed in **Chapter 5**. In late May 2022, we found an increasing tendency towards cannibalism, which coincided with a decline in abundance of *E. affinis* and *N. integer* during this period (compare **Chapter 2** and **3**). This trend may reflect top-down control within the food web and a subsequent food limitation for *O. eperlanus*.

### **The maximum turbidity zone**

The maximum turbidity zone (MTZ) is characterised by high turbidity due to a significant load of suspended particles accumulated by tidal mixing processes (Day *et al.*, 2013). In our studies, this zone was often located near the station Schwarztonnensand (ST) and occasionally extended to the station Brunsbüttel (BB) during high river discharge, especially in winter. According to Papenmeier *et al.* (2014), the MTZ extends for approximately 30 km, typically centred around the city of Glückstadt, near the station ST. This zone experienced reduced primary production due to increasing salinity and high turbidity (Muylaert and

Sabbe, 1999), as indicated by low Chl *a* concentrations and poor POM quality throughout the year (**Chapter 2 and 4**)

In the MTZ, we found low species diversity in the zooplankton community, consisting mainly of *E. affinis*, *N. integer* and the amphipod *Gammarus zaddachi* (**Chapter 2**). We suspect that the planktonic organisms in this zone rely on carnivorous feeding behaviours, as they have limited access to algal sources and exhibited significantly higher  $\delta^{15}\text{N}$  values (**Chapter 4**). Potential food sources may include microzooplankton taxa or detrital sources, which are often inhabited by microbial organisms that are consumed through the ingestion of suspended particles (Stoecker and Capuzzo, 1990; Gasparini and Castelt, 1997; Cabrol *et al.*, 2015). Notably, Martens *et al.* (2024b) observed a high dominance of mixotrophic flagellates in this zone, which are able to acquire energy by grazing on bacteria under low light conditions (Calderini *et al.*, 2022). Similarly, we found increased abundances of the picoeukaryote *Mychonastes* in the MTZ (**Chapter 6**), which can also feed mixotrophically (Martens *et al.*, 2024a). We also identified  $^{15}\text{N}$ -enriched juvenile smelt in the MTZ (**Chapter 5**). These individuals had even higher  $\delta^{15}\text{N}$  values than adults, suggesting a diet consisting of  $^{15}\text{N}$ -enriched zooplankton taxa, which corresponds to the stable isotopic signatures of zooplanktonic species found in **Chapter 4**. Consequently, we suggest that the presence of mixotrophy and the shift towards carnivorous feeding may have a cascading effect on the entire food web in the MTZ of the Elbe estuary.

### **The river mouth**

The environmental conditions at the river mouth were influenced by the inflow of coastal waters from the North Sea. As a result, this zone exhibited oligo- to mesohaline characteristics, especially at the station Medemgrund (MG) and BB. This area was characterised by decreasing turbidity and moderate levels of phytoplankton biomass during spring and summer. POM collected at station MG had the highest  $\delta^{13}\text{C}$  signature, indicating an increased proportion of marine sources in the local organic matter mixture (**Chapter 4**). This finding was further supported by the presence of marine picophytoplankton taxa examined in **Chapter 6**.

The zooplankton community in this area included not only estuarine species such as *E. affinis* and *N. integer*, but also euryhaline taxa like *Acartia* spp., *Paracalanus parvus*, *Temora longicornis* and *Mesopodopsis slabberi* (**Chapter 2**), which are native to the North Sea (Fransz *et al.*, 1991; Marques *et al.*, 2023). During winter, when river discharge was high, marine species were almost completely absent from the lower reaches of the estuary, being replaced by brackish species from upstream areas. Both zooplankton taxa (**Chapter 4**) and juvenile and adult smelt (**Chapter 5**) exhibited the highest dietary diversity at the river mouth compared to the other stations, as reflected in their variable stable isotopic composition. We attributed this aspect to the tidal mixing processes in this area, which provide a greater variety of potential riverine and marine carbon sources to the local POM (De Jonge and Van Beusekom, 1992; Geerts *et al.*, 2017).

## Outlook

The doctoral thesis provides important insights into the spatial and temporal dynamics of zooplankton populations and their feeding interactions in the Elbe estuary. We have gained new knowledge on the intricate interplay between natural and anthropogenic stressors affecting zooplankton distribution patterns and food web dynamics in this temperate and highly modified estuarine environment. Our studies show that both natural stressors and anthropogenic changes in the hydrodynamics were likely associated with changes in food availability, quality and species composition of planktonic taxa in the Elbe estuary. These aspects were particularly evident in the contrasting findings from station BH, located in the autotrophic zone, compared to station ML in the port area. Our results underscore the need to consider the effects of these stressors on estuarine zooplankton, especially in terms of food web dynamics and overall ecosystem functioning, when developing sustainable management strategies for the Elbe estuary. In addition, ongoing climate change poses a considerable risk to coastal and riverine ecosystems, including the Elbe estuary, with increased threats from eutrophication, hypoxia and sea level rise (Statham, 2012; Cloern *et al.*, 2016; Robins *et al.*, 2016). Previous research indicates that the Elbe estuary is already experiencing climate change-induced shifts in the water regime (e.g. Weilbeer *et al.*, 2021), and further changes are expected (e.g. Hein *et al.*, 2018; Pein *et al.*, 2023). There is an urgent

need for the implementation of time series studies on Elbe zooplankton to better understand how these organisms may respond to future climatic conditions and further human-induced hydrological changes (e.g. recurrent deepening events). Mesocosm experiments could also help to elucidate the complex responses of estuarine zooplankton to stressful environmental conditions, thereby supporting both ecological research and the development of effective ecosystem-based management strategies.

## References

- Adams, M. S., Kausch, H., Gaumert, T., and Krüger, K.-E. 1996. The effect of the reunification of Germany on the water chemistry and ecology of selected rivers. *Environmental Conservation*, 23(1), 35–43. <https://doi.org/10.1017/S0376892900038236>.
- Aksnes, D. L., and Ohman, M. D. 1996. A vertical life table approach to zooplankton mortality estimation. *Limnology and Oceanography*, 41(7), 1461–1469. <https://doi.org/10.4319/lo.1996.41.7.1461>.
- Alegria Zufia, J., Farnelid, H., and Legrand, C. 2021. Seasonality of Coastal Picophytoplankton Growth, Nutrient Limitation, and Biomass Contribution. *Frontiers in Microbiology*, 12, 1–13. <https://doi.org/10.3389/fmicb.2021.786590>.
- Allan, J. D. 1976. Life History Patterns in Zooplankton. *The American Naturalist*, 110(971), 165–180. <https://doi.org/10.1086/283056>.
- Allan, J. D., Kinsey, T. G., and James, M. C. 1976. Abundances and Production of Copepods in the Rhode River Subestuary of Chesapeake Bay. *Chesapeake Science*, 17(2), 86. <https://doi.org/10.2307/1351050>.
- Alldredge, A. L., and Silver, M. W. 1988. Characteristics, dynamics and significance of marine snow. *Progress in Oceanography*, 20(1), 41–82. [https://doi.org/10.1016/0079-6611\(88\)90053-5](https://doi.org/10.1016/0079-6611(88)90053-5).
- Amann, T., Weiss, A., and Hartmann, J. 2012. Carbon dynamics in the freshwater part of the Elbe estuary, Germany: Implications of improving water quality. *Estuarine, Coastal and Shelf Science*, 107, 112–121. Elsevier Ltd. <https://doi.org/10.1016/j.ecss.2012.05.012>.
- Amundsen, P. -A., Gabler, H. -M., and Staldvik, F. J. 1996. A new approach to graphical analysis of feeding strategy from stomach contents data—modification of the Costello (1990) method. *Journal of Fish Biology*, 48(4), 607–614. <https://doi.org/10.1111/j.1095-8649.1996.tb01455.x>.
- Ankjærø, T., Christensen, J., and Grønkjær, P. 2012. Tissue-specific turnover rates and trophic enrichment of stable N and C isotopes in juvenile Atlantic cod *Gadus morhua* fed three different diets. *Marine Ecology Progress Series*, 461, 197–209. <https://doi.org/10.3354/meps09871>.
- Appeltans, W. 2003. Zooplankton in the Schelde estuary (Belgium/The Netherlands). The distribution of *Eurytemora affinis*: effect of oxygen? *Journal of Plankton Research*, 25(11), 1441–1445. <https://doi.org/10.1093/plankt/fbg101>.
- Azam, F., Fenchel, T., Field, J., Gray, J., Meyer-Reil, L., and Thingstad, F. 1983. The Ecological Role of Water-Column Microbes in the Sea. *Marine Ecology Progress*

## REFERENCES

- Series*, 10(3), 257–263. <https://doi.org/10.3354/meps010257>.
- Azeiteiro, U. M. M., Jesus, L., and Marques, J. C. 1999. Distribution, Population Dynamics, and Production of the Suprabenthic Mysid *Mesopodopsis Slabberi* in the Mondego Estuary, Portugal. *Journal of Crustacean Biology*, 19(3), 498–509. <https://doi.org/10.2307/1549259>.
- Azémar, F., Maris, T., Mialet, B., Segers, H., Van Damme, S., Meire, P., and Tackx, M. 2010. Rotifers in the Schelde estuary (Belgium): a test of taxonomic relevance. *Journal of Plankton Research*, 32(7), 981–997. <https://doi.org/10.1093/plankt/fbq030>.
- Ban, S., and Minoda, T. 1994. Induction of diapause egg production in *Eurytemora affinis* by their own metabolites. *Hydrobiologia*, 292–293(1), 185–189. <https://doi.org/10.1007/BF00229940>.
- Ban, S. 1994. Effect of temperature and food concentration on post-embryonic development, egg production and adult body size of calanoid copepod *Eurytemora affinis*. *Journal of Plankton Research*, 16(6), 721–735. <https://doi.org/10.1093/plankt/16.6.721>.
- Barnett, A. J., Finlay, K., and Beisner, B. E. 2007. Functional diversity of crustacean zooplankton communities: towards a trait-based classification. *Freshwater Biology*, 52(5), 796–813. <https://doi.org/10.1111/j.1365-2427.2007.01733.x>.
- Bartl, S., Schümberg, S., and Deutsch, M. 2009. Revising time series of the Elbe river discharge for flood frequency determination at gauge Dresden. *Natural Hazards and Earth System Sciences*, 9(6), 1805–1814. <https://doi.org/10.5194/nhess-9-1805-2009>.
- Barton, S., Jenkins, J., Buckling, A., Schaum, C. E., Smirnov, N., Raven, J. A., and Yvon-Durocher, G. 2020. Evolutionary temperature compensation of carbon fixation in marine phytoplankton. *Ecology Letters*, 23(4), 722–733. <https://doi.org/10.1111/ele.13469>.
- Basu, S., and Mackey, K. R. M. 2018. Phytoplankton as key mediators of the biological carbon pump: Their responses to a changing climate. *Sustainability (Switzerland)*, 10(3). <https://doi.org/10.3390/su10030869>.
- Bělehrádek, J. 1935. Temperature and living matter. *Protoplasma*, 24(1), 332–333. <https://doi.org/10.1007/BF01605675>.
- Belkinova, D., Teneva, I., Basheva, D., Neykov, N., Moten, D., Gecheva, G., Apostolova, E., *et al.* 2021. Phytoplankton composition and ecological tolerance of the autotrophic picoplankton in Atanasovsko lake (Black sea coastal lagoon, Bulgaria). *Applied Ecology and Environmental Research*, 19(2), 849–866. [https://doi.org/10.15666/aeer/1902\\_849866](https://doi.org/10.15666/aeer/1902_849866).
- Bemal, S., and Anil, A. C. 2019. Picophytoplankton *Synechococcus* as food for nauplii of

## REFERENCES

- Amphibalanus amphitrite and Artemia salina. *Hydrobiologia*, 835(1), 21–36. <https://doi.org/10.1007/s10750-019-3923-x>.
- Benfield, M. C. 2012. Estuarine Zooplankton. *In* Estuarine Ecology, pp. 285–302. Ed. by J. W. Day, B. C. Crump, W. M. Kemp, and A. Yáñez-Arancibia. John Wiley & Sons, Hoboken, New Jersey. <https://doi.org/10.1002/9781118412787.ch11>.
- Benner, I., Irwin, A. J., and Finkel, Z. V. 2020. Capacity of the common Arctic picoeukaryote *Micromonas* to adapt to a warming ocean. *Limnology And Oceanography Letters*, 5(2), 221–227. <https://doi.org/10.1002/lol2.10133>.
- Bergkemper, V., and Weisse, T. 2018. Do current European lake monitoring programmes reliably estimate phytoplankton community changes? *Hydrobiologia*, 824(1), 143–162. <https://doi.org/10.1007/s10750-017-3426-6>.
- Bernát, N., Köpcke, B., Yasseri, S., Thiel, R., and Wolfstein, K. 1994. Tidal variation in bacteria, phytoplankton, zooplankton, mysids, fish and suspended particulate matter in the turbidity zone of the Elbe estuary; Interrelationships and causes. *Netherlands Journal of Aquatic Ecology*, 28(3–4), 467–476. <https://doi.org/10.1007/BF02334218>.
- Biederbick, J., Möllmann, C., Hauten, E., Russnak, V., Lahajnar, N., Hansen, T., Dierking, J., et al. 2024. Spatial and temporal patterns of zooplankton trophic interactions and carbon sources in the eutrophic Elbe estuary (Germany). *ICES Journal of Marine Science*, 0(0). <https://doi.org/10.1093/icesjms/fsae189>.
- Blaber, S. 2000. Effects of fishing on the structure and functioning of estuarine and nearshore ecosystems. *ICES Journal of Marine Science*, 57(3), 590–602. <https://doi.org/10.1006/jmsc.2000.0723>.
- BMUV/UBA. 2022. Water Framework Directive - The status of German waters 2021. Progress and Challenges. Bonn, Dessau. 1–124 pp.
- Boehlich, M. J., and Strotmann, T. 2008. The Elbe estuary. *Die Küste*, 1(74), 288–306.
- Bogdan, K. G., and Gilbert, J. J. 1982. Seasonal patterns of feeding by natural populations of *Keratella*, *Polyarthra*, and *Bosmina*: Clearance rates, selectivities, and contributions to community grazing. *Limnology and Oceanography*, 27(5), 918–934. <https://doi.org/10.4319/lo.1982.27.5.0918>.
- Borcard, D., Gillet, F., and Legendre, P. 2011. Numerical Ecology with R. Springer New York, New York, NY. <https://link.springer.com/10.1007/978-1-4419-7976-6>. <https://doi.org/10.1007/978-1-4419-7976-6>.
- Borchardt, D. 1988. Long-term correlations between the abundance of smelt, (*Osmerus eperlanus eperlanus* L.), year classes and biotic environmental conditions during the period of spawning and larval development in the Elbe River. *Arch. FischWiss.*, 38(3), 191–202.

## REFERENCES

- Bouillon, S., Mohan, P., Sreenivas, N., and Dehairs, F. 2000. Sources of suspended organic matter and selective feeding by zooplankton in an estuarine mangrove ecosystem as traced by stable isotopes. *Marine Ecology Progress Series*, 208, 79–92. <https://doi.org/10.3354/meps208079>.
- Boutton, T. W. 1991. Stable Carbon Isotope Ratios of Natural Materials: II. Atmospheric, Terrestrial, Marine, and Freshwater Environments. *In* Carbon Isotope Techniques, pp. 173–185. Ed. by D. C. Coleman and B. Fry. Academic Press, London. <https://doi.org/10.1016/B978-0-12-179730-0.50016-3>.
- Boynton, W. R., Ceballos, M. A. C., Bailey, E. M., Hodgkins, C. L. S., Humphrey, J. L., and Testa, J. M. 2018. Oxygen and Nutrient Exchanges at the Sediment-Water Interface: a Global Synthesis and Critique of Estuarine and Coastal Data. *Estuaries and Coasts*, 41(2), 301–333. <https://doi.org/10.1007/s12237-017-0275-5>.
- Brandl, Z. 2005. Freshwater copepods and rotifers: Predators and their prey. *Hydrobiologia*, 546(1), 475–489. <https://doi.org/10.1007/s10750-005-4290-3>.
- Breine, J., Maes, J., Ollevier, F., and Stevens, M. 2011. Fish assemblages across a salinity gradient in the Zeeschelde estuary (Belgium). *Belgian Journal of Zoology*, 141(2), 21–44. <https://doi.org/10.26496/bjz.2011.148>.
- Breteler, W. C. M. K., Fransz, H. G., and Gonzalez, S. R. 1982. Growth and development of four calanoid copepod species under experimental and natural conditions. *Netherlands Journal of Sea Research*, 16(C), 195–207. [https://doi.org/10.1016/0077-7579\(82\)90030-8](https://doi.org/10.1016/0077-7579(82)90030-8).
- Brown, S. C., Bizzarro, J. J., Cailliet, G. M., and Ebert, D. A. 2012. Breaking with tradition: redefining measures for diet description with a case study of the Aleutian skate *Bathyraja aleutica* (Gilbert 1896). *Environmental Biology of Fishes*, 95(1), 3–20. <https://doi.org/10.1007/s10641-011-9959-z>.
- Buchheister, A., and Latour, R. J. 2010. Turnover and fractionation of carbon and nitrogen stable isotopes in tissues of a migratory coastal predator, summer flounder (*Paralichthys dentatus*). *Canadian Journal of Fisheries and Aquatic Sciences*, 67(3), 445–461. <https://doi.org/10.1139/F09-196>.
- Burdloff, D., Gasparini, S., Sautour, B., Etcheber, H., and Castel, J. 2000. Is the copepod egg production in a highly turbid estuary (the Gironde, France) a function of the biochemical composition of seston? *Aquatic Ecology*, 34(2), 165–175. <https://doi.org/10.1023/A:1009903702667>.
- Burkill, P., and Kendall, T. 1982. Production of the Copepod *Eurytemora affinis* in the Bristol Channel. *Marine Ecology Progress Series*, 7(1977), 21–31. <https://doi.org/10.3354/meps007021>.
- Busch, A., and Brenning, U. 1992. Studies On the Status of *Eurytemora Affinis* (Pope,

## REFERENCES

- 1880) (Copepoda, Calanoida). *Crustaceana*, 62(1), 13–38. <https://doi.org/10.1163/156854092X00028>.
- Cabana, G., and Rasmussen, J. B. 1996. Comparison of aquatic food chains using nitrogen isotopes. *Proceedings of the National Academy of Sciences*, 93(20), 10844–10847. <https://doi.org/10.1073/pnas.93.20.10844>.
- Cabrol, J., Winkler, G., and Tremblay, R. 2015. Physiological condition and differential feeding behaviour in the cryptic species complex *Eurytemora affinis* in the St Lawrence estuary. *Journal of Plankton Research*, 37(2), 372–387. <https://doi.org/10.1093/plankt/fbu111>.
- Calderini, M. L., Salmi, P., Rigaud, C., Peltomaa, E., and Taipale, S. J. 2022. Metabolic plasticity of mixotrophic algae is key for their persistence in browning environments. *Molecular Ecology*, 31(18), 4726–4738. <https://doi.org/10.1111/mec.16619>.
- Christianen, M. J. A., Middelburg, J. J., Holthuijsen, S. J., Jouta, J., Compton, T. J., van der Heide, T., Piersma, T., *et al.* 2017. Benthic primary producers are key to sustain the Wadden Sea food web: stable carbon isotope analysis at landscape scale. *Ecology*, 98(6), 1498–1512. <https://doi.org/10.1002/ecy.1837>.
- Christiansen, B. 1988. Vergleichende Untersuchungen zur Populationsdynamik von *Eurytemora affinis* POPPE und *Acartia tonsa* DANA, Copepoda, in der Schlei (Comparative studies on the population dynamics of *Eurytemora affinis* POPPE and *Acartia tonsa* DANA, Copepoda, in the Schlei). Dissertation. Universität Hamburg. 141 pp.
- Cloern, J. E., Canuel, E. A., and Harris, D. 2002. Stable carbon and nitrogen isotope composition of aquatic and terrestrial plants of the San Francisco Bay estuarine system. *Limnology and Oceanography*, 47(3), 713–729. <https://doi.org/10.4319/lo.2002.47.3.0713>.
- Cloern, J. E., Abreu, P. C., Carstensen, J., Chauvaud, L., Elmgren, R., Grall, J., Greening, H., *et al.* 2016. Human activities and climate variability drive fast-paced change across the world's estuarine-coastal ecosystems. *Global Change Biology*, 22, 513–529. <https://doi.org/10.1111/gcb.13059>.
- Coe, A., Biller, S. J., Thomas, E., Boulias, K., Bliem, C., Arellano, A., Dooley, K., *et al.* 2021. Coping with darkness: The adaptive response of marine picocyanobacteria to repeated light energy deprivation. *Limnology and Oceanography*, 66(9), 3300–3312. <https://doi.org/10.1002/lno.11880>.
- Coello-Camba, A., and Agustí, S. 2021. Picophytoplankton Niche Partitioning in the Warmest Oligotrophic Sea. *Frontiers in Marine Science*, 8. <https://doi.org/10.3389/fmars.2021.651877>.
- Cole, M. L., Valiela, I., Kroeger, K. D., Tomasky, G. L., Cebrian, J., Wigand, C., McKinney, R.

## REFERENCES

- A., *et al.* 2004. Assessment of a  $\delta^{15}\text{N}$  Isotopic Method to Indicate Anthropogenic Eutrophication in Aquatic Ecosystems. *Journal of Environmental Quality*, 33(1), 124–132. <https://doi.org/10.2134/jeq2004.1240>.
- Corkett, C. J., and McLaren, I. A. 1970. Relationships between development rate of eggs and older stages of copepods. *Journal of the Marine Biological Association of the United Kingdom*, 50(1), 161–168. <https://doi.org/10.1017/S0025315400000680>.
- Dähnke, K., Sanders, T., Voynova, Y., and Wankel, S. D. 2022. Nitrogen isotopes reveal a particulate-matter-driven biogeochemical reactor in a temperate estuary. *Biogeosciences*, 19(24), 5879–5891. <https://doi.org/10.5194/bg-19-5879-2022>.
- Dalerum, F., and Angerbjörn, A. 2005. Resolving temporal variation in vertebrate diets using naturally occurring stable isotopes. *Oecologia*, 144(4), 647–658. <https://doi.org/10.1007/s00442-005-0118-0>.
- Dalsgaard, J., St. John, M., Kattner, G., Müller-Navarra, D., and Hagen, W. 2003. Fatty acid trophic markers in the pelagic marine environment. *In* pp. 225–340. [https://doi.org/10.1016/S0065-2881\(03\)46005-7](https://doi.org/10.1016/S0065-2881(03)46005-7).
- Das, K., Lepoint, G., Leroy, Y., and Bouquegneau, J. 2003. Marine mammals from the southern North Sea: feeding ecology data from  $\delta^{13}\text{C}$  and  $\delta^{15}\text{N}$  measurements. *Marine Ecology Progress Series*, 263, 287–298. <https://doi.org/10.3354/meps263287>.
- David, V., Sautour, B., Chardy, P., and Leconte, M. 2005. Long-term changes of the zooplankton variability in a turbid environment: The Gironde estuary (France). *Estuarine, Coastal and Shelf Science*, 64(2–3), 171–184. <https://doi.org/10.1016/j.ecss.2005.01.014>.
- David, V., Sautour, B., Galois, R., and Chardy, P. 2006. The paradox high zooplankton biomass–low vegetal particulate organic matter in high turbidity zones: What way for energy transfer? *Journal of Experimental Marine Biology and Ecology*, 333(2), 202–218. <https://doi.org/10.1016/j.jembe.2005.12.045>.
- David, V., Selleslagh, J., Nowaczyk, A., Dubois, S., Bachelet, G., Blanchet, H., Gouillieux, B., *et al.* 2016. Estuarine habitats structure zooplankton communities: Implications for the pelagic trophic pathways. *Estuarine, Coastal and Shelf Science*, 179, 99–111. Elsevier Ltd. <https://doi.org/10.1016/j.ecss.2016.01.022>.
- Davis, A. M., Blanchette, M. L., Pusey, B. J., Jardine, T. D., and Pearson, R. G. 2012. Gut content and stable isotope analyses provide complementary understanding of ontogenetic dietary shifts and trophic relationships among fishes in a tropical river. *Freshwater Biology*, 57(10), 2156–2172. <https://doi.org/10.1111/j.1365-2427.2012.02858.x>.
- Day, J. W., Crump, B. C., Kemp, M. W., and Yáñez-Arancibia, A. 2013. *Estuarine Ecology*. John Wiley & Sons, Hoboken, New Jersey. 1–554 pp.

## REFERENCES

- De Jonge, V. N., and Van Beusekom, J. E. E. 1992. Contribution of resuspended microphytobenthos to total phytoplankton in the EMS estuary and its possible role for grazers. *Netherlands Journal of Sea Research*, 30(1992), 91–105. [https://doi.org/10.1016/0077-7579\(92\)90049-K](https://doi.org/10.1016/0077-7579(92)90049-K).
- Debus, L., and Winkler, H. M. 1996. Frischmasserekonstruktion mit dem Programm FINA. Hinweise zur computergestützten Auswertung von Nahrungsanalysen. *Rostocker Meeresbiologische Beiträge*, 4, 97–110.
- DeNiro, M. J., and Epstein, S. 1978. Influence of diet on the distribution of carbon isotopes in animals. *Geochimica et Cosmochimica Acta*, 42(5), 495–506. [https://doi.org/10.1016/0016-7037\(78\)90199-0](https://doi.org/10.1016/0016-7037(78)90199-0).
- DeNiro, M. J., and Epstein, S. 1981. Influence of diet on the distribution of nitrogen isotopes in animals. *Geochimica et Cosmochimica Acta*, 45(3), 341–351. [https://doi.org/10.1016/0016-7037\(81\)90244-1](https://doi.org/10.1016/0016-7037(81)90244-1).
- Devreker, D., Souissi, S., and Seuront, L. 2004. Development and mortality of the first naupliar stages of *Eurytemora affinis* (Copepoda, Calanoida) under different conditions of salinity and temperature. *Journal of Experimental Marine Biology and Ecology*, 303(1), 31–46. <https://doi.org/10.1016/j.jembe.2003.11.002>.
- Devreker, D., Souissi, S., Forget-Leray, J., and Leboulenger, F. 2007. Effects of salinity and temperature on the post-embryonic development of *Eurytemora affinis* (Copepoda; Calanoida) from the Seine estuary: A laboratory study. *Journal of Plankton Research*, 29. <https://doi.org/10.1093/plankt/fbl071>.
- Devreker, D., Souissi, S., Winkler, G., Forget-Leray, J., and Leboulenger, F. 2009. Effects of salinity, temperature and individual variability on the reproduction of *Eurytemora affinis* (Copepoda; Calanoida) from the Seine estuary: A laboratory study. <https://doi.org/10.1016/j.jembe.2008.10.015>.
- Die Flussgemeinschaft Elbe (FGG Elbe). 2017. Elbebericht, Entwicklung des ökologischen und chemischen Zustands der Elbe 2009-2012, Schwerpunktthema Nährstoffe. Magdeburg. [https://www.fgg-elbe.de/files/Download-Archive/Gewaesserguete/Elbeberichte\\_ab\\_2008/08Elbebericht.pdf](https://www.fgg-elbe.de/files/Download-Archive/Gewaesserguete/Elbeberichte_ab_2008/08Elbebericht.pdf) (Accessed 7 March 2022).
- Die Flussgemeinschaft Elbe (FGG Elbe). 2024. FGG Elbe database (Flussgebietsgemeinschaft Elbe/ Elbe River Basin Association).
- Donázar-Aramendía, I., Sánchez-Moyano, J. E., García-Asencio, I., Miró, J. M., Megina, C., and García-Gómez, J. C. 2019. Human pressures on two estuaries of the Iberian Peninsula are reflected in food web structure. *Scientific Reports*, 9(1), 11495. <https://doi.org/10.1038/s41598-019-47793-2>.
- Dumont, H. J., Van de Velde, I., and Dumont, S. 1975. The dry weight estimate of biomass

## REFERENCES

- in a selection of Cladocera, Copepoda and Rotifera from the plankton, periphyton and benthos of continental waters. *Oecologia*, 19(1), 75–97. <https://doi.org/10.1007/BF00377592>.
- Dunn, O. J. 1961. Multiple Comparisons among Means. *Journal of the American Statistical Association*, 56(293), 52–64. <https://doi.org/10.1080/01621459.1961.10482090>.
- Eick, D., and Thiel, R. 2014. Fish assemblage patterns in the Elbe estuary: guild composition, spatial and temporal structure, and influence of environmental factors. *Marine Biodiversity*, 44(4), 559–580. <https://doi.org/10.1007/s12526-014-0225-4>.
- Eick, D. 2015. A spatial-temporal analysis of the fish fauna structure of the Elbe estuary. Dissertation. Universität Hamburg.
- Elliot, M., and Hemingway, K. L. 2002. Fishes in Estuaries. Blackwell Science Ltd, Hoboken, New Jersey. <https://doi.org/10.1002/9780470995228>.
- Elliott, M., and Whitfield, A. K. 2011. Challenging paradigms in estuarine ecology and management. *Estuarine, Coastal and Shelf Science*, 94(4), 306–314. <https://doi.org/10.1016/j.ecss.2011.06.016>.
- Elser, J. J., Fagan, W. F., Denno, R. F., Dobberfuhl, D. R., Folarin, A., Huberty, A., Interlandi, S., *et al.* 2000. Nutritional constraints in terrestrial and freshwater food webs. *Nature*, 408(6812), 578–580. <https://doi.org/10.1038/35046058>.
- Evans, L. E., Hirst, A. G., Kratina, P., and Beaugrand, G. 2020. Temperature-mediated changes in zooplankton body size: large scale temporal and spatial analysis. *Ecography*, 43(4), 581–590. <https://doi.org/10.1111/ecog.04631>.
- Fairbridge, R. W. 1980. The estuary: Its definition and geodynamic cycle. *In* Chemistry and biogeochemistry of estuaries, First edit, pp. 1–36. Ed. by E. Olausson and I. Cato. John Wiley & Sons, Chichester.
- Federal Waterways and Shipping Agency (WSV). 2023. River discharge Neu Darchau. <https://www.kuestendaten.de/Tideelbe/> (Accessed 17 April 2024).
- Fernandes, L. F., and Correr-Da-Silva, F. 2020. Diversity and distribution of nanoplanktonic Minidiscus (Bacillariophyta) in shelf waters of the Southwest Atlantic Ocean. *Diatom Research*, 35(4), 327–338. Taylor & Francis. <https://doi.org/10.1080/0269249X.2020.1845807>.
- Fiedler, M. 1991. Die Bedeutung von Makrozoobenthos und Zooplankton der Unterelbe als Fischnahrung (The importance of macrozoobenthos and zooplankton of the Lower Elbe as food for fish). Dissertation. Universität Hamburg. 1–226 pp.
- Finlay, J. C., and Kendall, C. 2007. Stable Isotope Tracing of Temporal and Spatial Variability in Organic Matter Sources to Freshwater Ecosystems. *In* Stable Isotopes in Ecology and Environmental Science, 2nd ed., pp. 283–333. Ed. by R. Michener and K. Lajtha.

## REFERENCES

- Wiley-Blackwell, Oxford. <https://doi.org/10.1002/9780470691854.ch10>.
- Flombaum, P., and Martiny, A. C. 2021. Diverse but uncertain responses of picophytoplankton lineages to future climate change. *Limnology and Oceanography*, 66(12), 4171–4181. <https://doi.org/10.1002/lno.11951>.
- Foflonker, F., Ananyev, G., Qiu, H., Morrison, A., Palenik, B., Dismukes, G. C., and Bhattacharya, D. 2016. The unexpected extremophile: Tolerance to fluctuating salinity in the green alga *Picochlorum*. *Algal Research*, 16, 465–472. <https://doi.org/10.1016/j.algal.2016.04.003>.
- Franek, D. 1988. 0+ smelt (*Osmerus eperlanus* L.) and herring (*Clupea harengus* L.) in the food chain of the Barther Bodden. *ICES Symposium. 1988 BAL/19*.
- Fransz, H. G., Colebrook, J. M., Gamble, J. C., and Krause, M. 1991. The zooplankton of the north sea. *Netherlands Journal of Sea Research*, 28(1–2), 1–52. [https://doi.org/10.1016/0077-7579\(91\)90003-J](https://doi.org/10.1016/0077-7579(91)90003-J).
- Fricke, K., Baschek, B., Jenal, A., Kneer, C., Weber, I., Bongartz, J., Wyrwa, J., *et al.* 2021. Observing Water Surface Temperature from Two Different Airborne Platforms over Temporarily Flooded Wadden Areas at the Elbe Estuary—Methods for Corrections and Analysis. *Remote Sensing*, 13(8), 1489. <https://doi.org/10.3390/rs13081489>.
- Fry, B. 1988. Food web structure on Georges Bank from stable C, N, and S isotopic compositions. *Limnology and Oceanography*, 33(5), 1182–1190. <https://doi.org/10.4319/lo.1988.33.5.1182>.
- Gasparini, S., and Castelt, J. 1997. Autotrophic and heterotrophic nanoplankton in the diet of the estuarine copepods *Eurytemora affinis* and *Acartia bifilosa*. *Journal of Plankton Research*, 19(7), 877–890. <https://doi.org/10.1093/plankt/19.7.877>.
- Gasparini, S., Castel, J., and Irigoien, X. 1999. Impact of suspended particulate matter on egg production of the estuarine copepod, *Eurytemora affinis*. *Journal of Marine Systems*, 22(2–3), 195–205. Elsevier. [https://doi.org/10.1016/S0924-7963\(99\)00041-X](https://doi.org/10.1016/S0924-7963(99)00041-X).
- Gearing, J. N., Gearing, P. J., Rudnick, D. T., Requejo, A. G., and Hutchins, M. J. 1984. Isotopic variability of organic carbon in a phytoplankton-based, temperate estuary. *Geochimica et Cosmochimica Acta*, 48(5), 1089–1098. [https://doi.org/10.1016/0016-7037\(84\)90199-6](https://doi.org/10.1016/0016-7037(84)90199-6).
- Geerts, L., Cox, T. J. S., Maris, T., Wolfstein, K., Meire, P., and Soetaert, K. 2017. Substrate origin and morphology differentially determine oxygen dynamics in two major European estuaries, the Elbe and the Schelde. *Estuarine, Coastal and Shelf Science*, 191, 157–170. Elsevier Ltd. <https://doi.org/10.1016/j.ecss.2017.04.009>.
- Ger, K. A., Urrutia-Cordero, P., Frost, P. C., Hansson, L. A., Sarnelle, O., Wilson, A. E., and Lürling, M. 2016. The interaction between cyanobacteria and zooplankton in a more

## REFERENCES

- eutrophic world. *Harmful Algae*, 54, 128–144. <https://doi.org/10.1016/j.hal.2015.12.005>.
- Gilbert, J. J. 2022. Food niches of planktonic rotifers: Diversification and implications. *Limnology and Oceanography*, 67(10), 2218–2251. <https://doi.org/10.1002/lno.12199>.
- Glippa, O., Souissi, S., Denis, L., and Lesourd, S. 2011. Calanoid copepod resting egg abundance and hatching success in the sediment of the Seine estuary (France). *Estuarine, Coastal and Shelf Science*, 92(2), 255–262. Elsevier Ltd. <https://doi.org/10.1016/j.ecss.2010.12.032>.
- Godhe, A., Asplund, M. E., Härnström, K., Saravanan, V., Tyagi, A., and Karunasagar, I. 2008. Quantification of diatom and dinoflagellate biomasses in coastal marine seawater samples by real-time PCR. *Applied and Environmental Microbiology*, 74(23), 7174–7182. <https://doi.org/10.1128/AEM.01298-08>.
- Gutkowska, A., Paturej, E., and Kowalska, E. 2012. Qualitative and quantitative methods for sampling zooplankton in shallow coastal estuaries. *Ecohydrology and Hydrobiology*, 12(3), 253–263. <https://doi.org/10.2478/v10104-012-0022-2>.
- Haedrich, R. L. 1983. Estuarine fishes. Elsevier, Amsterdam. 183–207 pp.
- Hamburg Port Authority (HPA). 2022. Auswirkungsprognose für die Verbringung von Baggergut zur Verbringstelle „Hamburger Außenelbe“ bei Elbe-km 749. [https://www.hamburg-port-authority.de/fileadmin/user\\_upload/aphhae2022.pdf](https://www.hamburg-port-authority.de/fileadmin/user_upload/aphhae2022.pdf) (Accessed 1 July 2024).
- Hamerlynck, O., and Mees, J. 1991. Temporal and spatial structure in the hyperbenthic community of a shallow coastal area and its relation to environmental variables. *Oceanologica Acta*, SP(11), 205–212.
- Hammar, J., Axenrot, T., Degerman, E., Asp, A., Bergstrand, E., Enderlein, O., Filipsson, O., *et al.* 2018. Smelt (*Osmerus eperlanus*): Glacial relict, planktivore, predator, competitor, and key prey for the endangered Arctic char in Lake Vättern, southern Sweden. *Journal of Great Lakes Research*, 44(1), 126–139. International Association for Great Lakes Research. <https://doi.org/10.1016/j.jglr.2017.11.008>.
- Hansen, H. P., and Koroleff, F. 2007. Determination of nutrients. *In* Methods of Seawater Analysis, pp. 159–228. Wiley. <https://doi.org/10.1002/9783527613984.ch10>.
- Harmelin-Vivien, M., Dierking, J., Bănaru, D., Fontaine, M. F., and Arlhac, D. 2010. Seasonal variation in stable C and N isotope ratios of the Rhone River inputs to the Mediterranean Sea (2004-2005). *Biogeochemistry*, 100(1), 139–150. <https://doi.org/10.1007/s10533-010-9411-z>.
- Harris, R., Wiebe, P., Lenz, J., Skjoldal, H. R., and Huntley, M. 2000. ICES Zooplankton Methodology Manual. Academic Press, London. 1–684 pp. <https://doi.org/10.1016/B978-0-12-327645-2.X5000-2>.

## REFERENCES

- Harvey, C. J., and Kitchell, J. F. 2000. A stable isotope evaluation of the structure and spatial heterogeneity of a Lake Superior food web. *Canadian Journal of Fisheries and Aquatic Sciences*, 57(7), 1395–1403. <https://doi.org/10.1139/f00-072>.
- Heaton, T. H. . 1986. Isotopic studies of nitrogen pollution in the hydrosphere and atmosphere: A review. *Chemical Geology: Isotope Geoscience section*, 59, 87–102. [https://doi.org/10.1016/0168-9622\(86\)90059-X](https://doi.org/10.1016/0168-9622(86)90059-X).
- Hein, B., Viergutz, C., Wyrwa, J., Kirchesch, V., and Schöl, A. 2018. Impacts of climate change on the water quality of the Elbe Estuary (Germany). *Journal of Applied Water Engineering and Research*, 6(1), 28–39. <https://doi.org/10.1080/23249676.2016.1209438>.
- Henderson, P. A. 1989. On the structure of the inshore fish community of England and Wales. *Journal of the Marine Biological Association of the United Kingdom*, 69(1), 145–163. <https://doi.org/10.1017/S002531540004916X>.
- Hirche, H.-J. 1992. Egg production of *Eurytemora affinis*—Effect of k-strategy. *Estuarine, Coastal and Shelf Science*, 35(4), 395–407. [https://doi.org/10.1016/S0272-7714\(05\)80035-6](https://doi.org/10.1016/S0272-7714(05)80035-6).
- Hitchcock, J. N., Mitrovic, S. M., Hadwen, W. L., Growns, I. O., and Rohlf, A.-M. 2016. Zooplankton responses to freshwater inflows and organic-matter pulses in a wave-dominated estuary. *Marine and Freshwater Research*, 67(9), 1374. <https://doi.org/10.1071/MF15297>.
- Hlawa, S., and Heerkloss, R. 1994. Experimental studies into the feeding biology of rotifers in brackish water. *Journal of Plankton Research*, 16(8), 1021–1038. <https://doi.org/10.1093/plankt/16.8.1021>.
- Hoffman, J. C., Bronk, D. A., and Olney, J. E. 2008. Organic Matter Sources Supporting Lower Food Web Production in the Tidal Freshwater Portion of the York River Estuary, Virginia. *Estuaries and Coasts*, 31(5), 898–911. <https://doi.org/10.1007/s12237-008-9073-4>.
- Holst, H. 1996. Untersuchung zur Ökologie der Rotatorien auf den Schwebstoffflocken und im Freiwasser der Elbe während des Frühjahrs (Investigations of the rotifer ecology on suspended matter and in the pelagic zone of the Elbe estuary during spring). Diploma thesis. Hamburg. 1–138 pp.
- Holst, H., Zimmermann, H., Kausch, H., and Koste, W. 1998. Temporal and Spatial Dynamics of Planktonic Rotifers in the Elbe Estuary during Spring. *Estuarine, Coastal and Shelf Science*, 47(3), 261–273. <https://doi.org/10.1006/ecss.1998.0364>.
- Horne, C. R., Hirst, A. G., Atkinson, D., Neves, A., and Kiørboe, T. 2016. A global synthesis of seasonal temperature–size responses in copepods. *Global Ecology and Biogeography*, 25(8), 988–999. <https://doi.org/10.1111/geb.12460>.

## REFERENCES

- Hromova, Y., Brauns, M., and Kamjunke, N. 2024. Lagrangian dynamics of the spring zooplankton community in a large river. *Hydrobiologia*. <https://doi.org/10.1007/s10750-024-05520-7>.
- Hu, Y. O. O., Karlson, B., Charvet, S., and Andersson, A. F. 2016. Diversity of pico- to mesoplankton along the 2000 km salinity gradient of the baltic sea. *Frontiers in Microbiology*, 7, 1–17. <https://doi.org/10.3389/fmicb.2016.00679>.
- Hughes, J. E., Deegan, L. A., Peterson, B. J., Holmes, R. M., and Fry, B. 2000. Nitrogen flow through the food web in the oligohaline zone of a New England estuary. *Ecology*, 81(2), 433–452. [https://doi.org/10.1890/0012-9658\(2000\)081\[0433:NFTTFW\]2.0.CO;2](https://doi.org/10.1890/0012-9658(2000)081[0433:NFTTFW]2.0.CO;2).
- Hydes, D., Aoyama, M., Aminot, A., Bakker, K., Becker, S., Coverly, S., Daniel, A., *et al.* 2010. Determination of dissolved nutrients (N, P, Si) in seawater with high precision and inter-comparability using gas-segmented continuous flow analysers. *The GO-SHIP Repeat Hydrography Manual: IOCCP Report*, 134(14), 1–87.
- Hyndes, G. A., Nagelkerken, I., McLeod, R. J., Connolly, R. M., Lavery, P. S., and Vanderklift, M. A. 2014. Mechanisms and ecological role of carbon transfer within coastal seascapes. *Biological Reviews*, 89(1), 232–254. <https://doi.org/10.1111/brv.12055>.
- Illing, B., Sehl, J., and Reiser, S. 2024. Turbidity effects on prey consumption and survival of larval European smelt (*Osmerus eperlanus*). *Aquatic Sciences*, 86(3). Springer International Publishing. <https://doi.org/10.1007/s00027-024-01103-9>.
- Irigoiien, X., and Castel, J. 1995. Feeding rates and productivity of the copepod *Acartia bifilosa* in a highly turbid estuary; the Gironde (SW France). *Hydrobiologia*, 311(1–3), 115–125. <https://doi.org/10.1007/BF00008575>.
- Jackson, A. L., Inger, R., Parnell, A. C., and Bearhop, S. 2011. Comparing isotopic niche widths among and within communities: SIBER - Stable Isotope Bayesian Ellipses in R. *Journal of Animal Ecology*, 80(3), 595–602. <https://doi.org/10.1111/j.1365-2656.2011.01806.x>.
- Jacob, U., Mintenbeck, K., Brey, T., Knust, R., and Beyer, K. 2005. Stable isotope food web studies: a case for standardized sample treatment. *Marine Ecology Progress Series*, 287(1), 251–253. <https://doi.org/10.3354/meps287251>.
- Jeffrey, S. W., and Humphrey, G. F. 1975. New spectrophotometric equations for determining chlorophylls a, b, c1 and c2 in higher plants, algae and natural phytoplankton. *Biochemie und Physiologie der Pflanzen*, 167(2), 191–194. Elsevier Masson SAS. [https://doi.org/10.1016/s0015-3796\(17\)30778-3](https://doi.org/10.1016/s0015-3796(17)30778-3).
- Johnson, J. K. 1980. Effects of temperature and salinity on production and hatching of dormant eggs of *Acartia californiensis* (copepoda) in an Oregon Estuary. *Fishery Bulletin*, 77(3), 567–584.
- Kafemann, R. 1992. Ökologische, fischereibiologische Gradienten in Haupt- und

## REFERENCES

- Nebenstromgebieten der unteren Tide-Elbe unter besonderer Berücksichtigung des Mühlenberger Lochs. Hamburg.
- Kamjunke, N., Brix, H., Flöser, G., Bussmann, I., Schütze, C., Achterberg, E. P., Ködel, U., *et al.* 2023. Large-scale nutrient and carbon dynamics along the river-estuary-ocean continuum. *Science of The Total Environment*, 890, 164421. <https://doi.org/10.1016/j.scitotenv.2023.164421>.
- Kennish, M. J. 2002. Environmental threats and environmental future of estuaries. *Environmental Conservation*, 29(1), 78–107. <https://doi.org/10.1017/S0376892902000061>.
- Kerner, M. 2004. Trophic diversity within the planktonic food web of the Elbe Estuary determined on isolated individual species by <sup>13</sup>C analysis. *Journal of Plankton Research*, 26(9), 1039–1048. <https://doi.org/10.1093/plankt/fbh094>.
- Kerner, M. 2007. Effects of deepening the Elbe Estuary on sediment regime and water quality. *Estuarine, Coastal and Shelf Science*, 75(4), 492–500. <https://doi.org/10.1016/j.ecss.2007.05.033>.
- Kimmel, D. G., and Roman, M. R. 2004. Long-term trends in mesozooplankton abundance in Chesapeake Bay, USA: Influence of freshwater input. *Marine Ecology Progress Series*, 267, 71–83. <https://doi.org/10.3354/meps267071>.
- Kjørboe, T., and Sabatini, M. 1995. Scaling of fecundity, growth and development in marine planktonic copepods. *Marine Ecology Progress Series*, 120(1–3), 285–298. <https://doi.org/10.3354/meps120285>.
- Kjørboe, T. 2006. Sex, sex-ratios, and the dynamics of pelagic copepod populations. *Oecologia*, 148(1), 40–50. <https://doi.org/10.1007/s00442-005-0346-3>.
- Kjørboe, T. 2011. How zooplankton feed: mechanisms, traits and trade-offs. *Biological Reviews*, 86(2), 311–339. <https://doi.org/10.1111/j.1469-185X.2010.00148.x>.
- Kjørboe, T., Ceballos, S., and Thygesen, U. H. 2015. Interrelations between senescence, life-history traits, and behavior in planktonic copepods. *Ecology*, 96(8), 2225–2235. <https://doi.org/10.1890/14-2205.1>.
- Kirk, K. L., and Gilbert, J. J. 1990. Suspended Clay and the Population Dynamics of Planktonic Rotifers and Cladocerans. *Ecology*, 71(5), 1741–1755. <https://doi.org/10.2307/1937582>.
- Kirk, K. L. 1992. Effects of suspended clay on Daphnia body growth and fitness. *Freshwater Biology*, 28(1), 103–109. <https://doi.org/10.1111/j.1365-2427.1992.tb00566.x>.
- Klarian, S. A., Schultz, E. T., Hernández, M. F., Valdes, J. A., Fernandoy, F., Barros, M. E., Neira, S., *et al.* 2022. Stomach contents and stable isotope analysis reveal ontogenetic shifts and spatial variability in *Brama australis* diet. *Environmental Biology of Fishes*,

## REFERENCES

- 105(11), 1673–1682. Springer Netherlands. <https://doi.org/10.1007/s10641-022-01365-y>.
- Kling, G. W., Fry, B., and O'Brien, W. J. 1992. Stable Isotopes and Planktonic Trophic Structure in Arctic Lakes. *Ecology*, 73(2), 561–566. <https://doi.org/10.2307/1940762>.
- Koch, E. W., Barbier, E. B., Silliman, B. R., Reed, D. J., Perillo, G. M. E., Hacker, S. D., Granek, E. F., *et al.* 2009. Non-linearity in ecosystem services: temporal and spatial variability in coastal protection. *Frontiers in Ecology and the Environment*, 7(1), 29–37. <https://doi.org/10.1890/080126>.
- Köpcke, B. 2002. Die Bedeutung der Nebenebenen und Flachwasserbereiche für den Populationserhalt von *Eurytemora affinis* (Calanoida; Copepoda) in der Tide-Elbe (The importance of side channels and shallow water areas for the conservation of the *E. affinis* population in the Elbe estuary). Dissertation. Universität Hamburg.
- Koppelman, R., Böttger-Schnack, R., Möbius, J., and Weikert, H. 2009. Trophic relationships of zooplankton in the eastern Mediterranean based on stable isotope measurements. *Journal of Plankton Research*, 31(6), 669–686. <https://doi.org/10.1093/plankt/fbp013>.
- Korpinen, S., Karjalainen, M., and Viitasalo, M. 2006. Effects of Cyanobacteria on Survival and Reproduction of the Littoral Crustacean *Gammarus zaddachi* (Amphipoda). *Hydrobiologia*, 559(1), 285–295. <https://doi.org/10.1007/s10750-005-1172-7>.
- Kottelat, M., and Freyhof, J. 2007. Handbook of European freshwater fishes. Publications Kottelat, Cornol, Switzerland.
- Krysanova, V., Kundzewicz, Z. W., Pińskwar, I., Habeck, A., and Hattermann, F. 2006. Regional socio-economic and environmental changes and their impacts on water resources on example of odra and elbe basins. 607–641 pp. <https://doi.org/10.1007/s11269-006-3091-4>.
- Layman, C. A., Winemiller, K. O., and Arrington, D. A. 2005. Describing a species-rich river food web using stable isotopes, stomach contents, and functional experiments. *In* Dynamic Food Webs: Multispecies Assemblages, Ecosystem Development, and Environmental Change, pp. 395–406. Ed. by A. R. Ives, P. Chesson, J. M. Cushing, M. Lewis, S. Rinaldi, and Y. Iwasa. Academic Press, London.
- Layman, C. A., Arrington, D. A., Montaña, C. G., and Post, D. M. 2007. Can stable isotope ratios provide for community-wide measures of trophic structure? *Ecology*, 88(1), 42–48. [https://doi.org/10.1890/0012-9658\(2007\)88\[42:CSIRPF\]2.0.CO;2](https://doi.org/10.1890/0012-9658(2007)88[42:CSIRPF]2.0.CO;2).
- Layman, C. A., Araujo, M. S., Boucek, R., Hammerschlag-Peyer, C. M., Harrison, E., Jud, Z. R., Matich, P., *et al.* 2012. Applying stable isotopes to examine food-web structure: an overview of analytical tools. *Biological Reviews*, 87(3), 545–562. <https://doi.org/10.1111/j.1469-185X.2011.00208.x>.

## REFERENCES

- Leblanc, K., Quéguiner, B., Diaz, F., Cornet, V., Michel-Rodriguez, M., Durrieu De Madron, X., Bowler, C., *et al.* 2018. Nanoplanktonic diatoms are globally overlooked but play a role in spring blooms and carbon export. *Nature Communications*, 9(1), 1–12. Springer US. <https://doi.org/10.1038/s41467-018-03376-9>.
- Leclerc, J., Riera, P., Noël, L. M. -L. J., Leroux, C., and Andersen, A. C. 2014. Trophic ecology of *Pomatoschistus microps* within an intertidal bay (Roscoff, France), investigated through gut content and stable isotope analyses. *Marine Ecology*, 35(2), 261–270. <https://doi.org/10.1111/maec.12071>.
- Lee, C. E., Moss, W. E., Olson, N., Chau, K. F., Chang, Y. M., and Johnson, K. E. 2013. Feasting in fresh water: Impacts of food concentration on freshwater tolerance and the evolution of food × salinity response during the expansion from saline into fresh water habitats. *Evolutionary Applications*, 6(4), 673–689. <https://doi.org/10.1111/eva.12054>.
- Lerner, J. E., Marchese, C., and Hunt, B. P. V. 2022. Stable isotopes reveal that bottom-up omnivory drives food chain length and trophic position in eutrophic coastal ecosystems. *ICES Journal of Marine Science*, 79(8), 2311–2323. <https://doi.org/10.1093/icesjms/fsac171>.
- Li, M., Ge, J., Kappenberg, J., Much, D., Nino, O., and Chen, Z. 2014. Morphodynamic processes of the Elbe River estuary, Germany: The Coriolis effect, tidal asymmetry and human dredging. *Frontiers of Earth Science*, 8(2), 181–189. <https://doi.org/10.1007/s11707-013-0418-3>.
- Li, S., Dong, Y., Sun, X., Zhao, Y., Zhao, L., Zhang, W., and Xiao, T. 2024. Seasonal and spatial variations of *Synechococcus* in abundance, pigment types, and genetic diversity in a temperate semi-enclosed bay. *Frontiers in Microbiology*, 14, 1–14. <https://doi.org/10.3389/fmicb.2023.1322548>.
- Lillelund, K. 1961. Untersuchungen über die Biologie und Populationsdynamik des Stintes *Osmerus eperlanus eperlanus* (Linnaeus 1758), der Elbe. *Arch. FischWiss.*, 12(1), 1–128.
- Lin, H.-J., Kao, W.-Y., and Wang, Y.-T. 2007. Analyses of stomach contents and stable isotopes reveal food sources of estuarine detritivorous fish in tropical/subtropical Taiwan. *Estuarine, Coastal and Shelf Science*, 73(3–4), 527–537. <https://doi.org/10.1016/j.ecss.2007.02.013>.
- Lindén, E., Lehtiniemi, M., and Viitasalo, M. 2003. Predator avoidance behaviour of Baltic littoral mysids *Neomysis integer* and *Praunus flexuosus*. *Marine Biology*, 143(5), 845–850. <https://doi.org/10.1007/s00227-003-1149-x>.
- Liu, C., Shi, X., Wu, F., Ren, M., Gao, G., and Wu, Q. 2020. Genome analyses provide insights into the evolution and adaptation of the eukaryotic Picophytoplankton *Mychonastes homosphaera*. *BMC Genomics*, 21(1), 1–18. BMC Genomics. <https://doi.org/10.1186/s12864-020-06891-6>.

## REFERENCES

- Lloyd, S. S., Elliott, D. T., and Roman, M. R. 2013. Egg production by the copepod, *Eurytemora affinis*, in Chesapeake Bay turbidity maximum regions. *Journal of Plankton Research*, 35(2), 299–308. <https://doi.org/10.1093/plankt/fbt003>.
- Mackas, D. L., Denman, K. L., and Abbott, M. R. 1985. Plankton patchiness: biology in the physical vernacular. *Bulletin of Marine Science*, 37(2), 652–674.
- Magath, V., and Thiel, R. 2013. Stock recovery, spawning period and spawning area expansion of the twaite shad *Alosa fallax* in the Elbe estuary, southern North Sea. *Endangered Species Research*, 20(2), 109–119. <https://doi.org/10.3354/esr00490>.
- Magath, V., Marohn, L., Fietzke, J., Frische, M., Thiel, R., and Dierking, J. 2013. Migration behaviour of twaite shad *Alosa fallax* assessed by otolith Sr:Ca and Ba:Ca profiles. *Journal of Fish Biology*, 82(6), 1871–1887. <https://doi.org/10.1111/jfb.12115>.
- Maksymowska, D., Richard, P., Piekarek-Jankowska, H., and Riera, P. 2000. Chemical and isotopic composition of the organic matter sources in the Gulf of Gdansk (Southern Baltic Sea). *Estuarine, Coastal and Shelf Science*, 51(5), 585–598. <https://doi.org/10.1006/ecss.2000.0701>.
- Malinsky-Rushansky, N., Berman, T., Berner, T., Yacobi, Y. Z., and Dubinsky, Z. 2002. Physiological characteristics of picophytoplankton, isolated from Lake Kinneret: Responses to light and temperature. *Journal of Plankton Research*, 24(11), 1173–1183. <https://doi.org/10.1093/plankt/24.11.1173>.
- Marion, A., Plourde, S., and Sirois, P. 2016. Mortality and recruitment in two copepod populations in a subarctic oligotrophic reservoir and the influence of environmental forcing. *Journal of Plankton Research*, 38(4), 915–930. <https://doi.org/10.1093/plankt/fbw040>.
- Marques, R., Otto, S. A., Pane, J. Di, and Boersma, M. 2023. Response of the meso- and macro- zooplankton community to long-term environmental changes in the southern North Sea. *ICES Journal of Marine Science*, 0, 1–14. <https://doi.org/10.1093/icesjms/fsad121>.
- Marques, S. C., Pardal, M. A., Pereira, M. J., Gonçalves, F., Marques, J. C., and Azeiteiro, U. M. 2007. Zooplankton distribution and dynamics in a temperate shallow estuary. *Hydrobiologia*, 587(1), 213–223. <https://doi.org/10.1007/s10750-007-0682-x>.
- Marsh, A. G., Grémare, A., and Tenore, K. R. 1989. Effect of food type and ration on growth of juvenile *Capitella* sp. I (Annelida: Polychaeta): macro- and micronutrients. *Marine Biology*, 102(4), 519–527. <https://doi.org/10.1007/BF00438354>.
- Martens, N., Ehlert, E., Putri, W., Sibbertsen, M., and Schaum, C. E. 2024a. Organic compounds drive growth in phytoplankton taxa from different functional groups. *Proceedings of the Royal Society B: Biological Sciences*, 291(2016). <https://doi.org/10.1098/rspb.2023.2713>.

## REFERENCES

- Martens, N., Russnak, V., Woodhouse, J., Grossart, H., and Schaum, C.-E. 2024b. Metabarcoding reveals potentially mixotrophic flagellates and picophytoplankton as key groups of phytoplankton in the Elbe estuary. *Environmental Research*, 252, 119126. Elsevier Inc. <https://doi.org/10.1016/j.envres.2024.119126>.
- Martens, N., Biederbick, J., and Schaum, C. -Elis. 2024c. Picophytoplankton prevail year-round in the Elbe estuary. *Plant-Environment Interactions*, 5(5), 1–11. <https://doi.org/10.1002/pei3.70014>.
- Martineau, C., Vincent, W. F., Frenette, J., and Dodson, J. J. 2004. Primary consumers and particulate organic matter: Isotopic evidence of strong selectivity in the estuarine transition zone. *Limnology and Oceanography*, 49(5), 1679–1686. <https://doi.org/10.4319/lo.2004.49.5.1679>.
- Martinez Arbizu, P. 2020. pairwiseAdonis: Pairwise multilevel comparison using adonis(R package version 0.4).
- Mason, C. F. 1986. Invertebrate populations and biomass over four years in a coastal, saline lagoon. *Hydrobiologia*, 133(1), 21–29. <https://doi.org/10.1007/BF00010798>.
- Massana, R. 2011. Eukaryotic picoplankton in surface oceans. *Annual Review of Microbiology*, 65, 91–110. <https://doi.org/10.1146/annurev-micro-090110-102903>.
- Mauchline, J., Blaxter, J. H. S., Southward, A. J., and Tyler, P. A. 1998. The Biology of Calanoid Copepods. Academic Press. 1–710 pp.
- McCarthy, I. D., Jones, N. J. E., Moore, D. M., and Berlinsky, D. L. 2019. Determining the optimum temperature and salinity for larval culture, and describing a culture protocol for the conservation aquaculture for European smelt *Osmerus eperlanus* (L.). *Journal of Applied Ichthyology*, 36(1), 113–120. <https://doi.org/10.1111/jai.13992>.
- McClelland, J. W., Valiela, I., and Michener, R. H. 1997. Nitrogen-stable isotope signatures in estuarine food webs: A record of increasing urbanization in coastal watersheds. *Limnology and Oceanography*, 42(5), 930–937. <https://doi.org/10.4319/lo.1997.42.5.0930>.
- McCutchan, J. H., Lewis, W. M., Kendall, C., and McGrath, C. C. 2003. Variation in trophic shift for stable isotope ratios of carbon, nitrogen, and sulfur. *Oikos*, 102(2), 378–390. <https://doi.org/10.1034/j.1600-0706.2003.12098.x>.
- McEwen, G. F., Johnson, M. W., and Folsom, T. R. 1954. A statistical analysis of the performance of the folsom plankton sample splitter, based upon test observations. *Archiv für Meteorologie, Geophysik und Bioklimatologie Serie A*, 7(1), 502–527. <https://doi.org/10.1007/BF02277939>.
- McLaren, I. A. 1963. Effects of Temperature on Growth of Zooplankton, and the Adaptive Value of Vertical Migration. *Journal of the Fisheries Research Board of Canada*, 20(3), 685–727. <https://doi.org/10.1139/f63-046>.

## REFERENCES

- Mees, J., Dewicke, A., and Hamerlynck, O. 1993. Seasonal composition and spatial distribution of hyperbenthic communities along estuarine gradients in the Westerschelde. *Netherlands Journal of Aquatic Ecology*, 27(2–4), 359–376. <https://doi.org/10.1007/BF02334798>.
- Mees, J., Abdulkerim, Z., and Hamerlynck, O. 1994. Life history, growth and production of *Neomysis integer* in the Westerschelde estuary (SW Netherlands). *Marine Ecology Progress Series*, 111, 43–57. <https://doi.org/10.3354/meps111043>.
- Mialet, B., Azémar, F., Maris, T., Sossou, C., Ruiz, P., Lionard, M., Van Damme, S., *et al.* 2010. Spatial spring distribution of the copepod *Eurytemora affinis* (Copepoda, Calanoida) in a restoring estuary, the Scheldt (Belgium). *Estuarine, Coastal and Shelf Science*, 88(1), 116–124. <https://doi.org/10.1016/j.ecss.2010.03.018>.
- Mialet, B., Gouzou, J., Azémar, F., Maris, T., Sossou, C., Toumi, N., Van Damme, S., *et al.* 2011. Response of zooplankton to improving water quality in the Scheldt estuary (Belgium). *Estuarine, Coastal and Shelf Science*, 93(1), 47–57. <https://doi.org/10.1016/j.ecss.2011.03.015>.
- Middelburg, J. J., and Herman, P. M. J. 2007. Organic matter processing in tidal estuaries. *Marine Chemistry*, 106(1–2), 127–147. <https://doi.org/10.1016/j.marchem.2006.02.007>.
- Modéran, J., Bouvais, P., David, V., Le Noc, S., Simon-Bouhet, B., Niquil, N., Miramand, P., *et al.* 2010. Zooplankton community structure in a highly turbid environment (Charente estuary, France): Spatio-temporal patterns and environmental control. *Estuarine, Coastal and Shelf Science*, 88(2), 219–232. <https://doi.org/10.1016/j.ecss.2010.04.002>.
- Modéran, J., David, V., Bouvais, P., Richard, P., and Fichet, D. 2012. Organic matter exploitation in a highly turbid environment: Planktonic food web in the Charente estuary, France. *Estuarine, Coastal and Shelf Science*, 98, 126–137. <https://doi.org/10.1016/j.ecss.2011.12.018>.
- Moreira-Turcq, P. F., Cauwet, G., and Martin, J. M. 2001. Contribution of flow cytometry to estimate picoplankton biomass in estuarine systems. *Hydrobiologia*, 462, 157–168. <https://doi.org/10.1023/A:1013138317897>.
- Morrissey, C. A., Boldt, A., Mapstone, A., Newton, J., and Ormerod, S. J. 2013. Stable isotopes as indicators of wastewater effects on the macroinvertebrates of urban rivers. *Hydrobiologia*, 700(1), 231–244. <https://doi.org/10.1007/s10750-012-1233-7>.
- Mosman, J. D., Gilby, B. L., Olds, A. D., Goodridge Gaines, L. A., Borland, H. P., and Henderson, C. J. 2023. Multiple Fish Species Supplement Predation in Estuaries Despite the Dominance of a Single Consumer. *Estuaries and Coasts*, 46(4), 891–905. <https://doi.org/10.1007/s12237-023-01184-z>.

## REFERENCES

- Motoda, S. 1959. Devices of simple plankton apparatus. *Memoirs of the faculty of fisheries hokkaido university*, 7(1–2), 73–111.
- Mouny, P., Dauvin, J. C., Bessineton, C., Elkaim, B., and Simon, S. 1998. Biological components from the Seine estuary: First results. *Hydrobiologia*, 373–374(1994), 333–347. [https://doi.org/10.1007/978-94-011-5266-2\\_26](https://doi.org/10.1007/978-94-011-5266-2_26).
- Mouny, P., and Dauvin, J.-C. 2002. Environmental control of mesozooplankton community structure in the Seine estuary (English Channel). *Oceanologica Acta*, 25, 13–22.
- Müller-Solger, A. B., Jassby, A. D., and Müller-Navarra, D. C. 2002. Nutritional quality of food resources for zooplankton (*Daphnia*) in a tidal freshwater system (Sacramento-San Joaquin River Delta). *Limnology and Oceanography*, 47(5), 1468–1476. <https://doi.org/10.4319/lo.2002.47.5.1468>.
- Mullin, M., and Brooks, E. R. 1970. Growth and metabolism of two planktonic copepods as influenced by temperature and type of food. *In* J. H. Steele. *Marine food chains*, 1st edn. Oliver & Boyd, Edinburgh.
- Muñoz-Marín, M. C., Gómez-Baena, G., López-Lozano, A., Moreno-Cabezuelo, J. A., Díez, J., and García-Fernández, J. M. 2020. Mixotrophy in marine picocyanobacteria: use of organic compounds by *Prochlorococcus* and *Synechococcus*. *The ISME Journal*, 14(5), 1065–1073. <https://doi.org/10.1038/s41396-020-0603-9>.
- Muylaert, K., and Sabbe, K. 1999. Spring phytoplankton assemblages in and around the maximum turbidity zone of the estuaries of the Elbe (Germany), the Schelde (Belgium/The Netherlands) and the Gironde (France). *Journal of Marine Systems*, 22(2–3), 133–149. [https://doi.org/10.1016/S0924-7963\(99\)00037-8](https://doi.org/10.1016/S0924-7963(99)00037-8).
- Muylaert, K., Tackx, M., and Vyverman, W. 2005. Phytoplankton growth rates in the freshwater tidal reaches of the Schelde estuary (Belgium) estimated using a simple light-limited primary production model. *Hydrobiologia*, 540(1–3), 127–140. <https://doi.org/10.1007/s10750-004-7128-5>.
- Newsome, S. D., Martinez del Rio, C., Bearhop, S., and Phillips, D. L. 2007. A niche for isotopic ecology. *Frontiers in Ecology and the Environment*, 5(8), 429–436. <https://doi.org/10.1890/060150.1>.
- Nielsen, J. M., Clare, E. L., Hayden, B., Brett, M. T., and Kratina, P. 2018. Diet tracing in ecology: Method comparison and selection. *Methods in Ecology and Evolution*, 9(2), 278–291. <https://doi.org/10.1111/2041-210X.12869>.
- Ning, M., Li, H., Xu, Z., Chen, L., and He, Y. 2021. Picophytoplankton identification by flow cytometry and high-throughput sequencing in a clean reservoir. *Ecotoxicology and Environmental Safety*, 216, 112216. <https://doi.org/10.1016/j.ecoenv.2021.112216>.
- NLWKN. 2023. Monitoring data NLWKN (Niedersächsischer Landesbetrieb für Wasserwirtschaft, Küsten- und Naturschutz) - Phytoplankton taxa and Biovolume

## REFERENCES

- (pers.Commun.).
- Nogueira, P., Barbosa, A. B., and Domingues, R. B. 2023. Impacts of sample storage time on estimates of phytoplankton abundance: how long is too long? *Journal of Plankton Research*, 45(6), 794–802. <https://doi.org/10.1093/plankt/fbad041>.
- Nöthlich, I. 1972. Trophische Struktur und Bioaktivität der Planktongesellschaft im unteren limnischen Bereich des Elbe-Ästuars. Kriterien zur saprobiellen Einstufung eines Tidegewässers (Trophic structure and bioactivity of the plankton community in the lower limnic area of the Elbe estuary. Criteria for the saprobic classification of tidal waters). *Archiv fuer Hydrobiologie, Supplement*, 43, 33–117.
- Oesmann, S. 1994. Nahrung und Wachstum clupeider Fische in der Unterelbe (Food and growth of clupeid fish in the Lower Elbe). Dissertation. Universität Hamburg.
- Ohman, M. D. 2012. Estimation of mortality for stage-structured zooplankton populations: What is to be done? *Journal of Marine Systems*, 93, 4–10. Elsevier B.V. <https://doi.org/10.1016/j.jmarsys.2011.05.008>.
- Oksanen, J., Simpson, G. L., Blanchet, F. G., Kindt, R., Legendre, P., Minchin, P. R., O'Hara, R. B., *et al.* 2022. Package 'Vegan'. Community Ecology Package. *Cran*, 2(9), 1–297.
- Omori, M., and Fleminger, A. 1976. Laboratory methods for processing crustacean zooplankton. The Unesco Press, Paris. 281–286 pp.
- OpenAI. 2023. GPT-4. <https://www.openai.com/gpt-4>.
- Paerl, H. W. 2006. Assessing and managing nutrient-enhanced eutrophication in estuarine and coastal waters: Interactive effects of human and climatic perturbations. *Ecological Engineering*, 26(1), 40–54. <https://doi.org/10.1016/j.ecoleng.2005.09.006>.
- Paerl, R. W., Venezia, R. E., Sanchez, J. J., and Paerl, H. W. 2020. Picophytoplankton dynamics in a large temperate estuary and impacts of extreme storm events. *Scientific Reports*, 10(1), 1–15. <https://doi.org/10.1038/s41598-020-79157-6>.
- Papenmeier, S., Schrottke, K., and Bartholomä, A. 2014. Over time and space changing characteristics of estuarine suspended particles in the German Weser and Elbe estuaries. *Journal of Sea Research*, 85, 104–115. <https://doi.org/10.1016/j.seares.2013.03.010>.
- Park, G. S., and Marshall, H. G. 2000. The trophic contributions of rotifers in tidal freshwater and estuarine habitats. *Estuarine, Coastal and Shelf Science*, 51(6), 729–742. <https://doi.org/10.1006/ecss.2000.0723>.
- Park, J. S., Jung, S. W., Ki, J. S., Guo, R., Kim, H. J., Lee, K. W., and Lee, J. H. 2017. Transfer of the small diatoms *Thalassiosira proschkiniae* and *T. spinulata* to the genus *Minidiscus* and their taxonomic re-description. *PLoS ONE*, 12(9), 1–20. <https://doi.org/10.1371/journal.pone.0181980>.

## REFERENCES

- Parnell, A., and Inger, R. 2016. Stable Isotope Mixing Models in R with simmr. Version 4.3.1. <https://cran.r-project.org/web/packages/simmr/vignettes/simmr.html> (Accessed 20 December 2024).
- Pasquaud, S., Elie, P., Jeantet, C., Billy, I., Martinez, P., and Girardin, M. 2008. A preliminary investigation of the fish food web in the Gironde estuary, France, using dietary and stable isotope analyses. *Estuarine, Coastal and Shelf Science*, 78(2), 267–279. <https://doi.org/10.1016/j.ecss.2007.12.014>.
- Pein, J., Eisele, A., Sanders, T., Daewel, U., Stanev, E. V., van Beusekom, J. E. E., Staneva, J., *et al.* 2021. Seasonal Stratification and Biogeochemical Turnover in the Freshwater Reach of a Partially Mixed Dredged Estuary. *Frontiers in Marine Science*, 8. <https://doi.org/10.3389/fmars.2021.623714>.
- Pein, J., Staneva, J., Mayer, B., Palmer, M. D., and Schrum, C. 2023. A framework for estuarine future sea-level scenarios: Response of the industrialised Elbe estuary to projected mean sea level rise and internal variability. *Frontiers in Marine Science*, 10, 1–19. <https://doi.org/10.3389/fmars.2023.1102485>.
- Peitsch, A. 1992. Untersuchungen zur Populationsdynamik und Produktion von Eurytemora affinis (Calanoida; Copepoda) im Brackwasserbereich des Elbe Ästuars (Studies on the population dynamics and production of Eurytemora affinis in the brackish waters of the Elbe estuary). Dissertation. Universität Hamburg.
- Peitsch, A., and Kausch, H. 1993. Distribution and tidal transport of different developmental stages of Eurytemora affinis (Copepoda: Calanoida) in the Elbe Estuary. *Archiv fuer Hydrobiologie, Supplement*, 75(3–4), 341–355.
- Peitsch, A. 1995. Production rates of Eurytemora affinis in the Elbe estuary, comparison of field and enclosure production estimates. *Hydrobiologia*, 311(1–3), 127–137. <https://doi.org/10.1007/BF00008576>.
- Peitsch, A., Köpcke, B., and Bernát, N. 2000. Long-term investigation of the distribution of Eurytemora affinis (Calanoida; Copepoda) in the Elbe Estuary. *Limnologica*, 30(2), 175–182. [https://doi.org/10.1016/S0075-9511\(00\)80013-4](https://doi.org/10.1016/S0075-9511(00)80013-4).
- Perkins, E. J. 1957. A Modification of the Hensen-Stempel Pipette. *Nature*, 179(4570), 1143–1143. <https://doi.org/10.1038/1791143b0>.
- Petersen, W., Schroeder, F., and Bockelmann, F.-D. 2011. FerryBox - Application of continuous water quality observations along transects in the North Sea. *Ocean Dynamics*, 61(10), 1541–1554. <https://doi.org/10.1007/s10236-011-0445-0>.
- Peterson, B. J., and Fry, B. 1987. Stable isotopes in ecosystem studies. *Annual review of ecology and systematics*, 18, 293–320. <https://doi.org/10.1146/annurev.es.18.110187.001453>.
- Peterson, W. T. 2001. Patterns in stage duration and development among marine and

## REFERENCES

- freshwater calanoid and cyclopoid copepods: A review of rules, physiological constraints, and evolutionary significance. *Hydrobiologia*, 453–454, 91–105. <https://doi.org/10.1023/A:1013111832700>.
- Pihl, L., and Rosenberg, R. 1982. Production, abundance, and biomass of mobile epibenthic marine fauna in shallow waters, Western Sweden. *Journal of Experimental Marine Biology and Ecology*, 57(2–3), 273–301. [https://doi.org/10.1016/0022-0981\(82\)90197-6](https://doi.org/10.1016/0022-0981(82)90197-6).
- Pihl, L., and Rosenberg, R. 1984. Food selection and consumption of the shrimp Crangon crangon in some shallow marine areas in western Sweden. *Marine Ecology Progress Series*, 15(1), 159–168. <https://doi.org/10.3354/meps015159>.
- Platell, M. E., Orr, P. A., and Potter, I. C. 2006. Inter- and intraspecific partitioning of food resources by six large and abundant fish species in a seasonally open estuary. *Journal of Fish Biology*, 69(1), 243–262. <https://doi.org/10.1111/j.1095-8649.2006.01098.x>.
- Plummer, M. 2003. DSC 2003 Working Papers JAGS: A program for analysis of Bayesian graphical models using Gibbs sampling. *Proceedings of the 3rd International Conference on Distributed Statistical Computing*, 1–10.
- Poiesz, S., Witte, J., van der Meer, M., van der Veer, H., and Soetaert, K. 2021. Trophic structure and resource utilization of the coastal fish community in the western Wadden Sea: evidence from stable isotope data analysis. *Marine Ecology Progress Series*, 677, 115–128. <https://doi.org/10.3354/meps13855>.
- Popov, A. P. 2006. Biology and reproduction of smelt (*Osmerus eperlanus* L.) in the eastern Gulf of Finland. *In* Ecological aspects of impact of hydroconstruction upon biota of the eastern Gulf of Finland, pp. 92–118. Ed. by Proceedings of FGNU GOSNIORH.
- Poppe, S. A. 1880. Über eine neue Art der Calaniden-Gattung Temora, Baird (On a new species of the Calanidae genus Temora, Baird). *Abhandlung des Naturwissenschaftlichen Vereins zu Bremen*, 7(3), 55–60.
- Post, D. M. 2002. Using Stable Isotopes to Estimate Trophic Position: Models, Methods, and Assumptions. *Ecology*, 83(3), 703. <https://doi.org/10.2307/3071875>.
- Pothoven, S. A., Vanderploeg, H. A., Ludsin, S. A., Höök, T. O., and Brandt, S. B. 2009. Feeding ecology of emerald shiners and rainbow smelt in central Lake Erie. *Journal of Great Lakes Research*, 35(2), 190–198. <https://doi.org/10.1016/j.jglr.2008.11.011>.
- Puigcorbé, V., Benitez-Nelson, C. R., Masqué, P., Verdeny, E., White, A. E., Popp, B. N., Prahl, F. G., *et al.* 2015. Small phytoplankton drive high summertime carbon and nutrient export in the Gulf of California and Eastern Tropical North Pacific. *Global Biogeochemical Cycles*, 29(8), 1309–1332. <https://doi.org/10.1002/2015GB005134>.
- Purcell-Meyerink, D., Fortune, J., and Butler, E. C. V. 2017. Productivity dominated by picoplankton in a macro-tidal tropical estuary, Darwin Harbour. *New Zealand Journal*

## REFERENCES

- of Botany*, 55(1), 47–63. <https://doi.org/10.1080/0028825X.2016.1231125>.
- R Core Team. 2024. R: A language and environment for statistical computing. R Foundation for Statistical Computing, Vienna, Austria. <https://www.r-project.org/>.
- Radach, G., and Pätsch, J. 2007. Variability of continental riverine freshwater and nutrient inputs into the North Sea for the years 1977–2000 and its consequences for the assessment of eutrophication. *Estuaries and Coasts*, 30(1), 66–81. <https://doi.org/10.1007/BF02782968>.
- Raven, J. A. 1998. The twelfth Tansley Lecture. Small is beautiful: The picophytoplankton. *Functional Ecology*, 12(4), 503–513. <https://doi.org/10.1046/j.1365-2435.1998.00233.x>.
- Read, D. S., Bowes, M. J., Newbold, L. K., and Whiteley, A. S. 2014. Weekly flow cytometric analysis of riverine phytoplankton to determine seasonal bloom dynamics. *Environmental Sciences: Processes and Impacts*, 16(3), 594–603. <https://doi.org/10.1039/c3em00657c>.
- Reinl, K. L., Harris, T. D., Elfferich, I., Coker, A., Zhan, Q., De Senerpont Domis, L. N., Morales-Williams, A. M., *et al.* 2022. The role of organic nutrients in structuring freshwater phytoplankton communities in a rapidly changing world. *Water Research*, 219, 118573. <https://doi.org/10.1016/j.watres.2022.118573>.
- Remane, A. 1934. Die Brackwasserfauna: Mit besonderer Berücksichtigung der Ostsee. *Verh. Dtsch. Zool. Ges.*, 36, 34–74.
- Richard, M., Bec, B., Bergeon, L., Hébert, M., Mablouké, C., and Lagarde, F. 2022. Are mussels and oysters capable of reducing the abundances of *Picochlorum* sp., responsible for a massive green algae bloom in Thau lagoon, France? *Journal of Experimental Marine Biology and Ecology*, 556, 151797. <https://doi.org/10.1016/j.jembe.2022.151797>.
- Riedel-Lorjé, J., Agatha, S., Holst, H., Köpcke, B., and Krieg, H. J. 1998. Kleinlebewesen der Tideelbe. Arbeitsgemeinschaft für die Reinhaltung der Elbe (ARGE).
- Riedel-Lorjé, J. C., and Gaumert, T. 1982. Hydrobiologische Situation und Fischbestand 1842 - 1943 unter dem Einfluß von Stromverbau und Sieleinleitungen. *Archiv für Hydrobiologie*, 61, 317–378.
- Robins, P. E., Skov, M. W., Lewis, M. J., Giménez, L., Davies, A. G., Malham, S. K., Neill, S. P., *et al.* 2016. Impact of climate change on UK estuaries: A review of past trends and potential projections. *Estuarine, Coastal and Shelf Science*, 169, 119–135. <https://doi.org/10.1016/j.ecss.2015.12.016>.
- Rochard, E., and Elie, P. 1994. La macrofaune aquatique de l'estuaire de la Gironde: contribution au livre blanc de l'Agence de l'eau Adour Garonne. 1–56 pp.

## REFERENCES

- Rosinski, C. L., Vinson, M. R., and Yule, D. L. 2020. Niche Partitioning among Native Ciscoes and Nonnative Rainbow Smelt in Lake Superior. *Transactions of the American Fisheries Society*, 149(2), 184–203. <https://doi.org/10.1002/tafs.10219>.
- Salujõe, J., Gottlob, H., Agasild, H., Haberman, J., Krause, T., and Zingel, P. 2008. Feeding of 0+ smelt *Osmerus eperlanus* in Lake Peipsi. *Estonian Journal of Ecology*, 57(1), 58. <https://doi.org/10.3176/eco.2008.1.04>.
- Sanders, T., Schöl, A., and Dähnke, K. 2018. Hot Spots of Nitrification in the Elbe Estuary and Their Impact on Nitrate Regeneration. *Estuaries and Coasts*, 41(1), 128–138. <https://doi.org/10.1007/s12237-017-0264-8>.
- Sathicq, M. B., Unrein, F., and Gómez, N. 2020. Recurrent pattern of picophytoplankton dynamics in estuaries around the world: The case of Río de la Plata. *Marine Environmental Research*, 161, 105136. <https://doi.org/10.1016/j.marenvres.2020.105136>.
- Sato, M., Yoshikawa, T., Takeda, S., and Furuya, K. 2007. Application of the size-fractionation method to simultaneous estimation of clearance rates by heterotrophic flagellates and ciliates of pico- and nanophytoplankton. *Journal of Experimental Marine Biology and Ecology*, 349(2), 334–343. <https://doi.org/10.1016/j.jembe.2007.05.027>.
- Schaum, C. E., Rost, B., and Collins, S. 2016. Environmental stability affects phenotypic evolution in a globally distributed marine picoplankton. *ISME Journal*, 10(1), 75–84. <https://doi.org/10.1038/ismej.2015.102>.
- Schelske, C. L., and Odum, E. P. 1962. Mechanisms maintaining high productivity in Georgia estuaries. *Proceedings of the Gulf and Caribbean Fisheries Institute*, 75–80.
- Schneider, C. A., Rasband, W. S., and Eliceiri, K. W. 2012. NIH Image to ImageJ: 25 years of image analysis. *Nature Methods*, 9(7), 671–675. <https://doi.org/10.1038/nmeth.2089>.
- Schöl, A., Blohm, W., Becker, A., and Fischer, H. 2009. Untersuchungen zum Rückgang hoher Algenbiomassen im limnischen Abschnitt der Tideelbe (Investigations concerning the decline of high algal biomass in the limnic part of the tidal Elbe). *In* German Society of Limnology: extended summary of the annual conference 2008 (Konstanz). Konstanz.
- Schöl, A., Hein, B., Wyrwa, J., and Kirchesch, V. 2014. Modelling water quality in the Elbe and its estuary -Large scale and long term applications with focus on the oxygen budget of the estuary. *Küste*(81), 203–232. <https://hdl.handle.net/20.500.11970/101692>.
- Schroeder, F. 1997. Water quality in the Elbe estuary: Significance of different processes for the oxygen deficit at Hamburg. *Environmental Modeling and Assessment*, 2(1–2), 73–82. <https://doi.org/10.1023/a:1019032504922>.
- Schulz, H. 1961. Qualitative und quantitative Planktonuntersuchungen im Elbe-Ästuar

## REFERENCES

- (Qualitative and quantitative plankton analyses in the Elbe estuary). *Archiv fuer Hydrobiologie, Supplement*, 26(1), 5–105.
- Selleslagh, J., and Amara, R. 2008. Environmental factors structuring fish composition and assemblages in a small macrotidal estuary (eastern English Channel). *Estuarine, Coastal and Shelf Science*, 79(3), 507–517. <https://doi.org/10.1016/j.ecss.2008.05.006>.
- Selleslagh, J., Lobry, J., N'Zigou, A. R., Bachelet, G., Blanchet, H., Chaalali, A., Sautour, B., *et al.* 2012. Seasonal succession of estuarine fish, shrimps, macrozoobenthos and plankton: Physico-chemical and trophic influence. The Gironde estuary as a case study. *Estuarine, Coastal and Shelf Science*, 112, 243–254. <https://doi.org/10.1016/j.ecss.2012.07.030>.
- Sendek, D. S., and Bogdanov, D. V. 2019. European smelt *Osmerus eperlanus* in the eastern Gulf of Finland, Baltic Sea: Stock status and fishery. *Journal of Fish Biology*, 94(6), 1001–1010. <https://doi.org/10.1111/jfb.14009>.
- Shi, X., Li, S., Fan, F., Zhang, M., Yang, Z., and Yang, Y. 2018. Mychonastes dominates the photosynthetic picoeukaryotes in Lake Poyang, a river-connected lake. *FEMS Microbiology Ecology*, 95(1), 1–11. <https://doi.org/10.1093/femsec/fiy211>.
- Sieburth, J. M., Smetacek, V., and Lenz, J. 1978. Pelagic ecosystem structure: Heterotrophic compartments of the plankton and their relationship to plankton size fractions 1. *Limnology and Oceanography*, 23(6), 1256–1263. <https://doi.org/10.4319/lo.1978.23.6.1256>.
- Sim, Z. Y., Goh, K. C., He, Y., and Gin, K. Y. H. 2023. Present and future potential role of toxin-producing *Synechococcus* in the tropical region. *Science of The Total Environment*, 896, 165230. <https://doi.org/10.1016/j.scitotenv.2023.165230>.
- Sluss, T. D., Jack, J. D., and Thorp, J. H. 2011. A comparison of sampling methods for riverine zooplankton. *River Systems*, 19(4), 315–326. <https://doi.org/10.1127/1868-5749/2011/0048>.
- Soetaert, K., and Van Rijswijk, P. 1993. Spatial and temporal patterns of the zooplankton in the Westerschelde estuary. *Marine Ecology Progress Series*, 97, 47–59. <https://doi.org/10.3354/meps097047>.
- Somogyi, B., Pálffy, K., Balogh, K. V., Botta-Dukát, Z., and Vóróes, L. 2017. Unusual behaviour of phototrophic picoplankton in turbid waters. *PLoS ONE*, 12(3), 1–15. <https://doi.org/10.1371/journal.pone.0174316>.
- Somogyi, B., Felföldi, T., Boros, E., Szabó, A., and Vörös, L. 2022. Where the Little Ones Play the Main Role—Picophytoplankton Predominance in the Soda and Hypersaline Lakes of the Carpathian Basin. *Microorganisms*, 10(4), 818. <https://doi.org/10.3390/microorganisms10040818>.

## REFERENCES

- Souissi, A., Souissi, S., and Hwang, J. S. 2016. Evaluation of the copepod *Eurytemora affinis* life history response to temperature and salinity increases. *Zoological Studies*, 55, 1–9. <https://doi.org/10.6620/ZS.2016.55-04>.
- Souissi, S., and Souissi, A. 2021. Promotion of the development of sentinel species in the water column: Example using body size and fecundity of the egg-bearing calanoid copepod *Eurytemora affinis*. *Water (Switzerland)*, 13(11). <https://doi.org/10.3390/w13111442>.
- Soulier, N., Walters, K., Laremore, T. N., Shen, G., Golbeck, J. H., and Bryant, D. A. 2022. Acclimation of the photosynthetic apparatus to low light in a thermophilic *Synechococcus* sp. strain. *Photosynthesis Research*, 153(1–2), 21–42. <https://doi.org/10.1007/s11120-022-00918-7>.
- Spieckermann, M., Gröngröft, A., Karrasch, M., Neumann, A., and Eschenbach, A. 2021. Oxygen Consumption of Resuspended Sediments of the Upper Elbe Estuary: Process Identification and Prognosis. *Aquatic Geochemistry*. <https://doi.org/10.1007/s10498-021-09401-6>.
- Statham, P. J. 2012. Nutrients in estuaries — An overview and the potential impacts of climate change. *Science of The Total Environment*, 434, 213–227. Elsevier B.V. <https://doi.org/10.1016/j.scitotenv.2011.09.088>.
- Steidle, L., and Vennell, R. 2024. Phytoplankton retention mechanisms in estuaries: a case study of the Elbe estuary. *Nonlinear Processes in Geophysics*, 31(1), 151–164. <https://doi.org/10.5194/npg-31-151-2024>.
- Sterner, R. W., and Elser, J. J. 2003. *Ecological Stoichiometry: The Biology of Elements from Molecules to the Biosphere*. Princeton University Press, Princeton. <https://doi.org/10.1515/9781400885695>.
- Stoecker, D. K. 1984. Particle production by planktonic ciliates. *Limnology and Oceanography*, 29(5), 930–940. <https://doi.org/10.4319/lo.1984.29.5.0930>.
- Stoecker, D. K., and Capuzzo, J. M. 1990. Predation on Protozoa: its importance to zooplankton. *Journal of Plankton Research*, 12(5), 891–908. <https://doi.org/10.1093/plankt/12.5.891>.
- Sweeting, C. J., Barry, J., Barnes, C., Polunin, N. V. C., and Jennings, S. 2007a. Effects of body size and environment on diet-tissue  $\delta^{15}\text{N}$  fractionation in fishes. *Journal of Experimental Marine Biology and Ecology*, 340(1), 1–10. <https://doi.org/10.1016/j.jembe.2006.07.023>.
- Sweeting, C. J., Barry, J. T., Polunin, N. V. C., and Jennings, S. 2007b. Effects of body size and environment on diet-tissue  $\delta^{13}\text{C}$  fractionation in fishes. *Journal of Experimental Marine Biology and Ecology*, 352(1), 165–176. <https://doi.org/10.1016/j.jembe.2007.07.007>.

## REFERENCES

- Taal, I., Saks, L., Nedolgov, S., Verliin, A., Kesler, M., Jürgens, K., Svirgsden, R., *et al.* 2014. Diet composition of smelt *O. smerus eperlanus* (Linnaeus) in brackish near-shore ecosystem (Eru Bay, Baltic Sea). *Ecology of Freshwater Fish*, 23(2), 121–128. <https://doi.org/10.1111/eff.12044>.
- Tackx, M. L. M., Herman, P. J. M., Gasparini, S., Irigoien, X., Billiones, R., and Daro, M. H. 2003. Selective feeding of *Eurytemora affinis* (Copepoda, Calanoida) in temperate estuaries: Model and field observations. *Estuarine, Coastal and Shelf Science*, 56(2), 305–311. [https://doi.org/10.1016/S0272-7714\(02\)00182-8](https://doi.org/10.1016/S0272-7714(02)00182-8).
- Tackx, M. L. M., De Pauw, N., Van Mieghem, R., Azémar, F., Hannouti, A., Van Damme, S., Fiers, F., *et al.* 2004. Zooplankton in the Schelde estuary, Belgium and The Netherlands. Spatial and temporal patterns. *Journal of Plankton Research*, 26(2), 133–141. <https://doi.org/10.1093/plankt/fbh016>.
- Takasu, H., Ikeda, M., Miyahara, K., and Shiragaki, T. 2023. High contribution of picophytoplankton to phytoplankton biomass in a shallow, eutrophic coastal sea. *Marine Environmental Research*, 184, 105852. <https://doi.org/10.1016/j.marenvres.2022.105852>.
- Tan, Y. H., Poong, S. W., Yang, C. H., Lim, P. E., John, B., Pai, T. W., and Phang, S. M. 2022. Transcriptomic analysis reveals distinct mechanisms of adaptation of a polar picophytoplankter under ocean acidification conditions. *Marine Environmental Research*, 182, 105782. <https://doi.org/10.1016/j.marenvres.2022.105782>.
- Telesh, I. V., Schubert, H., and Skarlato, S. O. 2011. Revisiting Remane's concept: Evidence for high plankton diversity and a protistan species maximum in the horohalinicum of the Baltic Sea. *Marine Ecology Progress Series*, 421, 1–11. <https://doi.org/10.3354/meps08928>.
- Theilen, J., Sarrazin, V., Hauten, E., Koll, R., Möllmann, C., Fabrizius, A., and Thiel, R. (n.d.). Environmental factors shaping fish fauna structure in a temperate mesotidal estuary: periodic insights from the Elbe estuary across four decades. *Estuarine, Coastal and Shelf Science*.
- Theilen, J., Sarrazin, V., Hauten, E., Koll, R., Möllmann, C., Fabrizius, A., and Thiel, R. 2022. Long-term changes in the ichthyofaunal composition in a temperate estuarine ecosystem - developments in the Elbe estuary over the past 40 years. *In* 18th conference of the Society for Ichthyology e.V. (GfI). Wien.
- Thiel, R., Sepúlveda, A., Kafemann, R., and Nellen, W. 1995. Environmental factors as forces structuring the fish community of the Elbe Estuary. *Journal of Fish Biology*, 46(1), 47–69. <https://doi.org/10.1111/j.1095-8649.1995.tb05946.x>.
- Thiel, R., Mehner, T., Köpcke, B., and Kafemann, R. 1996. Diet niche relationships among early life stages of fish in German estuaries. *Marine and Freshwater Research*, 47(2), 123–136. <https://doi.org/10.1071/MF9960123>.

## REFERENCES

- Thiel, R. 2001. Spatial gradients of food consumption and production of juvenile fish in the lower River Elbe. *River Systems*, 12(2–4), 441–462. <https://doi.org/10.1127/lr/12/2001/441>.
- Thiel, R., and Potter, I. C. 2001. The ichthyofaunal composition of the Elbe Estuary: an analysis in space and time. *Marine Biology*, 138(3), 603–616. <https://doi.org/10.1007/s002270000491>.
- Thiel, R. 2011. Die Fischfauna europäischer Ästuarie: eine Strukturanalyse mit Schwerpunkt Tideelbe. Abhandlungen des Naturwissenschaftlichen Vereins in Hamburg 43/2011. Dölling and Galitz Verlag.
- Thiel, R., and Thiel, R. 2015. Atlas der Fische und Neunaugen Hamburgs. Behörde für Stadtentwicklung und Umwelt, Hamburg. Freie und Hansestadt Hamburg. 1–170 pp.
- Thiemann, K. 1934. Das Plankton der Flußmündungen (The plankton of the estuaries). *Wiss. Erg. Dt. Atl. Exp. Meteor*, 12, 199–273.
- Thornton, S. F., and McManus, J. 1994. Application of Organic Carbon and Nitrogen Stable Isotope and C/N Ratios as Source Indicators of Organic Matter Provenance in Estuarine Systems: Evidence from the Tay Estuary, Scotland. *Estuarine, Coastal and Shelf Science*, 38(3), 219–233. <https://doi.org/10.1006/ecss.1994.1015>.
- Thyssen, M., Grégori, G., Créach, V., Lahbib, S., Dugenne, M., Aardema, H. M., Artigas, L. F., et al. 2022. Interoperable vocabulary for marine microbial flow cytometry. *Frontiers in Marine Science*, 9, 1–13. <https://doi.org/10.3389/fmars.2022.975877>.
- Tobias-Hünefeldt, S. P., van Beusekom, J. E. E., Russnak, V., Dähnke, K., Streit, W. R., and Grossart, H.-P. 2024. Seasonality, rather than estuarine gradient or particle suspension/sinking dynamics, determines estuarine carbon distributions. *Science of The Total Environment*, 926, 171962. <https://doi.org/10.1016/j.scitotenv.2024.171962>.
- Tragin, M., and Vaultot, D. 2019. Novel diversity within marine Mamiellophyceae (Chlorophyta) unveiled by metabarcoding. *Scientific Reports*, 9(1), 1–14. <https://doi.org/10.1038/s41598-019-41680-6>.
- Turner, R. E., Milan, C. S., Swenson, E. M., and Lee, J. M. 2022. Peak chlorophyll a concentrations in the lower Mississippi River from 1997 to 2018. *Limnology and Oceanography*, 67(3), 703–712. <https://doi.org/10.1002/lno.12030>.
- van Buuren, S., and Groothuis-Oudshoorn, K. 2011. mice: Multivariate imputation by chained equations in R. *Journal of Statistical Software*, 45(3), 1–67. <https://doi.org/10.18637/jss.v045.i03>.
- van Maren, D. S., van Kessel, T., Cronin, K., and Sittoni, L. 2015. The impact of channel deepening and dredging on estuarine sediment concentration. *Continental Shelf Research*, 95, 1–14. <https://doi.org/10.1016/j.csr.2014.12.010>.

## REFERENCES

- Vander Zanden, M. J., and Rasmussen, J. B. 2001. Variation in  $\delta^{15}\text{N}$  and  $\delta^{13}\text{C}$  trophic fractionation: Implications for aquatic food web studies. *Limnology and Oceanography*, 46(8), 2061–2066. <https://doi.org/10.4319/lo.2001.46.8.2061>.
- Vander Zanden, M. J., Clayton, M. K., Moody, E. K., Solomon, C. T., and Weidel, B. C. 2015. Stable Isotope Turnover and Half-Life in Animal Tissues: A Literature Synthesis. *PLOS ONE*, 10(1), e0116182. <https://doi.org/10.1371/journal.pone.0116182>.
- Venice System. 1958. The Venice System for the Classification of Marine Waters according to salinity. *In* Symposium on the Classification of Brackish Waters, pp. 243–248. Ed. by D. Anconda. Venice, Italy.
- Vinni, M., Lappalainen, J., Malinen, T., and Peltonen, H. 2004. Seasonal bottlenecks in diet shifts and growth of smelt in a large eutrophic lake. *Journal of Fish Biology*, 64(2), 567–579. <https://doi.org/10.1111/j.0022-1112.2004.00323.x>.
- Vinni, M., Lappalainen, J., and Horppila, J. 2005. Temporal and size-related changes in the frequency of empty stomachs in smelt. *Journal of Fish Biology*, 66(2), 578–582. <https://doi.org/10.1111/j.0022-1112.2005.00615.x>.
- Volk, R. 1903. Hamburgische Elbuntersuchungen I. *Mitt. Naturhist. Mus. Hamburg*, 19, 65–154.
- Wang, X., and Zauke, G. P. 2002. Relationship between growth parameters of the amphipod *Gammarus zaddachi* (Sexton 1912) and the permeable body surface area determined by the acid-base titration method. *Hydrobiologia*, 482, 179–189. <https://doi.org/10.1023/A:1021245715827>.
- Watkins, J., Rudstam, L., and Holeck, K. 2011. Length-weight regressions for zooplankton biomass calculations - A review and a suggestion for standard equations. *Cornell Biological Field Station Publications and Reports*, 17. <https://api.semanticscholar.org/CorpusID:126819925>.
- Wayland, M., and Hobson, K. A. 2001. Stable carbon, nitrogen, and sulfur isotope ratios in riparian food webs on rivers receiving sewage and pulp-mill effluents. *Canadian Journal of Zoology*, 79(1), 5–15. <https://doi.org/10.1139/z00-169>.
- Weilbeer, H., Winterscheid, A., Strotmann, T., Entelmann, I., Shaikh, S., and Vaessen, B. 2021. Analyse der hydrologischen und morphologischen Entwicklung in der Tideelbe für den Zeitraum von 2013 bis 2018 (Analysis of the hydrological and morphological development in the tidal Elbe estuary for the period from 2013 to 2018). *Die Küste*, 89, 57–129. <https://doi.org/10.18171/1.089104>.
- Wetz, M. S., Paerl, H. W., Taylor, J. C., and Leonard, J. A. 2011. Environmental controls upon picophytoplankton growth and biomass in a eutrophic estuary. *Aquatic Microbial Ecology*, 63(2), 133–143. <https://doi.org/10.3354/ame01488>.
- Whitfield, A. K., Elliott, M., Basset, A., Blaber, S. J. M., and West, R. J. 2012. Paradigms in

## REFERENCES

- estuarine ecology - A review of the Remane diagram with a suggested revised model for estuaries. *Estuarine, Coastal and Shelf Science*, 97, 78–90. <https://doi.org/10.1016/j.ecss.2011.11.026>.
- Whitfield, A. K., and Harrison, T. D. 2020. Fish species redundancy in estuaries: A major conservation concern in temperate estuaries under global change pressures. *Aquatic Conservation: Marine and Freshwater Ecosystems*, 31(4), 979–983. <https://doi.org/10.1002/aqc.3482>.
- Whitfield, A. K., Able, K. W., Blaber, S. J. M., and Elliott, M. 2022. Fish and Fisheries in Estuaries. Wiley, Hoboken, New Jersey. 1–1056 pp. <https://doi.org/10.1002/9781119705345>.
- Wilson, J. G. 2002. Productivity, fisheries and aquaculture in temperate estuaries. *Estuarine, Coastal and Shelf Science*, 55(6), 953–967. <https://doi.org/10.1006/ecss.2002.1038>.
- Wilson, S. E., and Steinberg, D. K. 2010. Autotrophic picoplankton in mesozooplankton guts: Evidence of aggregate feeding in the mesopelagic zone and export of small phytoplankton. *Marine Ecology Progress Series*, 412, 11–27. <https://doi.org/10.3354/meps08648>.
- Winkler, G., Dodson, J., Bertrand, N., Thivierge, D., and Vincent, W. 2003. Trophic coupling across the St. Lawrence River estuarine transition zone. *Marine Ecology Progress Series*, 251, 59–73. <https://doi.org/10.3354/meps251059>.
- Winkler, G., Martineau, C., Dodson, J. J., Vincent, W. F., and Johnson, L. E. 2007. Trophic dynamics of two sympatric mysid species in an estuarine transition zone. *Marine Ecology Progress Series*, 332, 171–187. <https://doi.org/10.3354/meps332171>.
- Winkler, G., Souissi, S., Poux, C., and Castric, V. 2011. Genetic heterogeneity among *Eurytemora affinis* populations in Western Europe. *Marine Biology*, 158(8), 1841–1856. <https://doi.org/10.1007/s00227-011-1696-5>.
- Wolanski, E., and Elliott, M. 2015. Estuarine Ecohydrology: An Introduction. Elsevier, Amsterdam. 1–320 pp. <https://doi.org/10.1016/C2013-0-13014-0>.
- Wolfstein, K., and Kies, L. 1995. A case study on the oxygen budget in the freshwater part of the Elbe estuary. Variation in phytoplankton pigments in the Elbe estuary before and during the oxygen minima in 1992 and 1993. *Archiv fuer Hydrobiologie, Supplement*, 1(110), 39–54.
- Wolfstein, K. 1996. Untersuchungen zur Bedeutung des Phytoplanktons als Bestandteil der Schwebstoffe für das Ökosystem Tide-Elbe (Investigations about the significance of phytoplankton as a component of suspended matter for the tidal Elbe ecosystem). Dissertation. Universität Hamburg.
- Yang, J., Lv, J., Liu, Q., Nan, F., Li, B., Xie, S., and Feng, J. 2021. Seasonal and spatial patterns of eukaryotic phytoplankton communities in an urban river based on marker gene.

## REFERENCES

- Scientific Reports*, 11(1), 1–13. <https://doi.org/10.1038/s41598-021-02183-5>.
- Yang, J., Zhang, X., Lü, J., Liu, Q., Nan, F., Liu, X., Xie, S., *et al.* 2022. Seasonal co-occurrence patterns of bacteria and eukaryotic phytoplankton and the ecological response in urban aquatic ecosystem. *Journal of Oceanology and Limnology*, 40(4), 1508–1529. <https://doi.org/10.1007/s00343-021-1214-7>.
- Zhang, F., He, J., Lin, L., and Jin, H. 2015. Dominance of picophytoplankton in the newly open surface water of the central Arctic Ocean. *Polar Biology*, 38(7), 1081–1089. <https://doi.org/10.1007/s00300-015-1662-7>.
- Zhao, B., Peng, W., Zhu, X., Zhang, H., Zhuang, X., Wang, J., Xi, S., *et al.* 2024. Research on the Relationship between Eukaryotic Phytoplankton Community Structure and Key Physiochemical Properties of Water in the Western Half of the Chaohu Lake Using High-Throughput Sequencing. *Water (Switzerland)*, 16(16). <https://doi.org/10.3390/w16162318>.
- Zimmermann-Timm, H., Holst, H., and Müller, S. 1998. Seasonal dynamics of aggregates and their typical biocoenosis in the Elbe Estuary. *Estuaries*, 21(4), 613–621. <https://doi.org/10.2307/1353299>.

## Acknowledgements

First of all, I would like to thank my supervisors, Prof. Dr. Christian Möllmann and Dr. Rolf Koppelman, for their incredible support and throughout my doctoral journey. We have come up with many great ideas and solutions together and I really appreciate all the guidance you provided along the way. A special thanks to Dr. Andrej Fabrizius, who supported me as chair of the thesis committee, for sharing valuable suggestions during our panel meetings. Many thanks to Dr. Jasmin Renz, Dr. Bettina Martin and Dr. Justus van Beusekom for their helpful comments and suggestions on my project. I would like to thank Prof. Dr. Jutta Schneider and Prof. Dr. Nicole Aberle-Malzahn for agreeing to be part of the examination committee. A big thank you to Prof. Dr. Kai Jensen, Monika Petersen and Dr. Susanne Stirn for all their hard work and for letting me be a part of the RTG2530 family. I truly appreciate all your help!

I would like to thank the IMF family for helping me navigate through the chaos of daily life as a doctoral candidate while I was on cruises, in the lab and office. A special thanks goes to my (partly former) colleagues in the office, especially Elena Hauten, Tobias Reißing, Jan Conradt, Alexandra Blöcker, Helene Gutte, Rene Plonus, Elvis Kamberi, Nele Martens, Widhi Putri, Marie Vogel, Michael Edetanlen, Raquel Marques, Dominik Auch, Gregor Börner and many other lovely people – thank you for all the coffee and brainstorming sessions, and so much more. I would also like to express my gratitude to my RTG2530 family for their help and contributions to the doctoral project. A special thanks goes to my colleagues Stephanie Kondratowicz, Stefanie Schnell, Sven Stärker, Joachim Lütke, and especially Martina Wichmann for their technical support in the lab and during the fieldwork. Without you, Martina, I would still be sitting in the lab counting and sorting my zooplankton samples under the microscope!

Thank you to the amazing people in my life, who I spend most of my time with, for constantly reminding me that there is a whole world of exciting things to explore beyond zooplankton. A special thank you to Annika Baumgartner, who has supported every one of my ideas since 2003 and has always been by my side, no matter what comes next. A thousand thanks to Vanessa Russnak and Marc Stammerjohann for all the laughs and cooking sessions – they really are balm for the soul. A heartfelt thank you to Daniel Pemsel for joining me on this rollercoaster ride and for always being there to support and ground me when I needed it most. And my biggest and deepest thanks go to my wonderful family – Petra, Robert, Franziska and Sebastian Biederbick. I can't express how grateful I am for all your support and love. THANK YOU!

## **Eidesstattliche Versicherung / Declaration on oath**

### **Eidesstattliche Versicherung:**

Hiermit versichere ich an Eides statt, die vorliegende Dissertationsschrift selbst verfasst und keine anderen als die angegebenen Hilfsmittel und Quellen benutzt zu haben.

Sofern im Zuge der Erstellung der vorliegenden Dissertationsschrift generative Künstliche Intelligenz (gKI) basierte elektronische Hilfsmittel verwendet wurden, versichere ich, dass meine eigene Leistung im Vordergrund stand und dass eine vollständige Dokumentation aller verwendeten Hilfsmittel gemäß der Guten wissenschaftlichen Praxis vorliegt. Ich trage die Verantwortung für eventuell durch die gKI generierte fehlerhafte oder verzerrte Inhalte, fehlerhafte Referenzen, Verstöße gegen das Datenschutz- und Urheberrecht oder Plagiate.

### **Affidavit:**

I hereby declare and affirm that this doctoral dissertation is my own work and that I have not used any aids and sources other than those indicated.

If electronic resources based on generative artificial intelligence (gAI) were used in the course of writing this dissertation, I confirm that my own work was the main and value-adding contribution and that complete documentation of all resources used is available in accordance with good scientific practice. I am responsible for any erroneous or distorted content, incorrect references, violations of data protection and copyright law or plagiarism that may have been generated by the gAI.

Hamburg, den 20. Februar 2025

## List of Publications

### Published articles:

#### Chapter 4:

**Biederbick, J.**, Möllmann, C., Hauten, E., Russnak, V., Lahajnar, N., Hansen, T., Dierking, J. and Koppelman, R. 2024. Spatial and temporal patterns of zooplankton trophic interactions and carbon sources in the eutrophic Elbe estuary (Germany), ICES Journal of Marine Science, 0(0). <https://doi.org/10.1093/icesjms/fsae189>

#### Chapter 6:

Martens, N., **Biederbick, J.**, and Schaum, C.-E. 2024. Picophytoplankton prevail year-round in the Elbe estuary. Plant-Environment Interactions, 5(5), 1–11. <https://doi.org/10.1002/pei3.70014>.

### In preparation:

#### Chapter 2:

**Biederbick, J.**, Möllmann, C., Russnak, V. and Koppelman, R. (*in prep.*). Spatial and temporal succession of zooplankton in an environment under anthropogenic pressure – the Elbe estuary in northern Germany

#### Chapter 3:

**Biederbick, J.**, Renz, J., Russnak, V., Möllmann, C. and Koppelman, R. (*in prep.*). Population dynamics and production of *Eurytemora affinis* in the Elbe estuary.

#### Chapter 5:

Hauten, E., **Biederbick, J.**, Funk, S., Koll, R., Theilen, J., Fabrizius, A., Thiel, R., Jensen, K., Grønkjær, P. and Möllmann, C. (*in prep.*). Characterising intraspecific habitat exploitation of anadromous key species *Osmerus eperlanus* along the salinity gradient of a large European estuary.

## Contribution of authors

### **Chapter 2: Spatial and temporal succession of zooplankton in an environment under anthropogenic pressure – the Elbe estuary in northern Germany**

Running title: Spatio-temporal population dynamics of estuarine zooplankton

Authors: **Johanna Biederbick**, Christian Möllmann, Vanessa Rusnak and Rolf Koppelman

This chapter is a draft that is currently being prepared for submission to a peer-reviewed journal. The contributions of the authors are as follows: **Johanna Biederbick (JB)**, Christian Möllmann (CM) and Rolf Koppelman (RK) developed the objectives and methodology of this study, with CM and RK supervising the study. Field and laboratory work was conducted by **JB** and Vanessa Rusnak (VR). Data analysis and visualisation was developed and carried out by **JB** with advice from CM and RK. The acquisition of funding was done by CM. All co-authors reviewed and edited the original draft written by **JB**.

#### **Confirmation of correctness**

Hamburg, 20. February 2025

---

Place, date

---

Prof. Dr. Christian Möllmann

### Chapter 3: Population dynamics and production of *Eurytemora affinis* in the Elbe estuary

Running title: Population dynamics of *Eurytemora affinis*

Authors: **Johanna Biederbick**, Jasmin Renz, Vanessa Russnak, Christian Möllmann and Rolf Koppelman

This chapter is a draft that is currently being prepared for submission to a peer-reviewed journal. The contributions of the authors are as follows: **Johanna Biederbick (JB)**, Christian Möllmann (CM), Rolf Koppelman (RK) and Jasmin Renz (JR) designed the objectives and methodology of this study. CM and RK supervised the study. **JB** and Vanessa Russnak (VR) collected field samples and carried out laboratory work. Data analysis was performed by **JB**, CM, RK and JR. Data visualisation was done by **JB** with advice from CM and RK. Funding was obtained by CM. All co-authors revised and agreed to the original draft written by **JB**.

#### Confirmation of correctness

Hamburg, 20. February 2025

---

Place, date

---

Prof. Dr. Christian Möllmann

## **Chapter 4: Spatial and temporal patterns of zooplankton trophic interactions and carbon sources in the eutrophic Elbe estuary (Germany)**

Running title: Estuarine zooplankton trophic dynamics

Authors: **Johanna Biederbick**, Christian Möllmann, Elena Hauten, Vanessa Russnak, Niko Lahajnar, Thomas Hansen, Jan Dierking and Rolf Koppelman

This chapter is a manuscript that is published in ICES Journal of Marine Science (31/12/2024). The contributions of the authors are as follows: **Johanna Biederbick (JB)**, Christian Möllmann (CM), Rolf Koppelman (RK) and Jan Dierking (JD) developed the objectives and methodology of this study, with CM, RK and JD supervising the study. **JB**, Elena Hauten (EH) and Vanessa Russnak (VR) conducted the field work. Laboratory work was carried out by **JB**, VR, EH, Niko Lahajnar (NL) and Thomas Hansen (TH). Data analysis was performed by **JB** with advice from RK and JD. Data was visualised by **JB**. Funding acquisition was done by CM. All co-authors revised and agreed to the original draft written by **JB**.

### **Confirmation of correctness**

Hamburg, 20. February 2025

---

Place, date

---

Prof. Dr. Christian Möllmann

**Chapter 5: Characterising intraspecific habitat exploitation of anadromous key species *Osmerus eperlanus* along the salinity gradient of a large European estuary**

Running title: Feeding ecology of *Osmerus eperlanus*

Authors: Elena Hauten, **Johanna Biederbick**, Steffen Funk, Raphael Koll, Jesse Theilen, Andrej Fabrizius, Ralf Thiel, Kai Jensen, Peter Grønkjær, Christian Möllmann

This chapter is a draft that is currently being prepared for submission to a peer-reviewed journal. The contributions of the authors are as follows: Elena Hauten (EH), Peter Grønkjær (PG) and Christian Möllmann (CM) developed the objectives of this study, whereby PG and CM supervised the work. Fieldwork was carried out by EH, **Johanna Biederbick (JB)**, Jesse Theilen (JT) and Raphael Koll (RK). Laboratory work was done by EH and **JB**. Data analysis was developed by EH, PG and Steffen Funk (SF) with the advice from CM, and conducted by EH. Data visualization was done by EH. Ralf Thiel (RT), Kai Jensen (KJ), Andrej Fabrizius (AF) and CM provided the funding for the study. All co-authors reviewed and edited the original draft written by EH.

**Confirmation of correctness**

Hamburg, 20. February 2025

---

Place, date

---

Prof. Dr. Christian Möllmann

## Chapter 6: Picophytoplankton prevail year-round in the Elbe estuary

Running title: Estuarine phytoplankton dynamics: Picophytoplankton

Authors: Nele Martens, **Johanna Biederbick**, C.-Elisa Schaum

This chapter is a manuscript that is published in Plant-Environment Interactions (27/10/2024). The contributions of the authors are as follows: Nele Martens (NM), **Johanna Biederbick (JB)** and C.-Elisa Schaum (C-ES) planned and designed the research objectives and methodology. NM and **JB** carried out sampling. C-ES was responsible for resource and funding acquisition. NM carried out laboratory measurements, analysed and visualised the obtained data and wrote the first draft of the manuscript. All authors contributed equally to subsequent versions of the manuscript.

### Confirmation of correctness

Hamburg, 20. February 2025

---

Place, date

---

Prof. Dr. Christian Möllmann